DISS. ETH NO. 19749

ENGINEERED 3D MODELS TO STUDY THE CANCER MICROENVIRONMENT AS A DETERMINANT OF DRUG RESPONSE

A dissertation submitted to

ETH ZURICH

for the degree of

Doctor of Sciences

presented by

MARIA HÅKANSON

M.Sc. Biology Engineering, Linköping University, Sweden
Born on January 30, 1980

accepted on the recommendation of

Prof. Dr. Marcus Textor, examiner
Dr. Mirren Charnley, co-examiner
Prof. Dr. Viola Vogel, co-examiner
Prof. Dr. Matthias Lütolf, external co-examiner
Prof. Dr. Edna Cukierman, external co-examiner

2011

Frühlingsglaube

Die linden Lüfte sind erwacht,
Sie säuseln und weben Tag und Nacht,
Sie schaffen an allen Enden.
O frischer Duft, o neuer Klang!
Nun, armes Herze, sei nicht bang!
Nun muß sich alles, alles wenden.

Die Welt wird schöner mit jedem Tag,
Man weiß nicht, was noch werden mag,
Das Blühen will nicht enden.
Es blüht das fernste, tiefste Tal:
Nun, armes Herz, vergiß der Qual!
Nun muß sich alles, alles wenden.

Ludwig Uhland *(1787 – 1862)*

Acknowledgements

A PhD thesis is typically not the result of only one man's mind. Instead it takes the support of a lot of people to reach this goal. After three years in the same project, with a distant goal and many disappointing experiments next to successful ones, it feels great to reach out to all the fantastic people that supported me on the way. This is my opportunity to thank you all officially.

First of all, I would like to thank my Professor, Marcus Textor. Almost four years ago I walked into your lab asking for the opportunity to do a PhD in your group. You were very welcoming and open and I feel that this spirit has followed throughout my PhD work. You have given me a lot of autonomy in this interdisciplinary project but at the same time helped me with structure and defining the end of the projects. One important part of my PhD has been establishing collaborations with various researchers within and outside of ETH. Thanks a lot for supporting me in getting into contact with the right people. I am also very grateful that you gave me the opportunity to participate in several international conferences. These conferences provided me with many ideas that helped me moving the project forward.

Secondly, I would like to thank Dr. Mirren Charnley, who continuously has supported me in my work over the last two and a half years. Without you this thesis could not have had the same biological emphasis. I am enormously grateful for the support you have given me along the way and for all the constructive input you provided in our meetings. Thanks to you, I am also stronger in writing scientific papers today. Your way of approaching research projects I find very impressive, you are passionate but at the same time you do it in a very professional and analytical way.

I got to know Prof. Edna Cukierman at a Gordon research conference in 2008. Later when I was in a phase where I found it challenging to define the direction of my project, I contacted you for advice. I am very grateful that you took time to discuss with me and give me valuable support. You have provided me with inspiration and ideas for making my research more relevant for *in vivo*. I am also very happy that you will be part of the thesis committee.

I would also like to thank Prof. Matthias Lütolf and Stefan Kobel for sharing the PEG hydrogel technology. Matthias, I very much appreciate that you will be part of the Thesis committee.

Prof. Viola Vogel acted as a discussion partner in the early stage of the project. I very much appreciate the input and ideas you provided in our meetings. I am glad that you will be part of my thesis committee.

Dr. Michelle Grandin, thank you for introducing me to LSST. In the beginning of the PhD project, I also interacted with Prof. Michael Smith. Thank you for teaching me confocal microscopy and mechanosensation.

I would also like to thank all the other researchers who worked with microwells: Dr. Mirjam Ochsner, Fabian Anderegg, Markus Rottmar and Dr. Katarina Maniura. Our discussions helped me define the direction of my PhD project.

During the PhD there are many techniques to learn, which can be very time-consuming without support. Therefore I would like to thank Sabrina Dilling for instructing me on protein quantification by Western blot, Dr. Peter Horvath for help on image analysis and all the people at LMC for help with the microscopy.

Special thanks to the three students who worked with me on different topics during the years: Helena Zec, Christoph Faigle and Elisabeth Sinner. Thank you for your enthusiasm and thorough work. To be more than one person on the project made the work more fun and interesting.

I have learned that good office mates are very important! They cheer you up at times when you are down. I shared office with many fantastic persons over the years. Especially I would like to thank Alireza for making my first months in the basement office very enjoyable. Thanks Martina, Katrin and Mirjam, I very much appreciated you being so welcoming and sharing your own experiences. Other great office mates have been Jia, Xiao, Tolga and Mateu.

Thank you also Josephine Baer and Esther Stähli who helped me with a lot of the administrative part of my work.

It was really special to work at LSST. The mix of nationalities and the cooperative atmosphere made LSST a place to feel good and get inspired. Last but not least I would like to thank all my colleagues for the great times we spent inside and outside of the lab!

Abstract

One of the major obstacles in cancer treatment is the failure of the initial therapy. One reason for cancer cell survival after the initial treatment is that the cells find sanctuary in their microenvironment. Cell adhesion-mediated drug resistance (CAM-DR) is defined as the signaling from the adhesive microenvironment that reduces the efficiency of therapy. CAM-DR is a transient effect, which is not linked to changes on the transcriptional level. Therefore the effect of CAM-DR is typically immediate and the extent of the effect is completely dependent on the cancer cell – microenvironment interaction. These effects are mediated both by adhesion to the extracellular matrix and to other cells and can be explained by signaling regulating both the apoptotic pathway and the cell cycle. It can be foreseen that the involvement of multiple signaling pathways leads to complex processes. Hence, while the promise of drugs targeting the microenvironment to improve the outcome of therapy is high, we are currently lacking in our understanding of the intricacies that lead to CAM-DR.

The aim of this thesis was to investigate the use of controlled *in vitro* culture models to study the role of extrinsic parameters on cell behaviour. Protein-coated microwell array platforms are advantageous compared to standard culture substrates such as the Petri dish as they allow for 3D culture, with a higher relevance for *in vivo*, but with a similarly high control of extrinsic parameters as can be obtained in 2D culture. Therefore, these platforms offer a unique opportunity for the independent interrogation of the role of different extrinsic parameters on cell behaviour. For this work we used two different platforms.

The PDMS microwell platform: surface functionalization improvement for long-term single cell studies

A PDMS-based microwell array was previously developed in our lab by M. Dusseiller and M. Ochsner in collaboration with the group of V. Vogel. With this platform we aimed at testing the concept of using microwells to study the role of extrinsic parameters on drug response.

Some cell assays studying, for example, differentiation, protein expression and drug response require long culture times of up to at least one week. To meet this demand we developed a new single-cell platform for long-term cell culture by optimizing the coating procedure of the previously developed PDMS microwell array. The original

protocol for fabrication of this microwell array used microfabrication/replication in PDMS and a surface modification protocol to provide a cell-adhesive protein coating exclusively inside the microwells (wall and floor). The microwell plateau areas were rendered non-adhesive for proteins and cells by a PLL-*g*-PEG coating. This surface functionalization strategy proved insufficient to constrain mesenchymal stem cells (MSCs) as single cells in the microwells for more than 2 days. Stability of patterned substrates for cell culture is a general issue, dependent on the type of substrate, the non-adhesive coating, as well as the cells that are cultured on the patterns.

In the new coating procedure we took advantage of the stable adsorption of the well-characterized amphiphilic triblock co-polymer PEG-PPO-PEG, Pluronics, onto the surface of native, hydrophobic PDMS. In addition to developing a printing-based protocol for functionalization of the array with proteins in the microwells and non-adhesive coating on the plateau, we used microfluidic patterning to create multiple patterns per array. The novel platform showed suitable for culturing mesenchymal stem cells inside the microwells for up to a week. These results were obtained in a collaborative project together with M. Rottmar in the group of K. Maniura at Empa St. Gallen, aimed at the application of the microwell array technology to study mesenchymal stem cell differentiation.

PEG hydrogel microwell platform: creating arrays of 3D cancer models and enabling analysis by high content information

In the second part of this thesis, we adapted the use of a microwell array prepared in a PEG hydrogel for cancer cell cluster formation and drug response studies. This work was aimed at creating a more *in vivo* relevant breast cancer model. The PEG-hydrogel microwell array was previously developed in the lab of M. Lütolf at EPF Lausanne to study the differentiation of isolated, single stem cells. The material characteristics of the PEG hydrogel made it very interesting for our approach. Firstly, the PEG polymer network has a high water content and a low and variable rigidity, approaching that of the tumour tissue, an important aspect given the central role of substrate stiffness for cell function. Secondly, the intrinsically inert nature of the hydrogel allowed for reproducible long-term cell culture and the formation of homogenous 3D cell clusters.

This platform was further development to meet the requirements on an *in vivo* relevant 3D culture model. This included the evaluation of the well bottom coating with proteins of importance to different stages of cancer progression; laminin, collagen I and fibronectin as well as the successful establishment of protocols that resulted in cell cluster formation with a relevant cell line, MCF-7. Furthermore, an imaging strategy based on confocal fluorescence microscopy and the use of fluorescent markers for proliferation and apoptosis enabled the analysis of cell behaviour throughout the 3D cluster. Thereby the signals from cells in contact with the matrix and cells in locations with only cell-cell adhesion could be separated. The

high-resolution imaging enabled sub-cellular resolution. Thereby high-content analysis protocols could be used to obtain a more precise determination of response.

Applying microwell platforms for the detailed study of drug response in 3D cancer cell clusters

A key part of this thesis involved the application of these models for the study of the microenvironment as a determinant of drug response. Taxol was used as a model drug for all experiments, as it is a chemotherapeutic that is commonly used in the treatment of breast cancer. MCF-7 cells are tumorigenic but not metastatic and express high levels of E-cadherin and were therefore used to model early stages of cancer.

Fundamental studies of the role of different extrinsic parameters and their interrelationship were performed on the PDMS platform, with the overall complexity kept to a minimum. Here, we compared drug response in relation to the type of matrix coating, dimensionality and presence/absence of cell-cell contacts by comparing the behaviour of single cells and pairs of cells located in the microwells of dimension 34 μm (diameter) and 10 μm (depth). A striking result was that small cell colonies of one to six cells cultured in the microwells showed a reduced drug response in comparison to cells cultured on flat (2D) substrates. Hence, in this reductionist 3D model with small cell clusters, we were able to mimic the dimensionality effect reported in the literature. These results were explained by differences in cell shape, which may indirectly also affect the extent of cell-cell adhesion. Specifically, we showed that cells forming cell-cell contacts were less susceptible to Taxol treatment than single cells. This parameter is a well-known determinant of drug response. However, we could demonstrate for the first time that this effect is experienced already in cells with only one cell-cell contact.

The *in vitro* models created on the PEG-hydrogel platform, represents a more *in vivo* relevant approach with larger cell clusters of dimension 90 μm (diameter) and 60 μm (depth). It was therefore interesting to explore again the mechanisms leading to CAM-DR and compare it to the results obtained in the PDMS microwell arrays. In an attempt to reveal the signaling pathways leading to CAM-DR in these models, we further measured proliferation in parallel to drug response. Initially, culture models for both the primary and the more progressed cancer environment were prepared by the use of laminin and collagen I coatings, respectively. With these models we found that matrix-induced drug resistance plays an important role also for cells in 3D cell clusters. Furthermore it was revealed that collagen I, present at more progressed stages of cancer progression, showed the strongest effect. Within this controlled model system it was easily confirmed that the matrix effects did not correlate to other extrinsic factors, such as cell morphology and density. Therefore we concluded that

the altered drug response with matrix-adhesion was a direct result of the signalling from the matrix.

Nevertheless, cell density was shown to be another important determinate of drug response. Crosstalk between these two effects was observed in 3D at high cell density where drug response was indifferent on different matrix coatings. To separate cell density from other extrinsic parameters, we cultured the cells at different cell densities on 2D collagen patterns (Ø = 200 μm). It was found that the cells at high cell density were less responsive to Taxol treatment in comparison to cell cultured at low density. This trend correlated with a reduction in proliferation. Furthermore, knocking down the expression of E-cadherin in the cancer cells inhibited the effect of density on proliferation. In summary, we could conclude that increased E-cadherin signaling at high cell density was a major factor in this model, completely explaining the effect of 3D culture on drug response.

Finally we compared the relationship between drug response and proliferation in the different experiments. Interestingly, while there was a direct relationship between drug response and proliferation with cell density changes, this was not observed for matrix-dependent changes of drug response. This result indicates that both cell-cycle regulation and anti-apoptosis signaling was involved in determining the drug response of the 3D cell clusters in this early cancer cell model. The final conclusions chapter of this thesis holds a comparison of the findings from the two platforms and a discussion on how these results may be generalized.

In summary, we developed and characterized two novel *in vitro* culture platforms. These reductionist platforms allowed the dissection of microenvironmental effects, in particular cell-matrix and cell-cell interaction in the context of drug response to Taxol. In the future, these controlled 3D models may not only be useful for further fundamental research, e.g. to evaluate additional microenvironmental parameters such as substrate mechanical properties. They could as well become important as drug discovery and screening platforms, as the controlled culture conditions ensures more reproducible and unequivocal results. Particularly the combination with multiplexing would make these platforms useful for example in the development of new concepts for combination therapy targeting the microenvironment.

Zusammenfassung

Eines der größten Hindernisse in der Krebstherapie ist das Versagen der Ersttherapie. Einer der Gründe für das Überleben von Krebszellen nach der ersten Behandlung ist, dass die Zellen durch ihre Mikroumgebung geschützt sind. Die Zelladhäsion-vermittelte Medikamenten-Resistenz (CAM-DR) ist durch Signale aus der Mikroumgebung der Zelle bedingt, welche die Effizienz der Therapie reduzieren. CAM-DR ist ein transienter Effekt, der nicht mit Veränderungen auf transkriptioneller Ebene verbunden ist. Daher tritt die Wirkung von CAM-DR in der Regel sofort ein. Das Ausmaß des Effekts ist dabei abhängig von der Interaktion zwischen der Krebszelle und ihrer Mikroumgebung. Er wird sowohl durch Adhäsion an die extrazelluläre Matrix und wie auch die Interaktion mit anderen Zellen vermittelt und kann dadurch Signalwege erklärt werden, die sowohl die Apoptose als auch den Zellzyklus regulieren. Die dabei ablaufenden Prozesse sind durch die Beteiligung mehrerer Signalwege sehr komplex. Während Medikamente sehr vielversprechend sind, welche die Mikroumgebung zugunsten eines besseren Therapieerfolgs beeinflussen, fehlt uns derzeit noch das Verständnis der Grundlagen der Zelladhäsion-vermittelten Medikamenten-Resistenz.

Das Ziel dieser Arbeit war es, die Anwendung von kontrollierte *in vitro* Modellen zu untersuchen. Vor allem für das Testen von den Einfluss extrazelluläre Parameter auf dem Zellverhalten. Dafür bieten sich ein Array mit Protein-beschichteten 3D Mikrostrukturen an, weil sie im Gegensatz zu konventionellen Zellkultursubstraten für die 3D-Kultur geeignet sind. Deren Relevanz für die *in vivo* Umgebung ist höher als die von 2D-Kulturen, gleichzeitig lassen sich aber auch die extrinsischen Parameter ähnlich gut kontrollieren. Daher bieten diese Plattformen die einmalige Gelegenheit, die Rolle verschiedener extrinsischer Parameter auf das Verhalten der Zelle unabhängig voneinander zu untersuchen. Für diese Arbeit benutzten wir zwei verschiedene Plattformen.

Die PDMS Plattform: Verbesserung der Oberflächenfunktionalisierung für Langzeit-Zellstudien

Mikrostrukturierte PDMS Substrate wurden zuvor in unserem Labor von M. Ochsner und M. Dusseiller in Zusammenarbeit mit der Gruppe von Viola Vogel entwickelt und für biologische Fragestellungen eingesetzt. In dieser Arbeit sollte gezeigt werden, inwieweit solche Mikrostrukturierten Plattformen geeignet sind, um die Rolle den extrinsischen Parametern auf die Medikamentenwirkung zu untersuchen.

Einige Zellassays, mit denen beispielsweise Zelldifferenzierung, Proteinexpression oder die Wirkung von Medikamenten untersucht werden, erfordern sehr lange Kulturzeiten von bis zu einer Woche. Um dieser Anforderung gerecht zu werden, wurde eine neue Einzel-Zell-Plattform entwickelt, die längere Zellkulturzeiten zulässt. Dies wurde durch Weiterentwicklung der zuvor entwickelten mikrostrukturierten PDMS Kultursubstrate erreicht. Das ursprüngliche Protokoll für die Herstellung dieses Microwell Array verwendet Mikrofabrikation in PDMS und ein Oberflächenmodifizierungs-Protokoll, das die Proteinbeschichtung ausschliesslich auf die Innenseite der Vertiefungen beschränkt. Die erhabenen Bereiche der Microwells wurden mittels Beschichtung mit PLL-g-PEG so modifiziert, dass sie nicht mehr adhäsiv für Proteine und Zellen waren. Diese Strategie der Oberflächen-Funktionalisierung erwies sich jedoch als unzureichend, um mesenchymale Stammzellen (MSCs) als einzelne Zellen in den Vertiefungen für mehr als 2 Tage wachsen zu lassen. Die Stabilität von strukturierten Substraten für die Zellkultur ist immer ein problematischer Aspekt. Sie ist abhängig von dem jeweiligen Substrat, der Antihaftbeschichtung sowie dem kultivierten Zelltyp.

In einem neuen Beschichtungsverfahren nutzten wir die stabile Adsorption eines gut charakterisierten Block-Co-polymers, Pluronics, auf der Oberfläche des nativen, hydrophoben PDMS. Für das neue Verfahren wurde eine Stempelmethode zur Funktionalisierung des Arrays mit Proteinen in den Vertiefungen und einer Antihaftbeschichtung auf der Oberseite entwickelt. Die Biofunktionalisierung durch Mikrofluidik, erlaubte es, einen einzelnen Array mit multiplen Proteinbeschichtungen zu erzeugen. Mit dieser neuartigen Plattform gelang es, mesenchymale Stammzellen bis zu eine Woche lang zu kultivieren. Diese Ergebnisse wurden in einem gemeinsamen Projekt zusammen mit K. Maniura und M. Rottmar an der Empa St. Gallen erzielt, bei dem die Differenzierung mesenchymaler Stammzellen untersucht werden sollte.

Die PEG Hydrogel Plattform: Herstellung von Arrays mit 3D Krebsmodellen und „High-Content-Information" Analyse der Zellkolonien

In einem nächsten Schritt nutzten wir ein Array mit einem mikrostrukturierten PEG-Hydrogel, wie er ursprünglich im Labor von M. Lütolf an der EPF Lausanne entwickelt wurde. Dieser Array wurde weiterentwickelt zu einer Plattform für

Krebszellenstudien. Das Ziel dabei war, ein Brustkrebs-Modell mit verbesserter *in vivo* Relevanz zu schaffen und so neue Einblicke in die Beziehungen zwischen verschiedenen CAM-DR Signalwegen zu gewinnen. Um diesem Ziel nachzugehen, wurde in dieser Studie Zellwachstum parallel zur Medikamentenantwort bestimmt. Diese Plattform wurde ursprünglich entwickelt, um die Differenzierung von isolierten, einzelnen Stammzellen zu untersuchen. Wir wählten diese Plattform, da die Materialeigenschaften der PEG Hydrogele die Möglichkeit boten, Krebszellen mit hoher *in vivo* Relevanz zu züchten. Das Polymer-Netzwerk von Hydrogelen hat eine geringe Steifigkeit, die der von Tumorgewebe ähnlich ist. Zudem erlaubt das inerte Material, reproduzierbare Langzeit-Zellkultur-Experimente durchzuführen und die Bildung von homogenen 3D Zellkolonien zu erreichen.

Die Entwicklung der Plattform hin zu einem relevanten *in vivo* 3D-Modell beinhaltete die Beschichtung mit Proteinen aus verschiedenen Stadien der Tumorprogression. Dazu gehörten Laminin, Kollagen I und Fibronectin. Mit Hilfe von konfokaler Mikroskopie und für Zellwachstum und Apoptose spezifischen Fluoreszenzmarkern gelang es, das Verhalten der Zellen innerhalb der 3D-Cluster zu beobachten. Dabei konnten die Signale von Zellen, die nur Kontakt mit anderen Zellen hatten, von solchen zu unterscheiden werden, die zusätzlich Kontakt zur Matrix hatten. Hochauflösende Bildgebung ermöglichte die subzelluläre Auflösung und die Verwendung von High-Content-Screening-Protokollen zur genaueren Bestimmung der Zellantwort.

Die Anwendung von mikrostrukturierten Plattformen für detaillierte Studien der Antwort auf Medikamente in den 3D Krebszellen Kolonien

In dieser Arbeit wurden die beschriebenen Modelle eingesetzt, um den Einfluss der Mikroumgebung auf die Medikamentenantwort von Zellen zu bestimmen. Für alle Experimente verwendeten wir als Modellmedikament Taxol, da es ein bekanntes Chemotherapeutikum ist, das üblicherweise zur Behandlung von Brustkrebs eingesetzt wird. MCF-7 Zellen haben Tumorzelleigenschaften, metastasieren jedoch nicht und exprimieren grosse Mengen E-Cadherin. Sie werden deshalb dazu eingesetzt, frühe Krebsstadien zu untersuchen.

Es wurden grundlegende Untersuchungen der verschiedenen extrinsischen Parameter und deren Wechselwirkungen mit der PDMS-Plattform durchgeführt, wobei die Komplexität auf ein Minimum beschränkt wurde. In diesem Setup konnte nachfolgend der Einfluss von extrazellulärer Matrix-Beschichtung, Dimensionalität und Zell-Zell Kontakte auf die Medikamentenantwort untersucht werden. Ziemlich unterwartet konnten wir feststellen, dass auch bei kleineren Zellkolonien von lediglich ein bis sechs Zellen die Dimensionalität der Zellkultursubstrate eine signifikante Auswirkung hat. Zellen, die innerhalb der 3D-Mikrostrukturen kultiviert wurden, haben weniger stark auf Taxol geantwortet als Zellen auf flachen (2D) Substraten.

Dabei konnte mit dieser 3D Plattform das in der Literatur beobachtete Benehmen von Zellen in 3D Umgebungen nachgestellt werden.

Wir nehmen an, dass unsere Resultate vor allem durch Zellform-Veränderungen erklärt werden können, die vermutlich auch indirekt eine Auswirkung auf die Zell-Zell Adhäsion haben. In einem weiteren Experiment wurde gezeigt, dass Zellen, die Zell-Zell Kontakte gebildet haben, weniger stark als einzelne Zellen auf die Taxol Behandlung reagierten. Dieser Parameter ist zwar bekannt für seine Auswirkungen auf die Medikamentenantwort. Es war jedoch interessant zu sehen und neu, dass dieser Effekt bereits für Zellen gilt, welche lediglich einen einzelnen Zell-Kontakt ausgebildet haben.

Die PEG-Hydrogel Plattform repräsentiert ein *in vitro* Modell mit höherer Relevanz für die *in vivo* Situation. Mit dieser Plattform haben wir das Verhalten von Zellen in größeren Zell-Clustern untersucht. Eine Zielsetzung mit diesen weiteren Experimenten war es, die Mechanismen von CAM-DR näher anzugehen. In ersten Experimenten haben wir Modelle für die ganz frühe sowie die teils fortgeschrittene Phase der Krebsentwicklung genutzt. Diese wurden dadurch verwirklicht, dass wir verschiedene adhäsive ECM Proteine verwendeten, welche zu den respektiven Krebs-Phasen gehören, nämlich Laminin und Kollagen I. Mit diesem Modellsystem fanden wir, dass die Adhäsion zu Matrixproteinen eine wichtige Rolle spielt bezüglich Medikamentenantwort, auch dann wenn Zellen in grösseren Kolonien vorliegen. Im weiteren wurde festgestellt, dass die Interaktion zu Kollagen I (entsprechend der fortgeschritteneren Krebsphase) die grösste Auswirkung auf die Zellen hatte. Mit diesem kontrollierten Modellsystem wurde weiterhin bestätigt, dass dieser Effekt nicht von anderen Parametern wie Zellenmorphologie und Zelldichte erklärt werden kann. Andererseits konnten wir auch zeigen, dass die Dichte, mit der die Zellen wachsen, ein wichtiger Parameter für die Antwort auf die Medikamente war. Wenn Zellen in hoher Dichte kultiviert wurden, wurde ein Crosstalk zwischen diesen beiden Effekte festgestellt. An dieser Stelle war nämlich der Unterschied, den wir vorher bei unterschiedlichen Matrixproteinen beobachtet hatten, nicht mehr vorhanden.

In einem weiteren Schritt haben wir den Einfluss der Zelldichte genauer untersucht, in dem wir Zellen in unterschiedlichen Dichten auf 2D Kollagenmustern (Ø = 200 μm) wachsen liessen. In diesem Experiment konnten wir zeigen, dass Zellen, die in höherer Dichte wuchsen, weniger stark auf die Behandlung mit Taxol antworteten. In diesem Modell konnten wir daher feststellen, dass die Zelldichte den Einfluss der 3D-Zellkultur auf die Medikamentenantwort komplett erklärt.

Schliesslich haben wir das Verhältnis zwischen Zellwachstumsrate und Medikamentenantwort genauer untersucht. Das Verhältnis zwischen der Auswirkung der Zelldichte auf Zellwachstum und der Medikamentenantwort war proportional. Allerdings war dies nicht der Fall für den Einfluss der Matrixadhäsion. Diese

Resultate deuten darauf hin, dass sowohl Zell-Zyklus-regulierende Proteine als auch Anti-Apoptosis Signalwege für die Medikamentenantwort in diesem 3D Krebsmodell involviert sind. In der Schlussdiskussion dieser Dissertation werden die Resultate der beiden Zellkulturplattformen verglichen und mögliche Generalisierungen dieser Schlussfolgerungen diskutiert.

Die *in vitro* Modelle, die innerhalb dieser Dissertation entwickelt wurden, könnten sich daher als nutzbare Plattformen in der Krebsforschung erweisen, vor allem in Bezug auf die Erforschung der Bedeutung der extrazellulären Umgebung für die Medikamentenantwort. In Zukunft sollten Plattformen, wie die hier präsentierte, nicht nur in der Grundlagenforschung einsetzbar sein, sondern könnten auch Anwendung in der Pharmaindustrie finden, zum Beispiel bezüglich Entwicklung neuer Konzepte für Kombinationstherapien, welche die Mikroumgebung der Zellen als Target haben.

Contents

Abbreviations

2D	Two-dimensional
3D	Three-dimensional
APS	Ammonium persulfate
CLSM	Confocal laser scanning microscope
ADR	Acquired drug resistance
ECM	Extracellular matrix
EDTA	Ethylenediaminetetraacetic acid
FBS	Fetal bovine serum
FCS	Fetal calf serum
Fn	Fibronectin
Lam	Laminin
Col-I	Collagen-I
PBS	Phosphate buffered saline
PDMS	Polydimethylsiloxane
PEG	Poly(ethylene glycol)
PLL-g-PEG	Poly(L-lysine)-graft-poly(ethylene glycol)
HRE	Human renal epithelial cells
MCF-7	Breast mammary carcinoma, tumorigenic
MDA-MB-231	Breast mammary carcinoma, metastatic
PS	Polystyrene
TCPS	Tissue culture polystyrene
TEMED	N, N, N, N-tetramethylethylenediamine
BrdU	Bromodeoxyuridin
EMT	Epithelial mesenchymal transition
MET	Mesenchymal epithelial transition
CAM-DR	Cell adhesion mediated drug resistance
SiO_2	Silicon oxide
Borax	Sodium-Tetraborat
PI	Propidium iodide
MMP	Mitochondria membrane potential

CHAPTER 1

Introduction

This chapter describes the state of the art for the use of microfabricated models in cancer drug discovery. It provides background information on cell-based methods in cancer drug discovery, the role of the microenvironment in cancer progression and drug response as well as a presentation of different applications of microfabricated models. This is a highly interdisciplinary research area that spans from device technology development to fundamental studies of cell behaviour to more application-oriented research in drug discovery and screening. Since the first exploration of microfabricated cell culture devices in the 1990s (Chen *et al.*, 1997) it was predicted that investigators would provide new and improved solutions for cell-based screening (Wlodkovic and Cooper, 2010) (Gidrol *et al.*, 2009). Today, this technology has been widely exploited for numerous applications in cell handling, sorting and analysis.

Three main advantages make microfabricated models interesting to use in cell-based testing. First, the miniaturization of cell testing platforms makes it possible to test several conditions per substrate, thereby increasing throughput and reducing the number of cells needed per experiment. This enables the assaying of primary cells or patient derived cells. Second, microfabrication techniques make it possible to integrate several functions within a system, coupling the cell handling system to actuators for pumping or sensors for analysis. Such designs minimize the number of pipetting steps needed for an assay, hence reducing the time-consumption for an assay, increasing reproducibility and ultimately also minimizing the required sample size. The third advantage of microfabricated systems, over conventional methods, is that they offer the possibility to control the microenvironment of the cells. In microfabricated systems, the biochemical environment as well as solute concentrations and flow characteristics may be controlled on the length scale of single cells. Thus, microfabricated systems can be used to mimic the in *vivo* environment of the cell and conversely, allow the effects of the microenvironment on cell behaviour to be explored.

In this background chapter we will show why these advantages of microfabricated systems can be especially profitable in cancer research and drug discovery. One way to tackle the problem of heterogeneity in cancer would be to move from generalized treatment to patient-specific treatment (Rønnov-Jessen and Bissell, 2008). This would require methods that can obtain information from the small cell number typically available in a patient sample, which would in principle be feasible by miniaturization. In addition, cancer is a disease where the microenvironment has shown to both directly (Aoudjit and Vuori, 2001) and indirectly (Grantab *et al.*, 2006) modulate drug response. Therefore, models that can control certain parameters of the microenvironment could be powerful tools to elucidate such effects and in the development of treatment against them. In the final part of this chapter the use of microfabricated models for combinatorial screening of drug and microenvironmental effects and for the analysis of patient cells are presented as two particularly promising areas of application.

1.1 Cell-based methods in cancer drug discovery

The WHO predicted cancer to become the leading cause of death in 2010 (Boyle and Levin, 2008). Thus, it is unsurprising that the majority of drug candidates in development today are targeted at cancer therapy (Maziasz *et al.*, 2010), with over 800 drugs and vaccines in clinical development as of 2009 (Christel, 2009). However, cancer drug development suffers from a very low success rate with a three times lower success rate of new compounds in clinical development compared to cardiovascular disease (Kola and Landis, 2004) (Fig. 1.1a).

Two major factors complicate the development of drugs that can effectively treat cancer. Firstly, there is a high heterogeneity in this disease (Fig. 1.1b), which makes it difficult to develop drugs that have general success. Probably the range of the disease is wider than for any other therapeutic area (Kamb et al., 2007). Secondly, resistance to treatment originating from the interactions within the tumour microenvironment and from repeated treatment complicates the therapeutic picture (Teicher, 2009).

High clinical failure results in escalating downstream costs, which has led to an increased focus on the early drug development steps, including target validation and lead optimization (Bleicher *et al.*, 2003) (Fig. 1.1c). In order to remove poor candidates as early as possible in the drug development process, cell-based assays are increasingly used (Landro, 2000; Roberge, 2000) (Fig. 1.1c). The approach for anti-cancer drug discovery has evolved from empiric cell-based screening for anti-proliferative effects to more mechanistically cell-based approaches for the targeting of specific proteins involved in signal transduction related to the cell cycle and

apoptosis. Today, cell-based assays are considered superior to molecular assays both for target-validation and pre-clinical screening (Balis, 2002). Experimenting directly within the complex environment of the cell is advantageous, as the pharmacologic effect of many drugs is due to the drug action within a protein network, which is only present within the cell. In addition, experimenting within the cell allows any unpredicted targets to be discovered.

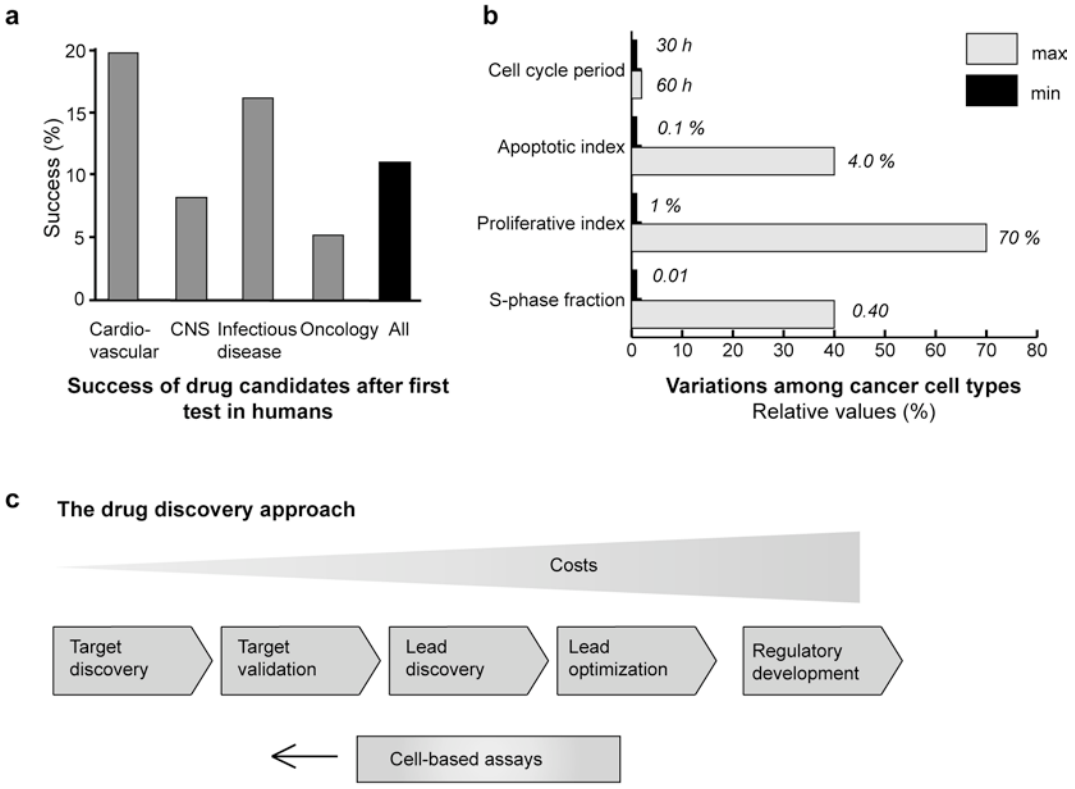

Figure 1.1: *Meeting the challenges in anti-cancer drug development*. a) Cell-based assays are increasingly used in the drug development process (Ramm, 2005) because of the greater relevance compared to biochemical assays (Balis, 2002). Early identification of poor candidates reduces costs. Hence, cell-based assays are implemented as early as possible in the drug development. b) Oncology compounds have historically had a significantly lower success rate in clinical development than compounds in other areas, such as cardiovascular disease. The rates shown are the success rates from first tests in human to registration for ten large pharmaceutical companies in the united states and Europe for the period 1991-2000. Data taken from (Kola and Landis, 2004). c) One reason for the low success of cancer drugs is the heterogeneity of this disease as exemplified by the large variation in basic cellular behaviour between cells from different cancers (Gardner and Fernandes, 2003). The graph shows the minimum and maximum value that can be expected for a certain characteristic of the cancer cells, such as apoptotic index and S-phase fraction.

However, it is clear that the methods in cell-based screening need to further develop, as the predictivity of preclinical screening for patient outcome is still unsatisfactory. This is one reason for an increasing interest in using primary tumour explants in

addition to cell lines as more relevant models in the cell-based screens (Cree *et al.*, 2010). Future anti-cancer drug development may use a combination of molecular, cell line and primary cell culture. However, crucial for a better translation from pre-clinical testing to patient outcome may be test models that better reflect the complexity of the cancer microenvironment (Friedrich *et al.*, 2009).

1.2 The cancer microenvironment and treatment response

Most eukaryotic cells exist in a complex environment in which they are in continuous contact with surrounding cells and extracellular matrix. This interaction is important for the constant regulation of cellular behaviour. In cancer, cells do not show a normal response to regulatory signals anymore. Therefore, tumour cells continue to grow where normal cells would not. Another hallmark of cancer is that they can escape the signals to induce cell death. Cancer can develop in most human tissues and in a more progressed stage of the disease the tumour cells may leave the primary site to form metastases in other organs. The mechanisms that can cause cancer are continuously explored. In the 1970s the Knudson theory was presented, in which a number of statistical investigations showed that at least two mutations are needed for cancer to occur (Knudson, 1971). In recent years, viruses that can cause cancer have been discovered. Another possibility for cancer causation is given by the tissue organization field theory, which explains cancer as an effect of aberrant tissue organization (Maffini *et al.*, 2004).

While the role of the microenvironment in the initiation of cancer remains controversial, there are currently several lines of evidences of how the microenvironment can affect cancer progression (Denys *et al.*, 2009), dissemination and metastasis (Joyce and Pollard, 2009). Hence, this shows that even though cancer may originate from DNA mutations, it is promoted by certain physiological conditions (Bissell *et al.*, 2002). This idea, as controversial as it was when it was first raised, is now well accepted in the cancer research community (Kumar and Weaver, 2009). The interaction between the cancer cell and its microenvironment has also shown to affect the outcome of treatment (Meads *et al.*, 2009) and we are just at the starting point for using this knowledge about the microenvironmental effects in the clinical procedures in diagnosis and treatment (Rønnov-Jessen and Bissell, 2008).

1.2.1 Microenvironmental changes in cancer progression

Changes to the cancer microenvironment

The vast majority (about 90 %) of human cancers are carcinomas, malignant tumours of epithelia (Morgan, 2007). In breast cancer, as one example of carcinomas, the cells at the primary site are surrounded by healthy epithelial cells and proteins in the

basement membrane (Fig. 1.2a). As the tumour progresses, the basement membrane, that physically separates the epithelial from the connective (mesenchymal) tissue, is degraded thus facilitating a direct interaction between cancer cells and the tumour-associated mesenchymal stroma (Kunz-Schughart and Knuechel, 2002) (Fig. 1.2a). This implies that tumour cells in an early tumour are in contact with epithelial cells and an ECM, which is mainly composed of collagen IV and laminin, while after basement membrane breakdown the cells come in contact with a completely different niche containing mainly collagen I and mesenchymal cells. Not only do the cancer cells therefore encounter many different microenvironments during progression, but these physiological niches can be changed by the tumorigenic process itself.

Such changes include the stiffening of the tumour stroma by increased collagen crosslinking (Levental *et al.*, 2009) and changes of the stromal cells (Bissell and LaBarge, 2005). Interestingly though, there is not a clear-cut division in cause and consequence in these relationships. *In vitro* experimentation has shown that on the one hand normal fibroblasts undergo conversion to myofibroblasts in response to tumour cells in culture (Ronnov-Jessen *et al.*, 1996). On the other hand, the activated, myofibroblast-rich stroma has shown to support cancer cell growth and metastasis (Castelló-Cros and Cukierman, 2009). Parameters that have shown to influence cancer progression include integrin signaling (Desgrosellier and Cheresh, 2010), matrix rigidity (Levental *et al.*, 2009), hypoxic conditions (Wittekind and Neid, 2005) and signaling from stromal cells (Jodele *et al.*, 2006).

Changes to the cancer cells

In order for cancer cells to survive in many different environments they have to go through certain phenotypical changes. In the primary cancer environment the cells still show many characteristics of an epithelial cell. In many cancers, such as breast cancer, the cancer cells escape this environment by going through the epithelial – mesenchymal transition (EMT), thereby losing E-cadherin expression (Wheelock *et al.*, 2008) and gaining a more mesenchymal like morphology. In this state the cells can invade the stroma and form distant metastases. Completed EMT is therefore a characteristic of advanced breast cancer, while other cancers can invade by other strategies not requiring the EMT (Friedl *et al.*, 1998).

Little is known about phenotypic changes at the metastatic site, as it is difficult to follow the cells through this cycle. However, a recent report found that the introduction of a metastatic cell line in a secondary organ environment, promoted a reversion back to an epithelial phenotype with E-cadherin expression as one characteristic (Chao *et al.*, 2010). The EMT transition changes the phenotypic and functional state of cells not only by downregulation of the cell-cell adhesion molecule E-cadherin (Sleeman and Cremers, 2007) but also by upregulation of several cancer-specific integrins (Desgrosellier and Cheresh, 2010).

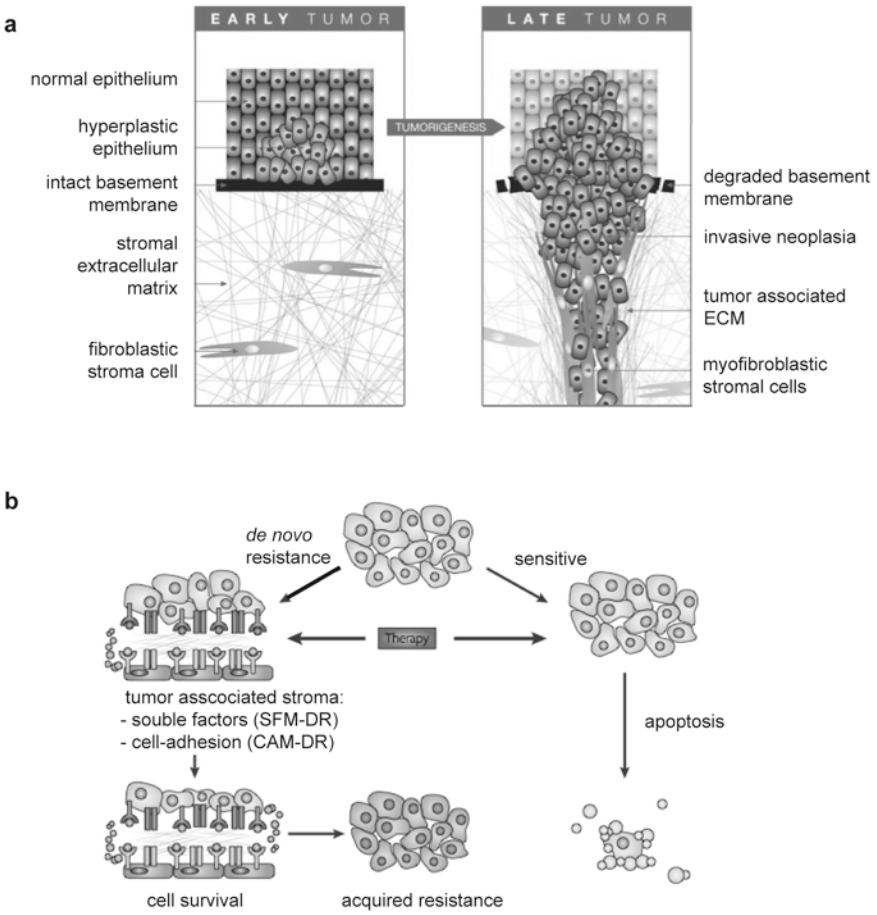

Figure 1.2: *The role of the microenvironment in cancer progression and drug response.* a) Cancer progression is accompanied by a change of the local microenvironment. Epithelial cells, which typically only form homotypic adhesions to other epithelial cells and matrix adhesions to the basement membrane, transform to an invasive neoplasia and come in contact with the tumour associated ECM. The image is adapted from (Cukierman, 2010, Biochemical pharmacology). b) Factors that are present in the tumour microenvironment induce environment-mediated drug resistance (EMDR) by two primary mechanisms: soluble factor-mediated drug resistance (SFM-DR) and cell adhesion-mediated drug resistance (CAM-DR). When the cancer is treated for the first time, most tumour cells respond to the drugs. However, the interaction with microenvironmental factors can give enough protective signaling for some of the cells to survive therapy. Over time, genetic instability inherent in cancer cells combined with the strong selective pressure of therapy leads to successive, random genetic changes that cause the gradual development of more complex, diverse and permanent acquired-resistance phenotypes (multidrug resistance). These persistent tumour cells eventually cause disease recurrence and are much less likely to respond to subsequent therapy after acquired resistance develops. Hence, therapeutic strategies that disrupt EMDR pathways would reduce the level of surviving cells and therefore the emergence of acquired resistance. The image is adapted from (Meads *et al.*, 2009) .

Studies correlating integrin expression levels in human tumours with pathological outcomes, such as patient survival and metastasis, have identified several integrins that might have an important role in cancer progression. For example β_1 integrin has shown to be up-regulated in invasive breast cancer cells and the detection of high levels of β_1 integrin in patient tissue is related to decreased survival (Yao *et al.*, 2007). Another work highlighted the importance of $\alpha_3\beta_1$ integrin for pulmonary metastasis (Wang *et al.*, 2004).

1.2.2 Adhesion mediated drug resistance

Signaling from the tumour microenvironment is known to affect the susceptibility of tumour cells to the treatment with chemotherapeutics. Cell-adhesion mediated drug resistance (CAM-DR) is mediated by the interaction of tumour cells to components of the extracellular matrix and to other cells in their environment (Meads *et al.*, 2009) (Fig. 1.2b). The protective signaling from the microenvironment is niche-specific, as it is dependent on the composition of the ECM and neighbouring cells. Using cell derived ECM matrices it has been shown that survival signaling was induced in the metastatic cell line MDA-MB-231 only at culture in a tumour associated ECM and not in a normal ECM control (Castelló-Cros *et al.*, 2009). Another example is the microenvironment in bone, which has shown to support increased survival in metastatic cells, hence complicating treatment of bone metastases (Onishi *et al.*, 2010).

Park *et al.* used blocking antibodies to show that β1 integrin is important for the growth of cancer cells in a 3D matrigel culture, while conversely it did not affect normal cells (Park et al., 2006). The same researchers later found that the combinatorial treatment of a β1-inhibiting antibody with ionizing radiation treatment increased the effect of treatment in mice (Park *et al.*, 2008). The effect of CAM-DR is immediate as it is mainly caused by degradation of activators of apoptosis (Hazlehurst *et al.*, 2007) or increased stability of suppressors of apoptosis and cell cycle regulators (Lwin *et al.*, 2007), and therefore is a non-transcriptional change. The importance of CAM-DR has been highlighted in recent years as it has been identified as one reason for the failure of initial treatment and therefore also a first stage towards acquired resistance (Meads *et al.*, 2009) (Fig. 1.2b).

1.2.3 Limited drug penetration in transformed tissue

Cell survival after treatment is also a consequence of poor drug penetration into the tumour tissue. Cancer drugs are typically administered by oral or intravenous injection. Hence, the drugs will accumulate in the blood stream and eventually reach all well-vascularised tissue. A characteristic of tumour tissue is in-complete vascularisation, leading to poor penetration of the drug. Drug penetration of tumour

tissue can be studied *in vitro* by measuring the penetration and effect of drugs in multicellular layers on top of a membrane. The packing density has shown to significantly affect drug penetration already in 200 μm thick layers (Grantab *et al.*, 2006). As a result, the common cancer drug Doxorubicin was less effective in closely packed cells. Poor tissue penetration of current cancer drugs (Minchinton and Tannock, 2006) is a considerable problem and substantial time and effort has been invested into the development of drug carriers that should prolong the circulation time of the drug in the blood and improve the tissue penetrating capabilities (Cukierman and Khan, 2010).

1.2.4 Therapeutic strategies targeting the cancer microenvironment

The growing knowledge of the signaling between the microenvironment and cancer cells has resulted in a new therapeutic area. For cancer therapies that target the microenvironment, different integrins are promising candidates (Hehlgans *et al.*, 2007). Integrin-associated proteins are involved in all major signal transduction pathways related to proliferation and survival.

After many years of preclinical studies, there are now several integrin targeting drugs in Phase III clinical trials (Desgrosellier and Cheresh, 2010). One area in which this strategy has become important is in the targeting of integrins expressed during neovascularisation, to suppress tumour angiogenesis. Patient tests have already been conducted with Vitaxin, an antibody that has specificity for the αvβ3 integrin (Patel *et al.*, 2001). Interestingly, Mori *et al.* showed that integrin blocking enhances the treatment with a cytotoxic drug in mice. They found that the combined treatment was more effective than any of the drugs alone (Mori *et al.*, 2004). With an increased understanding of the molecular difference between cancer cells and normal cells, there is a potential for therapies that specifically target cancer cells in their characteristic environment.

The cancer-specific environment has also been exploited for the targeting of drug carriers (Marlind *et al.*, 2006). Targeted treatment typically gives higher efficiency at a lower drug dose and reduced side effects. One strategy is to target the integrins specifically expressed in tumour vasculature (Hood *et al.*, 2002). Recent pre-clinical studies in mice showed very promising results in which the targeting of doxorubicin-loaded nanoparticles to integrin αvβ3 positive tumour vasculature improved the resultant treatment 15-fold compared to administration of the free drug (Murphy *et al.*, 2008).

1.3 Creating *in vivo* like culture conditions by microfabrication

The immense difference between the cell environments in standard 2D cell culture compared to *in vivo* likely contributes to the limited predictivity for patient outcome (Bhadriraju and Chen, 2002; Friedrich *et al.*, 2007). It is known that the 3D organization of cells within tissue affects several major cell functions, including proliferation, motility and cell fate (Griffith and Schwartz, 2006). Therefore the growth of cells in an artificial environment can induce phenotypes that do not represent their *in vivo* counterparts. There are many parameters that differ between the environment a cell sees *in vivo* and in the flat dish. Theoretically, with every step moving closer to the *in vivo* situation, more relevant culture conditions are obtained. Here we outline some directions taken in the area of cell culture development including improvements both at the level of cell type and the actual culture system (Fig. 1.3).

Firstly, cell lines are typically applied due to their ease of use and low cost. However, cell lines are often largely altered in comparison to their origin. Therefore, moving to the use of primary cell lines should increase predictivity (Cree *et al.*, 2010; van der Kuip *et al.*, 2006). Cancer, however, is not coherent even when the tissue origin remains the same and therefore the highest predictivity would be expected first when assays are performed with cells directly from the patient (Trusheim *et al.*, 2007) (Ganser *et al.*, 2009). Co-culture methods can account for parts of the signaling in the *in vivo* microenvironment that is not represented in a normal cell culture system. For example co-culture has been used to study the interaction between normal and cancerous cells (Spink *et al.*, 2006). On the other hand, the *in vivo* relevance and predictivity of the cell culture can also be increased by alterations of the cell culture substrate. In a system where culture conditions can be controlled, the *in vivo* organization of cells can be better recapitulated (Bhadriraju and Chen, 2002), for example making it possible to engineer capillaries in vitro. One of the most important parameters in making in vitro cell culture more relevant has shown to be dimensionality. The culture in a 3D environment has shown to regulate the growth of migratory cells (Serebriiskii *et al.*, 2008) and profoundly affect cell-cell interaction-dependent processes such as morphogenesis (Nelson and Bissell, 2005).

Secondly, other parameters that have shown to greatly impact predicitvity of cancer cell culture are related to the culture environment and include the composition of the extracellular matrix (Aoudjit and Vuori, 2001) and the 3D organization (St Croix *et al.*, 1998). In the worst case, the target or target-associated molecules are differently expressed *in vivo* and *in vitro*. Another important consideration is that standard 2D cultures do not take into account the effect of diffusion limitations for metabolites and drugs in the tissue (Ivascu and Kubbies, 2007).

Today, there are a vast number of approaches, using microfabrication and novel scaffolds materials, to develop new cell culture platforms that recapitulate the 3D characteristics of the *in vivo* environment. These models have been crucial for the understanding of the role of the *in vivo* environment on the behaviour of normal and malignant cells (Lee *et al.*, 2007) and are currently making the first steps into drug development (Hirschhaeuser *et al.*, 2010).

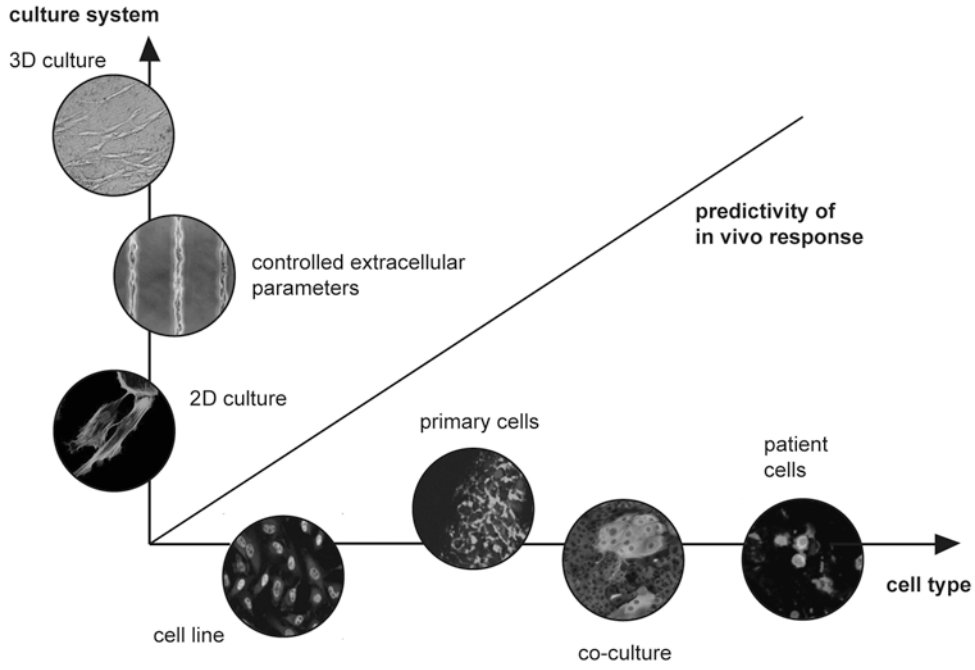

Figure 1.3: *More relevant models in cell-based assays.* The predictivity of drug development should theoretically improve when more *in vivo* relevant models are used. This graph outlines some directions taken in cell culture development to improve predictivity. Two parameters, cell type and culture system are plotted in an x-y graph. The linear curve thereby explains the hypothetical increase in predicitvity of a cell culture system, with the alteration of these parameters. Along the x-axis some examples of cell-types that have a higher relevance than cell lines in monoculture are plotted. This ranges from primary cells (van der Kuip *et al.*, 2006) to co-culture (Spink *et al.*, 2006). Patient cells (Ganser *et al.*, 2009) would be the most relevant model system. Systems that enable the culture and analysis of patient cells can be used for tailored treatment, which holds a high promise for the improvement of cancer therapy. On the y-axis the culture platforms of different relevance are plotted. Systems with controlled extrinsic parameters have a higher relevance than standard 2D culture platforms (Bhadriraju and Chen, 2002), as exemplified here were micropatterns make it possible to engineer capillaries in vitro. Platforms that enable 3D culture, recapitulates the organization of cells *in vivo* and are therefore probably the most relevant (Serebriiskii *et al.*, 2008).

Microfabricated cell culture platforms include open microfabricated system, which here are defined as cell culture substrates with 2D or 3D patterns that can control cell-adhesion into certain areas and support an *in vivo*-like 3D growth (Fig. 1.4a). In closed microfabricated systems the liquid volume is controlled and exchanged through inlet and outlet holes (Fig. 1.4b).

1.3.1 Open microfabricated systems

The first step towards controlling cell culture is to grow single cells or colonies of cells on protein patterns of controlled shape and biochemical composition. Protein patterns, as adhesive islands on an inert material, can be produced by stamping and spotting techniques or by applying photolithography directly on the substrate (Faia-Torres *et al.*, 2011; Falconnet *et al.*, 2006). The etching of a PLL-g-PEG coating through a mask produced adhesive patterns suitable for the culture of single cells (Azioune *et al.*, 2009), while spotting techniques can only be applied when larger islands are desired, i.e. for the patterning of cell colonies. Kuschel *et al.* used piezoelectric spotting to increase the throughput of *in vitro* cell adhesion assays, making it possible to determine different adhesive properties of 14 different ECM proteins on one single substrate (Kuschel *et al.*, 2006) (Fig. 1.4c).

Using arrays of 2D cell patterns, several relationships between extrinsic parameters and cell behaviour have been elucidated. Cell-cell contacts play an important role in proliferation of normal cells. A detailed study of this mechanism with patterns of different size for single and multiple cells showed that cell-cell contact actually promoted cell division, but only when cells were sufficiently spread (Nelson and Chen, 2002). As a result, round cells with many cell-cell contacts proliferated less than spread cells with none. Nelson *et al.* used single cell pattern of different size to show that a certain cell size was needed for EMT to occur. Restricting cell spreading prevented MMP3-induced EMT but not TGFβ-induced EMT (Nelson *et al.*, 2008b).

3D models, such as the *in vivo*-like protein matrix matrigel have been extensively used to study the influence of extrinsic parameters on mammary epithelial cells and their cancerous derivatives (Lee *et al.*, 2007). Because of the biochemical resemblance to the *in vivo* environment, the system can be used to distinguish normal from cancerous cells by their morphology and growth characteristics (Debnath *et al.*, 2003). The matrigel model has also been used as a more *in vivo* like model to study integrin-mediated resistance to radiotherapy (Park *et al.*, 2008). One problem with this 3D culture technique is that the cellular self-assembly is driven only by the cells and therefore the resulting microtissues become irregular in size and have a certain distribution in the z-direction throughout the gel, which complicates imaging.

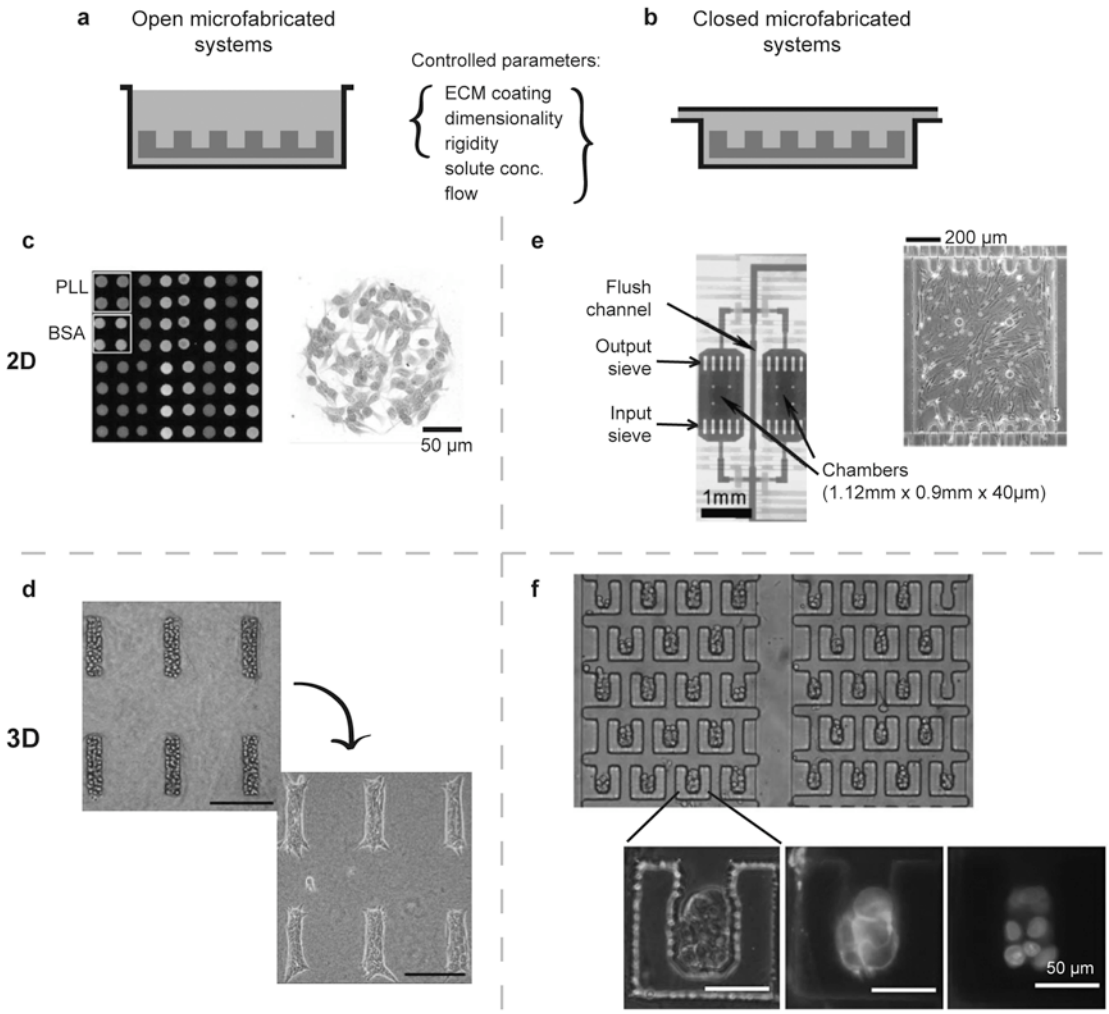

Figure 1.4: *Microfabricated cell culture models enables controlled cell culture.* Microfabricated cell culture models can be divided into two groups; open and closed microfabricated systems. a) Microfabrication enables the control of certain extrinsic parameters including ECM coating, dimensionality and substrate rigidity. b) Encapsulating the culture environment into a closed system further enables the control of solute concentration and flow. c) Piezoelectric spotting was used to increase the throughput of in vitro cell adhesion assays, making it possible to determine different adhesive properties of 14 different ECM proteins on one single substrate (Kuschel *et al.*, 2006). d) 3D cell culture can be obtained by microstructuring a protein matrix or an inert material. Here a collagen gel was microfabricated to give wells that can be filled with proteins. This model can be used to study cell branching into this *in vivo* relevant scaffold (Nelson *et al.*, 2008a). e) Closed microfabricated systems offer the possibility to individually address cell chambers on a substrate. In an automated system with electrically controlled valves, culture conditions in terms of cell density and culture medium was controlled in 96 independent culture chambers (Gómez-Sjöberg *et al.*, 2007). f) 3D culture can be facilitated inside closed microsystems by filling them with a 3D matrix or by 3D-cluster formation in wells. Using hydrodynamic trapping, cancer cells formed clusters with a very homogenous size distribution inside a device (Wu *et al.*, 2008).

To develop this model towards more high-throughput applications, soft lithography was used to microfabricate 3D matrigel circular structures with diameters of 100µm (Sodunke *et al.*, 2007). Single cells were then seeded onto the posts by matching cell density to the number of posts. With this novel platform it was possible to reduce the size polydispersity of the cell colonies, thereby reducing the number of variable parameters and ease imaging. While this approach is based on single cell seeding and needs several days for microtissue formation, Nelson *et al.* developed a method to obtain controlled cluster formation within a day after seeding. They also used soft lithography, but instead to produce microwells within a collagen I matrix (Nelson *et al.*, 2008a) (Fig. 1.4d). After seeding of mammary epithelial cells into thes cavities, microtissues with the size and shape determined by the design of the microwells were obatined. With this platform it was possible to show that cell branching is affected by the local geometry of the tissue (Nelson *et al.*, 2006) and further by biochemical signaling from the surrounding ECM (Pavlovich *et al.*, 2010). Such information is relevant for the control of invasion and metastasis. This shows another application for culture systems with controlled physical and biochemical cues, namely in the development of drugs aimed at the inhibition of metastasis and endothelial cell branching, important processes in tumour vascularisation. A drawback of the fabrication method used in this system was that the scaffold material was ECM based, thus allowing cell migration out of the cavities and consequently a collagen lid on top of the cavity was required.

A successful strategy to spatially control the position of microtissues in an array is therefore to culture cells in microwells surrounded by non-adhesive areas. Platforms based on this principle have been extensively investigated in our research group using microwells produced in PDMS (Ochsner *et al.*, 2007) (Ochsner *et al.*, 2010) and by Lütolf *et al.* in a PEG-hydrogel (Lutolf *et al.*, 2009). Such platforms provide flexibility in the biochemical interface presented to the cells, as the substrate used to fabricate the microwells can be coated with many different proteins.

With these examples we can show that open microfabricated cell culture arrays offer the advantage of greater control of the biochemical and physical culture environment. However, one disadvantage of the open format is that the microwells or spots in an array cannot be individually addressed to allow the application of different combinations of cells and drugs to specific spots. Hence, even though these open cell arrays contain a high number of experimental units with controlled environmental conditions, the full multiplexing potential of the array cannot be used. The problem with addressability has been innovatively solved by Lee *et al.* (Lee *et al.*, 2008). They used stamping to transfer the drugs spotted on one chip to specific areas of a micropatterned cell chip. Such combination of microfabrication and spotting may be a

promising approach even though there may be issues with the control of the final drug dose and the avoidance of cross-contamination in rinsing steps.

Addressability can also be added by the direct spotting of sample into larger microwells. A recent publication used robotic dispensing to spot a large range of plasmid-DNA on an array before cell seeding (Pla-Roca *et al.*, 2010). However, because the volume of each microwell on this chip was only 1 nl, it would have been very difficult to handle cell seeding in the same way and therefore cell culture was performed covering the whole chip with the cells suspension. Cross-contamination can only be avoided in this approach if the DNA is trapped on the substrate, e.g. in a protein matrix.

In summary, open microfabricated models show advantages in comparison to standard well-plate system as the adhesive and physical environment can be controlled at the micrometer range. This enables the creation of *in vivo* like culture conditions to study, for example, metastatic outgrowth. Furthermore, increased reproducibility is expected, as each sample contains repeated units of controlled culture conditions. Finally we discussed different possibilities to use open systems to increase throughput of standard assays by multiplexing.

1.3.2 Closed microfabricated systems

One advantage of using closed microfabricated system is that cells cultured in an array can be individually addressed without risking cross-contamination. This can be obtained by placing several channels in parallel over the substrate or by using a laminar flow. Laminar flow can easily be created in a microsystem because of the small dimensions and has been used to create concentration gradients over cultured cells and to avoid the mixing of adjacent solutions (Takayama *et al.*, 2001). Electrically or flow-controlled valves (Gómez-Sjöberg *et al.*, 2007) can be used to create a complex network of microchannels with automatic control of a series of additions and rinsing steps (Fig. 1.4e). Hence, these properties can be used to independently test the effect of a multitude of drugs and soluble factors on an array of cells.

Several groups have shown that 3D culture can be realized within a microchannel, simply by filling the channel with the desired gel forming material, such as matrigel, collagen or a synthetic peptide-based material (Choi *et al.*, 2007) (Lii *et al.*, 2008). An advantage of performing 3D culture within a closed system is that the concentration of secretion factors and metabolites can be controlled due to the small liquid volume and by means of controlled flow. Kim et al showed that the growth of cancer cells within a matrix in a microchannel increased their viability compared to in matrix alone, which may be explained by more *in vivo* like solute concentrations (Kim *et al.*, 2007). Choi *et al.* presented a model for the precise and cell-number corrected control

of metabolite concentration within a 3D scaffold (Choi *et al.*, 2007). This model was obtained by a combination of flow simulation and an empirical method based on fluorescence recovery after photobleaching.

The level of fluid exchange in the vessels and within the interstitial space determines drug uptake. Therefore, 3D scaffolds embedded within microchannels with controlled flow characteristics can serve as tools to investigate the tissue penetration of drugs. One example is a matrigel-filled microsystem, which was used to study the penetration of novel nano particles, with respect to particle size and the presence of interstitial fluid (Ng and Pun, 2008). In a particularly interesting application, 3D culture was combined with controlled flow characteristics to create an *in vivo* relevant organization of different tissues for pharmacokinetic and pharmacodynamic studies. In short, culture chambers in a connected circuit were used to culture colon cancer cells, liver cells and myeloblasts (Sung and Shuler, 2009). Optimization of the size of the culture chambers and using controlled flow enabled the creation of residence times in the different compartments similar to the residence times in the respective organs *in vivo*. The potential of this platform was shown in a feasibility test, in which Tegafur showed cytotoxicity even though this is only a prodrug to 5-fluorouracil, i.e. was metabolized within this model in the same way as *in vivo*.

The combination of an encapsulated compliant material with flow comes with a number of practical difficulties, including how to perform cell loading, mass transfer limitations and added operational complexity. A favourable approach to circumvent these issues relies on the inclusion of a 3D environment for cells directly in the design. One possibility is to integrate pillars in the channel design. This environment induces cells to grow with a 3D morphology (Ong *et al.*, 2008). Another strategy is to use u-shaped cell traps within a channel to create a high number of cancer cell clusters within a narrow size range. Wu *et al.* used hydrodynamic trapping of cells into 35 x 70 x 50 μm large traps (Wu *et al.*, 2008) (Fig. 1.4f). After optimization of the flow, the system could be used to create cell clusters with 10 cells per clusters with a very narrow size distribution.

In summary, closed microfabricated systems not only offer the opportunity to perform several assays in parallel for increased throughput but they also allow the precise control of the microenvironment with an emphasis on flow characteristics, even in 3D cultured cells. Hence, with these models it is possible to mimic an *in vivo* like solute exchange, which is one of the important factors in the creation of in vivo like culture conditions. In addition, this characteristic makes such models suitable for the development of drugs and drug carriers that have improved tissue penetration and retention characteristics.

1.4 Read-out of cell-based assays in microfabricated systems

1.4.1 State of the art in standard cell-based assays

In high-throughput screening, solution-based assays measuring metabolism and cytotoxicity are still standard (Niles *et al.*, 2008). A disadvantage of determining differences in solution is that the measured response is an integrated signal over the whole cell population. A favourable approach, which is increasingly used in anti-cancer drug discovery, is therefore the evaluation of cell behaviour using imaging (Tanaka *et al.*, 2005). An image-based readout can produce information on the sub-cellular level and therefore provides more detailed information on cell death in response to treatment and further to the mechanism of the drug.

Imaging can be used to detect apoptosis by measuring changes of cell and nuclei morphology or using fluorescent markers to determine membrane permeability, mitochondria membrane potential (MMP) and caspase activity. As apoptosis is a complex process with several pathways involved, a multiparametric evaluation of cell behaviour is desirable. This is called high content screening, a method that is already used in the drug industry to obtain a more reliable output (Lang *et al.*, 2006) (Fig. 1.5). An example of the multiparametric measurement of apoptosis was presented by Lövborg *et al.* (Lövborg *et al.*, 2004). In their work it was clear that different read-outs gave different information on the apoptotic death of the cells (Fig. 1.5). In particular, it was found that nuclear fragmentation, consistently over five drugs, gave an earlier signal of apoptosis than caspase-3 activity, while MMP activity in some cases did not change at all with apoptosis.

1.4.2 Challenges and opportunities for microscopy-based readout in microfabricated systems

Microfabricated systems are typically very well suited for image-based read-outs, as their dimensions allow the whole sample depth to fit within the focus depth of a normal objective. There are several transparent materials suitable for microscopy that can be microfabricated, such as polystyrene (Dusseiller *et al.*, 2005) and PDMS (Younan and Whitesides, 1998). To measure cytotoxicity and apoptosis in cells within microfluidic systems, several different assays that rely on simple staining procedures have been used, such as the LIVE/DEAD assay, which measures membrane permeability (Wang *et al.*, 2007), or the Annexin V binding assay, which measures reorganization of lipids in the cell membrane (Reif *et al.*, 2009). In microfabricated systems that are compatible with high-resolution imaging, cell responses can be evaluated using high content screening. Ye *et al.* used rhodamine123, Hoechst and propidium iodide to assess several parameters of cell death in parallel within a gradient device for anti-cancer drug testing (Ye *et al.*, 2007).

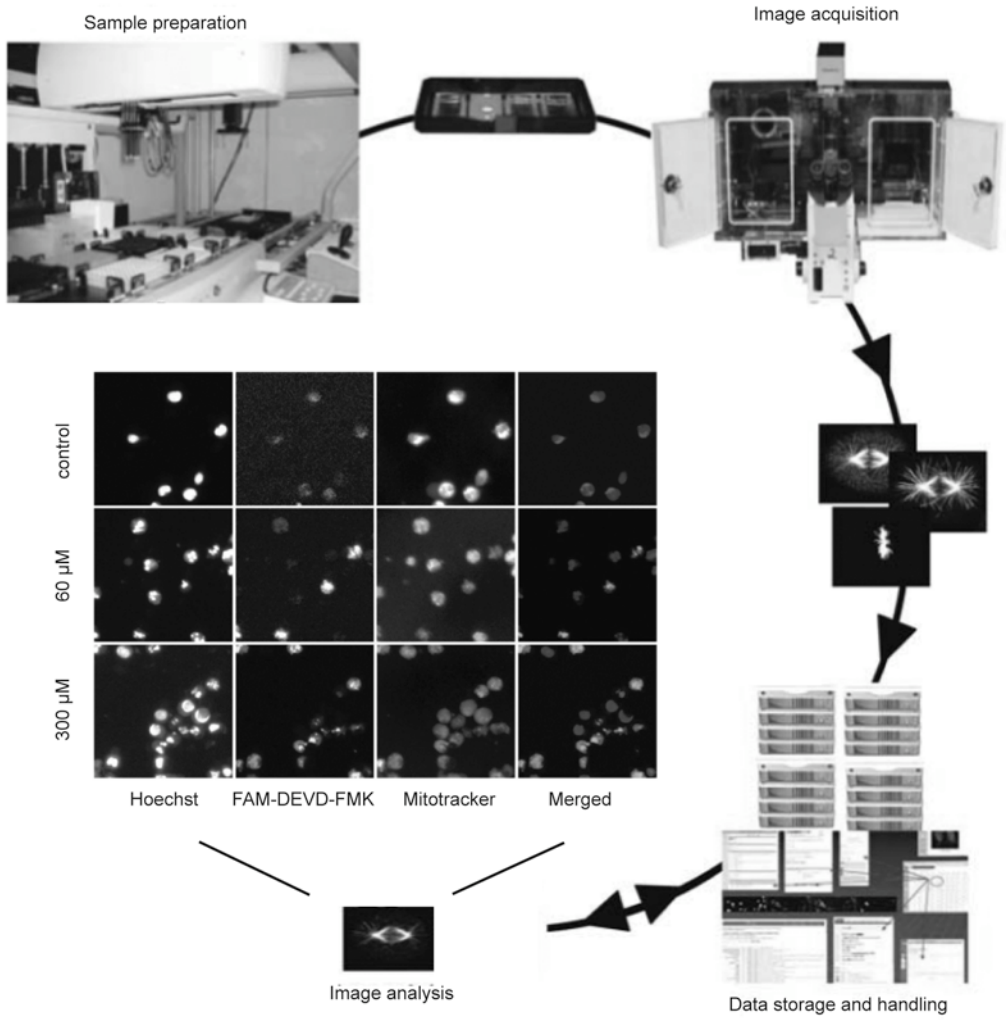

Figure 1.5: *High content screening in anti-cancer drug development.* High content screening is an information rich microscopy-based method to analyze cell assays. With subcellular resolution and using the plethora of dyes available today a multitude of parameters can be obtained per sample. Hence, this high-content screening gives a more complete picture of, for example drug response. High throughput high-content screening can be obtained by automating all steps in the process, from sample preparation to image acquisition to data storage and handling and image analysis. Image processing is central in this process and needs to be adapted for each new assay. Therefore it currently is the bottleneck of the technology.

The middle image shows an example images from an approach to determine the response to Etopside after 24 h treatment of in U-937 cells by multiparameteric evaluation of apoptotic signals. The nuclear fragmentation is determined by Hoechst-staining of the DNA, caspase-3 activity is determined by FAM-DEVD-FMK labeling and mitochondria activity is determined by Mitotracker. The figure is adapted from (Starkuviene and Pepperkok, 2007) with an insert from (Lövborg *et al.*, 2004) showing the three different stains for apoptotic cell death.

Challenges

The study of cell death within cells patterned in a 2D array is complicated by the fact that dying cells loose adhesion, round up and eventually leave the adhesive pattern. Therefore, in this situation not all cells originally residing in a certain area will be included in the end point measurement, which may complicate the interpretation of the results. This is also a problem that occurs in solution-based assays, particularly when a rinsing step is required, and is hence an inherent associated with 2D substrates, rather than the read-out. For such platforms, the possibility to detect apoptosis at an early stage would be beneficial. However, the assays most commonly used to measure cytotoxicity monitor late apoptosis or even necrosis (Martinez *et al.*, 2010).

Assays that do detect early stage apoptosis typically assess changes in the mitochondrial membrane potential or the activation of caspase pathways (Wu *et al.*, 2003). Novel assays based on initiator caspases could be promising for use in patterned cell assays. Kasili et al described an enzyme- based optical sensor that detected the cleavage of caspase-9 (Kasili *et al.*, 2004). While many apoptosis detection agents require fixing of cells, new developments, such as the Yo-Pro nuclear stain, can be used for continuous monitoring of apoptosis (Gawlitta *et al.*, 2004) (Muñoz-Pinedo *et al.*, 2005). Another innovative method allows for time-lapse apoptosis monitoring by the use of wavelength-dependent backscattering measurements to distinguish alive from apoptotic cells (Mulvey and Sherwood, 2009).

As we have discussed, modelling the cancer-specific microenvironment *in vitro* typically requires the implementation of 3D cell culture. This sets a new demand on fluorescence-based readouts. Confocal microscopy can be used to image samples that have a multicellular structure while maintaining single cell resolution (see Chapter 6 for details on this approach). Quantitative analysis of cell death can be obtained by measuring the integrated intensity of a 3D culture with low-resolution wide-field imaging or a microarray scanner (Lee *et al.*, 2008), although information at the single cells level is lost.

A 3D culture system optimal for microscopy-based read-out should allow for alignment of the cell cultures in the z direction. In addition the scaffold thickness should be minimized, as tissue or scaffold density hampers fluorescence detection (Paris and Sesboue, 2004). Strategies to optimize the image quality of thicker samples include the use of an optimal objective with correction collar to correct for spherical aberration, the use of multi-photon excitation and the employment of quantum dots that emit light in the near-infra red region, which has a greater penetration depth in tissue (Michalet *et al.*, 2005).

Opportunities

There are several examples of how microfabrication can lead to the development of new methods to read-out cell behaviour. By microfabrication, protein islands or physical traps in the size of single cells enables single cell analysis on a substrate (Lindstrom and Andersson-Svahn, 2010). Another application is the analysis of cells in suspension, cell samples that are otherwise restricted to fluorescence activated cell sorting (FACS) analysis. The simple principle is that the height of channel within a system can be designed to be within the focus depth of the optical system used, making it possible to analyze all cells within a certain volume.

Recently, a new substrate for microscopy-based read-out of the response to cytoskeleton-affecting anti-cancer drugs was presented. The idea was that cell morphology changes would be easier to detect in cells growing in etched 3D silicone microstructures compared to in cells on a 2D substrate. Indeed, after treatment with an experimental anti-cancer drug, suberoylanilide hydroxamic acid (SAHA), cells stretched and attached to the microstructures through actin-rich cell extensions, while control cells conformed to the microstructures (Strobl *et al.*, 2010).

An apoptosis assay that does not rely on high-resolution microscopy is the comet assay, which is used to quantify fragmented DNA. The original assay is tedious to perform, as drug treated cells first have to be removed from the substrate, then separated into a single cell suspension and finally placed in an agarose gel. Recently, microfabrication has been used to create an improved comet assay (Mercey *et al.*, 2010). In this innovative approach an agarose gel was patterned by deep-UV light to form microwells that was further functionalized with matrix protein to allow for cell culture. This array shows great promise, as it combines 3D cell culture and quantitative toxicity measurement. It can be concluded that not only can most standard microscopy based assays for cell analysis be adapted for application in a microfabricated system, miniaturized cell culture and handling can also enable the development of new methods for analysis.

1.5 Adaptation to automatic handling systems

In order for the described methods to find wider use it is important that they can be integrated into already established experimental platforms. One way to do this is to adapt the new methods for a standard well plate format that can then be handled in an automatic setup to exchange liquid, seed cells and perform read-outs. Meyvantsson *et al.* elegantly integrated their passive pumping channels into a 96-well plate format (Meyvantsson *et al.*, 2008) (Fig. 1.6a and b). These channels have some of the advantages already discussed in this review, including a small cell culture volume to control solute concentrations and ability to mimic *in vivo* environmental conditions.

The device can be operated for 2D culture or filled with a protein gel for 3D culture conditions, with or without flow. Recent results showed that this platform could be used for high content chemotaxis experiments with a 50-fold throughput compared to conventional assays (Berthier *et al.*, 2010).

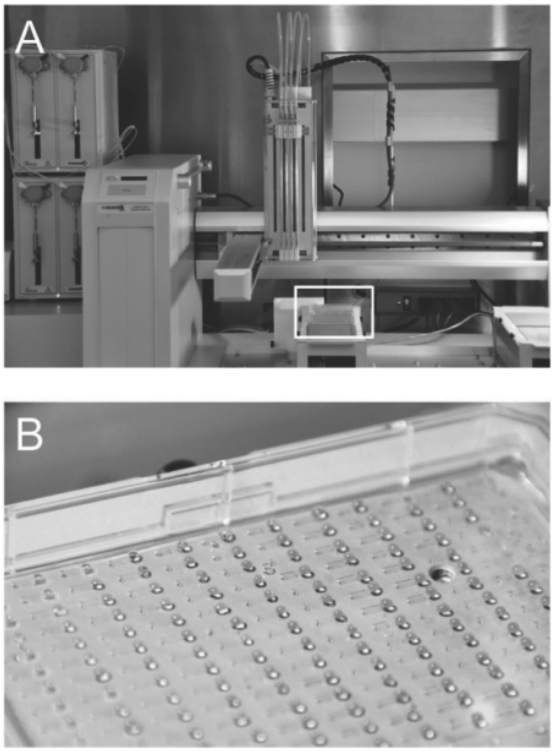

Figure 1.6: *Adaptation of microfabricated models to automatic handling systems.* In order for microfabricated cell culture platforms to find use outside of the academic community they need to be adaptable to standard methods, such as automatic liquid handling and imaging. In figure (a) a microchannel plate fabricated in a standard plate format (white box) is filled in an automated liquid handling system (Gilson Quad-Z 215 Liquid Handler, Middleton, WI, USA). In (b) an overview of the array with 192 microchannels in a standard microtiter plate format is shown. Straight microchannels contain access ports to allow passive pumping. The image is from (Young and Beebe, 2010).

Arrays of micropatterns to control the adhesive area of cells and ECM interface is another technique that can be easily integrated into a multi-well format. Furthermore, the arrayed format allows for easy automation of the imaging, as the positioning of the cells on the sample is known by the design of the array. While pattern generation by microcontact printing has been widely adapted in experimental biology, this method is less suitable for patterning over large areas and for the generation of stable patterns for long term studies (Fink *et al.*, 2007). Reproducible fabrication of adhesive patterns over large areas, that show pattern integrity over time, can be generated by microspotting (Flaim *et al.*, 2005) or by a photolithographic process, etching holes in a PLL-g-PEG coating with UV light through a mask (Azioune *et al.*, 2009).

The newly founded company Cytoo SA recently presented a product with single cell patterns based on this technology. One application of such a product would be to detect drug response at very low drug concentrations and cell number. As drug-promoted changes to the intracellular organization show very low variability between cells on patterns with the same shape (Schauer *et al.*, 2010), a reduced number of cells are needed for read-out.

1.6 Particularly promising applications of microfabricated systems

1.6.1 Combinatorial analysis of microenvironmental factors and drug treatment

Microfabrication of cell culture systems offers the possibility not only to do combinatorial testing of different drugs, but also to investigate the combinatorial effect of a drug with extrinsic microenvironmental parameters. Parameters of the microenvironment that can affect drug response include ECM composition, growth factor concentrations, and paracrine signaling (Meads *et al.*, 2009). While the high control of the extrinsic parameters facilitates this application, the miniaturized format increase the relevance of such systems as primary or patient-derived cells may be used. Additionally, closed microfabricated systems can be used to study the influence of paracrine signaling in a combinatorial assay.

There are several examples of how open cell arrays have been used to study the combinatorial effect of ECM components on cell responses. One of the first examples of an ECM array was presented by Flaim *et al.* (Flaim *et al.*, 2005). They used a DNA spotter to spot collagen I, -III, -IV, laminin and fibronectin in different combinations. This array was used to study stem cell differentiation, although a range of applications could be imagined, including the study of ECM-specific drug response in cancer. An array, produced by a similar technique, was used to test the role of different protein combinations in the niche of mammary progenitor cells (Labarge *et al.*, 2009) (Fig. 1.7a). They also investigated the role of E-cadherin by comparing cell behaviour directly after seeding and after 24 hrs, thus allowing enough time for the formation of cell-cell contacts.

In closed microsystems it is possible to combine the investigation of immobilized factors with solutes in a combinatorial setup. Liu *et al.* investigated the role of co-culture with hepatocellular carcinoma cells on the migration of fibroblasts (Liu *et al.*, 2010). This experiment is relevant for the understanding of the role of cancer – stroma interaction in cancer progression. In the presented design, a high control of the co-culture enabled the separation of different parameters in a time-dependent manner, to independently and in combination study the effect of cell-cell contacts and inter-cellular signaling. The findings show that fibroblast motility is increased by hepatocellular soluble signals. In addition, this behaviour is concentration-dependent as well as dependent on the time of stimulation after culture initiation. These results could be obtained with a high time-dependent accuracy, which may have been difficult in a standard 2D culture.

Another device was designed to study the effect of extrinsic factors on epithelial-mesenchymal transition (EMT), which is important in metastasis (Park *et al.*, 2010). This device was designed so that the streamline that passed through a particular

chamber did not pass through any other, thus avoiding cross-contamination. In a feasibility experiment the EMT of alveolar epithelial type II cells in response to pairwise combinations of immobilized (laminin and fibronectin) and soluble (TGF-β1) factors was studied (Fig. 1.7b). The epithelial vs. mesenchymal phenotype was characterized in images showing cell morphology and E-cadherin localization. In this work it was shown that fibronectin alone induced an elongated phenotype, while Lam alone induced an epithelial morphology and showed elongated cells first in combination with TGF-β1. These results are consistent with what has previously been shown using more traditional methods (Kim *et al.*, 2006).

There are numerous examples of how microfabricated systems have been used to screen the effect of the combinatorial application of drugs on cells. Combination therapies are used to enhance the potency of a drug and are widely applied in the treatment of cancer (Dancey and Chen, 2006). Liu *et al.* showed the use of an integrated combinatorial mixer to test the combination of three chemotherapeutics on a metastatic breast cancer cell line cultured in the device (Liu and Tai, 2011) (Fig. 1.7c). Synergistic effects of the two anti-cancer drugs vinorelbine and paclitaxel were observed, in addition to increased cell death when one of these drugs was used together with γ–lineolic acid. However, combining the three drugs did not give a significant death increase. These results are in agreement with what has previously been observed in vitro (Menendez *et al.*, 2002) and in the patient (Chang and Garrow, 1995).

In conclusion, the controlled culture conditions in both open and closed microfabricated models can be advantageously used for combinatorial studies of microenvironmental factors and drug treatment. In contrast to conventional experimental models, the microfabricated setup allows higher throughput because several conditions can be tested per chip and the higher control of the culture conditions enables the separation of different extrinsic parameters in a space and time-dependence manner.

1.6.2 Detection and analysis of cells from patients

An area in which microfabricated systems could be particularly beneficial is in the analysis of cells from patient samples. One reason why the efficiency of cancer treatment still remains low is that the success of treatment varies greatly between patients, even within groups that have a similar diagnosis. Failure of treatment of cancer patients is highly undesirable as chemotherapeutic drugs typically have strong side effects and prolonged treatment can lead to drug resistance (Shain and Dalton, 2001). Today, cancer patients are treated according to general guidelines, but because of the heterogeneity in cancer (Kamb *et al.*, 2007) the goal must be to develop

diagnostic tools that allow for patient-specific treatment. In extension, our increased knowledge about the effect of a certain microenvironment on cancer could make it possible to diagnose patients to receive a tumour cell- and stroma microenvironment-specific treatment (Rønnov-Jessen and Bissell, 2008).

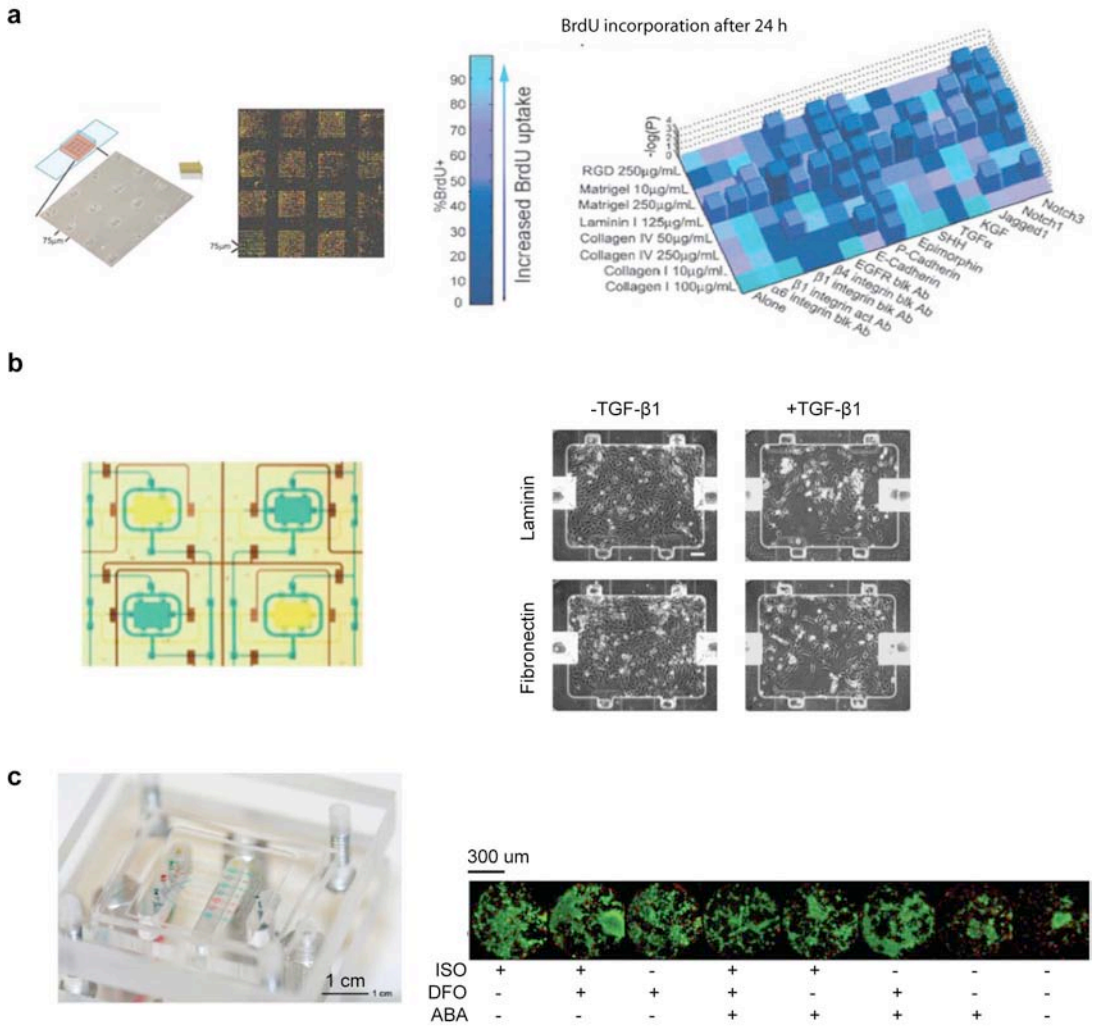

Figure 1.7: *Microfabricated platforms for combinatorial analysis of microenvironmental parameters and drugs.* a) Screening behaviour of mammary progenitor cells on an array of ECM proteins created by a printing on a microarrayer. At the end of the assays cells were stained with BrdU to monitor cell proliferation. The intensity of the BrdU stain relative total DNA versus adhesion protein is plotted in the bar graph. (Labarge *et al.*, 2009) b) A closed microfluidic system enables wells on a substrate to be continuously individually addressed. In this example the role of matrix interface in combination with soluble factors on epithelial-mesenchymal transition was investigated (Park *et al.*, 2010). c) A microfluidic device with a combinatorial mixer for testing of combinations of the three drugs; 1,5-dihydroxyisoquinoline (ISO), deferoxamine (DFO), and 3-aminobenzoic acid (ABA). The fluorescent image shows the live (green) dead (red) staining of cells in the chambers after treatment (Liu and Tai, 2011).

This problem can be tackled on several levels. On the one hand, there is a lack of reliable methods to predict the treatment outcome in a patient that can be used in the clinical practice (Shi *et al.*, 2008). In order to improve on this point we need to obtain a greater understanding of the mechanisms that determine drug sensitivity in cancer and normal cells and define markers that can provide improved prognostic information.

On the other hand, a complementary strategy is to develop reliable and cost-effective *in vitro* assays that can be used to acquire dose-response profiles of drugs on patient cell samples (Trusheim *et al.*, 2007). For this purpose, microfabricated systems may play an important role, as they offer a unique opportunity to handle and analyze samples with small cell numbers. Typically, there is only a limited supply of patient cells. If the cells are not explanted during surgery they normally have to be recovered at very low concentrations from blood or a biopsy.

Characterization and dose-response measurement of patient cell sample

In the future, ECM arrays used for combinatorial drug tests could be applied for detection of cancer phenotype and predict treatment in the patient. ECM arrays are not novel and have conventionally been performed in multiwell plates, presenting a different ECM coating in each well. Thanks to miniaturization they have found completely new applications. Kuschel et al applied piezoelectric spotting to increase the throughput of an ECM array. With optimized seeding conditions, only 500 cells per array was required and different adhesive properties for 14 different proteins were detected (Kuschel *et al.*, 2006). Hence, a miniaturized ECM array would be suitable for the analysis of patient cells, for example from biopsies.

Ganser *et al.* described a diffusion device, produced in a closed system, as an advantageous tool for personalized medicine (Ganser *et al.*, 2009). This device uses a diffusion gradient to obtain different drug concentrations over the cells. In the presented prototype only two pipetting steps were necessary to test all relevant combinations of two drugs on the cell samples. Furthermore, it was shown that only 3 $\times$ 10^6 cells primary leukemia cells were required to determine the dose response curves. This enabled the analysis of patient samples on this platform; typically around 10^8 cells are obtained from a patient with hematologic malignancy. An EC_{50} value close to the plasma concentrations reached in the clinic was obtained, hence the presented approach compared favourably with clinical concentrations.

Oncogenic kinase activity is a common driving force of cancer and hence an important diagnostic marker. Standard radiometric ^{32}P-ATP-labeled phosphate transfer assays are however not suitable for the diagnostic read-out of patient samples as millions of cells are needed per assay. In contrast, adaptation of this assay into a miniaturized system, the critical cell number was reduced to 3000 with maintained

signal-to-noise ratio (Fang *et al.*, 2010) (Fig. 1.8a and b). This therefore could become a promising diagnostic tool.

Using an image-based read-out with single cell resolution, the cell number needed per assay could be reduced even more. Wlodkovic *et al.* used hydrodynamic trapping to capture single hematopoietic cells in low shear stress zones and subsequently quantified anti-cancer drug-induced apoptosis. Using a simple assay based on Cytox green and propidium iodide nucleic acid labeling dyes, they obtained results from the analysis of only 300 cells with a similar statistical spread to that obtained in larger populations (Wlodkovic *et al.*, 2009).

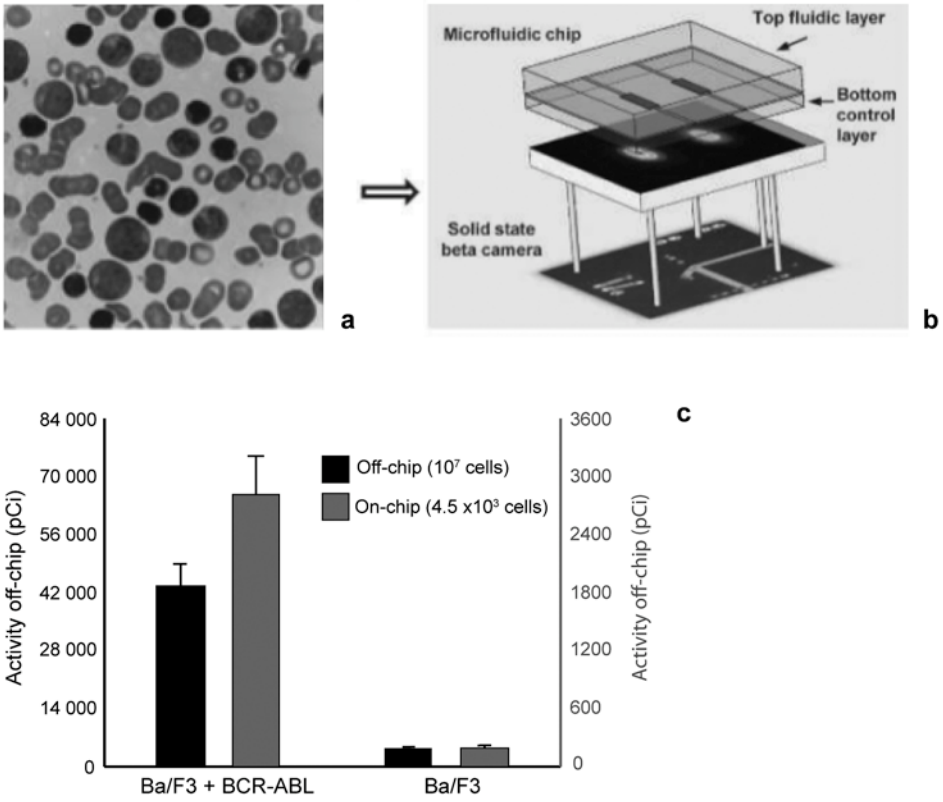

Figure 1.8: *Miniaturized cell culture systems enable the analysis of patient sample.* A kinase activity assay can be used to diagnose cancer cells. By miniaturization of this assay only 3000 leukemia cells (a) were needed to obtain a good signal from the assay in a microfabricated system (b). Hence, with this approach the diagnostic technique can be used directly on small patient cell samples. The miniaturized assay showed maintained reliability compared to when performed in a standard format (c). (Fang *et al.*, 2010).

Detecting circulating tumour cells in patient blood sample

A critical area of patient sample analysis is the detection of circulating tumour cells, which constitute a predictive signal of intractable metastatic disease (Steeg, 2006) (Pantel *et al.*, 2009). However, the lack of good methods to facilitate the detection has hindered the spread of this tool in the hospitals. An optimal tool would catch the specific tumour cells from the blood with high specificity and allow for subsequent

analysis by, for example PCR. The information about the expression-levels of certain cancer-specific proteins can help to predict treatment (Fehm *et al.*, 2007). Recently, microfabricated flow systems has shown promise as alternative systems with isolation efficiencies of cells in blood up to two orders of magnitude greater than conventional methods, such as FACS (fluorescent activated cell sorting) (Nagrath *et al.*, 2007) (Gleghorn, 2010).

In conclusion, there are many examples of how cell assays can advantageously be miniaturized for experimentation of patient cells without affecting the accuracy of the read-out. The next step would be to show that the measurement of dose-response curves in patient samples indeed improves the predictivity of the response to therapy. Furthermore, the characterization of patient cells in miniaturized systems by the use of novel predictive markers, can help in the cancer diagnostic and thereby also enable tailored treatments. Circulating tumour cells are strong predictors of certain types of cancers. Promising results show that sophisticated microfabricated systems can be used to capture these cells from very low concentration in whole blood.

1.7 Conclusions and Outlook

As summarized in this introduction chapter, the activities among interdisciplinary research groups active in the field of miniaturization have resulted in a large number of novel *in vitro* models for the handling and analysis of cancer cells. Much effort has been expended on the improvement of the technical qualities of these systems, such as advanced channel systems for improved control of the culture environment and the positioning of cells, as well as innovative methods for assay read-out. What has been missing for many years are examples of the application of these systems and the overall impact of microfabricated systems on modern biology, which continues to be marginal (Young and Beebe, 2010).

Here we show several examples of how these systems can be applied in cancer research as advantageous platforms over conventional methods. Initially it is shown how microfabrication can be used to better control the culture environment in terms of the biochemical coating and positioning of cells but also solute concentration. The controlled culture conditions not only enable the creation of an *in vivo*-like culture environment but also make it possible to elucidate the role of certain extrinsic parameters. This opens up for the combinatorial testing of microenvironmental conditions with drug exposure parameters that can be useful in drug development and especially in the development of novel treatment strategies targeting the microenvironment. In addition, the miniaturization approaches explained here make it possible to analyze small cell samples with retained accuracy. Thereby, there is a high

potential for these systems as methods for patient cell analysis, which would enable tailored treatments.

Many of the systems presented in this chapter, were developed with the motivation to find application in the clinic and pharmaceutical industry. Still, there are only a few researchers that focus on the realization of this translation to practise. This problem is especially true for the closed microfabricated systems, while open microfabricated systems have found a wider use. This can probably be attributed to the different levels of complexity of the two systems. While closed microfabricated systems often requires a complicated setup of pumps and optimization of imaging techniques, open microfabricated systems can be applied without additional equipment and more easily be integrated into conventional multi-well dishes for use in robotic handling setups. The general requirements that these systems must meet for broader application, is a major improvement compared to a conventional cell-based assay and further that they are easy to handle by people that are not specialized in the use of miniaturized assays. In addition, there must be a way to calibrate the output of the new system to that obtained by conventional methods, on which many laboratories already have a vast pool of data.

Hence, it can be predicted that open microfabricated systems, such as microwell arrays for 3D culture and ECM arrays for combinatorial drug testing, will find application in the near future. Conversely, closed microfabricated systems still need to be improved for adaptation by the cancer drug development community. Understanding in which applications such methods may be most beneficial is a challenging task. To tackle this problem we need researchers who bridge the specialized fields from developing relevant cell culture models and microfluidic tools to clinical researcher and engineers in industry to jointly search for solutions that fulfil the key requirements of the device-producing industry and clinical practice.

CHAPTER 2

Scope of the thesis

Background

Cancer drug development and diagnosis methods suffer from a low success rate in terms of predictivity of *in vivo* efficacy. The impediment to predictable cancer therapy lies in the heterogeneity of the disease, the occurrence of resistance and the difficulty of finding targets that are specific to cancer cells. A factor that makes the drug development process inefficient is the lack of relevant experimental models.

The development of more specific drugs would greatly profit from models that have a higher *in vivo* relevance. The properties of the cancer microenvironment have been shown to influence treatment, both indirectly, by affecting drug uptake and directly by active signaling from cells and proteins in the environment. Today, it is well accepted that cancer is not just caused by genetic mutations but that cancer progression is also greatly affected by interactions with the microenvironment. Fundamental cancer biology research has used *in vivo*-like culture models to study cancer progression for over a decade. Currently, there is a focus on starting to use more *in vivo*-relevant models also in cancer drug development.

Many studies have explored how extrinsic parameters, such as matrix coating, dimensionality of the culture environment and cell-cell contacts affect the response to anti-cancer treatments. However, the *in vitro* models that were used in these studies were typically either too simple or too complex to reveal the role of different extrinsic parameters on drug response in an *in vivo*-relevant environment. Simplistic models, e.g. the culture of cells on different proteins coatings on flat substrates (Aoudjit and Vuori, 2001), can enable the separation of the role of different parameters. However, the results from these models may have a low relevance for *in vivo*. On the other hand, complex models, such as cancer multi-cellular spheroids, successfully mimic some crucial aspects of the *in vivo* environment (Friedrich *et al.*, 2007). However, with these models it is difficult to separate the effect of the different extrinsic

parameters. Microfabricated models, which enable *in vivo* 3D culture but with controlled extrinsic parameters may therefore prove to be a useful alternative.

With microfabricated cell culture models, it is possible to engineer the microenvironment on the scale of single cells, thereby also enabling single cell studies. On the single cell level, fundamental information about the cell-microenvironment interactions may be revealed, that can in turn help to explain the tissue behaviour. Precise control of cell shape and the cell adhesive area makes it possible to study the role of cell shape for cell behaviour in a 3D environment (Ochsner *et al.*, 2010). In addition, controlling the position of single cells by microfabrication makes it possible to study the effect of single versus multiple cell-contacts (Nelson and Chen, 2002).

On the other hand, a multi-cellular system represents a more *in vivo*-like environment, as most cells exist within tissues composed of multiple cells. Many processes, such as tissue morphogenesis and cancerogenesis, depend on the signaling from multi-cellular contacts (Nelson and Bissell, 2005). Therefore, multi-cellular model systems are required for studies were tissue-relevance is important, for example in the evaluation of new drugs.

Objectives and Scope

The overall objective of this thesis was to establish novel *in vitro* culture models based on efficient microfabrication, replication and surface functionalization techniques that can be used to study the effect of microenvironmental parameters on drug response to cancer cell cultures in both a single-cell and cell-cluster array format. Hence, such models may find future application both in fundamental cancer research and in drug screening and development. The thesis covers four interrelated results & discussion parts presented in Chapters 4-7.

Two previously developed microfabricated models were used in this thesis, to cover both the study of single cells and multi-cellular clusters. For the study of single cells and cells with a few cell-contacts we used a microfabricated PDMS-based microwell platform (Fig. 2.1.I) that was previously developed in our lab (Dusseiller *et al.*, 2006) (Ochsner *et al.*, 2007). This platform has been used for fundamental studies of the role of dimensionality and substrate stiffness on cell survival, actin fiber formation and fibronectin rearrangement in single cells (Ochsner *et al.*, 2010). To transfer into multicellular clusters, a PEG hydrogel-based microwell array (Fig. 2.1.II) was used. This platform was originally established in the laboratory of Prof. Matthias Lütolf (Lutolf *et al.*, 2009) for the study of stem cell differentiation.

In part 1 of this work (**Chapter 4**), a new fabrication protocol for the production of the established PDMS microwell platform was developed with the objective of providing sufficient stability for application in longer-term cell culture assays ranging up to a week. The previous strategy to present an adhesive / non-adhesive contrast on the microwell array was based on the inverted micro-contact printing of PLL-g-PEG (Dusseiller *et al.*, 2005). In work with mesenchymal stem cells, this original strategy produced patterns, which were insufficiently stable for longer culture times. Therefore, we sought of an alternative patterning strategy based on the use of a PEO-PPO-PEO triblock copolymer (Pluronics) as a non-fouling coating applied to unmodified (hydrophobic) PDMS. In a collaborative project with Markus Rottmar and Katharina Maniura at Empa St. Gallen the quality of the new patterning strategy for mesenchymal stem cell patterning was investigated (cell culture tests were performed at Empa).

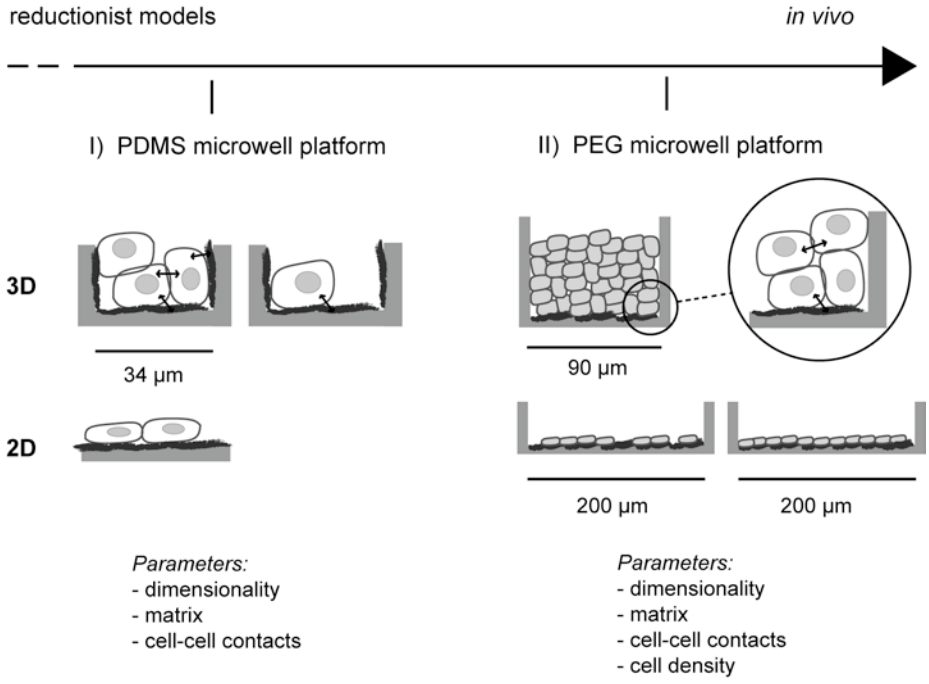

Figure 2.1: *Overview of the microfabricated platforms used in this thesis and the microenvironmental parameters that were investigated with respective platform.* I) The PDMS microwell array is a reductionist model that can be used to study single cells to small clusters of cells. II) The PEG microwell array platform was used to create a more *in vivo*-like model of early cancer, by culturing cells in multicellular clusters. Using the same technology to create 2D collagen patterns, the role of cell density on cell behaviour could be studied.

In part 2 of this work (**Chapter 5**), this platform was employed for the culture of MCF-7 breast cancer cells and to conduct a first series of drug testing experiments using Taxol as a well established anticancer drug. The main advantage of the PDMS microwell array is that it allows for the independent investigation of the effect of multiple extracellular stimuli on cell behaviour and function.

It has already been shown *in vivo* and in more complex 3D models that extrinsic cues play an important role in cancer progression and drug response. Therefore, we found it interesting to see if these factors would have an effect on drug response also in our reductionist model. Furthermore, with a high control of extrinsic parameters we thought to explore the interrelationship between these parameters. To preserve the envisaged advantages of a reductionist model, we studied the response of Taxol in single cells and small cell colonies of ≤ 6 cells within microwells. The specific objectives covered dissecting the role of cell-cell interaction (investigating colonies with different cell numbers), dimensionality and different ECM matrix coatings in the wells (collagen and fibronectin) on Taxol response. Flat PDMS substrates and cell-derived fibronectin matrix served as 2D and 3D controls, respectively, the latter in view of its claimed higher *in vivo* relevance compared to standard 2D substrates.

Part 3 of this thesis (**Chapter 6**) aimed at the establishment of a PEG-hydrogel based microwell array as a cancer *in vitro* model that may find wider application than can be expected for the PDMS platform. The PEG microwell array has several advantages over the PDMS platform. Firstly, the PEG hydrogel constitutes a softer and therefore more physiological relevant material than PDMS. Secondly, intrinsic to the fabrication procedure and the inert nature of the hydrogel, this platform allows for reproducible formation of larger clusters and long-term cell culture. In addition, the surface functionalization procedure results in a protein coating only at the bottom of the microwells. This allows for the exploration of the effect of cell-cell versus cell-matrix interactions within the clusters. Hence, this platform was believed to constitute a relevant multicellular-cluster-based culture model with higher *in vivo* relevance compared to single cell and conventional 2D studies.

The further development towards a cancer cell platform included the characterization of the coating of the microwell array with three different matrix proteins (collagen I, laminin, fibronectin) relevant for the different stages of cancer progression. Furthermore, in view of the known importance of substrate rigidity on cell function, we aimed at exploring the accessible rigidity range for the microfabricated PEG hydrogel. The fabrication of the microwell array into a thin hydrogel film on a thin solid support enabled high-resolution microscopy. Therefore, this hydrogel culture model was compatible with inverted-stage, confocal microscopy. This enable the evaluation of cell survival/death within 3D clusters based on high content analysis of fluorescent markers at a sub-cellular level and the analysis of the spatial distribution

of cell response in x-y-z. Finally, the cancer cell cluster formation was characterized for two cell lines representing different stages of cancer progression (MCF-7 and MDA-MB-231). This latter experiment was performed in order to interrogate the relevant applications of this model to study different cancer niche-specific questions.

In the final results part 4 (**Chapter 7**), we investigated the microenvironment as a determinant of drug response in an *in vivo* relevant model of early breast cancer. Laminin and collagen are relevant proteins of the cancer environment representing early and more progressed stages of cancer, respectively. The PEG microwell array offers a unique possibility to determined the role of these proteins on cell behaviour in a 3D environment and independently of other parameters. If successful, this would allow us to overcome limitations associated with other platforms including, for example, matrix-induced morphology changes.

In this part we aimed at studying the distribution of cell death along the z-axis as a factor of cluster culture time before treatment, in order to reveal information on matrix signaling as well as on the role of culture time and cell density. The effect of matrix was further investigated by integrin-blocking experiments. Increasing the culture time of the 3D clusters was found to affect drug response in the cells and thereby raised the question of the role of cell density. Increased cell density in 3D can lead to reduced drug response by several factors including diffusion effects, cell morphology changes and enhanced cell-cell interactions. The effect of cell density in cancer on drug response has been emphasized in the literature, especially for larger cancer clusters.

Here, we used the hydrogel microwell model, functionalized with collagen I to study the role of cell density in the dimensionality-dependent drug response, independently of other parameters. In a key experiment, we related density effects to E-cadherin levels by knocking down the expression of this protein. Finally the effect of the different extrinsic parameters on drug response and proliferation were compared to interrogate the underlying signaling pathways. Adhesion-mediated drug resistance can be related to both anti-apoptosis signaling and signaling regulating the cell cycle. Understanding the details of these signaling pathways and their interplay is believed to be key for the successful development of combination treatments targeting cell-microenvironment interactions.

The thesis ends with the Conclusions and Outlook Chapter, which discusses possible future directions in the engineering and application of the microwell platform (**Chapter 8**).

CHAPTER 3

Materials and Methods

In this chapter all the materials and the main methods used for the experiments of this thesis are explained. This includes cell culture substrate fabrication, general cell culture protocols as well as an explanation of the imaging methods used. Exact details and optimization procedures of new protocols are explained in the individual experimental chapters 4-7. For the sake of convenience, long names are listed as their abbreviations. List of abbreviations: see page 21.

3.1 Materials

3.1.1 Buffer

Water

Ultrapure water was used for buffers and other aqueous solutions. The water was purified using a milli-Q system Gradient A 10 (Millipore) equipped with an Elix 3 (three step purification process) and an ultraviolet lamp for photo-oxidation. The resistivity and TOC level were in the range of 18.2 MΩcm and <5ppb, respectively.

Phosphate buffered saline

Phosphate buffered saline (PBS); Sigma Aldrich, Switzerland) was diluted in ultrapure water. The final concentration was 137 mM NaCl, 10 mM Phosphate, 2.7 mM KCl and a pH of 7.4. PBS used in cell culture was autoclaved before use.

3.1.2 Poly (ethylene glycol)-grafted polymers

PLL-g-PEG

Poly(L-lysine)-graft-poly(ethylene glycol) (PLL-g-PEG) was purchased from SuSoS AG (Switzerland). PLL(20)-g[3.4]-PEG(2) was used to render negatively charged

surfaces protein resistant. The number in the "()" brackets is the molecular weight of the polymer chain in kDa. The number in the "[]" bracket describes the grafting ratio. Stock solution were prepared by dissolving PLL-g-PEG at 1mg/ml in HEPES 2 and stored at -20°C.

Pluronics

There are several different Pluronic molecules, both di-block PEO-PPO and tri-block PEO-PPO-PEO co-polymers that adsorb on hydrophobic surfaces rendering surfaces hydrophilic and stealth. In this work we used Pluronic F-127, purchased from Sigma, Switzerland. The powder was dissolved in PBS to a stock concentration of 0.2 % (w/v) and stored for up to one month at 4°C.

3.1.3 Proteins

Fibronectin

Human plasma Fibronectin (Fn) was isolated from fresh human plasma (Swiss Red Cross) using gelatin-sepharose chromatography based on established methods (Engvall, Int J Cancer, 1977) (Miekka, Thrombosis Res, 1982). For visualization of the fibronectin coating of substrates, Fn molecules were labelled with Alexa Fluor 488 (Molecular Probes, Switzerland). The labelling procedure was performed as already described (Antia, Biomaterials, 2006). First, Fn was incubated for 1 h with a 30-fold molar access of Alexa Fluor 488 succinimidyl ester. PBS with pH adjusted to 8.5 was used to ensure labelling of amines. The protein solution was then transfer to a dialysis cassette (Thermo scientific, U.S.) and dialyzed for 24 hrs in 1 l of PBS pH 7.4, changing the buffer twice.

The labelling ratio was determined by measuring the absorbance of the labelled Fn at 280 nm and 496 nm. Using published extinction coefficients for dyes and Fn, the labelling ratio could be calculated. With the above protocol a labelling ratio of about 4 fluorophores per Fn molecule was typically obtained. Fn was used in the studies presented in chapter 4 and 5. The Fn solution was typically diluted to 25 µg ml $^{-1}$ for coating of substrates.

Collagen I

Two different collagen batches were used. For coating of the PDMS microwells we used rat Col-I (Gibco, Switzerland) stored at 4°C. This collagen solution was diluted in PBS to a concentration of 46 µg ml $^{-1}$. Bovine Col-I, was purchased from Sigma and stored at 4°C. This solution was used to coat the PEG hydrogels. Dilutions in PBS were made on the same day as they were to be used.

Laminin

Mouse Lam was obtained from BD Biosciences and stored long term at – 80°C. Lam was labelled with a PEG-linker to ensure a stable binding to the PEG gel, see 2.2. After labelling and dialysis the protein concentration was determined by measuring the absorbance of the proteins at 280 nm. Functionalized protein was stored at a concentration of 0.5 mg/ml for up to 6 months at -20°C.

3.1.4 Antibodies

Several antibodies were used within this thesis for staining of cells in immunohistochemistry or in western blots. An integrin-blocking antibody was also used to block the function of integrin β1. See chapter 6. All antibodies used are listed in table.

Table 3.1. *A summary of all antibodies used in this work.*

Antibody	**Host animal**	**Prod Nr**	**Company**
α-E-cadherin (intracellular domain, human)	mouse	sc-1500	BD Biosciences
α-Collagen I	rabbit	sc- 8784-R	Chemicon
α-Laminin	rabbit	L 9393	Sigma (Switzerland)
α-GAPDH	rabbit	G 9545	Sigma (Switzerland)
α-mouse (HRP-labelled)	goat	A 4416	Sigma
α-rabbit (HRP-labelled)	goat	111-035-003	Jackson
α-mouse (Alexa 488 labelled)	goat	A 11001	Molecular probes
α-Integrin β1 (function blocking)	rat	mAb13	*
α-BrdU	mouse		BD Biociences
non specific IgG	rat	I 4131	Sigma (Switzerland)

* The mAb13 was a kind gift from Prof. Kenneth Yamada, NIH, Bethesda, MD.

3.1.5 Drugs

Taxol

Taxol was used as a model drug in all the drug response experiments with MCF-7, as presented in chapter 5 and 6. Pure Taxol was purchased from Sigma Aldrich (Switzerland), dissolved in DMSO to 20 mM and stored as a stock solution at – 20 °C until the day of use. Taxol was usually added to cell-media to give a final concentration of 10-1000 nM.

3.2 Substrates

3.2.1 Wafers and glass slides

Silicon wafers (p type, <100>, polished, ∅ = 100mm; Si-Mat Silicon Materials, Germany), glass slides (76 × 26 mm; Menzel GmbH, Germany) and glass cover slides (∅ = 10 – 24 mm, thickness 0; Menzel GmbH, Germany) served as substrates.

3.2.2 Well plates

Well plates were used to seed cells, as received or after coating with a protein or a microfabricated structure. 24-well polystyrene well plates (tissue culture treated, sterile; Corning, US). 8-well Ibidi dishes (tissue culture treated, sterile; Ibidi, Germany).

3.2.3 PDMS

Polydimethylsiloxane (PDMS) is a silicone rubber with the general chemical structure $CH_3[Si(CH_3)_2O]_nSi(CH_3)_3$. This elastomer has been intensively used to produce microstructured moulds for the structuring of other materials. This process is called soft lithography. PDMS is a favourable material for microfabricated cell culture as it is non-toxic, has a high permeability to O_2 and CO_2 but a very low permeability for H_2O. In addition PDMS is transparent between 230 – 1100 nm, which makes it suitable for microscopy based read-outs and live monitoring of experiments.

PDMS was used for wafer replication and to produce microwells (see section 3). Sylgard 184 (Dow Corning, Germany) was mixed at a ratio of 1:10 (w/w) curing agent to prepolymer, mixed thoroughly and degassed in a desiccator to remove air bubbles. The polymer was cured either at 80 °C for 4 h or at 60 °C overnight depending on the application. Detailed descriptions of the fabrication of microwells in both PDMS and a PEG hydrogel are given in 3.

3.3 Microwell fabrication

3.3.1 Preparing Si masters for microfabrication

Silicone masters containing the original structures for the replica molding of microwells were produced by photolithographic techniques in a clean room. All the clean room work needed for this project was performed by Mirjam Ochsner, Fabian Anderegg or Stefan Kobel. In short, silicon wafers were placed on a hot plate for 5 min at 190 C for dehydration. Then the wafers were spincoated with SU8 (2010 – 2100, negative resist, MicroChem, US) 90 sec at 2000 rpm. Softbake was performed for 2 min at 65 °C followed by 2 min at 95 °C. The photo resist was then crosslinked by exposure through a glass-chrome mask using a mask aligner (Karl Süss MA6, Germany).

Different exposure energy was used depending on the thickness of the resist, for example a 10 μm thick resist was exposed for 15 sec with 12 mW/cm^2. Finally the non-crosslinked resist was removed using a SU-8 developer (MicroChem, US). Excess developer was removed with isopropanol and the wafer was dried with nitrogen. The wafer was then placed on a hot plate at 65 °C to bake the resist hard. The hotplate was heated up to 150 °C, at which the wafer was subsequently baked for 5 min.

3.3.2 Producing microwells in PDMS

Replica molding

Soft lithography was used to generate arrays of microwells in PDMS with a diameter of 34 μm. A silicone master with the original array patterns in SU-8 photoresist was produced by standard photolithography as described above and fluorosilanized for a non-adhesive surface. Before the master was exposed to silane, the surface was activated with air- or O_2- plasma at 0.8 mbar for 30 s (PDC-002, Harrick Scientific, USA). Within 15 min after the treatment, the master was placed inside a desiccator next to an open bottle of fluorosilane (1H, 1H, 2H, 2H-Perfluorooctyltrichlorosilane, ABCR GmbH & Co. KG, Germany). The pressure within the desiccator was lowered using a vacuum pump to facilitate the release of fluorosilane molecules into the air. The incubation time was 1 h.

To produce the first PDMS master, PDMS base was thoroughly mixed with crosslinker at a ratio of 10:1 and subsequently degassed in a desiccator to remove air bubbles. The mixture was poured onto the fluorosilanized silicon wafer to a thickness of about 5 mm and cured for 4 h at 80 °C. After molding, 1×1 cm microstructured pieces of PDMS were cut out and fluorosilanzed as described above. These second PDMS masters could be reused > 10 times to mould microwell arrays onto thin glass

cover slips (Menzel-Gläser, Germany, strength 0, approx. 100 μm thickness). To do this, a small drop of PDMS was placed onto the glass and the PDMS master placed on top. After curing at 80 °C for 4 h the PDMS master was removed. The master was then functionalized with proteins and glued to the bottom of a small Petri dish with a hole (∅ = 8 mm) drilled in the bottom. Uncrosslinked PDMS was used as glue. After curing (4h at 80 °C or 48 h at 20 °C) the samples were sterilized with UV-light and used as a cell culture substrate. This fabrication procedure results in samples that are thin enough to be analyzed by high-resolution microscopy.

Protein functionalization

In order to discriminate cell attachment on the array to within the microwells, a method for creation of an adhesive / non-adhesive contrast is needed. The development of a new method for protein functionalization of the array is described in detail in chapter 4. This method was used to coat PDMS microwells with either Fn or Col-I.

In brief, the whole microwell arrays were coated with the desired protein, by incubation in a protein solution (25 μg/ml) for 1 h after air plasma treatment at 0.8 mbar for 30s. The arrays were rinsed with H_2O and blown dry with N_2 just before use. Stamps for μCP were cut out of crosslinked PDMS sheets, treated with plasma and functionalized with glutaraldehyde. To stamp the coated arrays, both the arrays and the stamps were rinsed with water and blown dry. The stamp was placed in contact with the array for 30 sec. Upon separation of the two substrates, the Fn on the flat areas between the microwells was removed from the array. This step was repeated 1-2 times to ensure complete removal of protein from the array surface. Samples were used 24-72 hrs after functionalization. Before cell seeding, the samples were sterilized with UV-light and incubated with Pluronic F-127 to render areas with no protein non-adhesive to cells.

3.3.3 Producing microwells in a PEG hydrogel

Replica molding

Microwells with a diameter of 100 or 200 μm were moulded into a PEG-hydrogel using a PDMS mould. To create a PDMS master capable of producing one microwell array in each one of the wells of an 8-well Ibidi dish, a special moulding frame was used. The moulding frame was designed by Stefan Kobel at EPFL. In principle it consisted of a PMMA frame, placed on top of a SU-8 silicone master. The silicone/SU8 master was made non-adhesive by fluorosilanization according to the protocol described for preparation of microwells in PDMS. About 5 ml of PDMS mixed base to crosslinker in a ratio of 10:1 was poured into the mould and cured at 60°C. The lower temperature was chosen to avoid deformation of the PMMA

polymer. After gentle removal from the mould, the PDMS master was used to make PEG hydrogel arrays. Typically the mould was used 24 h after moulding and within weeks.

The PEG hydrogel was prepared by mixing a solution of PEG-VS with a solution of PEG-TH to obtain a stoichiometric ratio of 1:1. The PEG-TH is commercially available with a functionalization of 100% while PEG-VS is synthesized in the laboratory of Prof. Matthias Lütolf and has a varying functionalization of around 80-90 %. The solvation of PEG-TH powder into H_2O and PEH-VS into 0.3 M Triethanolaminehydrochloride buffer, pH 7.4, was performed on ice. The solutions were vortexed thoroughly, filtered with a 0.2 um syringe filter, transferred into vials and immediately frozen down in liquid N_2. Working aliquots of the polymers were prepared with 10 % PEG and finally stored at -20 °C.

To prepare a 5 % gel the PEG solutions were thawed, mixed 1:2 with buffer and vortexed. Within a few minutes after mixing, the polymer solution was pipetted onto the microstructured area of the PDMS stamp. 10-15 µl was used per microwell array. The Ibidi dish was placed upside down on top of the PDMS mould with the gel-drops. Polymerization was finalized 45-60 min at RT. Afterwards, the Ibidi dish was carefully removed and the arrays covered with PBS and stored in 4C. The arrays were used the next day or after the weekend. Before use the arrays were sterilized with UV light and incubated with PLL-g-PEG (200 µg/ml in PBS for 1 h) to render the TCPS surface surrounding the gel, non-adhesive for proteins and cells. This limited cells adhesion to some extent and loosely adhered cells could be washed away after 24 h of culture.

Protein functionalization

The PEG microwells were functionalized with protein at the bottom by µCP the PDMS mould with protein before gel moulding. Col-I was used unmodified while Lam and Fn was first labelled with a maleimide-PEG-N-hydroxysuccinimide ester (MAL-PEG-NHS; mol wt 3.5 kDa; JENKEM TECH, USA). At a basic pH, the NHS ester group reacts specifically with the amino-terminus and the amine groups on lysines of the backbone peptide, to form covalent amide bonds between the MAL-PEG and the protein. The reaction occurs with an efficiency of 0.7, which was compensated by a 4× molar excess of NHS vs. protein. The MAL-PEG-NHS was dissolved in PBS buffer pH 8.5 at a relatively high concentration (~ 10 mg/ml) to minimize protein dilution and directly mixed with the protein. After 1 h incubation the protein mixture was dialyzed in 1 L PBS for 24 hrs with exchange of the buffer twice At the end of the dialysis the protein concentration was determined by measuring the absorption at λ= 280 nm and using the theoretical molar extinction

coefficient for the protein. A solution of 0.5 mg/ml protein in PBS pH 7.4 was prepared and stored at -20 °C until use.

The PDMS mould was printed with protein on top of the pillars using a wet- μCP process, as described in (Lutolf *et al.*, 2009). A 9 % polyacrylamide gel was prepared according to a standard protocol and crosslinked between two glass slides, using 3 mm plastic spacers to obtain a flat gel. The mixing ratios in the gel was 6.9 ml PBS, 3ml acrylamide 30 % (AppliChem, Germany), 50 μl APS (0.1 mg/ml) and 5 μl TEMED. The polymerized gel was removed from the glass support and immersed into PBS contained in a Petri dish.

The protein printing process was performed in a laminar flow hood. This environment, with a high airflow, was suitable to dry the gel in a convenient time frame. The gel first was cut into a suitable size to fit on a regular glass slide, which was placed inside a Petri dish. After 30 min 200 μl protein solution (0.3 mg/ml) was placed on top of the gel. The glass slide was tilted and a pipette tip was used to evenly distribute the solution on the gel. Let the gel with the protein coating dry in the Petri dish until you cannot distinguish any liquid on the gel anymore. Then the glass-slide with the gel was turned upside down and put in close contact with the PDMS mould. The protein-coated gel was left on the mould for 30 min before a PEG gel was moulded as described above.

3.4 Cell culture

3.4.1 Cells lines

MCF-7

The tumorigenic mammary carcinoma cell line MCF-7 was purchased from the American Type Culture Collection (ATCC, Manassas, VA, USA). These cells were maintained in culture for up to 20 passages. They were cultured in DMEM supplemented with fetal bovine serum (10% (v/v)), penicillin (100 Uml^{-1}) and streptomycin (100 μgml^{-1}) and were grown in a humidified atmosphere (95% (v/v) air, 5% (v/v) carbon dioxide at 37 °C). The cells were split at a ratio of 1:2 to 1:5 every 2-3 days.

MDA-MB-231

The metastatic mammary carcinoma cells MDA-MB-231 were purchased from the American Type Culture Collection (ATCC, Manassas, VA, USA). These cells were maintained in culture for up to 20 passages. They were cultured in DMEM supplemented with foetal bovine serum (10% (v/v)), penicillin (100 Uml^{-1}) and

streptomycin (100 μgml^{-1}) and were grown in a humidified atmosphere (95% (v/v) air, 5% (v/v) carbon dioxide at 37 °C). The cells were split at a ratio of 1:5 – 1:20 every 2-4 days.

HRE

Human renal epithelial cells (HRE) are primary cells that were purchased from Lonza. These cells were maintained for up to 12 passages in REBM^{TM} (Renal Epithelial Cell Basal Medium; Lonza) supplemented with REGM media supplements (Lonza), as recommended by the cell supplier. The cells were split at a ratio of 1:2 – 1:4 every 2-4 days.

NIH-3T3

The NIH-3T3 fibroblasts used were high-passage and no more controlled in growth by contact inhibition. The cells were maintained in DMEM (ATCC, US) supplemented with foetal calf serum (10% (v/v)), penicillin (100 Uml^{-1}) and streptomycin (100 μgml^{-1}) and were grown in a humidified atmosphere (95% (v/v) air, 5% (v/v) carbon dioxide at 37 °C). The cells were split at a ratio of 1:5 – 1:20 every 2-4 days.

3.4.2 Autoclaving of materials and liquids

All plastic materials that were not purchased in sterile conditions were autoclaved at 120C for how many hours? This includes pipette tips and Eppendorf tubes. PBS was sterilized by autoclaving at 120 °C for 20 min.

3.4.3 Immunohistochemistry

Actin and nucleus staining

Cell samples to be used for F-actin staining and the staining with E-cadherin antibodies were fixed in 3 % formalin in PBS for 10 min and subsequently permeabilized with 0.1 % Triton-X 100. The samples were rinsed twice in PBS before proceeding to staining procedures. Actin stress fibers were stained by incubation for 30 min in Alexa Fluor 488 Phalloidin (1:400 dilution in PBS; Molecular Probes, Switzerland). The nucleus was stained by incubation in Hoechst (1:4000 in PBS; Invitrogen, Switzerland).

E-cadherin staining

Cell samples were first fixed in 3 % formalin in PBS for 10 min and subsequently permeabilized with 0.1 % Triton-X 100. The samples were rinsed twice in PBS before

proceeding to the staining procedures. Before staining with antibodies the samples were incubated in 1 % BSA for at least 30 min to inhibit non-specific adsorption of antibodies. Then, primary anti-E-cadherin antibody was incubated on the samples at a dilution of 1:100 (stock solution to PBS), overnight at 4 °C. After rinsing with PBS the secondary Alexa-Fluor 488-conjugated anti-mouse antibody was added at a concentration of 1:500 (stock solution to PBS) for 1 h at RT. Then, the samples were rinsed again with PBS and imaged on the same day.

3.4.4 Western blot

Western blots were performed to control the knockdown efficiency of si-RNA. Cells were seeded in 24-well plates at the same cell number and for the same amount of time as used in the si-RNA experiments. At the end of the experiment the samples were dissolved in 2.5 x Laemmli buffer at 95°C. A volume of 40ul per well was used. Two wells were pooled into the same Eppendorf tube and lyzed at 95°C for 10 min. If the samples were not used directly, they were stored at -20°C until use. A SDS-PAGE was performed to allow for separation of the proteins within the samples. The samples were first collected in a 4 % PAAm-gel for 1 hr at 40 mA to obtain the same starting position for all the proteins. Thereafter they were separated in a 10% PAAm overnight at 9 mA.

A protein marker (Fermentas) was used to locate the different proteins in the gel. The proteins were then transferred from the gel onto a nitrocellulose membrane (Whatman, Switzerland) using an electric current of 300 mA for 2 h. To detect two different proteins, the membrane was cut in half and stained with the respective antibodies. Typically concentrations of 1:5 000 or 1:10 000 were used for primary antibodies with incubation overnight. Secondary HRP antibodies were incubated with the membrane at 1:5 000 for 1 h. Finally the stained proteins on the membrane were used to expose a photo film. The developed films were scanned and the evaluation of density of single bands was performed using the Gel Analysis plugin in Image-j.

3.5 Preparation of cell derived matrices

Cell derived matrices were prepared on Fn-coated tissue culture treated polystyrene substrates. For drug experiments, standard 96-well plates were used, while Ibidi dishes were applied when high-resolution imaging was required. All matrices were prepared according to a protocol that Dr. Kris Kubow, a previous PhD Student of Prof. Viola Vogel developed as a modification of already published protocols (Kubow, 2009, Integr Biol). First, the plastic was coated with Fn, by incubation with 20ug/ml Fn in PBS for 30 min at RT or overnight at 4 C. The wells were rinsed once with PBS before cell seeding.

NIH-3T3 fibroblasts were seeded at 80 x 10^3 cells/cm^2 and let adhere in the cell incubator, at 37 C. After 20 min the medium is replaced to medium containing 50 μg/ml Fn. The high Fn concentration causes the cells to produce Fn fibers, which make up the final matrix. The cells were cultivated on the samples for at least 4 days before the samples were decellularized. The decellularization in principle relies on the lysis of cells with a high concentration of Triton. First the samples were rinsed twice with PBS to removed cell culture media. Thereafter followed three rinses with Wash buffer I (0.1 M Na_2HPO_4, 2 mM $MgCl_2$ and 2 mM EGTA, pH 9.6). After this step the cells are lysed in Lysis buffer (8 mM Na_2HPO_4 and 1% v/v Triton X-100, pH 9.6), first for 15 min at 37 °C and thereafter again in new lysis buffer for 1 h at 37. After the lysis the matrices are rinsed twice with wash buffer II (10 mM Na_2HPO_4, 0.3 M KCl, pH 7.5). Finally the matrices are washed three times with de-ionized water. After completing this decellularization protocol, the matrices were rinsed with PBS and reseeded with MCF-7 breast carcinoma cells within a week.

3.6 Cell assays

3.6.1 Proliferation assay

There are several methods to detect proliferating cells in culture. Bromodeoxyuridin (BrdU) is a Thymidin-analog becomes inserted into newly synthesised DNA during the S-phase of the cell cycle. Therefore it is a specific marker for cells undergoing S-phase and can be used to give a quantitative measure of proliferation. The detection of proliferating cells is done via specific antibodies against BrdU.

BrdU stock solutions were prepared under sterile conditions. BrdU (Sigma, Switzerland) was dissolved in PBS to a concentration of 25 mM and stored at -20 C. The BrdU stock solution was diluted 1:2500 in cell culture media to a concentration of 10 μM and incubated with the cells; 6 or 8 h for MCF-7 and 2 h for MDA-MB-231 in the cell incubator at 37 °C. At the end of the incubation the cells were rinsed with PBS and fixed for 20 min in ice-cold methanol, 70 % in PBS. The samples were treated with 2 M HCl for 20 min, neutralized with 0.1 M Borax (Natriumtetraborate) for 2 minutes and permeabilized with 0.1% (v/v) Triton-X for 10 min.

All stages after fixation were performed at room temperature and in between each stage of the treatment the cells were washed three times with PBS. H2O. Finally the samples were blocked in 1 % BSA for at least 30 min. A staining buffer consisting of 0.5 % BSA and 0.5 % Tween-20 in PBS was used for all antibody dilutions and rinsing steps in the staining process. First the samples were incubated with a primary mouse anti-BrdU antibody (BD Biosciences) overnight at 4 °C. The antibody was diluted 1:50 for PEG hydrogel samples and 1:100 for polystyrene samples. The

secondary goat-anti mouse Alexa Fluor 488 (Molecular Probes) was diluted 1:200 and incubated for 1 h at RT. Finally the nuclei were counterstained with either Hoechst 33342 (1:3000 in PBS) or in undiluted PI/RNase buffer (BD Biosciences).

3.6.2 Apoptosis assays

Annexin V

This apoptosis assay uses the translocation of phosphatidylserine (PS) during apoptosis. In normal, viable cells, PS is located on the cytoplasmic surface of the cell membrane. However, in apoptotic cells, PS is translocated from the inner to the outer leaflet of the plasma membrane. Annexin V is a 35-36 kDa Ca^{2+}-dependent phospholipid binding protein that has a high affinity for PS. In this work we used Annexin conjugated to Alexa fluor 488 and therefore its binding to cells could be detected by fluorescent microscopy.

The cells were stained with Annexin before fixing. Cells were first washed with cold PBS and then with HEPES buffer (10 mM with 140 mM NaCl and 2.5 mM $CaCl_2$, pH 7.4). Subsequently the cells were labelled with the Annexin V conjugate (1:5 dilution in HEPES for 15 min at RT; Invitrogen, Switzerland). Finally, the cells were washed in the HEPES buffer and incubated with Propidium Iodide (1.5 µM in HEPES for 15 min at RT; Invitrogen, Switzerland). The cells were imaged directly after this step, without further rinsing.

Nuclear fragmentation

Nuclear fragmentation was assed on live or fixed cells. For live cell labelling, Hoechst 33342 was added directly to the cell media (1:3000 for 20 min at 37 °C; Invitrogen, Switzerland). Fixed cells were labelled either with Hoechst 33342 (1:3000 in PBS for 30 min at RT; Invitrogen, Switzerland) or in PI/RNase buffer (undiluted for 30 min at RT; BD Biosciences). The cells were imaged directly after this step, without further rinsing.

APOPercentage

The APOPercentage assay (Biocolor, UK) is based on a red dye that is only taken up by apoptotic cells, which have a slightly damaged cell membrane. The APOPercentage dye was added to live cells in cell culture medium at a dilution of 1:20. After incubation for 30 min at 37 °C, the cells were rinsed with PBS and imaged for red fluorescence.

Mitochondrie activity assessment

Tetramethylrhodamine ethyl ester (TMRE; Invitrogen, Switzerland) is a cell-permeable, cationic, red-orange fluorescent dye that is readily sequestered by active

mitochondria. The intensity of the signal corresponds to the mitochondria activity. We incubated TMRE with live cells (25 nM in cell culture media 30 min at 37°C). After incubation the cells were rinsed and imaged immediately. The TMRE signal is temperature-dependent and therefore it is important to keep the same temperature for all samples imaged.

In order to not have to image live cells we also used mitotracker mitochondrion-selective probes (Invitrogen, Switzerland), which is retained in cells after fixing. Before fixing the cells, mitotracker Deep-Red FM was added to the samples (200 nM in cell culture media at 37 °C for 30 min). Then the samples were rinsed in pre-warmed (37 °C) PBS and finally fixed in pre-warmed (37 °C) formaldehyde (2 % in PBS for 10 min). After fixing, the cells were rinsed again with PBS and imaged.

Blocking β1-integrin function with the mAb13 antibody

We used the well-characterized monoclonal antibody 13 (mAb13) that binds to integrin-β1 and favours its inactive conformation (Akiyama *et al.*, 1989). The mAb13 antibody was added 24 hours after cluster formation at a concentration of 50 μg/ml. After 24 h treatment with the antibody, cells were either assessed for proliferation by the BrdU assay or treated for another 24 h with a mixture of 50 μg/ml mAb13 and 100 nM Taxol.

E-cadherin knockdown with silencing RNA

E-cadherin expression in MCF-7 cells was inhibited by transfection with a si-RNA for E-cadherin. We used three different si-RNA Select; two for E-cadherin (s-2769 and s-2770) plus one si-control (Ambion, USA). Cells were transfected by reverse transfection, in which transfection agents and si-RNA are added to cells in suspension before seeding onto substrates. In short, Lipofectamine-2000 (Invitrogen) was mixed in Optimem (1:150, 5 min at RT). Then si-RNA was added and the mixture was incubated for 15 min before mixing with the cells. The final concentration of cells was 70 000 cells per 300 μl cell culture media and 100 μl Optimem. Final concentration of Lipofectamine and si-RNA was 1:1200 and 20 nM respectively.

3.7 Imaging techniques

3.7.1 Fluorescence microscopy

Fluorescence is a phenomenon where certain molecules or atoms can absorb light at one wavelength and at emit it at a longer wavelength. The energy-difference between the absorbed light and the emitted light is dependent on the electronic structure of the molecule. This phenomenon is extensively used to visualize biological samples. In the

1940s scientist explored the possibility of attaching fluorochromes to antibodies, making it is possible to visualize specific proteins and organelles within a cell (Alberts *et al.*, 2002).

Widefield microscopy

We used a widefield microscope (Zeiss, Germany) equipped with a 10x and a 20x air objective. This microscope was used to produce overview images of protein patterns, to monitor cell seeding quality on the microwell array and to analyze apoptosis and BrdU stain of cells cultured on flat substrates and of small cell clusters in microwells, as described in chapter 4. Widefield microscopy is a suitable technique to cover large areas of your sample at a high speed. Typical exposure times lies within 10 ms and 2 s. However, a disadvantage is that secondary fluorescence emitted by the specimen often occurs and can obscure resolution of features within the objective focal plane.

Confocal laser scanning microscopy

Clear images of thick samples can be obtained by confocal microscopy, as secondary fluorescence from areas distant from the focal plane is not collected in the image. In the confocal microscope a pinhole in the injected light path regulates the size of the volume of the sample that is excited by the light, the focal volume. After excitation the emitted light from the fluorescent molecules in the sample is collected back into the objective. Also scattered light and the reflected laser beam are collected into this objective. However, the wavelength of the emitted light is known by the Stokes-shift and therefore the unwanted light can be removed from the beam path by a wavelength filter.

A second pinhole suppresses out of focus light, keeping only the light from a certain focus plane. Hence, in this way a confocal microscope produces an image point by point as the laser is scanned across the specimen at a defined focal plane. Typically the light intensity of the scanned positions is detected on a photomultiplier. A computer is need for acquisition, processing and display of the images. The size of the confocal spot is determined by the microscope design, wavelength of incident light, objective characteristics, scanning unit settings and the specimen.

In this work the biggest challenge in image acquisition was to find a setup by which 3D images of sufficient resolution and with a low signal to noise ratio could be acquired. The resolution (r) of an image is defined as the smallest resolvable distance between two objects (Eq. 3.1). It is proportional to the wavelength (λ) and inversely proportional to the numerical aperture (NA). The NA is dependent on the objective and the immersion media. The brightness of an objective is proportional to the NA but inversely proportional to the magnification (Eq. 3.2). Therefore, an objective with

maximized NA and minimized magnitude would theoretically give the brightest image.

Equation 3.1: $$r = \propto \frac{\lambda}{NA}$$

Equation 3.2: $$brigthness = \frac{NA^4}{Mag^2}$$

When the distance between the objective and the sample deviates from an optimal thickness, spherical aberration occurs. It leads to a reduced brightness in the image. Therefore, it would preferable to use an objective with a correction collar to correct for spherical aberration, when imaging thick samples. Scattering and absorption of light has a major effect on the intensity of an image from thick samples. One way to reduce these effect are by increasing the power of the exciting light and also by choosing a fluorophore that is exited by long-wavelength light, as this is not as fast absorbed as short wavelength light.

We used two different confocal microscopes with water immersion objectives. On a Leica SP2-AOBS CLSM (Leica, Germany) we used a ×20 water immersion objective with a numerical aperture of 0.7. On an Olympus FV microscope (Olympus, Japan) we used a ×40 water immersion objective with a numerical aperture of 0.9. On both microscopes, the pinhole was automatically optimized for different wavelengths to give the highest z-resolution.

3.8 Statistic analysis

Quantitative data was plotted as the mean ± standard error of the mean (SEM) and normalised relative to the negative control (cells treated with media alone). Statistical analysis was performed using Student's unpaired two-way t-tests (using MinitabTM). Comparison between data sets was performed using one-way ANOVA (Tukey test) using MinitabTM. Differences were considered as statistically significant when $p < 0.05$.

CHAPTER 4

Protein patterning of a 3D single cell array

This chapter describes the development of a new method to pattern a 3D microwell array with matrix protein adsorbed exclusively to the wall and bottom of the microwells. A PDMS microwell array was developed by the former members of our lab Dr. Mirjam Ochsner and Dr. Marc Dusseiller (Dusseiller *et al.*, 2005) (Ochsner *et al.*, 2007). This platform was used to study the influence of the dimensionality of the culture environment on different cellular processes. Recently, it was applied as a unique platform for the study of dimensionality-dependent actin organization and contractility in fibroblasts (Ochsner *et al.*, 2010). However, while actin organization is a process that can be studied within hours, other biological processes require culture times of days to weeks. The original patterning strategy of the platform, based on PLL-g-PEG stamping (Ochsner *et al.*, 2007) showed loss of pattern stability for mesenchymal stem cells after only 2 days in culture, resulting in insufficient confinement of cells to the wells.

Therefore, an alternative methodology to functionalize the microwell array was developed, with the aim of creating a cell culture platform that is stable for longer culture times. The quality of the adhesive / non-adhesive contrast generated by this new method was evaluated by long-term culture of mesenchymal stem cells in the single-cell array format (Section 4.3.1). In addition, we created a protocol for the production of multiple protein coatings within one microwell array (Section 4.3.2). Finally, we demonstrated the feasibility of a completely new array design, aiming towards more efficient generation of the adhesive/non-adhesive contrast and improved reproducibility and reliability. First feasibility experiments towards this development are reported in Section 4.5.1. The second and third functionalization strategies were based on microfluidic approaches. Parts of the results presented in this chapter have been previously published (Rottmar M., Håkanson M., Smith M., Textor, M. and Maniura-Weber K., J Mater Sci: Mater Med, 2009). I contributed to this work by developing the method used to surface functionalize the platform while Marcus Rottmar performed the evaluation with mesenchymal stem cells.

4.1 Background

The current understanding of cell behaviour has greatly profited from the number of tools available to pattern cells on adhesive patterns, with a defined matrix-adhesion area and with a defined number of cell-cell adhesions. Such reductionist platforms will probably find increasing use in fundamental cell biology, where the role of the extracellular environment for different cell behaviour is elucidated. In addition, the controlled culture environment, may serve to increase reproducibility of standard assays in comparison to standard 2D culture, in which cells are present in a very heterogeneous environment.

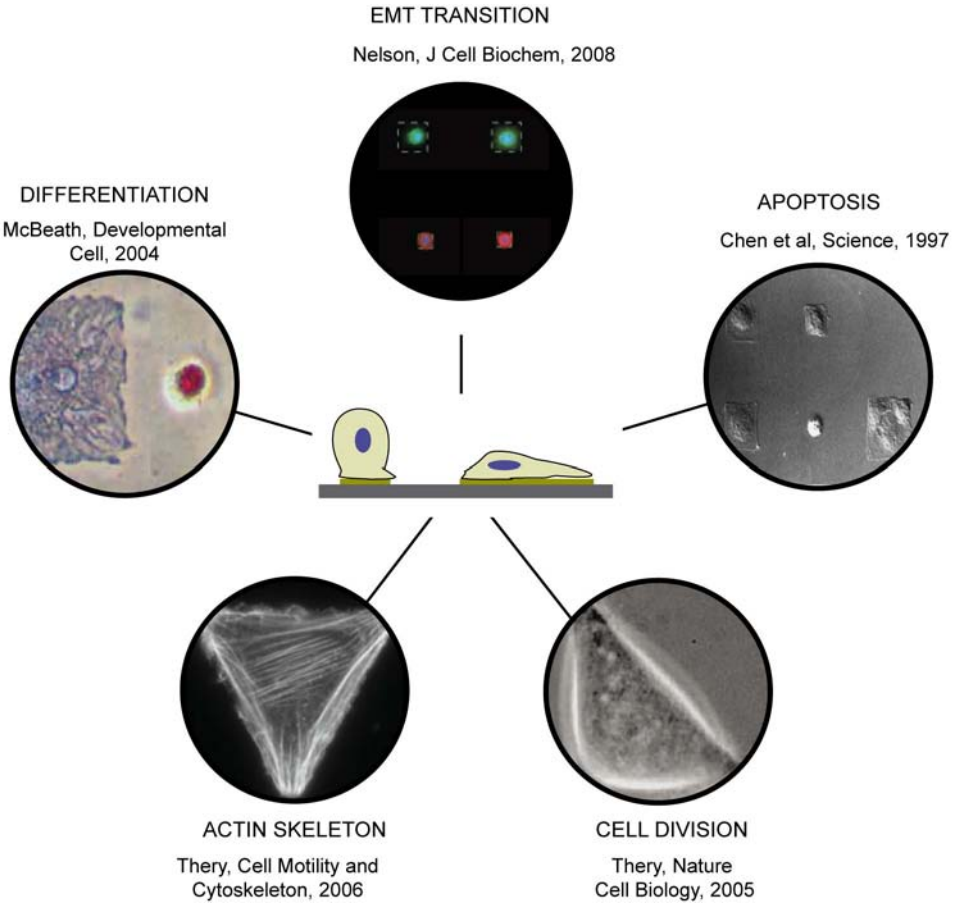

Figure 4.1: *The effect of cell shape on cell behaviour.* The images are explained clockwise. Apoptosis: Cells on a small spreading area undergo apoptosis, in contrast cells on bigger spreading areas survived (Chen *et al.*, 1997). Cell division: The cell shape guides the orientation of the cell division axis, and therefore the future position of the daughter cells (Théry *et al.*, 2007). Actin skeleton: Cells distribute stress fibers in response to the geometry of the adhesive environment (Théry *et al.*, 2006). Differentiation: Cell shape regulates commitment of human mesenchymal stem cells (hMSCs). hMSCs on small patterns differentiate into adipocyte cells and on bigger patterns into osteoblast (McBeath *et al.*, 2004). EMT Transition: Cells on large but not on the small patterns enter EMT induced by matrix metalloproteinase (Nelson *et al.*, 2008b). This figure is adapted from the PhD Thesis of Dr. Mirjam Ochsner.

4.1.1 Patterning single cells on substrates – bridging from 2D to 3D

A large set of tools enables us to study the influence of individual parameters of the microenvironment on cell behaviour. The role of physical parameters, such as matrix rigidity and cell shape, have been studied using polyacrylamide gels with tunable rigidity (Discher *et al.*, 2005) and two-dimensional (2D) cell patterning (Chen *et al.*, 1997), respectively. Technological advances, resulting in the continuous improvements of these tools, have enabled a large number of studies investigating the role of these parameters on cell behaviour and function. Controlling cell shape through the culture of cells on 2D patterns has shown the importance of cell shape in a vast number of cellular responses including proliferation and apoptosis (Chen *et al.*, 1997), stem cell differentiation (McBeath *et al.*, 2004), the orientation of the cell division axis (Thery *et al.*, 2005) and epithelial-mesenchymal transition (Nelson *et al.*, 2008b) (Fig. 4.1).

However, the cultivation of cells on planar surfaces is not optimal as it does not recapitulate the *in vivo* configuration of most cell types, in particular three dimensionality is lacking (Dunn *et al.*, 1989). Therefore, several strategies for 3D cell culture have been explored, including the culture of cells in 3D matrices of either natural polymers, such as Col-I, or synthetic polymers, such as PEO-based gels (Griffith and Schwartz, 2006).

The PDMS based microwell array developed within the group of Prof. Marcus Textor offers the opportunity to cultivate single cells in a controlled 3D environment. Several extrinsic parameters can be independently controlled on this platform including cell shape, stiffness and biochemical coating (Ochsner *et al.*, 2007) (Dusseiller *et al.*, 2006) (Fig. 4.2). By comparing cells cultured on this platform, with cells cultured on flat substrates it is possible to investigate dimensionality-dependent responses independently of the mentioned extrinsic parameters.

Creating patterns that are stable over extended culture times

Many cell processes such as cytoskeleton re-organization, metabolic activity and protein downregulation can be analyzed within 24 hours. However, processes such as cellular differentiation generally need at least one to two weeks to be observed. The analysis of such processes thus requires single-cell patterns, which are stable within this time frame.

Protein-patterned cell culture substrates are typically composed of at least these three components: a substrate material, an adhesive protein and a non-adhesive coating material that is linked to the substrate in areas in between the protein islands. The adhesive protein is chosen to be suitable for the cells of study, while the non-adhesive coating material is typically chosen to fit to the substrate. Single cell patterns usually have dimensions ranging from 20 – 50 μm in diameter. Today, patterns with μm-

resolution can be easily obtained by micro-contact printing, microfluidic patterning or by etching of a non-adhesive material (Faia-Torres *et al.*, 2011).

The emergence of impaired pattern fidelity with time of culture has been acknowledged as one of the major problems for current cell patterning techniques (Lussi *et al.*, 2006). It has been accredited to both cell-dependent and cell-independent processes (Nelson *et al.*, 2003) (Fig. 4.3). Fink *et al.* documented a cell-dependent failure of patterns, as fibroblasts consistently escaped the protein patterns before HeLa and RPE1 cells (Fink *et al.*, 2007).

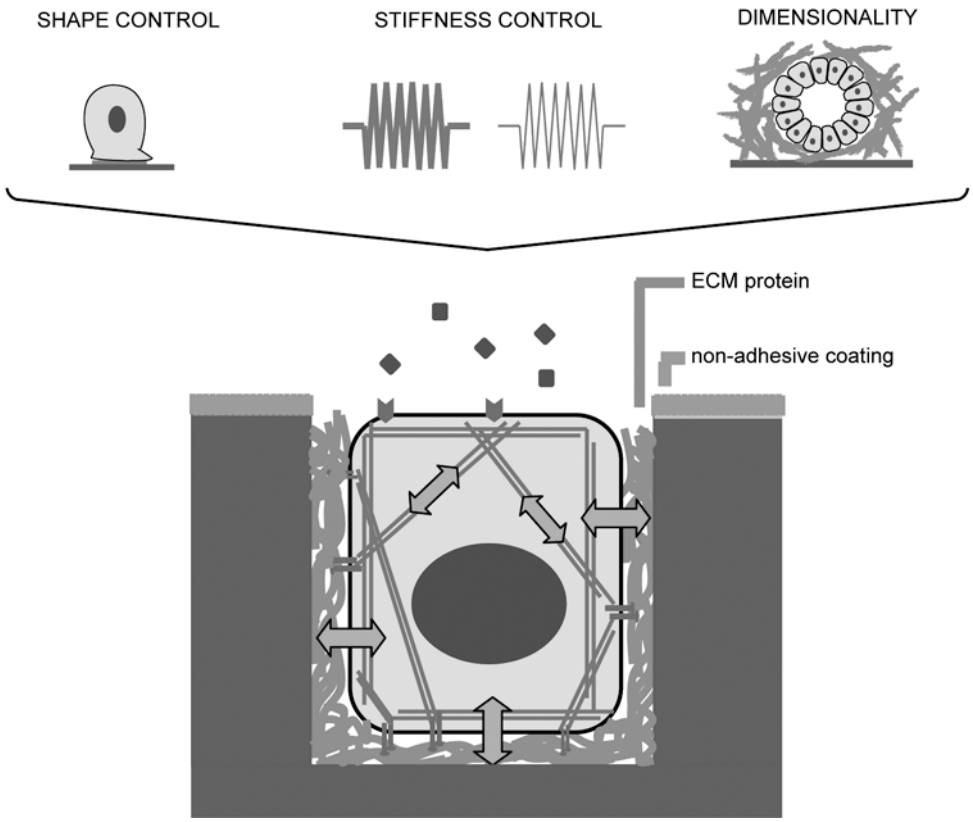

Figure 4.2: *The microwell structure combines the control of several extrinsic parameters.* It combines the shape control of 2D patterned substrates, the stiffness control of the substrate, and the dimensionality typical for 3D cell culture models. With microwells in the size of a single cell it is possible to control the 3D cell shape. Other factors, such as soluble factors are not controlled in this model. This figure is adapted from the PhD Thesis of Dr. Mirjam Ochsner.

The stability of an adhesive / non-adhesive contrast strongly depends on the stability of the non-adhesive coating and its linkage to the substrate. Therefore various approaches have been used to improve its stability. Lussi *et al.* increased the stability of a non-adhesive coating that binds to the substrate by electrostatic interaction, by choosing substrates that had the strongest interaction with the self-assembled polymer

coating (Lussi *et al.*, 2006). Another approach was to link the non-adhesive layer covalently to the substrate. This was used in an approach for patterning on glass, where a polyacrylamide gel constituted the non-adhesive coating. The covalent linkage of the polyacrylamide gel to the glass gave stable cell patterns for at least 28 days (Nelson *et al.*, 2003).

If the linkage to the substrate is not very strong, the non-adhesive coating may be replaced by serum proteins. The serum protein-dependent failure of cell patterns was observed for both a Pluronics coating on UV/Ozone treated PDMS and an agarose coating on glass (Nelson *et al.*, 2003). A last consideration deals with the strategy by which the polymer coating is formed on the surface. Self-assembling polymers can be applied either by adsorption from solution or by printing. In contrast to a printing procedure, adsorption from solution has shown to generate a more even coating, with fewer imperfections (Falconnet *et al.*, 2006).

Protein patterns can also fail the other way around, if the protein coating is not stable. This is often seen as a rounding up of cells on the patterns. In a comparative study protein patterns created by micro-contact printing on glass were more stable after a heat treatment, allowing cell attachment for more than 24 h (Fink *et al.*, 2007). However, even without heat treatment of protein patterns prepared with the same strategy on TCPS substrates, cells were successfully constrained to the patterns for more than 3 days. Therefore, also the quality of the protein coating should be considered in the choice of substrate.

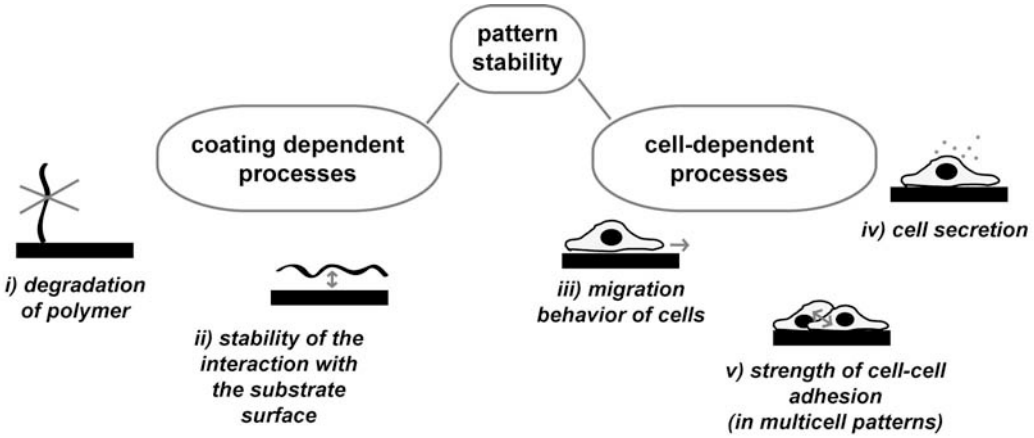

Figure 4.3: *The stability of adhesive / non-adhesive contrast is dependent on several parameters.* The parameters that affect the stability can be divided into cell-dependent and coating-dependent (Nelson *et al.*, 2003). Coating-dependent processes include degradation of the polymer on the substrate and the stability of the interaction with the substrate surface. Hence, one attempt to create a more stable coating is to achieve a stronger binding between the polymers and the substrate. Cell-dependent processes may be less obvious. However, three behaviours that are likely to influence the pattern stability are the migratory phenotype of the cells, the strength of the cell-cell contacts keeping the cells together on a multicellular pattern and their ability to secrete degrading enzymes (Nelson *et al.*, 2003).

Protein patterning of a microwell array

Many of the 2D patterning approaches mentioned in the previous section are not compatible with the 3D structure of the microwell array. It would, for example, be very difficult to align a mask over the microwells, for deposition or etching of a non-adhesive layer. There are three general principles for patterning of a microwell array with adhesive proteins inside microwells and a non-adhesive layer on the surrounding plateau. These approaches include selective deposition, inverted microcontact printing and subtractive microcontact printing (Fig. 4.4).

Selective deposition of proteins or polymer occurs on some materials. Proteins adsorb readily on most surfaces, but they do not adsorb on inert hydrogels. On the other hand, selective adsorption can be observed for many polymers. For example alkane phosphates form organized self-assembled monolayers on TiO_2 but not on SiO_2 (Michel *et al.*, 2002). Hence, if the microwell array is produced of two different materials, selective deposition can be used to generate the contrast (Fig. 4.4a). Chen *et al.* produced microwells in agarose by microfluidic patterning onto a glass substrate (Nelson and Chen, 2002). Subsequent deposition of protein only onto the bottom of the microwells allowed for cell adhesion with good pattern stability (Nelson and Chen, 2002). However, this method does not generate a 3D adhesive environment as the cells are prevented from adhering to the sides of the microwells, which is desired for some investigations.

Inverted microcontact printing (Fig. 4.4b) was developed by Dusseiller *et al.* (Dusseiller *et al.*, 2005) and relies on the printing of a non-adhesive polymer onto the microwell plateau surface before backfilling with an adhesive protein. While the resultant coating was useful for the study of short-term cell processes (Ochsner *et al.*, 2007), we noticed instability of the adhesive / non-adhesive contrast when mesenchymal stem cells were cultured in the wells for more than 2 days.

Lovchik *et al.* (Lovchik *et al.*, 2008) introduced subtractive microcontact printing (Fig. 4.4c), where they removed the protein from a hydrophobic PDMS surface with a hydrophilic silicon-wafer and backfilled with BSA. However, it is not clear how efficient this method is as it resulted in cell clusters adhered non-specifically outside of the microstructures. In addition, there is no information on the long-term stability of this method, which can expected to be moderate because of the poor non-adhesive properties of a BSA-coated surface (Nelson *et al.*, 2003).

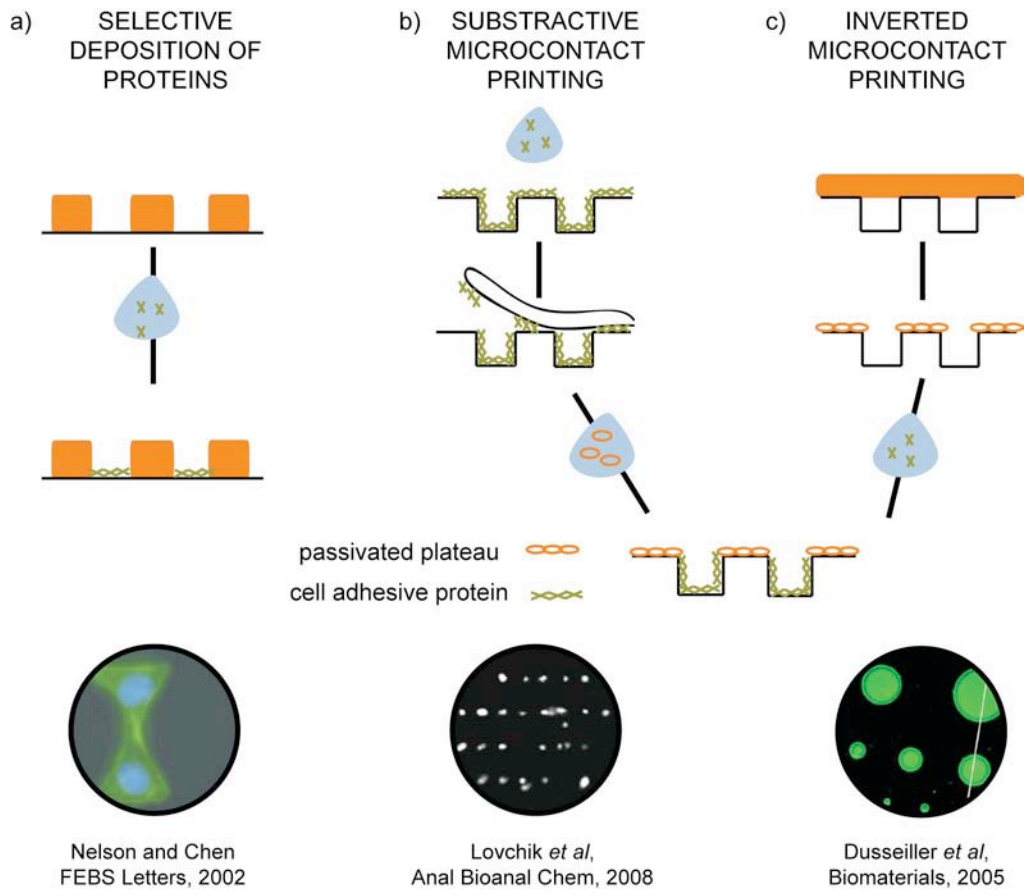

Figure 4.4: *Strategies to pattern microwells with protein only inside the microwells and surrounding areas with a non-adhesive coating.* a) The material contrast between glass and agarose was used to create selective deposition of protein only at the bottom of microwells (Nelson and Chen, 2002). b) In a first step the microwell platform is completely covered with a cell-adhesive protein. In a second step the protein on the plateau is removed (subtracted) and subsequent incubation in a BSA solution renders the plateau non-cell-adhesive (Lovchik *et al.*, 2008). c) First the plateau is passivated against protein adsorption via an inverted microcontact printing method and in a second step the cell-adhesive protein is adsorbed inside the microwell (Dusseiller *et al.*, 2005). This figure is adapted from the PhD Thesis of Dr. Mirjam Ochsner.

Generating non-adhesive contrasts by physisorption of Pluronic surfactants

PEO-PPO-PEO block copolymers, Pluronics have been previously used to render surfaces around protein patterns biopassive and showed the best performance on moderately hydrophobic substrates (Tan *et al.*, 2004). Pluronics self-assembles on hydrophobic surfaces to form a polymer layer with the hydrophobic block interacting with the surfaces and the two hydrophilic blocks extending into the aqueous solution (Fig. 4.5). Pluronics coatings of surfaces have the ability to suppress protein adsorption (Li and Caldwell, 1996). In the work of Li and Caldwell, the adsorption of fibrinogen on Pluronics-coated polystyrene beads was reduced to non-detectable levels.

In addition, various Pluronics have shown to adsorb on PDMS (Lee *et al.*, 2004) on which is also resulted in non-fouling properties (Boxshall *et al.*, 2006). Interestingly, optimum non-fouling properties of PDMS were obtained when Pluronics was adsorbed from solution with a polymer concentration marginally below CMC (critical micelle concentration) (Boxshall *et al.*, 2006). Pluronics has also been extensively used in cell patterning applications, for example to pattern endothelial cells on alkanethiol monolayers (Tan *et al.*, 2004) or mesenchymal stem cells on a polystyrene substrate (Tenstad *et al.*, 2010).

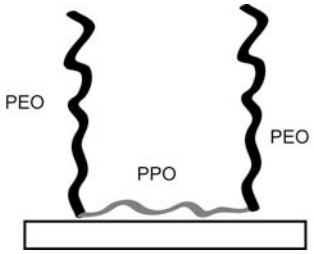

	Average MW	MW of PEO block	MW of PPO block
F-108	14600	1168	2920
F-127	1260	8820	3780

Figure 4.5: *Structure and adsorption behaviour of the Pluronics surfactants.* Triblock Pluronics are a class of block-co-polymers consisting of two hydrophilic poly(ethylene oxide) chains (PEO) and one hydrophobic poly(propylene oxide) chain (PPO). Different characteristics of the polymer can be obtained by varying the length of the different blocks. The PPO chain self-assembles on hydrophobic substrates by hydrophobic-hydrophobic interaction.

4.1.2 Motivation to study the effect of extrinsic cues on stem cell differentiation

Stem cells can be found both in the embryo and in adult tissue. Since methods for harvesting and *in vitro* culture emerged about a decade ago, stem cells have gained immense interest for the capability of differentiating into diverse specialized cells. One goal in stem cell research is therefore to use these cells for tissue engineering. Mesenchymal stem cells (MSCs) are multipotent cells that can differentiate into a variety of cell types including osteoblasts, chondrocytes and adipocytes. The development of distinct cell types from multipotent precursor cells is thought to occur in a two-phase process, comprising the commitment of a cell to a specific lineage, while retaining a certain degree of plasticity allowing trans- and de-differentiation, and terminal differentiation to become a specialized, functional cell (Oreffo *et al.*, 1998).

Encompassing a well-organized series of events, the gradual process of differentiation can be followed by monitoring different marker proteins being expressed at various time points. For osteogenic differentiation these comprise early genes, such as Runx2, bone-specific alkaline phosphatase and Col-I, as well as later genes, for example osteocalcin. Depending on the cues driving the lineage commitment, this progression

retains plasticity (Song and Tsuan, 2004) or is thought to arrest the cell in a differentiation-destined state (Engler *et al.*, 2006).

Previous studies have shown that adipogenesis versus osteogenesis is cell density-dependent phenomena (McBeath *et al.*, 2004). Further, using single cell patterns with a different size of the adhesive area it was shown that the culture of MSCs on small patterns, induced rounded cells and drove the commitment to adipocytes, while on larger patters the cells spread more and committed predominantly to the osteocyte lineage. Hence, physical cues, such as cell shape, have a dramatic effect on lineage commitment. 3D microwells could be used to study the role of cell shape and dimensionality on differentiation of stem cells.

4.2 Experimental section

4.2.1 Microwell array fabrication

The arrays of microwells were fabricated by soft lithography in PDMS as described in chapter 3, Materials and methods.

4.2.2 Surface functionalization

Subtractive micro-contact printing

PDMS microwell arrays (with and without plasma treatment) were coated with either unlabeled or fluorescently labeled Fn (25 μg ml^{-1} in PBS for 1 h at RT) (Fig. 4.6). Plasma treatment, if required, was performed in an air-plasma (PDC-002, Harrick Scientific, USA) at 0.8 mbar for 35s, and used to render the PDMS hydrophilic. The coated arrays were rinsed with H_2O and blow dried with N_2 just before stamping. Stamps for μCP were excised out of crosslinked PDMS sheets (1:10, curing agent to prepolymer). After plasma treatment of the PDMS stamps the surface was incubated with 2% 3-aminopropyldimethylmethoxysilane (Acros Organics, Belgium) in H_2O for 15 min. Subsequently, the stamps were rinsed with H_2O and incubated with glutaraldehyde (Sigma Aldrich), at 0.125% (v/v) in H_2O for 30 min (Goffin *et al.*, 2006). The stamps were rinsed again with water and dried in a stream of N_2 before being placed in contact with the Fn-functionalized microwell array.

Complete contact over the whole area was achieved by carefully pushing the stamp down with a pair of tweezers. After 30 sec the stamp was removed. The printing step was repeated 1-2 times to ensure complete removal of the Fn from the plateau surface. To enable hydrophobic recovery of the stamped areas the substrates were maintained for 24 to 48h at RT before further functionalization. The samples were sterilized with UV light in the sterile flow hood for 15 min. On the day of cell seeding Pluronic F-108 or F-127 (Sigma Aldrich) was adsorbed onto the substrates at 0.2 % or 0.04 %

(w/v) in PBS respectively. After 1h incubation, the substrates were rinsed with PBS and used for cell cultivation.

Visualization of the protein coating by immunohistochemistry

We also coated the microwell array with Col-I (40 µg/ml in 200 µl PBS). The protein removal from the plateau areas was performed as described above. To visualize the Col-I coating, the microwells were stained with a rabbit polyclonal anti-mouse collagen (1:100 for 1 h), rinsed with PBS before incubation in goat anti-rabbit Alexa 488 secondary antibody (1:200 for 1 h). The quality of the staining was visualized using an upright Zeiss microscope (Zeiss, Germany).

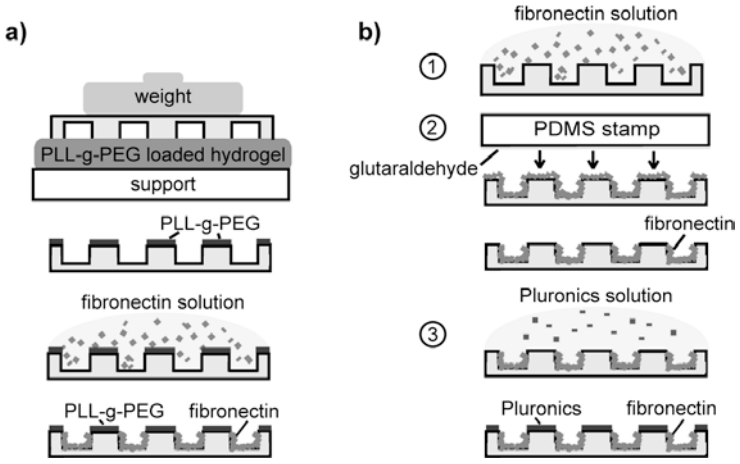

Figure 4.6: *Comparison of two procedures to pattern the PDMS microwell array with protein.* In the previously established patterning procedure (a) inverted microcontact printing was used to print PLL-g-PEG onto the plateau surface of the microwell array. This step was followed by adsorption of Fn on solution. Because of observed pattern instability of this method when cultures times over 2 days were required, a new patterning procedure was developed. The development of the new patterning procedure is described in detail in this chapter. It relies on the strong contact between Pluronics and hydrophobic PDMS. In this procedure (b) the microwell array is first coated with Fn from solution. In a second step, the dried protein coated surface is then placed in contact with a glutaraldehyde-coated PDMS stamp to remove the Fn on the plateau by covalent interaction between the NH_2-groups of the protein and the aldehyde groups on glutaraldehyde. Finally, the substrate was incubated in Pluronics solution to obtain a non-adhesive coating on the plateau areas, where the protein had been removed.

Patterning by microfluidics

A microfluidic approach was explored for the initial protein functionalization of the microwell array. A PDMS three-channel system with 100 µm wide channels and injection holes was moulded on a silicon wafer. The PDMS was cut into slices, each containing one of the channels systems. Holes for injection of liquid were made with

a hole puncher. Finally the PDMS was cleaned in isopropanol for 5 min in an ultrasonic bath, dried in a stream of nitrogen and then left to dry for additionally 4 h at RT to ensure complete evaporation of the isopropanol.

Then the channel system was mounted on top of the microwell array and treated with an air-plasma for 2 min. Finally a protein solution (Fn at 100µg ml^{-1}) was added to each injection hole and the solution allowed to enter the hydrophilic channels by capillary forces. After 1 h incubation, the system was demounted and rinsed. The Fn coating on the plateau surface could be subsequently removed with a glutaraldehyde stamp as described above, incubated in Pluronics and used for cell culture.

We also performed microfluidics in very narrow channels to evaluate a patterning approach based on microwells connected by small channels. The channels and the cover substrate were made hydrophilic either by; i) plasma treatment of channels mounted on the substrate for 2-4 min or ii) plasma treatment of channels and substrate separately. When the second approach was used, the channels were assembled with the substrate at least 1 h after treatment, in order to avoid covalent linkage. Capillary action was used to fill and coat the channels with a protein solution as described above. Before use, the substrates were incubated in a solution of Pluronic F-108 at 0.02 % in PBS for 1h.

4.2.3 Cultivation of cells on the patterned substrates

Testing the Pluronics contrast with different cell lines

The quality of the substrate passivation was tested, as renal epithelial cells (HRE) and NIH-3T3 fibroblasts were seeded on the substrates. These cells were considered suitable for this test as they spread well on fibronectin and are highly motile. The cells were maintained in culture as described in Materials and Methods, Chapter 3. Cells were seeded onto the different substrates, after sterilization and incubation in Pluronics, at a concentration of about 20 000 cells per cm^2. After completed culture time, ranging from 1-7 days, cells were fixed and stained for the actin cytoskeleton. First, the samples were fixed in 3% formaldehyde for 10 min. Then they were permeabilized with 0.1% Triton X-100 for another 10 min and finally stained with Phalloidin Alexa Flour 488 or 633 (1:400 dilution; Molecular Probes, Switzerland). The cell spreading on the substrates was imaged with an Olympus confocal microscope using a 10x air or a 40x water objective.

Isolation and culture expansion of hMSC

The study of mesenchymal stem cells differentiation was conducted by Markus Rottmar, Empa St Gallen, Switzerland. My contribution to this work was the

development of the new single cell platform. The planning, conducting and interpretation of the work with the mesenchymal stem cells was entirely performed by Markus Rottmar.

Human bone marrow stromal cells (MSC) were isolated as described previously (Oreffo *et al.*, 1998) from bone marrow specimens of a patient (female, age 58) undergoing hip surgery after informed consent. In brief, samples including trabecular bone pieces were incubated in isolation medium (25 mM HEPES, 128.5 mM NaCl, 5.4 mM KCl, 5.5 mM D(+)-glucose, 51.8 mM D(+)-saccharose, 0.1% BSA) over night at 4°C before centrifugation at 110×g for 15 min. The supernatant was discarded and the pellet washed several times to rinse out cells from the bone pieces. After filtrating the cell suspension three times through a 200µm filter and subsequent centrifugation at 110×g for 15 min, the pelleted cells were resuspended in expansion medium (α-MEM supplemented with 10 % FBS, 1% PSN, 1 ng/ml FGF-2) and 10^7 cells were seeded into T75 culture flasks. After 24 h the non-adherent cells were removed and medium was changed twice weekly thereafter. Cells were subcultured pre-confluent and used at passage one for experiments.

Osteogenic differentiation

HBMC were seeded at a density of 240 cells cm^{-2} in Petri dishes (P60) in either expansion or osteogenic medium (α-MEM supplemented with 10 % FBS, 1 % PSN, 10 nM dexamethasone, 50 mM ascorbic acid phosphate, 2 mM β-glycerophosphate and 10 nM 1,25-dihydroxyvitamine D_3) for 18 days before subculturing at the same density in either osteogenic or expansion medium for one or seven more days. Cells were fixed and permeabilised with 4% Paraformaldehyde/0.2% Triton X-100 for 8 min and stored in PBS without glucose until stained for bone specific alkaline phosphatase (bALP) (1:1000, Developmental Hybridoma Bank, B4-78), actin (phalloidin, 1:40, Molecular Probes, B607) and DAPI (4,6-Diamidino-2-phenylindole, 1:1000, Sigma Aldrich D9542).

Seeding hMSC onto the microwell array

After surface functionalization the 3D microwells were rinsed extensively with sterile PBS, which was thereafter replaced with either expansion or osteogenic medium. Human bone derived MSC were harvested and seeded at 10'000 cells per microwell array (~1 cm^2). The cells were allowed to settle for 15 minutes before washing off the non-adhering cells with the respective medium and were cultivated at 37°C / 5% CO_2 for seven days. Medium was changed every 2-3 days.

4.3 Results and discussion

4.3.1 Development of a novel single cell array platform

When inverted microcontact printing of PLL-g-PEG was used to generate the microwell platform we observed impaired pattern fidelity after only 2 days of cell culture (Fig. 4.7). Therefore we decided to explore the possibility to develop a new patterning method. This work is focused on contrast generation by the stable interaction between Pluronics surfactants and native PDMS.

Pluronics is a block-co-polymer that adsorbs with the middle, hydrophobic PPO chain onto hydrophobic substrates, such as PDMS. The hydrophilic side chains will extend into an aqueous solution to form a highly hydrated brush-like polymer structure. Hence, the principle for inhibition of protein adsorption is the same for PLL-g-PEG and Pluronics. The difference between the two polymers lies in the binding to the substrate. This work relies on the hypothesis that Pluronics could be more stable than PLL-g-PEG on the PDMS surface, because it binds to the native state of PDMS. In contrast, PLL-g-PEG binds only to negatively charged substrates, which can be achieved by plasma treatment of PDMS.

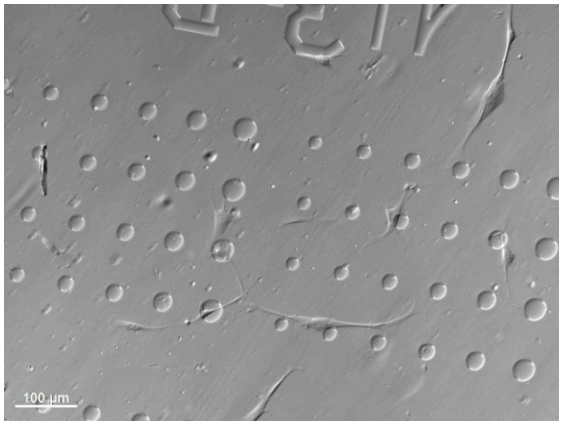

Figure 4.7: *Failure of PLL-g-PEG printing strategy for long-term cell culture.* A PDMS substrate was coated with PLL-g-PEG and Fn using inverted micro contact printing as described in Fig. 6a. When mesenchymal stem cells were seeded on the array, the cells first adhered within the wells but as little as 2 days after seeding, mesenchymal stem cells started to grow on the plateau of microwell array. An example of the failed cell patterning is shown in this DIC image of mesenchymal stem cells cultured on a substrate with round microwells of different size. Image courtesy of Marcus Rottmar, Empa St Gallen.

Initial investigation of the protein / Pluronics contrast

We first examined the ability of a protein / Pluronics contrast on PDMS to control cell adhesion. The contrast was obtained by treating a PDMS substrate with an air-plasma and incubating it in a Fn solution, with a part of the substrate covered by another piece of PDMS. After removal of this cover, the substrate was incubated in Pluronics, which should theoretically absorb only on the covered, and thus hydrophobic, region of PDMS. A fluorescent image of the substrate showed that Alexa Fluor 488 conjugated Fn adsorbed only in the areas of the PDMS substrate that had not been covered by the PDMS substrate (Fig. 4.8a). We then went on to test the quality of the

engineered adhesive/non-adhesive contrast. Indeed, the Pluronics coating was very efficient at inhibiting cell adhesion. 7 days after seeding renal epithelial cells on the patterned substrates, cells were still restricted to the part of the substrate, which was coated with Fn and no cells were observed on the Pluronics-coated areas (Fig. 4.8b).

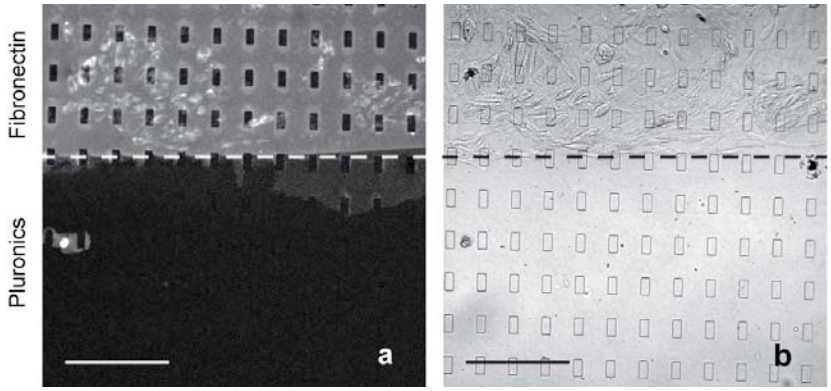

Figure 4.8: *First test of the Pluronics / protein contrast.* A microstructured PDMS substrates, was covered to 50 % by a PDMS substrate during plasma treatment and Fn adsorption. The covered area is shown in the lower parts of (a) and (b). The image (a) is a fluorescent image of the fibronectin staining and the image (b) is a transmission image showing the cultured cells. As can be expected, Fn was only present on the substrate in areas which had not been shielded by the PDMS cover, as shown by the fluorescent signal of adsorbed Fn-Alexa Fluor 488 conjugate (a). After 7 days in culture, renal epithelial cells were highly confluent, but still stayed strictly on the Fn-coated area (b). Scale bar is 100 µm.

Development of a subtractive printing method with Pluronics backfill

To use the Pluronics / protein contrast for patterning of the microwell array we used an inverted coating procedure, in which protein is first adsorbed on the sample and subsequently removed in a printing step. We used an optimized version of the previously described procedure for subtractive microcontact printing (Lovchik *et al.*, 2008). The new protocol is described in Fig. 4.6b, next to the method for inverted micro-contact printing of PLL-g-PEG (Fig. 4.6a). In this subchapter we describe the development towards the final coating procedure.

First we investigated the role of the wettability of PDMS on Fn adsorption. It was observed that adsorption onto hydrophilic, plasma treated PDMS resulted in a coating with higher protein surface density compared to when the protein was adsorbed onto hydrophobic PDMS. This can be observed by comparing the contrast between the Alexa Flour 488 labelled Fn and the background in images 9 and 10.

A major problem with the Fn coating of hydrophobic PDMS, was poor filling of microwells (Fig. 4.9a), obviously a consequence of low degree of wetting and trapped air, hindering the protein solution to enter these small cavities.

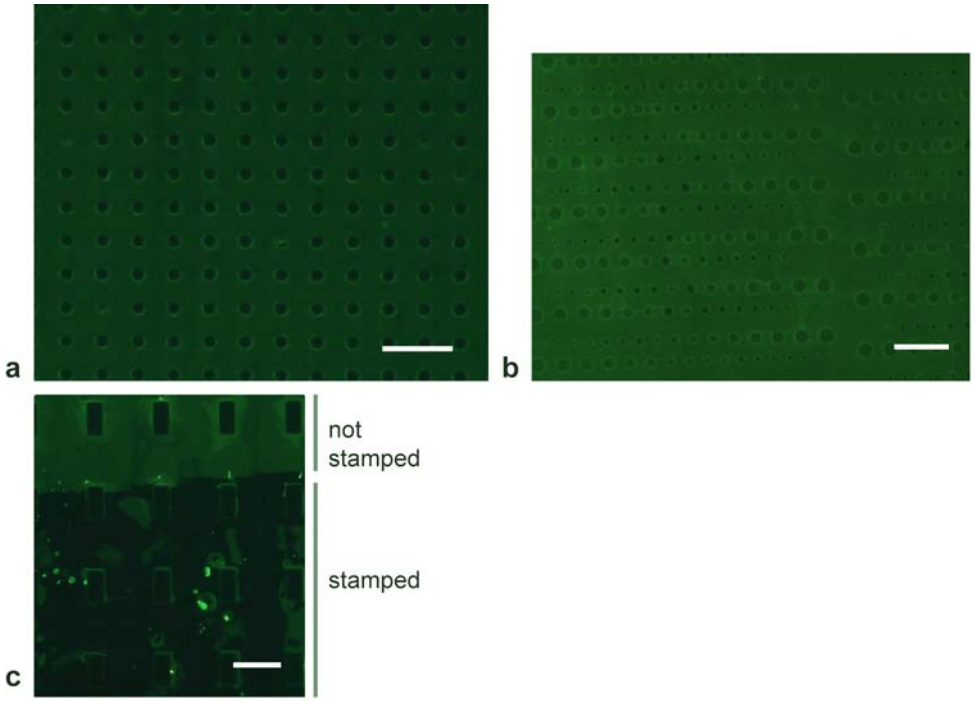

Figure 4.9: *Surface functionalization of hydrophobic PDMS.* Widefield fluorescence microscopy images of Alexa-Fluor labelled Fn on hydrophobic PDMS substrates. Adsorption of Fn from solution onto hydrophobic substrates resulted in a coating with low contrast between coated and uncoated areas (a,c). The low contrast indicates the coating is thin. One problem that occurred when adsorbing Fn onto hydrophobic PDMS was that the microwells were poorly filled with the protein solution (a). This can be partly solved by removing the gas bubbles in a desiccator (b). Fn adsorbed on hydrophobic PDMS can be removed by contacting with a plasma-treated, hydrophilic, PDMS stamp. After stamping one can clearly detect the area of contact, but with some patches of Fn left on the substrate (c).

This problem was partly solved by placing the sample in a desiccator, during the Fn adsorption step. As can be seen in Fig. 4.9b, the wells are also fluorescently stained, but with a lower signal when compared to the plateau regions.

Filling the holes with the Fn solution was revealed to be a delicate process, as Fn easily polymerizes into fibers at the liquid/air interface of bubbles (data not shown). This problem could be partly solved by first filling the microstructures with buffer and then exchange to a protein solution. Preliminary results show that it was possible to remove Fn from the hydrophobic PDMS surface with a hydrophilic PDMS stamp, even if there were areas at which Fn coating still remained (Fig. 4.9c). However, because of the mentioned drawbacks of Fn adsorption on hydrophobic PDMS substrates, we decided not to further investigate this approach.

Fn adsorption onto the PDMS microwell array after plasma treatment generated an even coating, which was clearly also present inside the microwells (Fig. 4.10a). Removal of Fn coating on a hydrophilic substrate was achieved by the use of a glutaraldehyde-coated substrate. Glutaraldehyde is a simple bi-functional crosslinker

that crosslinks proteins by covalent attachment to their NH_2-groups. It has therefore been used in multiple applications as a fixing agent, but also for covalent attachment of proteins to surfaces (Kubow *et al.*, 2009). The principle relies the initial functionalization of the surface with aminosilane. Glutaraldehyde can then act as a crosslinker with one aldehyde group binding to the surface and the other to the protein.

Initially, we tested glutaraldehyde-functionalized glass slides to stamp the array. However, these often did not cover the whole array because of an uneven PDMS surface and sometimes broke. Therefore glutaraldehyde-coated PDMS stamps were used instead, which were flexible enough to conform to a slightly uneven surface. A crucial step for efficient removal was to dry both substrates completely before stamping. However, when this parameter could be controlled, a good protein contrast between the wells and the plateau was obtained, as shown by the differing signal

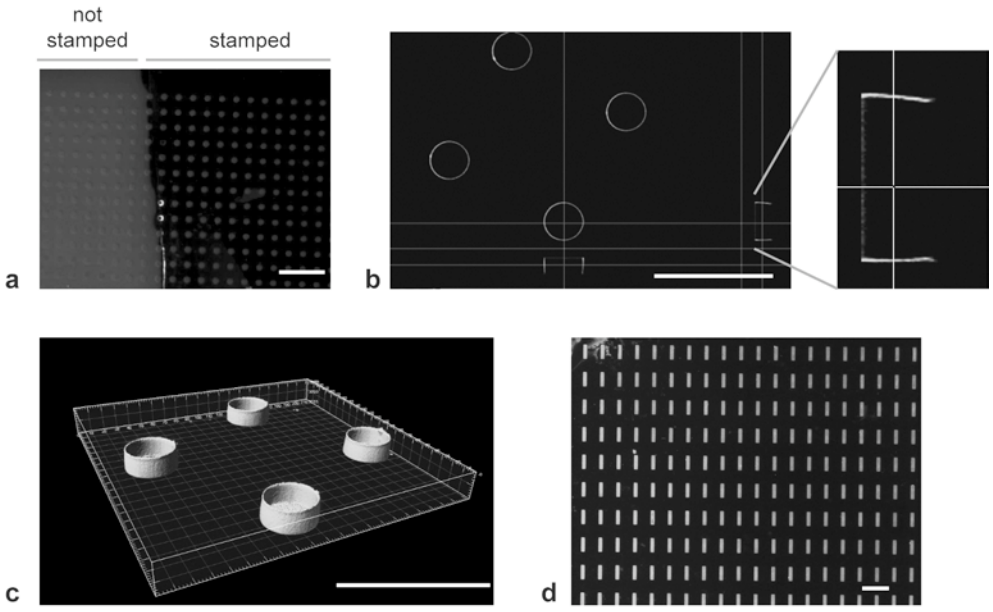

Figure 4.10: *Surface functionalization of hydrophilic PDMS using subtractive micro-contact printing.* Widefield fluorescence microscopy images of Alexa-Fluor labelled Fn on hydrophilic PDMS substrates. Microwell arrays were treated with an air-plasma and subsequently Fn was adsorbed onto the substrates from solution. This generated a homogenous Fn coating that was clearly visible in a fluorescent microscope. Stamping with a glutaraldehyde functionalized PDMS stamp for 30s removed the Fn from the plateau surface with a strong contrast to the microwells (a). Z-stacks of the fluorescent coating were taken after removal of Fn from the plateau by printing with glutaraldehyde-coated stamps. The intensity profile of a microwell show that no Fn is present on the plateau surface (b). The image was further processed in the Imaris software to better visualize the coating. By interpolation, a surface area was rendered (c). This image further confirms that the sides and the bottom of the microwells are homogenously coated with Fn, while no protein can be detected on the plateau surface. Finally, the coating procedure is compatible with large surface areas, as shown in (d). Scale bars are 100 μm.

intensity of the fluorescent Fn coating (Fig. 4.10b). The low fluorescence intensity on the plateau surface demonstrates that most Fn was removed from the plateau in the μCP step. Surface area visualization, constructed in the Imaris software, shows that the wells are evenly coated at the bottom and on the sides (Fig. 4.10c). The new method for subtractive micro-contact printing was shown to be compatible with large surface areas (Fig. 4.10d). We created patterned areas of up to 4 cm^2 with retained pattern quality, but it may be possible to create even larger surface areas. To test the versatility of this method we conducted the same protocol for patterning of Col-I. The resulting coating, as visualized by immunohistochemistry, was homogenous and showed a similarly good contrast between the wells and the plateau, as obtained with Fn (Fig. 4.11).

The final protocol for patterning of the microwell array with Pluronics backfill, described in Fig. 4.6b, was based on a recently published protocol for subtractive microcontact printing (Lovchik *et al.*, 2008). However, the new protocol was optimized for the microwell platform by adjusting the published methodology in three ways. Firstly, we adsorbed Fn onto plasma-treated, hydrophilic PDMS instead of hydrophobic. Fn adsorption on hydrophilic substrates has been shown to produce a protein coating with superior cell adhesion qualities (Tan *et al.*, 2004). Secondly, the use of a flexible glutaraldehyde-functionalized stamp instead of a rigid Si-wafer should ensure reliable removal of Fn by good conformation capabilities and covalent protein binding. Thirdly, in this new process Pluronics instead of BSA is used for the non-adhesive coating, which has shown to have better long-term pattern stability (Nelson *et al.*, 2003).

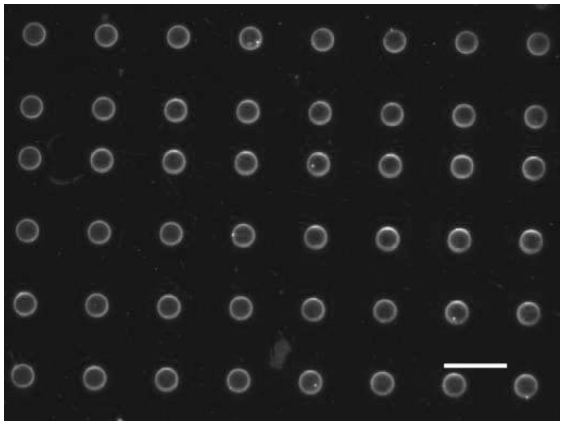

Figure 4.11: *Coating the microwells with Col-I.* After Col-I adsorption on the plasma-treated PDMS stamp, protein was removed from the plateau surface by subtractive microcontact printing. Areas without Col-I were rendered non-adhesive by incubation in a Pluronics solution. Finally immunohistochemistry was used to visualize the localization and homogeneity of the protein coating. Using a secondary Alexa Fluor 488 conjugated antibody we can clearly see that the Col-I is present inside the microwells with almost no protein on the plateau. Scale bar is 100 μm.

4.3.2 Multiplexed microwell protein array for single cell studies

The microwell array can be a useful tool to study dimensionality-dependent cell responses. However, the current setup allows the testing of only one experimental condition at a time. If it would be possible to create several areas of different protein composition per array, several conditions could be tested in parallel. This is important when studying complex biological processes and may lead to wider use of this platform. One way to generate multiple protein coatings per chip is by the use of patterning with microfluidics. The feasibility of this approach was tested with a setup in which a three- channel system with 100 µm wide channels was mounted on top of the microwell array (Fig. 4.12a).

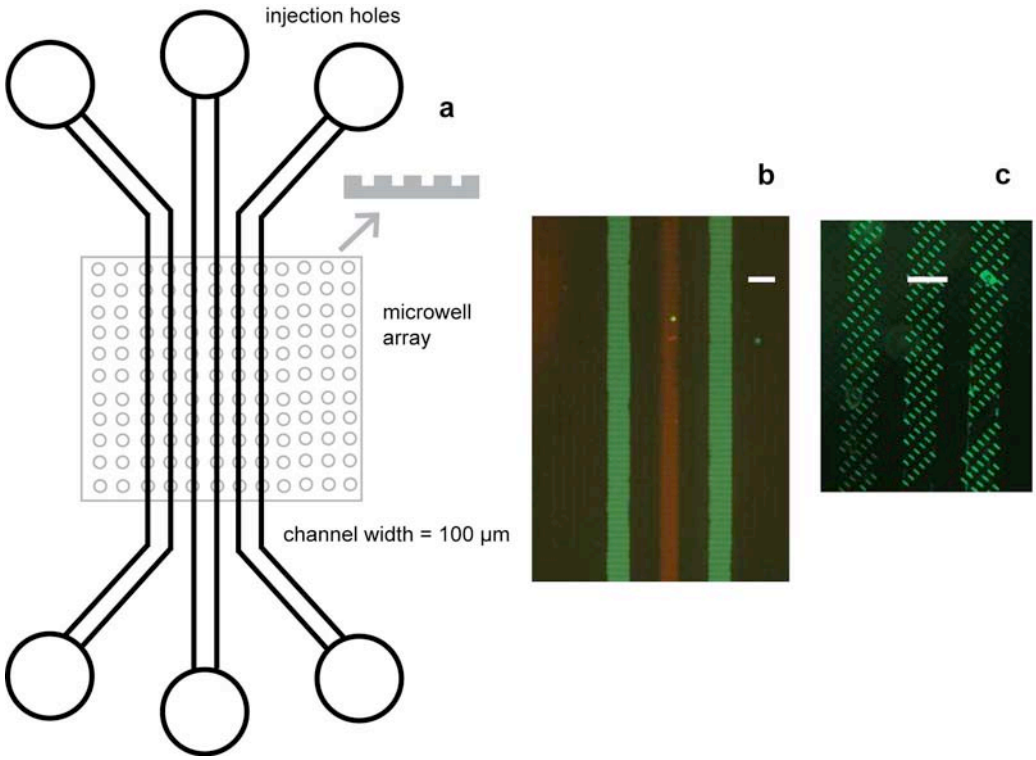

Figure 4.12: *Multiple protein patterning of a microwell array.* A microfluidic approach was tested for the patterning of the microwell array with different proteins in different areas of a microwell array. A PDMS channel system consisting of 3 x 100 µm wide channels with respective inlet and outlet was mounted on top of the microwell array (A). Three solutions were added, one at each inlet hole, which entered and filled the channels by capillary forces. The result was a microwell array with protein coating only in the areas covered by the channels (B). In this image solutions of Fn (100µg ml^{-1}) labelled with Alexa Fluor 488 (green) or Alexa Fluor 543 (red) were used. The substrates were subsequently rinsed in H_2O and dried. Finally, the protein was removed from the plateau surface by printing with glutaraldehyde-coated stamps (C). In this image only Fn labelled with Alexa Fluor 488 was used. Scale bars are 100 µm.

The assembled structure was treated with an air-plasma to render the inside of the channels hydrophilic. When different protein solutions were added at the injection holes, the solutions entered the channels by capillary forces. We used Fn-solutions with different fluorescent labels, to confirm that solutions were not mixed. After 1 h incubation, the substrate with the channels was removed and the microwell array rinsed with PBS.

A protein coating was clearly visible on the microwell array only in the areas, which had been in contact with the channels (Fig. 4.12b) and it was clear that the solutions could be separated by this methodology. In addition, we confirmed that the three solutions could be separated from each other. We further showed that this methodology could be combined with subtractive printing (Fig. 4.12c) to theoretically generate a large number of areas on a chip in which microwells are functionalized with different proteins.

There are many ways to generate ECM arrays, using for example spotting techniques (Flaim *et al.*, 2005). However, with the new platform it would be possible to investigate the role of the cell-ECM interaction in 3D cultured cells. This could become a promising tool for the screening of adhesive-dependent cell behaviour, such as differentiation and drug response. This topic was not further developed in this thesis, as the main direction was the application of controlled cell culture platforms for drug testing.

4.3.3 Osteogenic differentiation of single cells in 3D microwells

The culture of mesenchymal stem cells within the microwells was used to test the long-term stability of the new platform. Differentiation of stem cells into different lineages is a process that can take 1 – 2 weeks. This study was conducted by Markus Rottmar, Empa St Gallen, Switzerland. My contribution to this work was the development of the new single cell platform. The planning, conducting and interpretation of the work with the mesenchymal stem cells was entirely performed by Markus Rottmar.

Primary MSCs were cultivated in square shaped microwells, a shape shown to promote osteogenesis of single cells on 2D patterns (McBeath *et al.*, 2004). MSCs retained the cell shape given by the well for up to seven days in culture, which could be observed by staining for actin filaments (Fig. 4.13a and b). This result is in contrast to the results obtained with the previously established platform, based on PLL-g-PEG stamping, where cells were no longer confined to the microwells less than 2 days after seeding (Fig. 4.7). As individual cells can vary in volume, not every cell completely filled the wells. We further observed that single, as well as multiple cells, can bridge between functionalized wells, which was due to the close proximity (20µm edge to edge distance) of the individual microwells, as well as due to the presence of small

clusters of cells during the initial cell seeding procedure. Increasing the spacing between the individual wells to at least the same distance as the well diameter completely abolished the unwanted bridging of cells (unpublished observations).

When cultivated within the square shaped microwells for seven days, single isolated cells stained positive for bone-specific alkaline phosphatase only when provided with osteogenic stimuli (Fig. 4.13b). No staining for bALP could be observed when these stimuli were absent in the medium. Single primary MSC can therefore commit to the osteogenic lineage and are not hampered by the three-dimensional nature of the microwells when cultivated in osteogenic medium.

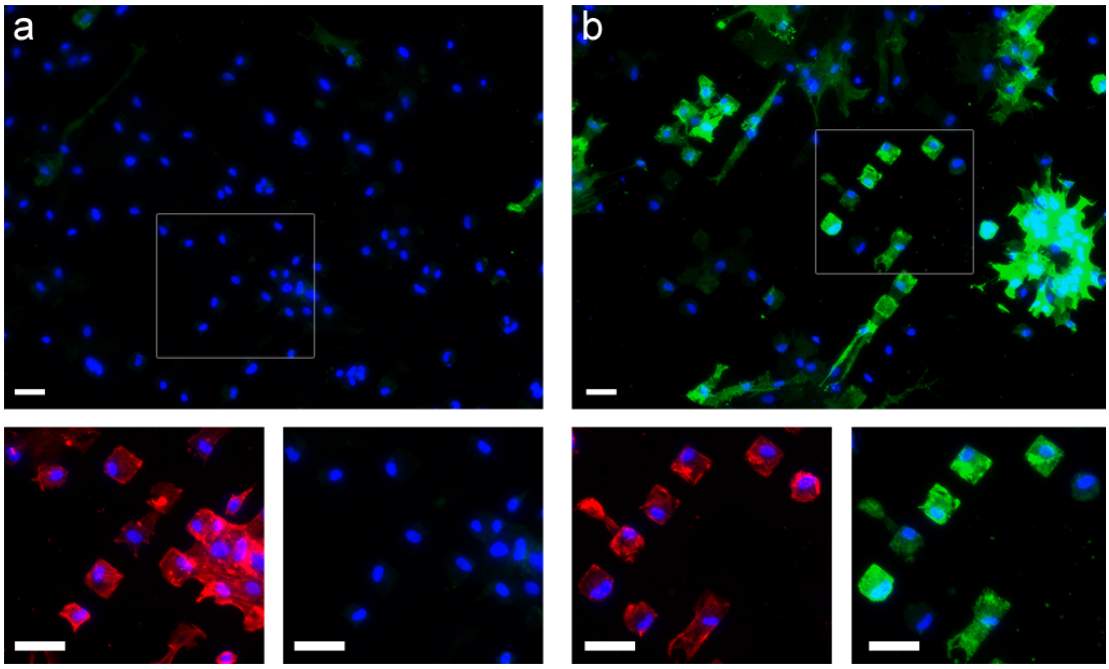

Figure 4.13: *Osteogenic differentiation of single stem cells in microwells*. After 7 days in square shaped microwells coated with Fn, some HBMCs are still successfully constrained to the microwell. The different images show the cells cultured in expansion (a) or osteogenic (b) medium and subsequently stained for bALP (green), actin (red) and the nucleus (blue). The bALP staining of the cells in microwells show that cells are able to differentiate to the osteogenic lineage, although constrained to the microwells. The lower images show the areas within the white square with higher resolution. Scale bars are 50 µm. These images are reprinted in courtesy of Markus Rottmar (Empa) who performed all the work with the mesenchymal stem cells.

4.4 Conclusions

Initial results showed that the novel platform allowed for long-term cultivation of single cells. Mesenchymal stem cells showed good confinement to 30 μm wide microwells after 7 days in culture. The improved pattern fidelity over time compared to the old method based on inverted microcontact printing of PLL-g-PEG, could probably not be explained by a single factor. The reason for failure of the old strategy during long-term cell culture is most likely due to the PLL-g-PEG coating. The stamping of PLL-g-PEG onto plasma treated PDMS may be a sensitive process that is dependent on a stable plasma source and a good contact between the PLL-g-PEG loaded stamp and the PDMS surface. Imperfections in the PLL-g-PEG coating on a hydrophilic PDMS substrate can be expected to lead to immediate protein adsorption, in these areas, and subsequent cell adhesion. PLL-g-PEG is also sensitive to degradation, however degradation should not occur within the tested time frames. Lussi *et al.* found that pattern stability of PLL-g-PEG coatings was substrate-dependent, and further was dependent of the presence of serum (Lussi *et al.*, 2006). Therefore, it may be that if PLL-g-PEG is not strongly adsorbed on PDMS it may be exchanged by serum protein over time.

We hypothesize that both the interaction of the PEO-based non-adhesive layer with the PDMS through strong hydrophobic-hydrophobic forces between PPO and hydrophobic PDMS, as well as the hydrophobic nature of the underlying substrate play important roles for the success of the new patterning strategy. It is known that hydrophobic PDMS substrates only poorly supports the adhesion of several cell types (De Silva *et al.*, 2004) potentially making any defects in the non-adhesive layer less problematic in comparison to when a non-adhesive layer on a hydrophilic substrate is used. The proven long-term stability of the new platform makes it suitable to study processes, such as stem cell plasticity and lineage commitment. The 3D environment of the microwell array allow for high control of extrinsic parameters, such as dimensionality, biochemical coating and mechanical properties of the environment. Therefore this platform may lead to new insight in the role of extrinsic parameters on stem cell differentiation.

Furthermore we showed that the new patterning strategy is compatible with multiple coatings on a chip, as achieved by simple microfluidic patterning. Hence, in combination these two techniques could enable the testing of several extrinsic cues per chip.

4.5 Outlook

Even though the developed patterning method showed very promising results for long-term cell culture, it also has some drawbacks. The preparation of stamps is a tedious process and it is difficult for a person who is not already trained in micropatterning to perform the stamping procedure. Therefore, we were motivated to continue the development, towards a methodology for more rapid functionalization of a 3D array with adhesive / non-adhesive contrasts.

4.5.1 Rapid fabrication of a protein / non-adhesive contrast

One idea would be to connect the microwells by small channels, 5 µm in width, hence creating a large connected channel system. (Fig. 4.14) This would enable microfluidic functionalization of these areas with protein. Using different injection holes connected to the channels, it would even be possible to functionalize one chip with a large number of different coatings.

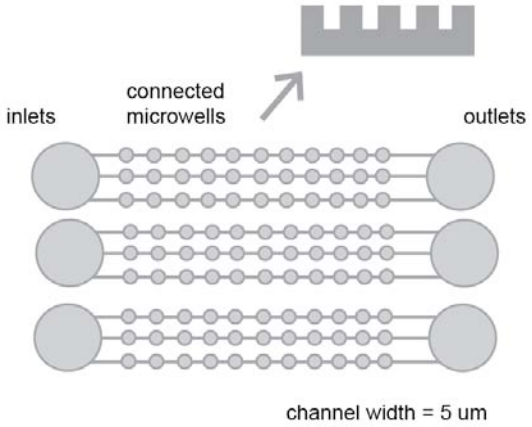

Figure 4.14: *Proposal for a new array design with connected microwells.* With narrow channels connecting the microwells, here 5µm, microfluidic patterning could be used to coat the surface of the microwells with protein. The aim of this approach is to provide a fabrication method that is faster and easier to use for unexperienced users. In addition, this approach may offer a higher reproducibility of the substrate pattern than the developed patterning method, as it does not rely on a stamping step.

The first step in the development of this method was to evaluate the optimum method to create hydrophilic and protein-coated channels and a hydrophobic, Pluronics-coated plateau surface. Covering the channel network with a PDMS cover, it would be possible to use an air-plasma to treat the surface of the channels only. However, air plasma is not very efficient in penetrating long, narrow channels and hence another system such UV-ozone treatment (Nelson *et al.*, 2003) or chemical treatment in solution could be more useful.

Another possibility that was investigated was to treat the substrate with the channels and the cover separately with air-plasma. If the substrates are not immediately

assembled, they did not covalently bond. Our initial results show that this may be a simple approach to generate hydrophilic channels for microfluidic coating with protein (Fig. 4.15a). After hydrophobic recovery and incubation with Pluronics, 3T3 cells showed preferential adhesion in the microchannels (Fig. 4.15b). To further evaluate this approach for contrast generation a new photolithographic mask, that contains microwells connected by channels, would need to be produced.

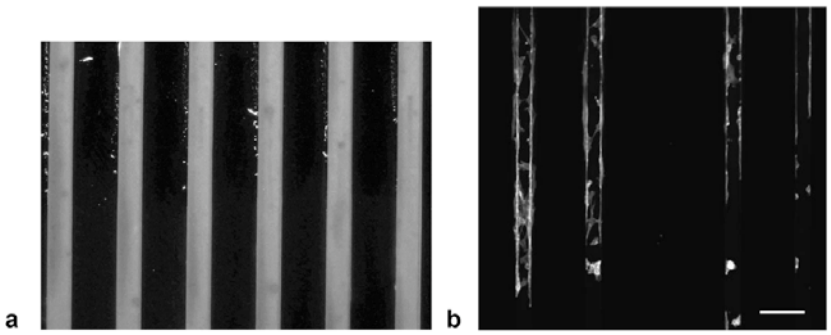

Figure 4.15: *Feasibility test for the connected microwell system.* 50 µm wide channels were treated for 30s with an air-plasma before mounting them on a glass slide. The channels were filled by capillary force with a 100 µg ml^{-1} Fn-Alexa Fluor 488 solution. This procedure resulted in a protein coating only inside the channels (a). The protein samples were then left for >24 h at RT before they were UV-sterilized and incubated with Pluronics. 3T3 cells that were seeded onto the substrates adhered preferentially inside the microgrooves, as shown by the phalloidin-staining of the actin cytoskeleton (b). Scale bars are 100 µm.

CHAPTER 5

Engineered 3D environments to elucidate the effect of environmental parameters on drug response in cancer

In the previous chapter a new single cell platform based on a PDMS microwell array was presented. The improved surface patterning allowed the culture of cells in controlled 3D conditions for up to a week. This opens up the possibility of new applications for the microwell array, including its use as an *in vitro* model for drug testing. This application would be particularly interesting in an area where the microenvironment has been shown to play a key role. Drug response in cancer is one area that may encompass many interesting questions to the role of the microenvironment. There is increasing evidence, that signaling from extrinsic parameters is important in the response to anti-cancer drugs (Meads *et al.*, 2009).

There are several 3D *in vitro* models present for cancer. However, these models seldom enable the study of different extrinsic parameters independently. Therefore we decided to evaluate the microwell array as a reductionist approach to study the effect of different extrinsic parameters on the response of cancer cells to anti-cancer drugs.

As a model experiment we studied Taxol-induced apoptosis in breast carcinoma cells. In section 5.3.3 the use of the microwell array to investigate the effect of the 3D culture on Taxol response is presented. In addition, we investigated the role of matrix composition together with dimensionality. By controlling the cluster size, the role of cell-cell contacts on cellular response could be determined, as outlined in section 5.3.4. In a central experiment we compared the results obtained using this model to a more complex 3D Fn matrix, which has been previously used as an *in vitro* model of the tumour stroma (Serebriiskii *et al.*, 2008). These results are presented in section 5.3.5. The results in this chapter have been previously published (Håkanson M., Charnley, M. and Textor, M., 2011), except for the Taxol adsorption studies (section 5.3.1).

5.1 Background

A central reason for the low predictivity of patient outcome of current *in vitro* models is their inability to mimic key aspects of the *in vivo* environment of cancer cells. Pharmaceutical companies are still using 2D cell cultures in the early screening process, which do not accurately reflect the physiological environment of the tumour *in vivo*. Hence, in order to improve the *in vivo* to *in vitro* translation efficiency, we need to increase our understanding of the effect of intrinsic factors on drug response and further develop new culture models that better mimic the *in vivo* environment.

5.1.1 *In vitro* models that can be used to understand the role of the microenvironment on drug response

There are several *in vitro* cancer models available. One of the oldest and most used is the multicellular tumour spheroid (MCTS) model (Sutherland, 1988) (Fig. 5.1a). MCTS are formed by culturing cells in a non-adhesive environment and can be composed of one or more cancer cell types. These experimental models are appreciated, because they resemble a cancer *in vivo* environment. In a size-dependent manner, nutrient and metabolite gradients will form similar to in a non-vascularised tumour (Friedrich *et al.*, 2007). MCTS obtain these characteristic at a size of several hundreds μm in diameter.

Another possibility to model the 3D cancer environment is to use porous polymeric scaffolds (Fig. 5.1b). This can be an advantageous approach as such scaffolds are easy to handle and to reproduce and have shown to induce *in vivo* like behaviour (Fischbach *et al.*, 2007). Growth within a scaffold showed to induce a more *in vivo* like metabolism in cells (Dhiman *et al.*, 2005) and enhanced their malignant potential (Fischbach *et al.*, 2007).

Bissell and co-workers came to many of their discoveries of morphogenesis in the mammary environment and carcinogenesis using a model based on the 3D culture of cells embedded within or on top of matrigel (Weaver and Bissell, 1999) (Fig. 1c). Matrigel is a protein matrix derived from sarcoma in mouse, which main components are Col-IV and Lam-I. It therefore serves as a good model of the basal lamina surrounding epithelial cell and early tumours, but suffers from batch-to-batch variations due to its *in vivo* origin.

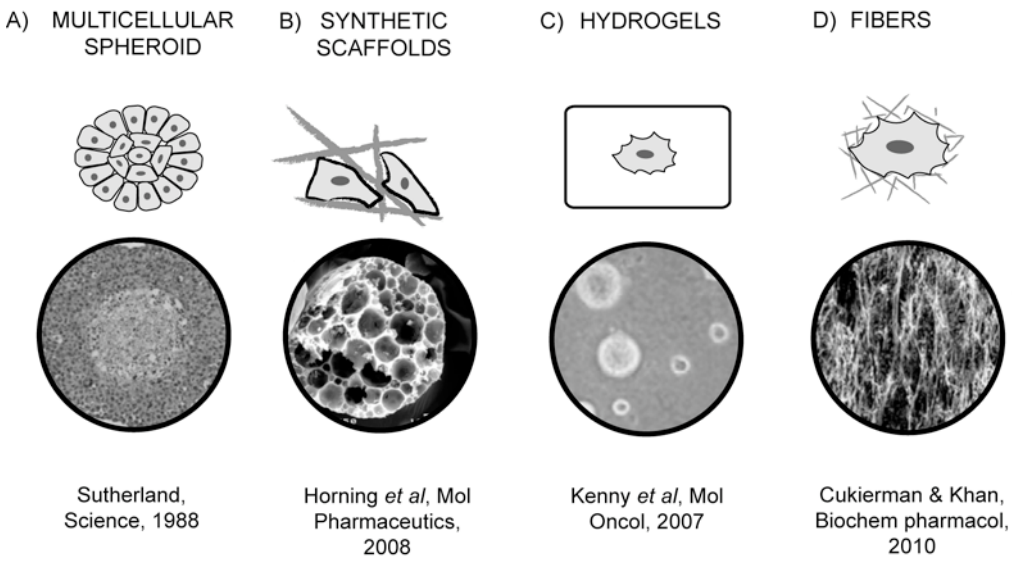

Figure 5.1: *3D cell culture models in cancer research.* A) In the multicellular spheroid model, the cell itself provides the 3D environment for other cells. This system shows an intermediate complexity with *in vivo* characteristics such as for example oxygen and metabolism gradients (Sutherland, 1988). B) Synthetic scaffolds composted of hollow ceramics, fibers etc. can be used as inert 3D models. Current methodologies allow for control of pore size (Horning *et al.*, 2008). C) Hydrogels made of synthetic or biological polymers can be used as a 3D scaffold. By control of crosslinking ratio of such system, rigidity can typically be controlled to be in the range of tissue. In addition, Col-I and matrigel form hydrogels that have an *in vivo*-like biochemical composition (Kenny *et al.*, 2007). D) Finally, cell derived matrices may be even more relevant, as they are derived directly by mesenchymal cells from the stroma. It has for example been shown that cells from different stages of cancer progression derive differentiating matrices (Cukierman and Khan, 2010).

In later stages of breast cancer, the cancer cells come in contact with the activated collagenous stroma. Hence, another very relevant model is to culture the cells within a Col-I gel. With this approach Gudjonsson *et al.*, found that normal epithelial cells could not polarize into their normal structure in this environment, and in addition that Lam-I signaling was enough to rescue this situation (Gudjonsson *et al.*, 2003). This observation would clearly not have been possible on 2D TCPS. Castello-Cros *et al.*, took this model one step further by using a cell-derived protein matrix (Castelló-Cros *et al.*, 2009) (Fig 5.1c). After decellularization of the matrix, a 3D protein matrix is obtained that can be used for reseeding of cancer cells. Hence, this is an approach with high *in vivo* relevance. Different cells can be used to produce a matrix that is specific for the type and stage of cancer to be studied.

5.1.2 Extrinsic parameters that have shown to influence drug response

Dimensionality

It has long been known that cells in 3D multicellular tumour spheroids (MCTSs) typically have a lower susceptibility to cytotoxic drugs compared to cells grown on 2D substrates (Durand and Olive, 2001). The altered drug response in these models has been argued to be an effect of lower drug penetration, development of a hypoxic core and decreased growth. (Friedrich *et al.*, 2007) The reduced drug response in a 3D environment was also observed in synthetic 3D scaffolds, where it was explained by a more *in vivo* like phenotype compared to the cells in standard 2D culture (Dhiman *et al.*, 2005) (Fischbach *et al.*, 2007).

Cell-cell contacts

Closely related to dimensionality is the parameter of cell-cell adhesion. Increased signaling from enhanced cell-cell contacts in 3D culture could be one important factor in the reduced drug responsiveness in spheroids, (Ivascu and Kubbies, 2007) which could in turn be the determinant of decreased growth (St Croix *et al.*, 1998). Indeed, it has been shown that in the presence of E-cadherin interfering antibody, cells within spheroids were sensitized to several chemotherapeutic drugs (Green *et al.*, 2004).

Matrix adhesion

The composition of the ECM is another parameter that has shown to have an important effect on drug response. In initial work it was found that the growth of cancer cells on flat substrates coated with different ECM proteins affected their response to anti-cancer drugs (Aoudjit and Vuori, 2001). A recent paper uses a more *in vivo*-like Fn matrix, produced by fibroblast cells, to study matrix induced alteration of drug response (Serebriiskii *et al.*, 2008). With this model it was possible to show that not only the presence of the matrix but also the organization of the matrix in 2D or 3D influences drug response. In addition, matrix from normal or transformed fibroblasts induced significantly different signaling in reseeded cancer cells (Castelló-Cros *et al.*, 2009). Park *et al.* highlighted the importance of β1 integrin signaling in drug response (Park *et al.*, 2008). In a matrigel model, they showed that blocking this integrin in combination with radiotherapy worked synergistically to increase the effect of treatment.

5.1.3 The advantage of *in vitro* models with controlled extrinsic parameters

However, there are several drawbacks of the aforementioned models. One disadvantage is that most of the models are limited to studying the effect of only one or a few parameters of the extracellular environment. An even more important consideration is the inability of many of these models to differentiate between the effects of different extrinsic parameters. In fundamental studies of cell biology, reductionist models of the *in vivo* environment have shown promise in the deconvolution of the importance of extrinsic factors on cell behaviour (Bhadriraju and Chen, 2002) (Ochsner *et al.*, 2010). Such models typically rely on micropatterned substrates, for example protein patterns in the size of a single cell that have been used to study the effect of cell spreading on different cell behaviours (Liu and Chen, 2007). However, until recently there has been a lack of tools that enable the investigation of cells cultured within structurally and biochemically controlled 3D environments.

Therefore, within our lab we have developed a PDMS-based microwell array for the culture of cells in a 3D environment, in which not only dimensionality but also cell cluster size and protein coating can be controlled independently (Ochsner *et al.*, 2007).

5.2 Materials and methods

5.2.1 Preparation of cell culture substrates

Arrays of microwells with a diameter of 34 µm and depth of 10 µm were fabricated in PDMS as described in chapter 3. Briefly, soft lithography was used to mould thin PDMS arrays onto glass cover slips to allow for high-resolution microscopy on an upright microscope. The arrays were functionalized with protein only in the wells using the new method developed during the course of this project and described in chapter 4. In short, the arrays were first coated with protein, and then subtractive µCP was used to remove the protein from the plateau surface using glutaraldehyde functionalized PDMS stamps. In a final step the surface was rendered non-adhesive for cells by backfilling with Pluronics. 2D samples were prepared by moulding thin PDMS films on thin glass cover slips and subsequently rendered hydrophilic in an air-plasma to facilitate coating with protein. All samples were glued onto the bottom of a Petri dish into which a hole was previously drilled to facilitate cell culture and imaging of the samples.

5.2.2 Preparation of cell-derived fibronectin matrices

Fn matrices were produced as previously described (Kubow *et al.*, 2009). In short, over-confluent NIH 3T3 fibroblasts were cultured in 96-well plates coated with Fn for at least 4 days and subsequently decellularized. After complete decellularization the matrices were rinsed with PBS and reseeded with MCF-7 breast carcinoma cells within a week. This protocol is described in detail in chapter 3.

5.2.3 Taxol adsorption measurements using HPLC

The different platforms; flat PDMS substrates, microwell arrays and Fn matrices were prepared as usual, covered with cell culture media containing 100 nM Taxol and incubated for 24 hours at 37^{o}C in a humidified atmosphere (95% (v/v) air, 5% (v/v) carbon dioxide). Prior to analysis the samples were mixed 1:1 (v/v) with acetonitrile to ensure the denaturation of the proteins in the solution, which were subsequently removed by filtration. The HPLC analysis was run on an 18 cm long, reverse phase, separation column. A mobile phase of H_2O and acetonitrile 1:1 ensured that the samples were detected ca. 4 min after injection. The chromatograms were printed and evaluated manually.

5.2.4 Confocal microscopy for characterization of cell morphology

MCF-7 cells were seeded onto the substrates at $3x10^{-5}$ cells/ml. After 2 hrs the microwell substrates were rinsed twice to remove any non-adherent cells. After 24 hrs the cells were fixed using paraformalehyde (4% (w/v) for 10 min at RT) and permeabilized with triton-X (0.1 % (v/v) for 20 min at RT). The cells were stained for F-actin with Phalloidin-Alexa Fluor 488 and nuclei were stained with propidium iodide/RNAse buffer (BD Biosciences). Imaging was performed on inverted confocal microscopy (Olympus, Switzerland) using at least 40x magnification.

5.2.5 Drug treatment and apoptosis determination

MCF-7 breast carcinoma cells and human renal epithelial (HRE) cells were cultured as described in Materials and Methods, Chapter 3. For experimentation MCF-7 or HRE cells were seeded onto the substrates at $3x10^{-5}$ cells/ml and allowed to adhere for ca 2 hrs before rinsing twice with cell culture media to remove any non-adherent cells. Cells were cultured on the substrates for 16 hours prior to incubation with Taxol (100 nM, including 0.1% (v/v) DMSO) for 24 or 48 hours. Control samples consisted of cells cultured in DMEM media with 0.1 % (v/v) DMSO to match test samples.

Cell viability was determined using the LIVE/DEAD assay (Invitrogen). Calcein (2 μM in cell culture media) and Ethidium Homodimer (4 μM in cell culture media)

were added simultaneously to live cells and incubated at 37 °C for 30 min before imaging. Apoptosis was detected by nuclear fragmentation, as described previously (Aoudjit and Vuori, 2001). Nuclei were stained with Hoechst 33342 (0.3 µg/ml for 20 min at 37 °C) and total nuclei and number of fragmented nuclei was then directly determined by imaging. For both the LIVE/DEAD assays and nuclear fragmentation assessment, we used an inverted widefield microscope (Zeiss, Germany) with a 20x air objective (Fig. 3C). Experiments were always performed in duplicates and repeated three times. In every experiment > 100 cells were counted, with an exception for the analysis of single cells in microwells, in which a minimum of 20 cells per experiment were counted.

5.2.6 Assessment of proliferation

Proliferation was assessed using the BrdU assay as explained in Chapter 3. Samples preparation and seeding of cells was performed as described above for the drug treatment experiments. After overnight cell adhesion the media was exchanged for media containing 10 µM BrdU (Sigma Aldrich, Switzerland) and the samples were incubated at 37 °C for 6 hrs before fixing and staining of the BrdU. The samples were counterstained with Hoechst 33342, to label cell nuclei, and imaged using a 20x objective on an inverted Zeiss widefield microscope. BrdU-labelled versus Hoechst labelled nuclei were manually counted with at least 100 cells per experiment. The experiments were performed in duplicates and repeated three times.

5.3 Results

5.3.1 Taxol adsorption on substrates

One potential problem associated with 3D cell culture scaffolds is the high surface area, resulting in an increased adsorption of test compounds, thereby reducing the effective concentration to which the cells are exposed. Therefore, Taxol adsorption onto the different platforms tested, namely flat substrates, microwells and cell-derived matrices, was assessed using HPLC. The light absorption detection after separation of Taxol from DMSO and components of cell culture media showed to be directly proportional to the Taxol concentration (Fig. 5.2a). This indicates that the read-out is reliable, even at these very low Taxol concentrations of 50 – 200 nM. However, the Taxol adsorption in the samples occurred at the lower part of this curve. Therefore, the measured values probably have an error of ± 20 %.

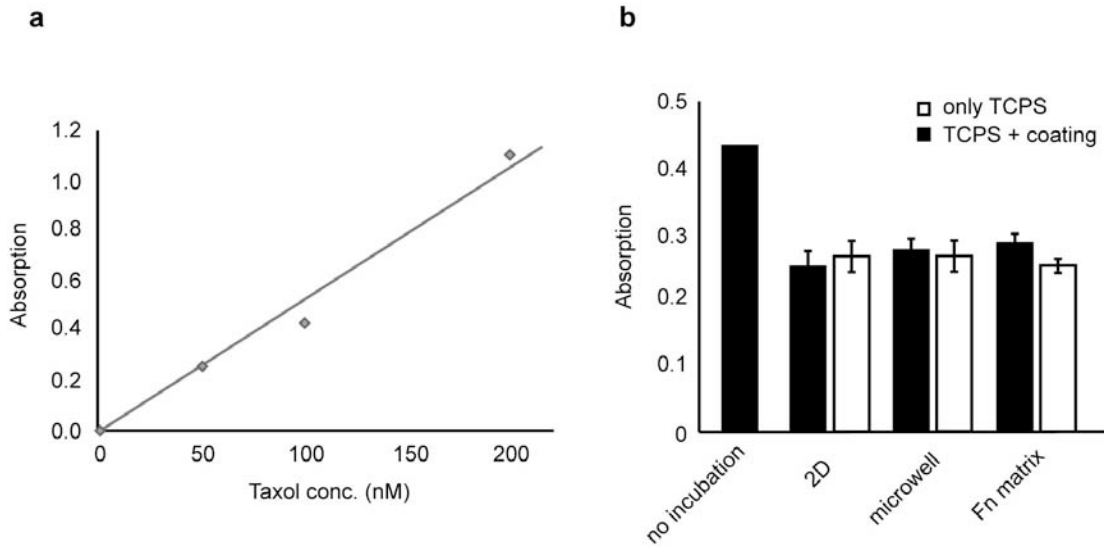

Figure 5.2: *Taxol concentration after incubation on the different substrates.* Taxol concentration was measured by absorption after separation of the Taxol with HPLC. The concentrations that were of interest were in the range of 100 nM. Interestingly, even at these very low concentrations we obtained a fairly linear relationship between adsorption and Taxol concentration (a). Different samples were then incubated with cell culture media containing 100 nM Taxol for 24 h at 37 h. Subsequently, Taxol adsorption in these samples were measured and compared to a control sample, which had not been stored in a falcon tube. We found no differences in Taxol concentration between samples that had been incubated on the different substrates, indicating that there were no differences in adsorption (b). However, the control sample showed a 40 % higher adsorption. This may be explained by adsorption onto the polystyrene containers, used to hold the samples.

Still, it was interesting to see that the HPLC analysis detected no differences in Taxol concentration in the cell culture media after exposure to the different substrates (Fig. 5.2b). This indicates that Taxol did not adsorb more on one of the samples. However, exposure to any of the substrates resulted in a 40 % decrease in Taxol concentration compared to the original solution. This decrease in Taxol concentration could be due to adsorption of the hydrophobic Taxol molecule to the polystyrene dishes during incubation or onto the pipette tips in the handling of the solutions. It is less likely to be due to degradation, as Taxol is known to keep stable at 37 ºC for days (Ringel and Horwitz, 1987).

5.3.2 Determining the rate and type of cell death induced by Taxol

Taxol acts by suppressing microtubule dynamics, which leads to a mitotic block and apoptosis in cancer cells (Jordan and Wilson, 1998), and is a standard drug in the treatment of breast cancer (Holmes *et al.*, 1991; Mamounas *et al.*, 2005). Taxol is typically applied *in vitro* in a concentration range of 10 nM – 100 nM (Aoudjit and Vuori, 2001) (Serebriiskii *et al.*, 2008), as determined to be suitable by IC_{50}-values.

We initially investigated Taxol response in our system using two different assays. In a first experiment we measured the number of both apoptotic and necrotic cells in a population of cells grown on flat Fn-coated PDMS substrates and treated with 100 nM Taxol. The LIVE/DEAD assay identifies dead cells on the basis of membrane integrity and was used to differentiate necrotic from apoptotic cells (Morley *et al.*, 2006; Prozialeck *et al.*, 2009), while apoptosis was detected by nuclear fragmentation, which is an easily identifiable characteristic of apoptosis (Lövborg *et al.*, 2004).

It was observed that the number of apoptotic cells, as determined by nuclear fragmentation, increased by 24 ± 4 % from 24 hrs to 48 hrs of treatment (57 ± 3 % and 81 ± 1% cell death respectively) (Fig. 5.3). Apoptosis levels of untreated samples, i.e. after incubation with media alone, were less than 5 %. The LIVE/DEAD assay revealed that the level of necrosis in these cell populations remained below 10 %, even after incubation with Taxol for 48 hrs. In all of the following experiments the cells were analyzed after 24 hrs of Taxol treatment, as at this time-point the rate of apoptosis was in a range where differences in drug response were detectable (i.e. before the cell death had reached a plateau).

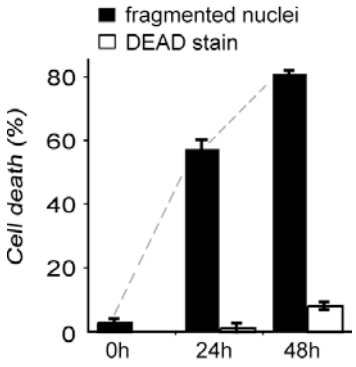

Figure 5.3: *Response to Taxol with time of treatment in MCF-7 cells.* Cell viability of MCF-7 cells cultured on flat Fn-coated PDMS after Taxol treatment was determined by counting the number of non-viable cells, as determined by the presence of a fragmented nucleus (black bar) or uptake of Ethidium homodimer (white bar), relative to the total number of cells present. MCF-7 cells cultured on flat Fn coated substrates showed an increase in fragmented nuclei over 48 hrs. The low number of cells stained with Ethidium homodimer DEAD stain indicates that most cells undergo apoptosis.

5.3.3 Using the microwell array to study the effect of dimensionality on drug response

Dimensionality was the first extrinsic factor that was evaluated, as it has previously been shown to be an important factor in governing altered drug responsiveness (Dhiman *et al.*, 2005) (Horning *et al.*, 2008). The individual microwells within the array were 34 μm in diameter by 10 μm in depth and MCF-7 breast carcinoma cells cultured in the microwells formed small clusters (≤ 6 cells per well after 16 hours culture (Fig. 5.4b). At this time point the clusters seldom filled the full volume of the well, however from confocal images it was clearly visible that the cells interacted with both the sides and the bottom of the microwell to form 3D clusters. This

contrasted to cells cultured on flat substrates, also coated with Fn, which were visibly more flat and stretched (Fig. 5.4a). Thus we found it interesting to explore whether the culture of small clusters of cancer cells in the engineered 3D environments of microwells has an effect on drug response.

MCF-7 breast carcinoma cells cultured either within microwells or on flat substrates coated with Fn showed very low levels of cell death after 24 hrs, regardless of the substrate. Treatment with 100 nM Taxol significantly increased cell death after culture either on flat PDMS (59 ± 3 % death) or within microwells (42 ± 4 % death) (Fig. 5.4c and Table 1). Intriguingly, the response to Taxol was significantly lower for cells cultured within the microwells (17 ± 5 % decrease, $p < 0.001$).

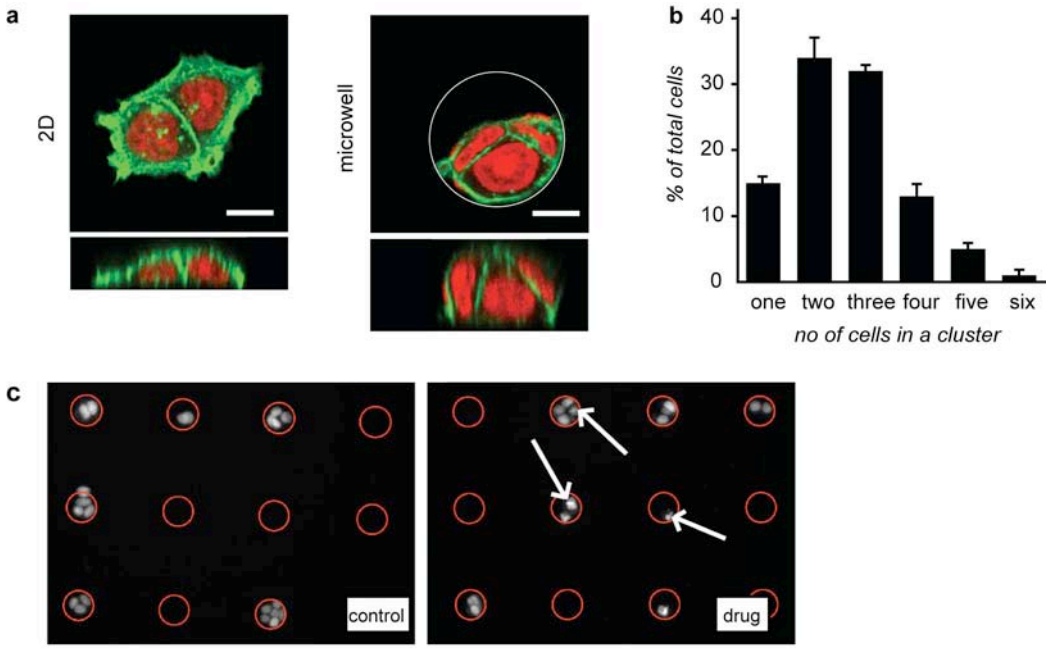

Figure 5.4: *Overview of cell cluster morphology in microwells.* A) Confocal images and cross section of z-reconstruction of the cell organization on flat substrates (left) and in the microwells (right). The cells were cultured for 24 hrs in 34 µm wide Fn-coated microwells and then stained for F-actin (green) and nuclei (red). In microwells the cells are inhibited from spreading in comparison to cells cultured on flat substrates, but were observed to interact with both the bottom and sides of the microwells to form small 3D clusters. Scale bar is 10 µm. B) Microwells coated with Fn contained 1 to 6 cells per well, with two thirds of the cells existing in pairs or clusters of 3 cells. C) MCF-7 cells that are seeded in 34 µm wide microwells show normal nuclei after 40 hrs cell of culture (A). 24 hrs Taxol treatment induced apoptosis in the cells. This is shown by the fragmented nuclei in B (white arrows).

The effect of dimensionality on drug response was also investigated for normal cells, namely human primary renal epithelial (HRE) cells, to determine whether the effect of dimensionality was specific to cancer cells. It was observed that Taxol induced cell death was significantly lower for normal cells than observed for the cancer cells

(Table 1). On flat substrates, Taxol induced cell death was 20 ± 2 % and within microwells 14 ± 3 %, which was significantly lower than the cell death which occurred when MCF-7 breast carcinoma cells were cultured either on flat substrates or in microwells (39 ± 4 % lower; $p < 0.001$ and 28 ± 4 % lower; $p < 0.001$ respectively). Further, the normal cells showed no significant difference in drug response between the flat and the 3D substrates.

Table 5.1 Summary of the level of cell death determined as percent of fragmented nuclei, on flat substrates and in 34 µm wide microwells after 24 hrs exposure to Taxol

		 2D		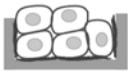 microwell		
		control	drug	control	drug	significance
Fibronectin	MCF-7	3 ± 1	59 ± 3	2 ± 1	42 ± 3	$p < 0.001$
	HRE	4 ± 1	20 ± 2	1 ± 1	14 ± 2	Not Sign.
Collagen I	MCF-7	3 ± 1	70 ± 2	3 ± 1	59 ± 2	$p < 0.05$

Studying the effect of dimensionality in combination with different matrix coating

The effect of dimensionality on drug-induced cell death was further explored in combination with different matrix coatings. Hence, we coated both the microwells and the flat substrates with Col-I, another common cell adhesion protein and assessed the responsiveness of MCF-7 breast carcinoma cells after culture in both 2D and 3D. We found, in coherence with the Fn results, that cells grown in Col-I coated microwells showed a small, but significant, reduction in cell death after treatment with 100 nM Taxol compared to cells cultured on flat Col-I coated substrates (12 % ± 4 lower, $p<0.01$) (Table 1). This difference in drug response between the two substrates was lower than observed for Fn-coated substrates. Further, it can be concluded that MCF-7 breast carcinoma cells were more sensitive to Taxol treatment after culture on Col-I, in comparison to Fn, on both flat substrates (12 ± 5 % higher, $p<0.05$) and within microwells (17 ± 5 % higher, $p<0.001$).

5.3.4 Using the microwells to differentiate between cell death in single cells and in cells forming cell-cell contacts

The microwell array offers a unique opportunity to study the importance of cell-cell contacts on the responsiveness to treatment. By controlling the well size and seeding density it is possible to form cell clusters in the microwells in different size ranges. Here we compared the level of cell death for single cells versus pairs of cells. The level of cell death within Fn coated microwells was 61 ± 7 % for single cells and 40 ± 4 % for cells with cell-cell contacts, thus revealing that single cells were significantly more sensitive to drug treatment (21 ± 9 % higher, $p < 0.01$) (Fig. 5.5).

In contrast to cells cultured in Fn-coated microwells, there was no significant difference in drug response for single cells and cell pairs cultured in Col-I coated microwells (39 ± 6 % for single cells versus 54 ± 4 % for pairs of cells). Further, the inter-dependency between cluster size and matrix coating was explored using the microwell platform and revealed that while single cells cultured on Fn were more sensitive to drug treatment than those cultured on Col-I, this trend was reversed after the formation of cell-cell contacts and within larger clusters.

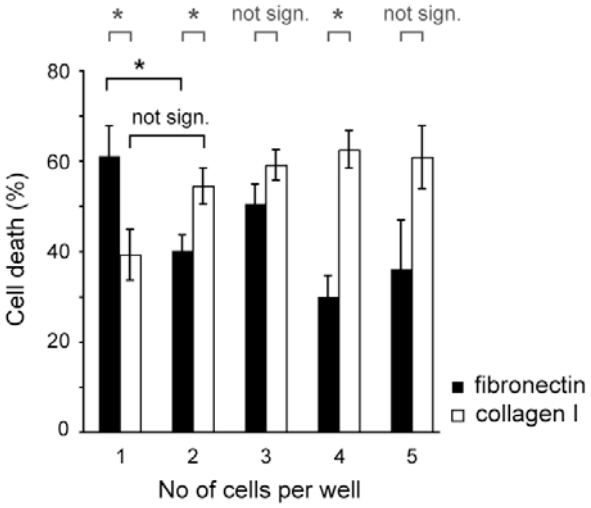

Figure 5.5: *The effect of cell number on Taxol-induced cell death in small cell clusters.* The level of cell death versus number of cells present within the microwell coated with either Fn (black bars) or Col-I (white bar) was plotted. It was found that single cells cultured in Fn-coated microwells were more sensitive to drug treatment than cells that had formed cell-cell contacts. This phenomenon was not observed for MCF-7 cells cultured in Col-I coated microwells, as no significant difference in cell death was observed between single and pairs of cells. Further, single cells cultured on Fn were more sensitive to drug treatment than those cultured on Col-I. Conversely, this trend was reversed when 2 or more cells were present within the microwells. Key: * $p < 0.05$: not sign. = not significant, grey symbols refer to Col-I versus Fn, while black symbols refer to single cells versus pairs of cells.

5.3.5 Comparison of cell behaviour in microwells and in a 3D fibronectin matrix

Taxol response

Fn matrix, derived from fibroblasts, is considered to be a mimic of the 3D environment which cancer cells experience *in vivo* and has been used previously to assess the response to Taxol for a number of different cancer cell lines (Serebriiskii *et al.*, 2008). It was therefore interesting to compare cell behaviour after culture within the microwells to that of cells cultured in the more complex Fn matrices. MCF-7 cells reseeded into the cell-derived matrices interacted with the Fn fibres (Fig. 5.6a) and showed only negligible cell death (2 ± 1 % death) (Fig. 5.6b).

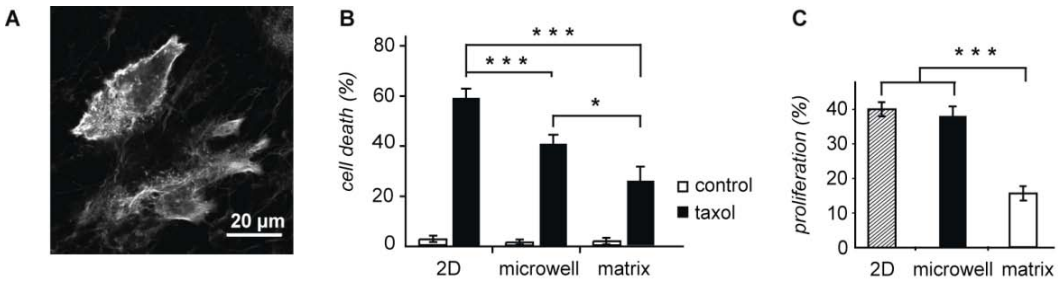

Figure 5.6: *The effect of 3D culture on drug response.* A) MCF-7 cells seeded into cell-derived Fn matrices were observed to interact tightly with the Fn fibres. This example image shows F-actin staining of cells cultured within the matrix for 24 hours. B) MCF-7 cells were cultured within cell-derived Fn matrices for 16 hrs before exposure to Taxol for a further 24 hrs. The level of apoptosis was significantly lower in the Fn matrices compared to on flat substrates. In comparison to the microwells the drug response was slightly lower. C) Levels of proliferating cells were determined by incubation of the cells for 6 hrs with the DNA-intercalating molecule BrdU. The proliferation of the cells cultured in microwells (black bar) was unchanged in comparison to cells cultured on flat substrates (striped bar). Conversely proliferation in cell-derived matrices (white bar) was significantly reduced. Key: * $p < 0.05$; *** $p < 0.001$.

Treatment with Taxol induced a significant increase in cell death in the matrices (26 ± 5 % death), however cell death was significantly lower in comparison to cells cultured on flat substrates (33 ± 6 % lower, $p<0.001$). Hence, the cells were less sensitive to Taxol treatment after culture within the cell-derived Fn matrix, which correlates well with the results observed in the 3D environment of the microwell array and highlights the importance of dimensionality in governing drug responsiveness. However, while both platforms followed the same biological trend, the cell death observed after culture in the microwells was slightly greater (16 ± 7 % higher, $p< 0.05$) than observed after culture in the matrix.

Proliferation

One factor that influences the cellular response to Taxol is cell turn-over rate, as the mode of action of this drug requires cell cycle transition (Henley *et al.*, 2006). To determine the extent to which the lower drug response observed in the 3D environments was influenced by proliferation rate changes, we determined the proliferation rates in the different environments studied. Proliferation rates were assessed using the BrdU proliferation assay, for MCF-7 cells cultured in Fn coated microwells and in cell derived matrices, in comparison to cells grown on Fn coated flat substrates. No difference in proliferation was observed between cells cultured in microwells (40 ± 2 % proliferation) and on flat substrates (38 ± 3 % proliferation) (Fig. 5.6c). However, in cell-derived matrices the proliferation was significantly lower than on flat substrates (24 ± 6 % decrease, $p<0.001$).

5.4 Discussion

In order to improve the development process of new anti-cancer drugs, we need to understand the effect of the signaling from the extracellular environment on drug response. Typically, *in vitro* models used to study such effects are based on polymer scaffolds or protein-based matrices. One drawback of such models is that they often constitute a complex environment in which it can be difficult to separate the effect of different environmental parameters. Therefore we have investigated the possibility of using a microwell array to study the effect of the extracellular context on drug response in a controlled 3D environment.

5.4.1 Dimensionality alone affects the response to Taxol

It was observed that the cancer cells cultured within the 3D environment of the microwells were less responsive to treatment with Taxol than cells cultured on 2D substrates. Our findings are in agreement with previous research, which revealed that the 3D culture of cancer cells induces a reduction in drug sensitivity (Dhiman *et al.*, 2005) (Horning *et al.*, 2008). Typically the reduced drug responsiveness in 3D environments has been demonstrated in MCTSs or 3D scaffolds, where cells are present in large clusters. However, the formation of smaller cancer cell clusters (10-20 cells) in matrigel has also previously shown to alter both cell morphology and gene expression in comparison to culture on tissue culture plastic (Kenny *et al.*, 2007). Nevertheless, the effect of these phenotypic and genotypic changes on drug response was not investigated.

It is therefore interesting to see that these small cell clusters, with ≤ 6 cells per cluster, show differences in drug response depending on the dimensionality of the environment. This indicates that dimensionality can alter drug responsiveness even in

the absence of dense packing of the cells and oxygen gradients provided by more complex *in vitro* models, such as MCTS. The dimensionality effects observed in microwells may instead be due to altered adhesion signaling from the reduced spreading and thereby an increase in cell-cell contacts.

In contrast to the behaviour of the cancer cells, normal renal epithelial cells showed no significant difference in response in 3D versus 2D, even though the response followed the same trend observed for cancer cells. We propose that the drug response in these cells is either not affected by the 3D environment or it is affected to a lesser extent. However, it should be borne in mind that these cells are derived from kidney and thus the difference observed between cancer and normal cells may in part be due to the differing tissue origin.

5.4.2 The effect of dimensionality is also observed in a collagen I environment

The reduced drug responsiveness after culture within a 3D environment was observed for two different interfacing proteins; Fn and Col-I. These proteins were chosen for the experiment as they have shown to affect the response to Taxol in breast cancer cells previously (Aoudjit *et al.*, 2001). In addition, increased fibronectin expression has been correlated to more aggressive forms of cancer (Yao *et al.*, 2007). Intriguingly, the effect of dimensionality was more dramatic when the cells were adhered to Fn. In addition, there was an overall reduced sensitivity to treatment on Fn compared to Col-I, observed both on flat substrates and within the microwells. Both proteins are important constituents of the stroma surrounding tumours but are known to engage different integrins (Heino, 2000; Siebers *et al.*, 2008), which could explain the differences observed. The higher cell death observed after interaction with Col-I in comparison to Fn could also be due to the increased turn-over rate for MCF-7 on Col-I (Hirtenlehner *et al.*, 2002), thus rendering the cells more susceptible to the effects of Taxol. Furthermore, *in vivo* studies have shown that increased β1- and extracellular Fn expression has been associated with more aggressive and invasive breast cancer (Ioachim *et al.*, 2002; Yao *et al.*, 2007), which may in part explain the reduced responsiveness to drug treatment observed after interaction with Fn, as revealed in this work.

5.4.3 Reduced apoptosis in cells forming cell-cell contacts is matrix-specific

Cell-cell contacts have been hypothesized to be one important parameter in governing reduction in drug response (Hazlehurst *et al.*, 2003), and thus we used the microwell platform to explore the effect of this parameter. Intriguing differences in the effect of forming cell contacts was observed depending on the matrix protein. On Col-I coated

substrates the formation of cell-cell contacts had little effect on the drug responsiveness of the cells. Interestingly, previous work has emphasized that crosstalk between adhesion proteins in cell-matrix contacts and in cell-cell contacts may disrupt E-cadherin interaction, as was shown for cancer cells adhering on Col-I (Koenig *et al.*, 2006). It is possible that a similar crosstalk takes place in the MCF-7 cells in this study and therefore would explain why there was no significant effect of the formation of one cell-cell contact on drug response for cells adhering on Col-I. On the other hand, the difference between single and multiple cells is higher for three and four cells. This effect is surprising, as the literature typically reports that cell-cell contacts make cells less responsive to drug treatment.

Conversely, our experiments could nicely reveal that cells in Fn-coated microwells lacking cell-cell contacts were more sensitive to treatment. Thus the formation of cell-cell contacts, leading to reduced drug responsiveness, would appear to be one contributing factor of the increased overall resistance observed when cells were cultured in the presence of Fn, as opposed to Col-I. On Fn/cadherin patterned surfaces it was found that the dominant role of integrin interactions over E-cadherin interactions in MCF-7 cells was rigidity dependent and could be ruled out on soft substrates (Tsai and Kam, 2009). Hence, if matrix interactions are reduced in a system, as is typically observed on soft substrates (Yeung *et al.*, 2004), this may strengthen the cell-cell contacts, which could in turn lead to reduced drug responsiveness. Intriguingly this may also explain in part the effect of dimensionality observed. It is probable that cells within the microwells have reduced matrix interactions, and thus increased cell-cell contacts, as they are restricted in both their spreading and migration.

5.4.4 The dimensionality effect in the microwells partly mimics that observed in a 3D Fibronectin matrix

If the advantage of a reductionist model is that different extrinsic factors may be studied separately, then the disadvantage is clearly that one fails in mimicking the complexity of the *in vivo* environment. Therefore, we found it interesting to compare our results to a cell-derived Fn matrix, which is a more complex *in vivo* model that has been previously used to study matrix induced changes in drug response (Serebriiskii *et al.*, 2008). After culture within the matrix, the cells were less responsive to drug treatment in comparison to cells grown on flat substrates. This correlates well with our results with the microwell platform, and further indicates that we were able to mimic some aspects of the complex environment of the matrices within the 3D environments of this *in vitro* model. However, even though the drug response was reduced in both 3D systems, the effect was enhanced in the matrices.

In addition we found that the proliferation rate in the two 3D systems was significantly different. In the microwells the proliferation rate was unchanged in

comparison to flat substrates, while it was significantly reduced in cell-derived matrices. This result is coherent with previous research using these matrices (Serebriiskii *et al.*, 2008), however the difference in proliferation was more pronounced in this work, possibly due to differences in the proliferation assays utilized. As Taxol is an anti-mitotic drug it is probable that the lower proliferation rate observed in the cell-derived matrix could at least partially explain the reduced drug response in the matrix. However, this is not the case for cells cultured in the microwells, for which there was no difference in proliferation in comparison to cells on flat substrate. There is not always a correlation between high mitotic frequency and elevated response to chemotherapeutic drugs (Aas *et al.*, 2003; Serebriiskii *et al.*, 2008). Instead, the response to Taxol should be regarded as a function of both turnover rate and drug sensitivity. For highly aggressive cancers, low sensitivity to treatment may even rule out an increased susceptibility to anti-cancer drugs due to a high turnover rate (Meads *et al.*, 2009).

Another aspect to consider when comparing these two 3D systems is the organization of the ECM, as a coating in the microwells or as fibres in the matrix. The organization of the ECM is known to affect integrin signaling (Even-Ram and Yamada, 2005), which could in turn lead to differences in drug response (Hazlehurst *et al.*, 2003).

Hence, we suggest that the effect of dimensionality observed in the two systems is not only related to changes in proliferation rate and also not only induced by the 3D characteristic of the environment. Instead, other environmental parameters, such as the scaffold pliability, the type and amount of cell-cell interactions and the conformation of the matrix molecules, may play additional roles in determining responsiveness to drug treatment.

5.5 Conclusions

In summary, with this platform it was possible to demonstrate the individual effect of dimensionality, adhesive proteins and cell-cell contacts on the responsiveness of breast cancer cells to drug treatment. Further it was possible to explore the inter-relationship between these environmental parameters and reveal a cumulative effect of dimensionality and matrix composition on drug response.

The lowest sensitivity to Taxol was acquired after culture in 3D in the presence of Fn, significantly lower than for Col-I. This drug response pattern can be expected to be different for different cancer cell types and would be interesting to explore. In addition, this could be extended to larger clusters of cells, using microwells with a greater volume, to provide more predictive results for cells residing in dense tumours.

In chapter 7, a similar approach is used to study microenvironment induced drug response. There is probably not one major extrinsic factor that alters the responsiveness to treatment *in vivo* and it is clear that a crucial step in the development of more effective treatments must be the understanding of the interdependence of signaling from different constituents of the environment.

CHAPTER 6

Cluster formation in a PEG hydrogel based microwell array: first steps towards high content screening in 3D

This chapter describes the development of a method to study drug response in 3D cell clusters with sub-cellular resolution. The read-out of current 3D culture models is often population based (Herrmann *et al.*, 2008) and hence information about spatial and temporal distribution of cell behaviour within a population is lost. On the other hand, microscopy-based high content screening (HCS) is increasingly used in the early stages of drug discovery. It allows for the multi-parametric read-out of sub-cellular events, which should ease bottlenecks formed at, for example, target validation (Gasparri, 2009). With few exceptions, cell-based HCS assays employ TCPS as the standard culture substrate.

In chapter 4 and 5 a PDMS-based microwell array was used to study the effect of extrinsic parameters on the culture of single cells and small clusters of cells. This work showed the advantage of using a platform with controlled extrinsic parameters to study the effect of extrinsic parameters on drug response. For example we found an interrelationship between the effect of matrix composition and dimensionality. However, it would be important to have a platform with a more *in vivo* like culture environment in order to obtain results that could have some value for translational research. A more *in vivo* like culture environment could be obtained by culturing cells in larger multicellular tissue to better mimic the tumour microenvironment. In addition, the stiffness of the culture platform should be similar to that of the tissue and adhesion proteins should be relevant for the cancer niche that is to be studied. These are two important parameters in cancer progression, as discussed in Chapter 1, Introduction.

To this end, we got interested in a microwell array created in a PEG hydrogel as a platform for 3D cancer cell culture. This platform has been previously used to study single stem cell fate (Lutolf *et al.*, 2009). An advantage of the hydrogel-based platform over PS and PDMS based platforms is that it has a high water content and mechanical properties closer to that of the organs in the human body (Lutolf and Hubbell, 2005).

Furthermore, intrinsic to the fabrication procedure of the PEG-hydrogel platform, the protein coating can easily be created only at the bottom of microwells, which favours the formation of homogenous 3D cell clusters. The inert nature of the PEG hydrogel material reduces the need for an additional non-adhesive coating. These properties improves the stability of the platform, enables longer cell culture experiments to be performed with increased reproducibility.

In order to establish the new platform we first investigate the possibilities to vary the materials properties of the array, including the coating with different ECM proteins (Section 6.3.1) and altering the rigidity by changing the PEG concentration (Section 6.3.2). In the next step, we develop a method for quantification of cell behaviour within 3D clusters with spatial information (Section 6.3.4). Finally, the cluster formation and growth behaviour of two different breast cancer cell lines in the microwells is characterized (Section 6.3.5)

6.1 Background

6.1.1 Cell-based drug testing in anti-cancer drug development

Cell-based assays are widespread in anti-cancer drug development. Cell-based testing is advantageous in comparison to biochemical assays as it reflects the complex system of a whole cell. Further, the effect of targeted treatment may be highly dependent on non-specific interactions within the cell, termed off-target effects (Lang *et al.*, 2006), which would not be observed in a biochemical assay. In the development of anti-cancer drugs, one of the most studied cellular processes is apoptosis (Lövborg *et al.*, 2004). There exist several markers for different stages in the apoptotic process such as nuclear morphology, caspase activation and lipid reorganization in the cell membrane (Martinez *et al.*, 2010).

Recent advances in automated imaging and memory storage have made high content screening (HCS) a widespread method in both academia and in the pharmaceutical industry (Gasparri, 2009) (Starkuviene and Pepperkok, 2007). See also the Introduction Chapter 1, Section 1.4. In HCS a composite signal of different cell parameters is obtained for every sample. This makes it possible to acquire a more detailed picture of the response to a certain drug. Ultimately, this multidimensional data could make it easier to accurately compare the effect of different drugs. HCS has

so far been limited to 2D samples, as a high image quality with sub-cellular resolution is required (Prestwich, 2008).

6.1.2 Cell lines to model different stages of cancer

In vitro cancer studies can be performed using primary cancer cells but most commonly cancer cell lines are used, due to their availability. There exist several cell lines derived from female patients with breast cancer. These originate from different stages of cancer progression and can therefore be used to study these stages *in vitro*. For more information on cancer progression, see Introduction chapter, Section 1.2.1.

A cell line that represents primary cancer is the tumorigenic MCF-7 cell. This cell line has been used to study the role of E-cadherin in growth suppression (St Croix *et al.*, 1998) and treatment response (Green *et al.*, 2004). It has also shown valuable when studying the importance of other adhesion molecules in explaining the different behaviour of cancerous and normal cells (Debnath and Brugge, 2005). The tumorigenic / metastatic MDA-MB-231 cells are E-cadherin negative and behaves more like cells in the progressed decease. By induced expression of E-cadherin in MDA-MB-231 cells, the role of E-cadherin in inhibition of metastasis could be determined (Wong and Gumbiner, 2003). These two cell lines also represent two different types of breast cancers in terms of their oestrogen receptor (ER) expression as MCF-7 is ER+ and MDA-MB-231 is ER-.

Recently, this cell line was used to study mesenchymal – epithelial reversion transition. It has been found that patients with E-cadherin negative breast cancer tumours could have E-cadherin positive metastases (Chao *et al.*, 2010). This indicates a possibility for cancer cells to revert back from mesenchymal to epithelial phenotype. The same group found that the introduction of a metastatic cell line in a secondary organ environment, promoted a reversion back to an epithelial phenotype with E-cadherin expression as one characteristic (Chao *et al.*, 2010). In a more simple approach, the metastatic niche was mimicked by the growth of MDA-MB-231 on a Lam matrix (Benton *et al.*, 2009). Surprisingly, the induced morphology change and the signaling from the Lam showed to be enough to induce E-cadherin re-expression.

6.1.3 Mechanical sensing in cancer

It is known that matrix rigidity is altered at cancer progression and the detection of stiffening of the tissue has been routinely used to detect cancer (Butcher *et al.*, 2009) (Fig. 6.1). The relevance of this extrinsic parameter for cancer progression has only recently been examined, but with very interesting first results. By the use of cell culture substrates of varying rigidity, it was revealed that normal and cancer cells did respond differently to increasing matrix rigidity, indicating a major change in the

outside-in signaling of the transformed cells (Paszek *et al.*, 2005). The relevance of matrix stiffening was confirmed by mouse *in vivo* experiments, which showed that inducing Col-I cross-linking promoted tumorigenic behaviour and invasion of injected pre-malignant cells (Levental *et al.*, 2009). Recently, Kostic *et al.* detected differences within a cell population in the preferred rigidity for growth. Intriguingly, they found that the preferred rigidity for growth *in vitro* matched the tissue rigidity of the preferred metastatic site in mouse (Kostic *et al.*, 2009). Hence, the phenotype of the cancer cell may determine its site of migration.

There are only very few reports to how flexibility may be one factor to regulate drug response. Rehfeldt *et al.* found that lung cancer cells were significantly more responsive to an integrin-related drug on rigid substrates, which could be correlated to their spreading on soft and rigid substrates (Rehfeldt *et al.*, 2007). In contrast, transformed fibroblasts did not respond to rigidity in their growth and apoptosis patterns (Wang *et al.*, 2000). Hence, the importance of this parameter in cancer drug response is unclear. It likely depends on the rigidity responsiveness of the cancer cell type and the mechanism of the drug.

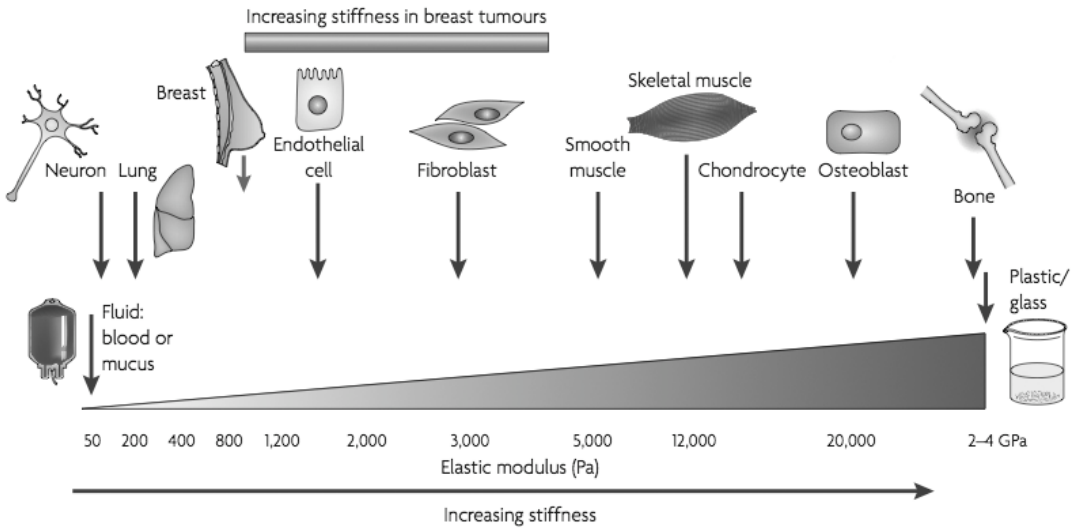

Figure 6.1: *Rigidity of different tissues.* All tissues are softer than plastic, making it a very artificial platform for cell culture. Also within the organs of the human body, there is a wide stiffness range, from the softest tissues like brain and lung-tissue of only a few hundred Pa to bone-tissue, which has a rigidity of 1 GPa. With tumour development in breast, the Elastic modulus increases from around 800 Pa to 3-5 kPa. (Figure from (Butcher *et al.*, 2009).)

6.1.4 Hydrogel-based 3D culture methods in cancer

3D culture of cancer cells can be obtained using polymeric scaffolds (Fischbach *et al.*, 2007), synthetic or protein hydrogels (Debnath *et al.*, 2003) as well as through the culture of cells on microfabricated materials (as described in detail in chapter 1,

Introduction). The advantage of hydrogel-based cell culture is that the rigidity can often be tuned to very low values, similar to the rigidity of tissues *in vivo*. Human tissues show very different rigidities, from very soft tissues such as breast tissue to very rigid tissue, such as cartilage (Fig. 6.1). Thus, protein-coated polyacrylamide gels are increasingly used as simple platforms to study the role of substrate rigidity in different cell behaviour (Engler *et al.*, 2007). Another advantage of a hydrogel culture platform is that it allows the encapsulation of cells without dramatically affecting diffusion properties, depending on its permeability for H_2O, minerals and lipophilic molecules.

3D culture in soft hydrogels has been performed both in purely protein-based gels such as Matrigel (Lee *et al.*, 2007) and in gels based on synthetic peptides (Prestwich, 2008). Typically this is facilitated by mixing the cells into the gel-forming material before crosslinking and hence is a simple approach for 3D cell culture. Recently a system for cell encapsulation based on both synthetic peptides and ECM protein was developed. The advantage of this system, was that the mechanical properties of the gel could be tuned without affecting the pore size of the gel (Miroshnikova *et al.*, 2011), which is another characteristic that plays an important role for how the cell sense the mechanical properties of a material (Levental *et al.*, 2007).

However, this methodology leads to a random positioning of cells in the gel, which complicates imaging in a more high throughput fashion (Nelson, 2008, Nature protocols). For more rigid hydrogels, micromolding by soft lithography can be used to allow for 3D culture with controlled cell positioning. This has shown feasible with crosslinked Col-I (Nelson *et al.*, 2008a), agarose (Nelson and Chen, 2002) and PEG hydrogels (Lutolf *et al.*, 2009). The Col-I gel approach has the advantage that it closely mimics the *in vivo* extracellular matrix. However, as the PEG-hydrogel is an inert material, it may be used as a platform to study the interaction with many different matrix proteins.

Proteins can be linked to the PEG hydrogel pre-mixture, which contains the reactive groups vinylsulfone and thiol (Fig. 6.2a). Lutolf *et al.* recently developed a micro-contact printing method that used this property of the gel to specifically coat only the bottom of microwells with protein in a micro-contact printing process. Hence, the PEG microwell array makes a versatile platform in dissecting the role of specific signals on cell behaviour (Lutolf *et al.*, 2009). Lutolf *et al.* showed that this platform could be used to assess the effects of protein characteristics of the *in vivo* microenvironment, or niche, on both hematopoietic and neural stem cell fate in an attempt to find bioengineering strategies to promote and control stem cell renewal *in vitro* (Lutolf *et al.*, 2009).

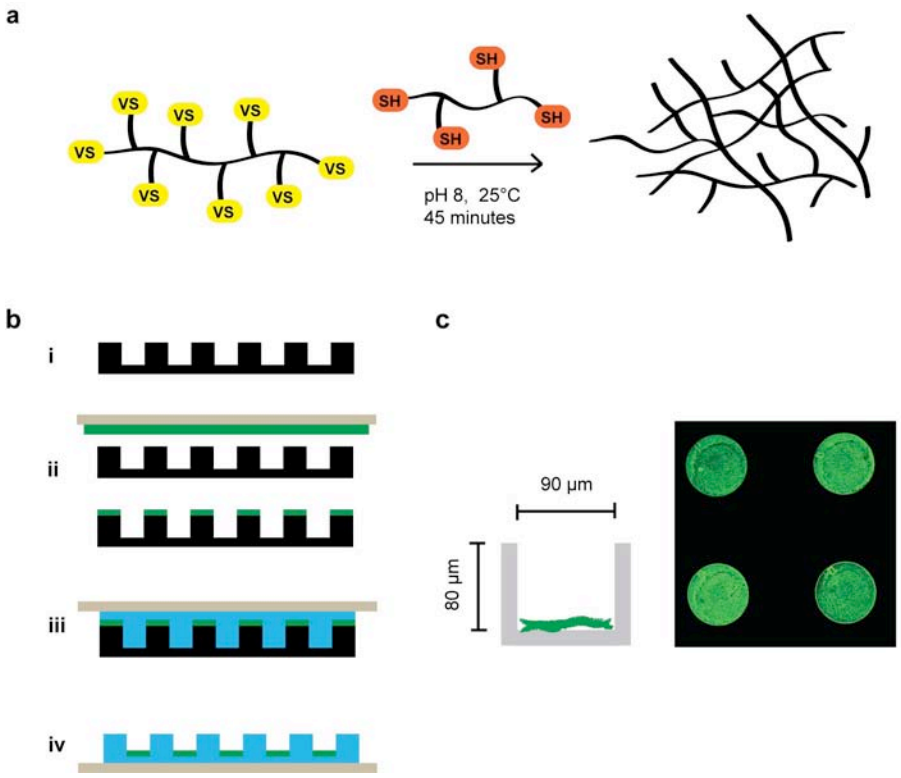

Figure 6.2: *Preparation of a microwell array in a PEG hydrogel: molding and protein coating.* The PEG hydrogel is formed by mixing the two components PEG-VS (vinylsulfone) and PEG-SH (thiol) in a Triethanolaminehydrochloride buffer (Lutolf *et al.*, 2009). After vigorous mixing for 30 s, the solution is moulded on a TCPS substrate, as explained in (b). In the first step in the molding process a PDMS mould is coated with protein by wet microcontact printing for 30 min (ii). Thereafter a small drop (15 µl / 0.7 cm^2) pre-gel mixture is placed on the PDMS mould and covered by a TCPS substrate (iii). After 45 min the gel may be removed from the mould (iv). The procedure results in a microwell array with protein only at the bottom of the microwells (c). The CLSM image shows Lam coating at the bottom of 100 µm microwells, as visualized by immunohistochemisty using a primary antibody against Lam and a secondary antibody conjugated to Alexa Fluor 488.

6.2 Experimental section

6.2.1 Fabrication of the PEG microwell arrays

Preparing arrays for 2D and 3D cell culture

Microwell arrays were produced at the bottom of 8-well Ibidi dishes by micromolding, as described in Materials and Methods (Fig. 6.2b). The bottom of the microwells was functionalized with protein according to a standard protocol, which was followed for all proteins. First, a protein solution at a high concentration (0.3 mg/ml for Col-I and Lam and 0.5 mg/ml for Fn) was distributed on the surface of a polyacrylamide gel. After drying the gel until no more drops of liquid were visible on

the surface, the gel was placed upside down on the PDMS mould for 30 min (see process step ii in Fig. 6.2b). The protein-functionalized polyacrylamide gel was then removed and the PEG-hydrogel was moulded on top of the protein-coated PDMS mould for 1 h (see process step iii in Fig. 2b). After demoulding it from the PDMS stamp, the gel was immersed in PBS overnight before cell seeding. The protein integration with the gel was achieved using two strategies.

Non-functionalised Col-I was applied and is theoretically incorporated into the first layer of the PEG-gel network, as it polymerizes simultaneously with the PEG-polymers at a basic pH and at high concentration. Fn and Lam do not have the same capability for self-polymerization, and therefore a maleimide -PEG-linker was attached to these proteins, see Materials and Methods, which covalently binds the proteins to the PEG gel. For all 3D cluster formation experiments we prepared microwells from a PDMS master with 100 μm wide pillars. This resulted in microwells with a diameter of about 90 μm.

Creating PEG gels with different rigidity

The rigidity of the PEG-gel is determined by the concentration of PEG polymer in the gel. We prepared gels with varying PEG concentration, from 2.5 % to 7.5 % (w/v). At lower PEG ratios, the gel did not form or was very fragile. The solutions were prepared on ice, as the higher the PEG-concentration the faster is the polymerization of the gel. Molding into microwells was performed as described above. For rheology measurement we moulded circular gels between two glass slides, which were rendered hydrophobic by coating them with Sigmacote. The PEG mixture was placed on the glass slide in drops of 75 μl. Another slide was placed on top using a 1 mm spacer. After polymerizing for 1 h the samples were allowed to swell in PBS for at least 1 h before rigidity measurements.

Determining stiffness by rheometry

The stiffness of the gel was measured at RT using a rheometer with a plate –plate geometry (Fig. 6.3a). Prior to each measurement, the thickness and the diameter of the gel disks were determined. The gel was placed at the bottom plate and the upper plate adjusted to the position, which correlated to 80% of the determined gel thickness (Fig. 6.3b). Target strain was set to a constant value of 5% and the shear modulus was measured over an oscillation range from 0.1 to 10 Hz.

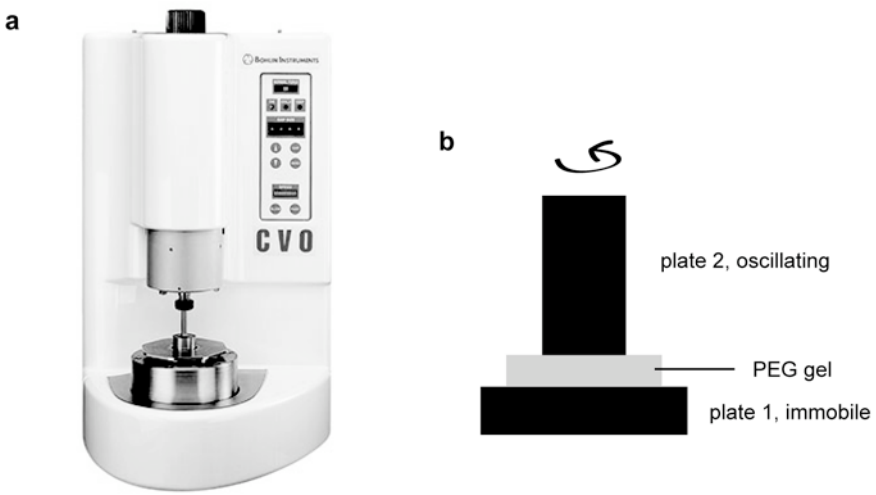

Figure 6.3: *Determining the rigidity of the PEG hydrogel.* The rigidity of gels with different polymer composition was measured at RT using a rheometer with a plate –plate geometry (a). Prior to each measurement, the thickness and the diameter of the gel disks were determined. The gel was placed on the bottom plate (b) and the upper plate adjusted to a position measuring 80% of the determined gel thickness. Target strain was set to a constant value of 5% and the shear modulus was measured over an oscillation range from 0.1 to 10 Hz.

6.2.2 Cell culture experiments in PEG microwells

Evaluation of different apoptosis assays

Several different apoptosis assays were tested for the detection of apoptosis in MCF-7 cells in response to Taxol treatment. For this evaluation, 3×10^4 MCF-7 cells were seeded into a 24-well plate. After 24 h preculture, the medium was exchanged for medium containing 100 nM Taxol. Thereafter, the apoptosis detection dyes Annexin V (Invitrogen, Switzerland), Propidium iodide (Invitrogen, Switzerland), APOPercentage (Biocolor, UK), TMRE (Molecular Probes, Switzerland) and mitotracker red (Invitrogen, Switzerland) were added at concentrations recommended by the manufacturer (section 3.6.2). For comparison cells were stained with Hoechst to detect nuclear fragmentation. Hoechst 33342 (Invitrogen, Switzerland) was incubated with the live cells at a concentration of 1:3000 in cell culture media, for 30 min. Images of the fluorescently labelled live cells were obtained with a Zeiss inverted microscope, using a 10x air-objective.

Cell seeding in microwells

The Ibidi-dishes with PEG microwell arrays were prepared as described in section 3.3.3. The day after the PEG microwells were prepared, the PBS in the Ibidi dish was carefully exchanged for cell culture media. During the cell seeding procedure we made sure never to let the hydrogel dehydrate. MCF-7 or MDA-MB-231 from 70 % confluent flasks, were seeded into the microwells at a seeding density of 1.5×10^5 cells

per Ibidi dish well. For E-cadherin re-expression studies, Col-I or Lam-I was added at a concentration of 60 µg/ml to the cell culture media during culture to simulate a 3D protein interaction, according to the protocol described in Benton *et al.* (Benton *et al.*, 2009).

BrdU assay

Proliferation was measured using the BrdU assay as described in detail in Chapter 3. In short, BrdU was incubated with live cells at the end of the culture period for 2h and 6h with MDA-MB-231 and MCF-7 cells respectively. Then the samples were fixed in methanol and stained for BrdU incorporation.

Immunohistochemisty

Cells were fixed in paraformaldehyde (3 % in PBS for 10 min) and thereafter permeabilized with triton x-100 (0.1 % in PBS for 10 min). The primary mouse E-cadherin antibody was applied at a concentration of 1:100 for an overnight incubation at 4°C. Secondary goat anti-mouse antibody conjugated to Alexa-fluor 488 was incubated at a concentration of 1:500 for 1 h. Cells were counterstained with either Hoechst (nuclei) or phalloidin (actin cytoskeleton).

6.2.3 Imaging with single cell resolution in 3D

Confocal microscopy was predominantly used to obtain the cell images. We used either a 20x or a 40x water-immersion objective. With the 20x objective sixteen 90 µm wells were imaged per image, while the 40x objective only imaged four wells per image. Confocal microscopy was also used to determine the dimensions of MCF-7 cell clusters. For this, samples were prepared in duplicates and repeated twice.

6.3 Results and discussion

6.3.1 Coating the microwells with different ECM proteins

The PEG hydrogel material is inert in nature and has to be coated with protein to allow cell attachment (Lutolf and Hubbell, 2005). Here, we evaluated the coating of the gel with three different ECM proteins; Lam, Col-I and Fn. These proteins are important at different stages in cancer progression (See Introduction, chapter 1) and were therefore of interest. After coating the proteins at the bottom of the gel using microcontact printing (Fig 6.2, process step ii) we imaged the direct or indirect (antibody labelled) fluorescent signal of the coating. In all cases, a distinct contrast between coated and non-coated areas in terms of fluorescent intensity could be

determined. Both Fn and Lam (Fig. 6.4a and c) were homogenously distributed across the bottom of the microwell, while Col-I was more unevenly distributed (Fig. 6.4b). This may be explained by polymerization of Col-I during the printing step, promoted by the high Col-I concentration and the basic pH of the PEG-mixture.

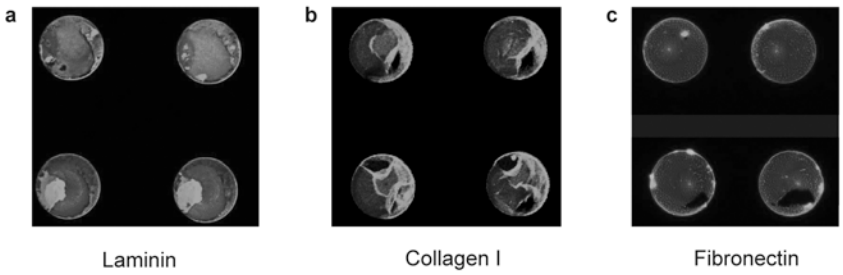

Figure 6.4: *Coating the wells with an ECM facilitates cell adhesion at the bottom of the microwells.* The protein coating is visualized by indirect fluorescence from left to right for Lam, Col-I and Fn. Lam and Col-I are stained with respective primary antibodies and visualized by secondary antibody staining using an Ab-Alexa Fluor 488 conjugate. In the case of Fn we immobilized Fn directly conjugated to Alexa Fluor 488. Lam and Fn coatings were very homogenous, while Col-I coatings were slightly more fibrous, probably due to polymerization of Col-I at the printing step.

6.3.2 Evaluating cluster formation in the array

The microwell array platform enables the production of 3D clusters within a short time frame, as microwells can be seeded with a high number of cells. When 1.5×10^5 MCF-7 cells per microwell array were seeded, 3D clusters formed within 24h (Fig. 6.5a) that, however, were small enough to still fit inside the microwells (90 µm diameter, 60 µm depth, $V = 0.4\times10^6$ µm^3) after 48h preculture (Fig. 6.5b). Clusters showed a rather low size distribution in x-y and most clusters filled the wells so that clusters in 90 µm wells had a diameter of 80-90 µm.

To measure cluster heights, we stained the cells' actin cytoskeleton using phalloidin and analyzed the average cluster heights by means of confocal microscopy. After seeding of 1.5×10^5 cells onto the platform, the clusters in 90 ×80 µm wide microwells reached an average height of 56 ± 3 µm (Fig. 10).

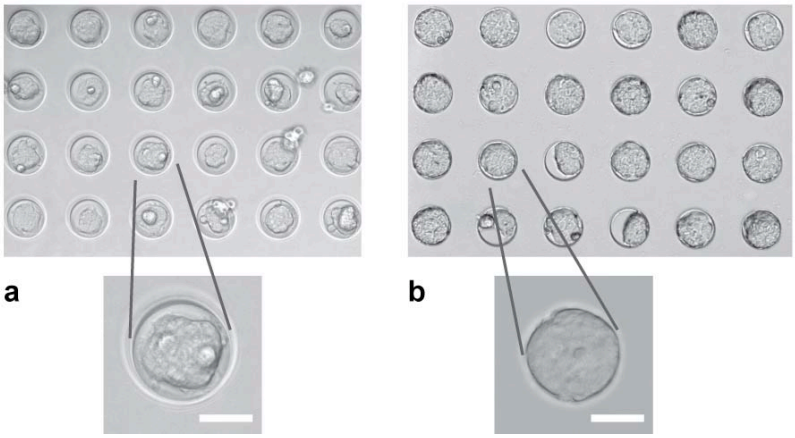

Figure 6.5: *Cluster formation in collagen-coated microwells.* With a seeding density of 1.5×10^5 cells per Ibidi dish well, clusters form in 90 µm wide wells after 24 h (a) but do not grow out of the bounds of the microwells after 48 h (b). The microwells used for cluster formation were 90 µm wide and 80 µm high. Scale bars are 50 µm.

6.3.3 Creating PEG gels with different rigidity

The rigidity of the cell culture environment has shown to influence cell behaviour *in vitro* and is probably important for various physiological behaviours (Levental *et al.*, 2007), including cancer progression and metastasis (Tilghman *et al.*, 2010). Recently it was shown that increased crosslinking of the Col-I matrix in the tumour stroma forced tumour progression by enhancing integrin signaling (Levental *et al.*, 2009). Here we determined the relationship between PEG concentration and rigidity of the PEG hydrogel. Furthermore the suitability of these gels for cancer cell culture was investigated at two different rigidities.

The relationship between PEG concentration and gel rigidity

Shear modulus (G) was measured for five different gel disks with different PEG concentrations on a rheometer with plate - plate geometry. The shear modulus was measured at a high range of frequencies. However, the measurement of the softest gels was only stable at lower frequencies and therefore an average shear modulus was determined from seven values between 0.1 and 2.5 Hz. For the calculation of the elastic modulus we used the 7 values with the lowest strain from each measurement. The measured shear modulus (G) was corrected for the area of the gel disks before we calculated approximate values for the Young's modulus (E). E is a measure of rigidity that is more commonly used to express the rigidity of tissues and substrates for cell culture. E relates to G as described by Equation 6.3, where v is the Poisson ratio. The hydrogel contains mainly water, therefore this material is almost incompressible and we can safely assume v = 0.5, which gives Equation 6.2. From the relationship

between E and G we determined Young's modulus versus the percentage of PEG as shown in Fig. 6.6a.

Intriguingly, the relationship between PEG concentration and gel rigidity was almost linear. Comparing these results with previously published data on tissue rigidity revealed that the gel with 2.5 % PEG, with a rigidity of around 8 kPa, is closest to the rigidity of the breast tumour, which is around 5 kPa (Fig. 6.1).

Equation 6.1 $$E = 2G(1+\nu)$$

Equation 6.2 $$E[\nu - 0.5] \approx 3G$$

Finally we investigated the possibility to micromould gels with different rigidity. Figure 6.6b shows transmission images of wells made in PEG hydrogel using a 100 μm PDMS mould. Hence, microfabrication in these dimensions was possible in all gels tested with a PEG concentration of 2.5 – 7.5 %. In addition, we found that the well diameter did not change with PEG concentration. The average diameter of wells moulded using the 100 μm was determined from microscopy images to 90 ± 2, 92 ± 1, 89 ± 2 and 88 ± 2 for the respective gels ranging from 2.5 – 7.5 %, (4 repeats).

Cell culture on PEG gels with different rigidity

To determine which gel that was most suitable for our experiments we used two gels with different rigidity as cell culture substrates for MCF-7 cells. We choose to test the two gels with the lowest rigidity, namely the 2.5 and 5 % gel, as these showed rigidity values closest to the rigidity of breast tumour.

MCF-7 cells were allowed to adhere for 7 hrs on Col-I-coated gels and subsequently fixed and stained with phalloidin to visualize the actin cytoskeleton. It was found that cells spread poorly on the 2.5 % gel (Fig. 6.7c) in comparison to the 5 % gel (Fig. 6.7d). Inhibited spreading is a common behaviour of cells on soft substrates (Rehfeldt *et al.*, 2007). However, the 2.5 % gel is actually still in the moderate rigidity range, with a Young's modulus of about 8 kPa. For example, Paszek *et al.* found that both cancer and normal cells spread well on poly (acrylamide) gels with a rigidity of 4 kPa (Paszek *et al.*, 2005). Therefore, it can be expected that the obtained differences in cell spreading were due to another parameter that is linked to substrates stiffness, such as protein coating.

The protein coating of the PEG gel is dependent on the amount of PEG in the network, the tighter the PEG network, the more protein may be linked to it via entrapment or covalent linkage via the PEG-maleimide linker. Indeed, this

assumption was backed up by lower fluorescent signal on both Lam and Col-I coated 2.5 % gels (Fig. 6.7a) in comparison to the 5 % gel (Fig. 6.7b). This is evidence that the reduced cell spreading on the 2.5 % PEG was due to insufficient Col-I coating.

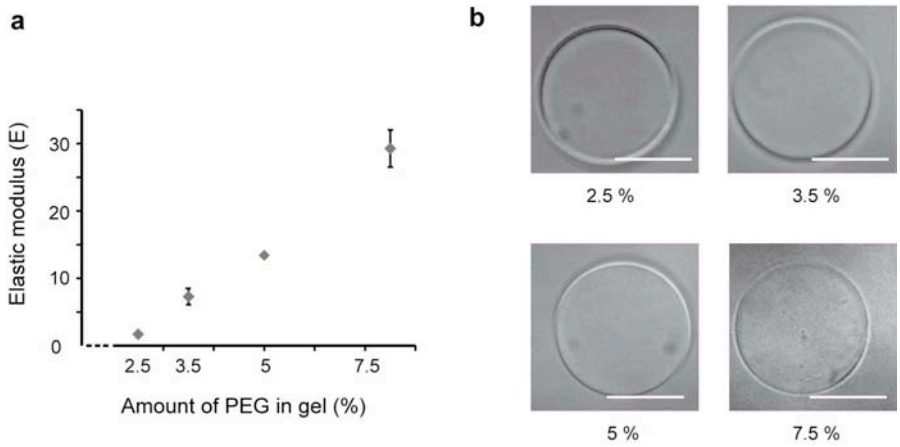

Figure 6.6: *Rigidity of PEG-gels with different polymer concentrations.* Rheology measurements indicate that there is linear relationship between PEG concentration and Elastic modulus (E). The gel rigidities are within a tissue relevant range. The 5 % PEG gel corresponds to the rigidity of skeletal muscle. In addition, microwell fabrication was performed in the tested gels. Transmission images show that microwells could be prepared by molding into all tested PEG gels (b), with concentrations ranging from 2.5 to 7.5 %. The well diameter remained similar, independent of the polymer concentration in the gel. Scale bars are 50 μm.

Because the protein coating of these gels was dependent on the PEG concentration, this system was not suitable for studies in which rigidity should be an independent parameter. It may be, that at higher PEG concentrations the protein coating is saturating. In that case, the cells would sense no differences in the protein coating of the gels in this rigidity range. However, while this is a hypothesis, in order to prove it, further investigation is needed. It may also be possible to find a way to coat the hydrogel that is independent of the density of the PEG network. This may be possible by blocking reactive groups on the PEG or by non-specific linkage of the protein.

A concrete strategy would be to mix a non-interactive protein such as BSA with the matrix protein to tune the amount of matrix protein to a constant level at different levels of total protein immobilization. However, this would not solve the problem with the low protein density on 2.5 % PEG. Compensating for the lower amount of PEG-TH at lower PEG concentration by adding extra PEG-TH would be another possibility to control the binding of PEG-maleimide functionalized protein. However, this would not solve the problem with different amount of trapped protein in differently dense PEG-gel networks.

It is clear that a large amount of engineering is needed until protein-coated PEG microwell arrays would be a suitable to study the effect of stiffness on cell behaviour without interference from other parameters. Another parameter that influences how a cell senses the mechanical properties of a material is the network pore size (Levental *et al.*, 2007). However, the PEG hydrogel is in principal non-porous, with a mesh size in the range of tens of nanometers, and thus in this instance this parameter is less relevant. For our studies we wanted to use a gel that had a constant rigidity with high *in vivo* relevance. We decided to use gels with a constant PEG concentration of 5 %, corresponding to a rigidity of 13 kPa. When these gels were coated with protein, they showed to support cell attachment well, as discussed above.

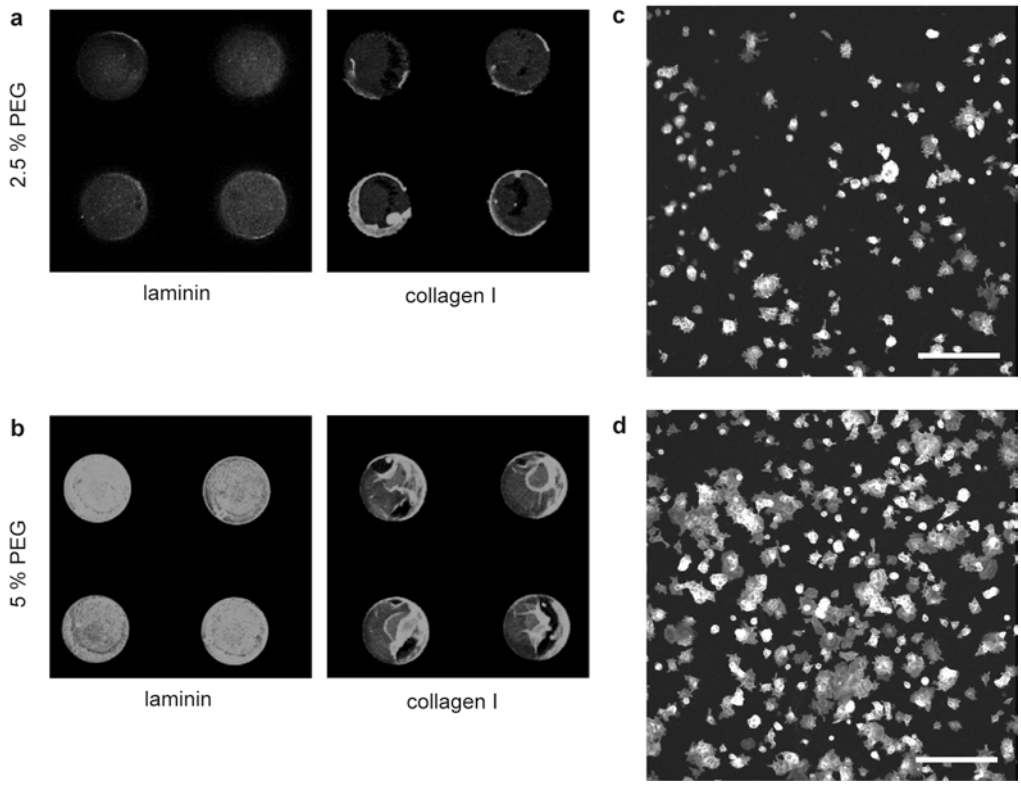

Figure 6.7: *Protein coating and MCF-7 cell spreading on gels with different rigidity.* Immunostaining of Lam-coating as well as Col-I-coating show lower fluorescent intensity on the 2.5 % PEG-gel (a) than on the 5 % PEG-gel (b). This indicates that the protein density is higher on the 5 % gel. In addition, MCF-7 cells spread less on flat Col-I-coated 2.5 % PEG-gel (c) than on the Col-I-coated 5 % gel (d). The images show the actin cytoskeleton (phalloidin-488 staining) of MCF-7 cells 7 h after seeding, i.e. enough time for cell spreading.

6.3.4 Optimization of the apoptosis detection by microscopy and automated image analysis

Evaluation of different apoptosis detection assays

As a next step we evaluated the suitability of different methods for the detection of apoptosis. Early apoptosis detection would be advantageous for this system as late stage apoptosis affects cell adhesion, leading to a change in the cluster morphology. For this purpose we tested several different assays, but many of them were sub-optimal.

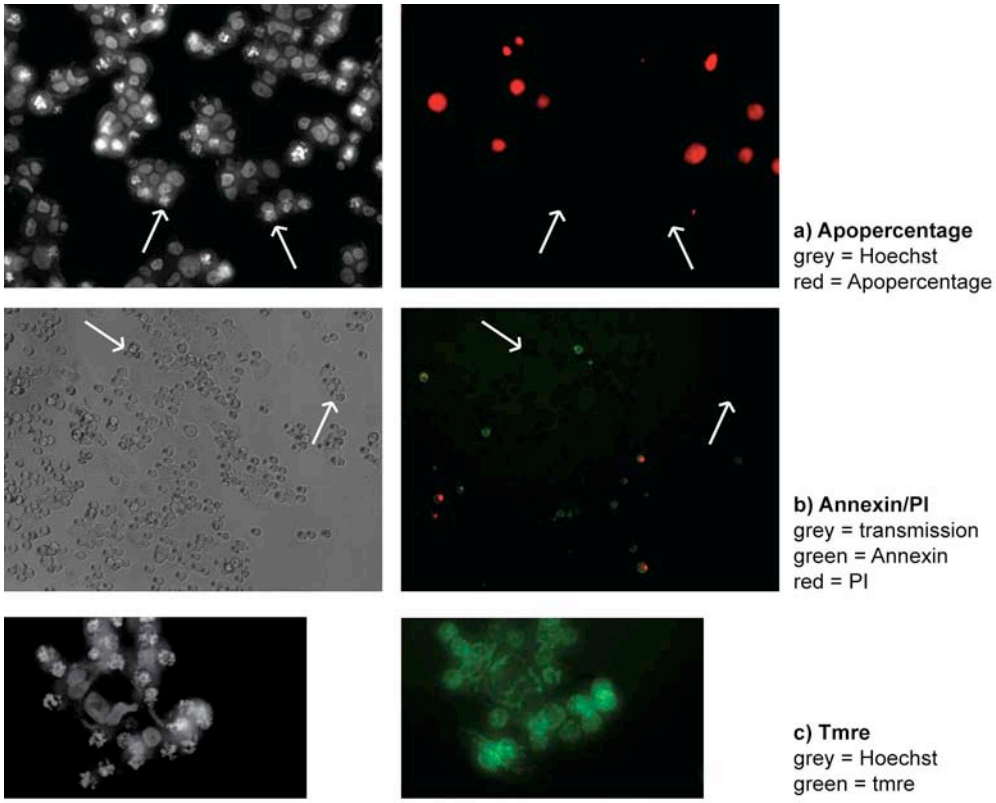

Figure 6.8: *Evaluation of apoptosis assays by widefield microscopy.* Different apoptosis assays were evaluated in order to find one that allowed the earliest detection of apoptosis. MCF-7 cells were seeded onto TCPS substrates for 24 h before treatment with 100 nM Taxol. In the figure, different assays based on fluorescent markers of apoptosis are compared to nuclear fragmentation and cell morphology. It was found that all assays showed lower apoptosis than the fragmentation of the cell nuclei. In a) less cells are stained with the APOPercentage dye than cells with a fragmented nuclei. The white arrows show two cells that have a fragmented nucleus, but are not stained with APOPercentage. Similarly, the green Annexin stain (b) showed very low apoptosis and almost correlates to the propidium iodide staining, which shows necrotic cells. In the corresponding transmission image it is clear that many of the unstained cells were rounded up, frequently a sign of apoptosis. The arrows are pointing at two cells that show a rounded morphology in the transmission image, but are not stained with Annexin. Tmre is a fluorescent dye (c) that stains mitochondria, to indirectly determine cell metabolism. It is however, very difficult to distinguish differences in the Tmre stain in cell with a normal and a fragmented nuclei, partly complicated by the rounding up of cells.

Some assays only gave a very weak signal after staining, such as the nick-end labelling, TUNEL assay (not shown). Other assays showed very low apoptosis signal, even when cells were clearly apoptotic, as determined by cell morphology and nuclear fragmentation (Fig. 6.8). Both Annexin V and APOPercentage were assays that showed a signal comparable to that of propidium iodide incorporation, which is a signal for necrosis or very late stage apoptosis. Nuclear fragmentation, determined by Hoechst staining of DNA, showed to be the most sensitive assay leading to the earliest apoptosis signal of the assays tested.

Quantification of apoptosis in images from wide-field microscopy

Image-based evaluation of drug response in 3D cell clusters can be done by comparing image parameters of whole clusters, as shown in an image obtained by widefield microscopy (Fig. 6.9). Intensity values of nuclear and viability stains (Lee *et al.*, 2008) as well as cluster granularity are different parameters that can be used as a read-out. Drawbacks of analyzing 3D cultured cells by widefield imaging are that on one hand, the read-out will be population based, so that parameters related to single cell information are lost. On the other hand, widefield imaging of thick samples often includes errors from out of focus blur and scattered fluorescent light.

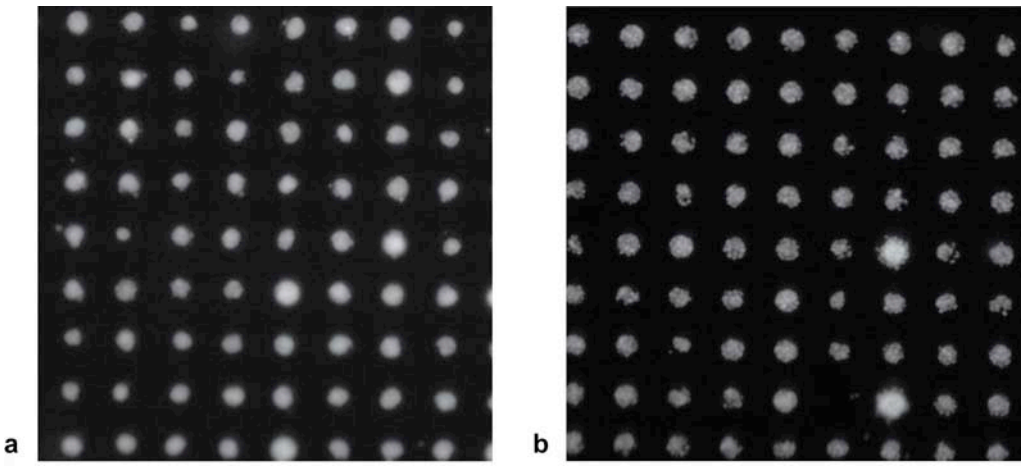

Figure 6.9: *Detecting apoptosis signals in cluster stained by widefield microscopy imaging.* Nuclear stain showed more homogenous staining in control cells (a) than in drug treated cells (b). However, light scattering leads to large errors to intensity measurements of these images. The method has a major drawback compared to confocal imaging based methods, in which spatial information can be obtained.

Quantification of apoptosis in images from confocal microscopy

Confocal microscopy reduces out of focus blur and therefore enables images with sub-cellular resolution. As discussed in the background section, this is a requirement of HCS, which is extensively used in drug development. This motivated us to develop a method to quantify apoptosis on the single cell level, which would be compatible with other HCS approaches. Images of the 3D clusters can be obtained by making a 3D reconstruction of z-stacks with inter-plane distance of 1 µm, however the image acquisition can be very time consuming, especially with thicker samples. An approach that needs less time for image acquisition is to take just a few confocal images at different z-positions within the 3D cluster and then evaluate them as 2D images. This method would also give spatial information on cell behaviour. In order to establish a protocol for this method, we first measured the mean nuclei size of cells cultured in 3D clusters. The nuclei diameter was determined to be 11 ± 4 µm. In order to avoid overlapping assessments, confocal images were therefore acquired at z-planes separated by 15 µm (Fig. 6.10). The high resolution of these images would enable a type of high content screening in 3D.

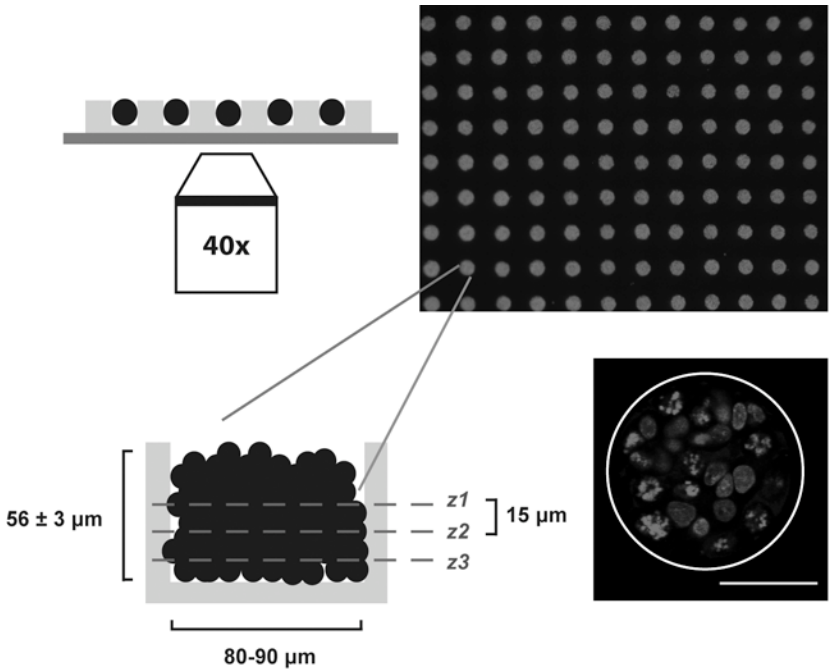

Figure 6.10: *In situ imaging of single cell information in 3D clusters.* MCF-7 cells seeded into the microwell array form clusters that are very homogenous in size. Confocal imaging is used to image the clusters at three different images planes.

This is exemplified in Fig. 6.11, which shows an image where cells are labelled with three different dyes to visualize cell health. Hoechst shows nuclei morphology (Fig. 6.11a), which gives information about apoptotic cells and in addition secondary parameters, such as cell density can be calculated from this stain. BrdU incorporation (Fig. 6.11b) shows a relative proliferation index. Resolution on the single cell level allows regional differences in proliferation to be determined. Mitotracker red (Fig. 6.11c) is a fluorescent dye that shows mitochondrial activity, thus providing information about cell metabolism within the cluster.

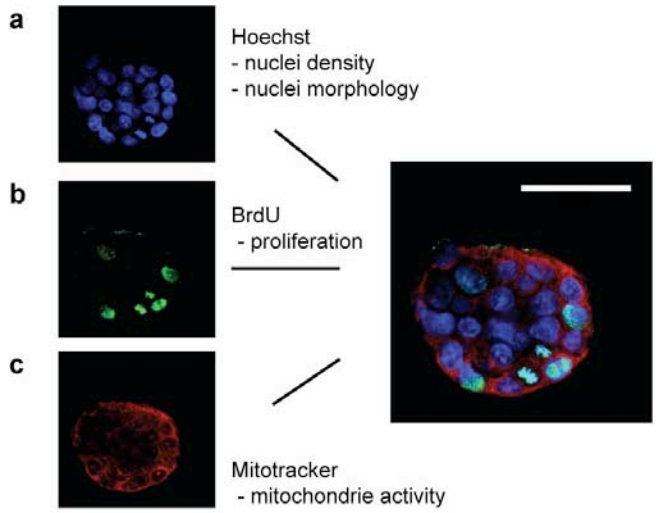

Figure 6.11: *Sub-cellular resolution enables high content screening methods to be used for analysis of the 3D clusters.* Here three different dyes are used to visualize cell health. Hoechst (a) shows nuclei morphology, which gives information about apoptotic cells. Also secondary parameters, such as cell density can be calculated from this stain. BrdU incorporation (b) shows a relative proliferation index. With resolution on the single cell level, regional differences in proliferation can be determined. Finally, Mitotracker red (c) a fluorescent dye that shows mitochodrial activity gives information about cell metabolism.

One problem that occurs when imaging thick samples is the loss of signal intensity further away from the objective, due to scattering of the fluorescent light and spherical aberration. In the cell cluster samples, it was possible to notice a light intensity drop already at 30 μm into the samples. This low penetration depth of the fluorescent light was probably due to the high nuclear density of the clusters. We hypothesized that a reduction in the intensity decrease in the z direction could be obtained by using a dye with excitation and emission maxima at longer wavelengths. Therefore we stained the nuclei with Propidium iodide (Ex/Em = 536/617) instead of Hoechst (Ex/Em = 346/460). With this, some improvement was observed.

Further steps towards an optimized strategy would include the use of an objective, which is designed for thick samples, the use of multi-photon excitation to increase the

intensity of the exciting light and an optimized light detection to avoid the leakage of scattered light. Finally we should note that this imaging issue is likely to be less problematic for cell clusters with a lower cell density e.g. the MDA-MB-231 cells. For our experiments the establishment of a standard method for analysis, which would then be comparable over the samples, solved this issue. This imaging protocol included three images at different z-planes per cluster, starting with the first image at the plane of the first cell nuclei in the cluster (Fig. 6.10).

Automatic object segmentation of confocal images

Counting of nuclei and the determination of differences in nuclear morphology can be performed manually, but would be very time consuming for larger experiments. Therefore we evaluated different strategies for automatic evaluation of the images based on object segmentation in 2D or 3D images. 3D image segmentation can theoretically be advantageous as no information is lost. The information gathered from whole 3D objects, in this case the nuclei position and morphology, should generate more information than in a 2D image to distinguish, for example, morphological differences.

Because the focus of our experiments was culture of MCF-7 cells we developed the algorithm based on these cells. From an image analysis perspective, these cells are not ideal. The problem is that they grow so densely that it can be difficult to distinguish between two nuclei in adjacent cells. Both in 2D and 3D images, standard image thresholding and segmentation by the standard watershed function (Fig. 6.12a and c) generates imperfect object recognition.

For 3D images we exploited a recently published segmentation algorithm called the gradient vector flow algorithm (Li *et al.*, 2007). This algorithm was developed especially for 3D object segmentation of touching objects. The segmentation results with this algorithm clearly improved the result compared to the watershed function (Fig 6.12b). It is likely that this algorithm could be further improved by introducing boundary and selection criteria, such as nuclear size and morphology (Master thesis, C. Faigle, 2010). However, because this method requires high computer capacity both in image acquisition and processing, image segmentation of 2D images would probably be a more attractive alternative in a screening activity.

We found that the Advanced Cell Classifier, an open source software developed by Dr. Peter Horvath at ETH Zurich, gave reasonable image segmentation results (Fig. 6.12d). This program also includes some machine learning algorithms (Jones *et al.*, 2009), which can be used to distinguish between complex phenotypes in an image. The machine learning algorithms proved useful when distinguishing between apoptotic and healthy cell nuclei.

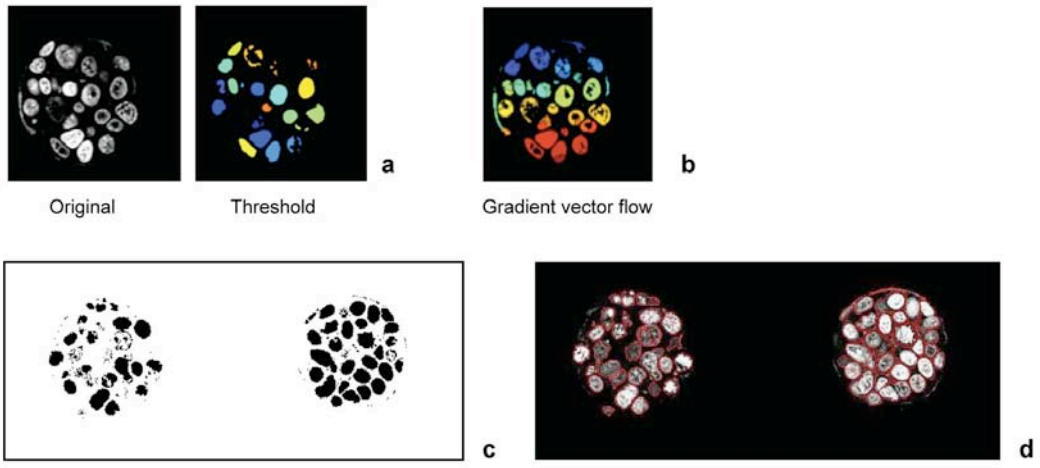

Figure 6.12: *Automatic object segmentation in 2D and 3D.* Two different methods for object segmentation of 3D images were employed. Only thresholding (a) resulted in a poor segmentation of the original image with both the loss of objects and difficulty in separating object. However, a newly developed image segmentation algorithm based on gradient flow tracking was shown to better recognize the nuclei in the example image b. Object segmentation of 2D images is a faster method to analyze the 3D clusters. Normal thresholding and watershed segmentation gave a rather poor result with much information lost (b). The result of segmentation was improved using the more sophisticated Open source Cell profiler software. This software uses several different segmentation algorithms to separate the nuclei. The segmentation result using the Cell Profiler is shown by the red lines in the original image (d).

6.3.5 The effect of 3D culture on growth after cluster formation in two cancer cell lines

We then went on to compare the growth behaviour of two different cancer cell lines upon culture in 3D clusters in 90 µm wide microwells. MCF-7 and MDA-MB-231 are two cell lines that are used to study early and more advanced stages of cancer, respectively. Interestingly, the proliferation relative to 2D after 3 days culture in 90 µm Col-I coated microwells, was significantly lower for MDA-MD-231 (Fig. 6.13). The relative proliferation reached 58 ± 6 % in MCF-7, which is 26 ± 9 % higher than in MDA-MB-231 ($p < 0.05$).

Furthermore we can confirm a significantly higher cell density in MCF-7 clusters than in clusters of MDA-MB-231 cells. The cell density after 3 days in culture was 27 ± 2 nuclei per unit area for MCF-7 cells, which is 6 ± 3 cells per unit area higher than for MDA-MB-231, where cell density only reached 21 ± 3 cells per unit area ($p<0.05$). Intriguingly, we could expect different signals to be responsible for the growth reduction. For the tumorigenic MCF-7 cell line, the reduced growth could be explained by increased E-cadherin-signaling because of enhanced cell-cell contacts in 3D culture and at increased cell density (Perrais *et al.*, 2007). On the other hand, the

growth reduction in the metastatic MDA-MB-231, that do not express E-cadherin, is probably more likely due to reduced integrin-signaling in 3D culture.

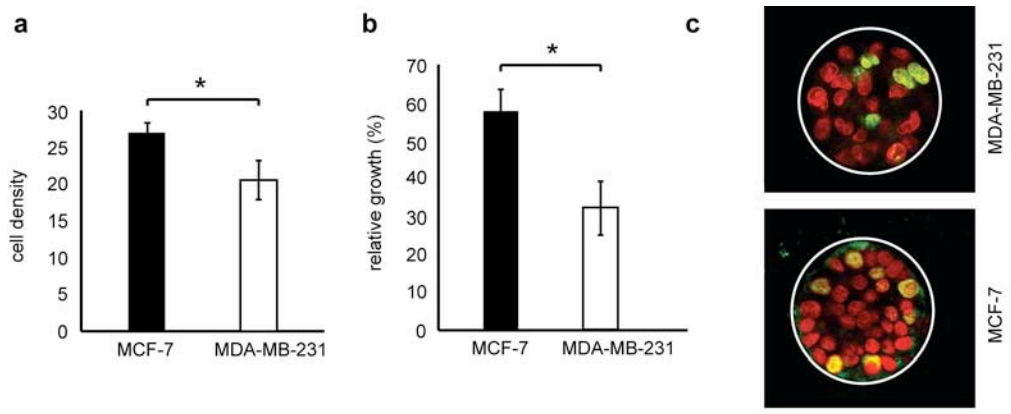

Figure 6.13: *Cell density and proliferation in the microwells for MDA-MB-231 and MCF-7.* We found significantly differences in growth behaviour and in the packing density when the two examined cell lines MCF-7 and MDA-MB-231 were grown in Col-I-coated microwells. First, after 72 h cluster growth, the cells in the MCF-7 clusters were significantly denser than the cells in the MDA-MB-231 clusters (a). This may relate to the strong cell-cell contacts in the MCF-7 cells. In addition, it was observed that the growth within the 3D cell clusters was reduced in comparison to the growth rate on a Col-I-coated TCPS substrate, here referred to as "relative growth". Interestingly, the relative growth was significantly lower in the MDA-MB-231 cells compared to the MCF-7 cells.

6.3.6 Investigating the possibility to use the microwell platform for the study of different niches in cancer progression

It was interesting to see that MDA-MB-231 cells grown in 90 µm microwells also formed proper 3D clusters, in which it is impossible to differentiate between single cells (Fig. 6.14a). Metastatic cells, such as MDA-MB-231 cells, have shown to change phenotype and re-express E-cadherin in the metastatic niche (Chao *et al.*, 2010). This could explain how metastases are formed. While it is known that the microenvironment participate in the regulation of metastasis, there are many open questions to the details on how the metastatic niche regulates cell behaviour (Joyce and Pollard, 2009). Therefore, experimental systems that could be used to study these questions would be highly useful. A recent paper showed that the phenotypic change of metastatic cells into 3D cluster formation and E-cadherin expression, can be induced by the culture on a Lam gel (Benton *et al.*, 2009). When the same cells were cultured on a Col-I 3D gel, cells spread and did not express E-cadherin. Therefore we were curious to explore if the PEG hydrogel system could be suitable to study these effects of extrinsic factors in the metastatic niche. In the microwells we could compare the effect of matrix coating independent of morphology.

To investigate this application, MDA-MB-231 cells were cultured in Col-I and Lam coated wells, as this would reveal if the phenotypic changes observed in (Benton *et al.*, 2009), were morphology or Lam dependent. Staining the F-actin of the cells in the clusters showed that stress fibers were produced at the interfaces with the coating on both Col-I and Lam (Fig. 6.14b), while further away from the protein the F-actin staining showed mainly cortical actin. This indicates that the MDA-MB-231 cells form matrix adhesions to both coatings. We were interested to see if the actin cytoskeleton looked qualitatively differently depending on the coating. However, even though the stress fibers were maybe a little more stretched on Col-I, the differences were very small.

We then investigated whether E-cadherin expression was induced by the culture within microwells. However, after 3 days in culture, MDA-MB-231 cells did not show any E-cadherin localized at the cell-cell contacts (Fig. 6.14c). Some intracellular E-cadherin was observed in the cells, but this was similar to cells cultured on flat Col-I-coated TCPS (Fig. 6.14d). The behaviour was independent of protein coating, as it was observed both in Col-I and Lam microwells and did not change after 5 days in culture. The control MCF-7 cells, that do express E-cadherin, form dense clusters in 3D with clear E-cadherin staining at the cell-cell contacts (Fig. 6.14e). These cells show E-cadherin expression even in 2D culture, where it is even more obvious that E-cadherin is localized only at the cell-cell contacts, as not all sides of the cells are in contact with other cells (Fig. 6.14f).

One possible explanation for the differing results between our work and the work reported in (Benton *et al.*, 2009) could be the stiffness of the substrates, as a pure Lam gel is expected to be much softer than the 5 % PEG gel. This could affect the adhesion of the cells. In a more recent report, the stimulation by both hepatocyte derived extracellular matrix and soluble factors from liver cells was needed to induce phenotypic changes in the MDA-MB-231 cells (Chao *et al.*, 2010). Hence, it is also plausible that the signal from the Lam interaction and the morphology effect is generally not strong enough to induce E-cadherin expression.

These results also provide evidence that the MCF-7 cell, as a tumorigenic cell line, would be the most appropriate choice for further experiments. Previous literature shows that these cells, as a model of early stages of cancer, typically grow in dense colonies in *in vivo* like ECM gels (Kenny *et al.*, 2007) similar to what we observed in the microwells.

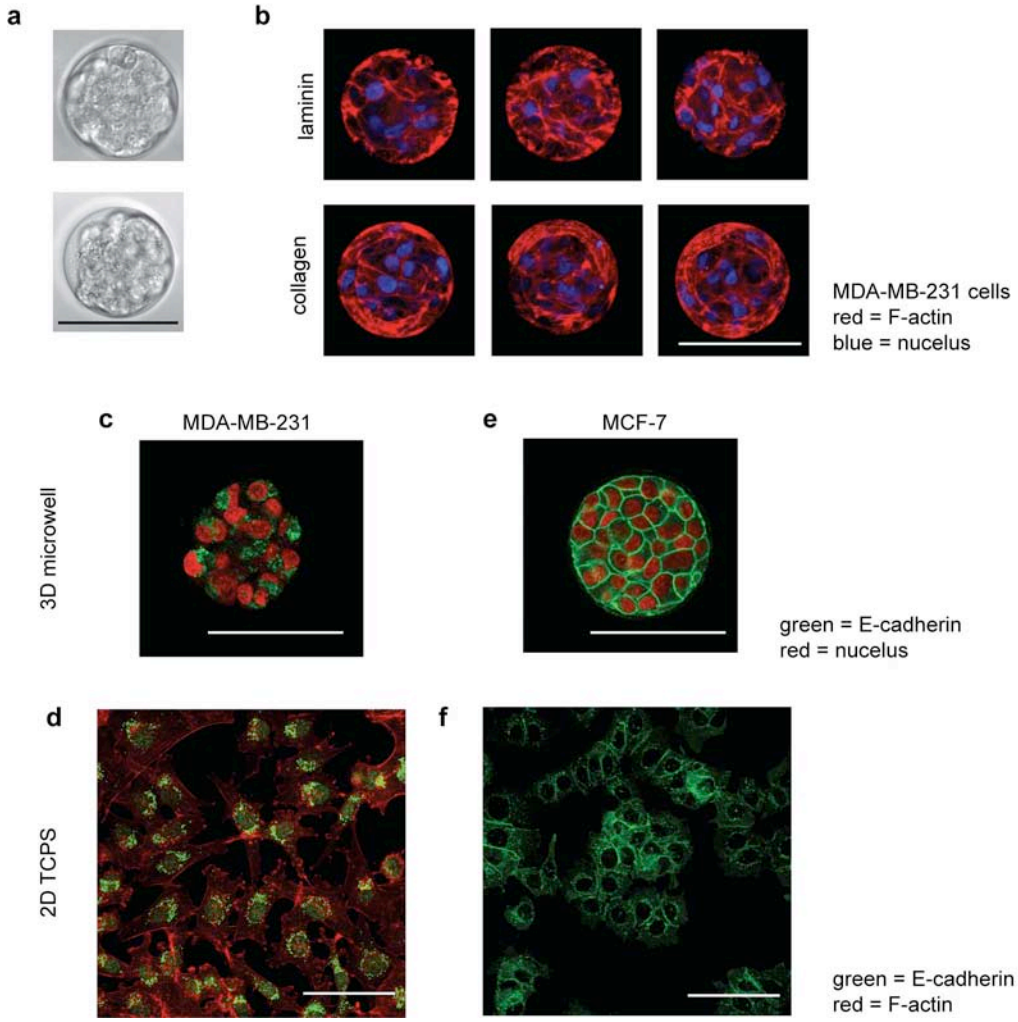

Figure 6.14: *Morphology and E-cadherin expression of MDA-MB-231 cells in microwells.* MDA-MB-231 cells form clusters in the microwells 48h after seeding (a). The transmission images of the clusters show that the cells are merged into a cluster and it is difficult to distinguish individual cells. In (b) confocal microscopy was used to image the cytoskeleton of the cells only at the matrix interphase. It can be seen that MDA-MB-231 interact with the coating and form actin stress-fibers (red) on both Lam and Col-I. A slight difference towards more stretched actin fibers on Col-I can be seen in these images. MDA-MB-231 cells did not show any E-cadherin staining at the cell-cell contacts after 72 h culture in the microwells (c). This behaviour was independent of the coating of the microwells (Lam versus Col-I) and if the cells were cultured for 3 or 5 days before fixation. In the confocal image of the MDA-MB-231 cluster, there seems to be some E-cadherin localized in the cytoplasm. However, this staining is also seen after culture in 2D on TCPS (d). In the MCF-7 control ells, E-cadherin expression was very strong after 72 h culture and the protein is predominantly localized at cell-cell contacts (e). The E-cadherin expression in MCF-7 is also present on 2D TCPS substrates (f), even though it may be enhanced by the increased cell-cell contacts in 3D. All scale bars are 100 μm.

6.4 Conclusions

In this chapter we described the characterization of the PEG hydrogel platform and the development of additional methods for the use of the platform to study cancer cell behaviour in 3D clusters. We were originally interested in this platform as it enables the creation of more *in vivo* like environment, including tissue relevant scaffold stiffness, 3D cell cluster formation and long term cell culture. Furthermore, as protein could be attached to the gel by a generic linker, any cancer-relevant protein could in principal be attached to the gel (Lutolf *et al.*, 2009). In addition, the PEG hydrogel offers similar advantages to the PDMS microwell array in terms of controlled culture conditions.

In a first step, we analyzed the rigidity range in which the platform can still be microstructured and support cell adhesion. It was found that with a PEG concentration of 2.5 % it was still possible to mould microwells. However, cells only poorly attached to the Col-I-coated 2.5 % gel in comparison to the 5 % gel. We concluded that this is probably due to reduced protein density in the coating of a less dense gel. Therefore, we finally decided to use only the 5 % gel for our drug testing experiments, and thus no longer investigate the role of substrate stiffness.

It is important to bear in mind that until now, only little is known about the effect of rigidity on drug response in cancer. Therefore, an initial investigation of this relationship would probably be better as a screen, testing a large range or rigidities, cell types and drugs. A first step in this direction was recently presented by Tilghman *et al.*. They investigated rigidity-dependent growth patterns of 17 different cancer cells and found both rigidity responsive and non-responsive cells (Tilghman *et al.*, 2010).

In the further development of this platform we tested different methods for apoptosis determination in the 3D clusters. First, different apoptosis assays were tested for their suitability to show apoptosis in MCF-7 cells in response to Taxol. It was found that all assays tested showed lower apoptosis than nuclear fragmentation. Therefore, we decided to use nuclear fragmentation, as it is beneficial to be able to study the early signs of apoptosis when a microscopy-based analysis is used.

The PEG hydrogel is moulded as a thin film on a thin solid support, which makes the platform compatible with high-resolution imaging. High-resolution confocal imaging would be an advantageous imaging method for these 3D samples, as with a low-resolution wide-field microscope only a population-based signal could be obtained. High-resolution microscopy is typically used in high-content screening during, for example, drug screening procedures. With the sub-cellular resolution it is possible to collect a multitude of parameters per sample. However, HCS has so far only been used for 2D samples, due to the ease of image acquisition and sample preparation.

Therefore, we were eager to evaluate the feasibility of extending this to 3D high content screening. We established a protocol for the imaging of the cell cluster at three positions at different distances from the protein coating. The information in the images could then be quantified by manual or automatic analysis.

We found that MCF-7 cells are particularly difficult to automatically quantify, as in the images nuclei were often touching. However, we found that the software "Advanced cell classifier", developed at ETH, managed to both segment the nuclei and classify nuclei according to their morphology. For the evaluation of the drug experiments presented in the next chapter we used the automatic image segmentation with the "Cell classifier" and manual cell counting to determine apoptosis levels.

Finally, we tested the culture of two different cancer cell lines in the microwells. While both cells lines showed cluster formation, MCF-7 cells seemed more suitable for the culture in the 3D environment of the microwells as they shown an *in vivo* like morphology and continued proliferating in the new culture environment. We originally hypothesized, that MDA-MB-231 cells could be very interesting to study in the microwells, because the 3D culture in contact with Lam may offer the environmental impulses that these cells encounter in a metastatic niche. However, as no phenotype change or alteration in E-cadherin expression was observed we decided to only continue with the MCF-7 cells.

CHAPTER 7

A comparative study of drug response and cell proliferation in a 3D model provides insights into signaling from the microenvironment

In the previous chapter we presented the development of a platform for the formation and analysis of 3D cancer clusters, based on the PEG hydrogel microwell array. This microwell array was recently developed for use as a cell culture platform and has been predominantly employed for stem cell cultures (Lutolf *et al.*, 2009). It has several advantages over conventional 3D culture models including the high control of the culture environment enabling the study of the role of, for example, matrix composition independently of other parameters. In addition, the micromolding of the hydrogel into a thin film enables high-resolution microscopy, which makes it possible to analyze cell behaviour on the single cell level. As discussed in Chapter 6, this model system has also advantages when compared to the PDMS model (Chapter 4 & 5) including an *in vivo* relevant rigidity and improved stability of the non-adhesive contrast.

The objective of the study presented in this chapter was to investigate matrix-dependent drug response in 3D with an experimental setup of high *in vivo* relevance and further to elucidate the relationship between alterations in drug response and proliferation. In section 7.3.2 we focused on two important matrix proteins in cancer, Lam and Col-I, and studied their role in the response to Taxol in 3D cultured cells. The matrix-dependent drug response observed in these experiments, was not observed at high cell densities. Therefore we were interested in interrogating the effect of cell density, in addition to matrix interaction, on drug response (Section 7.3.3). To investigate the importance of cell-density for 3D-specific drug response, 2D Col-I patterns on the hydrogel with varying cell density were used. An interesting result from the experiments in this chapter was that the relationship between proliferation

and drug response was affected differently by different parameters, as discussed in section 7.4.3. This points out two different mechanisms for microenvironment induced drug resistance. A publication based on the results presented in this chapter is currently in preparation.

7.1 Background

7.1.1 Microenvironment induced drug responses

Cancer development and progression is typically followed by microenvironmental changes that can in turn be cancer promoting. In breast cancer, there exist a number of known cancer-associated changes in the environment, explained in more detail in Chapter 1. These include the production of cancerous stroma by activated myofibroblasts (Cukierman and Bassi, 2010) and the stiffening of the matrix by Col-I crosslinking (Levental *et al.*, 2009).

Not only can the microenvironment promote cancer, an effect called cell adhesion-mediated drug resistance (CAM-DR) has been shown to protect cells from standard treatment with chemotherapy (Meads *et al.*, 2009). Interestingly, tumour-stroma cooperativity during cancer progression correlates with increased CAM-DR. In a pertinent example of this, Sherman-Baust et al showed that over-expression of collagen IV in ovarian cancer correlates with tumour grade and that adhesion of these tumour cells to collagen IV *in vitro* mediates CAM-DR (Sherman-Baust, 2003, Cancer Cell).

CAM-DR typically relates to extrinsic signals that lead to reduced drug-induced DNA damage, anti-apoptosis signaling or alterations of the cell cycle (Hazlehurst, 2003). The effects on cell behaviour induced by the signaling from matrix adhesion are typically not on the transcriptional level and are therefore transient and immediate (Meads *et al.*, 2009). *In vitro* experiments with myeloma cells adhering to fibronectin, showed survival signaling already 2h after initiation of adhesion (Damiano and Dalton, 2000). Matrix-induced drug response in breast cancer cells has repeatedly been shown to relate to upregulation of Akt (Aoudjit and Vuori, 2001; Park *et al.*, 2008). This protein reduces apoptotic activity, possibly by modulating the balance between anti- and pro-apoptotic proteins in the cell (Aoudjit and Vuori, 2001). It was recently shown that the matrix-induced resistance was not only dependent on matrix composition, but also its organization as a 2D coating or 3D matrix (Serebriiskii *et al.*, 2008).

In addition to matrix-dependent effects on drug response, the three-dimensionality of the culture environment has been shown to induce reduced response to chemotherapeutic drugs in numerous investigations (Dhiman *et al.*, 2005) (St Croix *et al.*, 1996) (Fischbach *et al.*, 2007). The effect of 3D organization on cell behaviour, in comparison to 2D cell culture, can be attributed to a number of parameters. In addition to a morphology difference and change in cell size, the culture in 3D increases cell-cell adhesion and it can influence the exchange of nutrients and soluble factors. St. Croix at al. showed that reduced drug responsiveness in 3D could be partially explained by increased levels of the cyclin-dependent kinase $p27^{Kip1}$ and decreased proliferation, rather than anti-apoptosis signaling (St Croix *et al.*, 1996). In a recent review, E-cadherin downstream signaling was postulated to be a combination of both anti-apoptosis signaling via activation of Akt and signaling that lead to growth reduction (Bewick and Lafreine, 2006). Hence, the modulation of different signaling pathways is involved in adhesion-mediated drug resistance, and the resultant effect on the cell can be attributed to alterations in the apoptosis and proliferation regulatory machinery.

An additional factor that complicates treatment in the 3D environment is poor drug penetration over long diffusion distances, due to poor vascularisation (Grantab *et al.*, 2006). In larger tumour areas low O_2-pressure can occur and lead to hypoxic conditions. Hypoxic conditions can induce metastasis and angiogenesis of the tumour (Wittekind and Neid, 2005). However, the role in drug response is less clear (Sminia *et al.*, 2003). Zahir *et al.* propose that the growth of cells in 3D per se alters the cell response to apoptotic stimuli (Zahir and Weaver, 2004) by inducing a phenotype change, independent of the presence of hypoxic conditions. This argument was strengthened by results showing that normal cells were more sensitive to apoptotic stimuli in 2D than in 3D in an experimental setup where proliferation rate and oxygen tension were constant (Weaver *et al.*, 2002).

7.1.2 Current anti-cancer drugs

There are nearly 200 cancer drugs on the market with many more in the development pipeline. Cancer therapy today still relies largely on standard chemotherapeutic drugs, which usually have a general effect on the cancer cells, inhibit their survival. Some examples include DNA modifying agents, such as Cisplatin, Taxol and several other molecules, that interfere with the microtubule polymerization, metabolite synthesis inhibitors (e.g. Methotrexate) and drugs, such as Irinotecan, which interfere with chromosome topology.

The common denominator of these drugs is that they interfere with essential functions of cells in the body and are therefore also toxic to normal cells. Thus, these drugs have a narrow therapeutic window and the specificity of the drug lies in the difference

in dose response between normal and cancer cells, as well as asymmetric distribution of the drug in the body. The therapeutic window is wider for drugs that target non-essential functions. However, efficient treatment with these drugs requires an exact diagnosis of the tumour type. Commonly used drugs within this category include hormonal therapy, such as Tamoxifen, which modulates oestrogen receptors in breast cancer.

More novel drugs have been developed to have a more specific action against different biochemical mechanisms in cell division, such as cyclin-dependent kinase inhibitors. However, even though these drugs have a more sophisticated target, their effect on the cancer cells, may not be indifferent from traditional cytotoxic drugs. Therefore, these drugs can be just as toxic to normal cells as traditional drugs. However, if these more specific strategies could be targeted at a member of a protein family that is prominent only in tumour, then the therapeutic window for these cytotoxic drugs could be increased (Kamb *et al.*, 2007).

For this work we chose to work with Taxol, as it is still a commonly used drug in breast cancer therapy. There is a wealth of literature on Taxol response, while drugs with a more specific action are still in development or not yet so studied. We were also motivated to use Taxol, as effects of the signalling from the microenvironment on the response to Taxol have been reported (Aoudjit and Vuori, 2001). Finally, using Taxol for these studies enable the comparison back to the results in the first study on the PDMS platform.

7.1.3 Combination therapy targeting the microenvironment

The increasing knowledge of the influence of the microenvironment on cancer progression and drug response has initiated an interest in drugs, which target the microenvironment. A combination therapy of traditional chemotherapeutics with a drug targeting the cell-microenvironment interaction, to prevent the influence of CAM-DR, may help to increase the efficiency of the original therapy. The drug area that has progressed furthest in development includes drugs targeting integrins (Desgrosellier and Cheresh, 2010).

Integrin β1 is one interesting candidate, as it has been shown that upregulation of this molecule is associated with more aggressive forms of cancer (Yao *et al.*, 2007), and the blocking of its activity increased the response to radiotherapy (Park *et al.*, 2008). One integrin drug in clinical trial is Vitaxin, an antibody that has specificity for the αvβ3 integrin (Patel *et al.*, 2001) (see Introduction, section 1.2.4 for further details).

7.2 Experimental section

7.2.1 Fabrication of the PEG microwell arrays

Microwell arrays were produced at the bottom of 8-well Ibidi dishes by micromolding as described in Materials and Methods, Chapter 3. Here, microwells functionalized with either Col-I or Lam were used. All cluster formation experiments were performed in 90 μm wide and 80 μm deep microwells, as described in Chapter 6. For the 2D experiments we used 200 μm wide and 200μm deep, Col-I-coated, microwells.

7.2.2 Cell culture experiments in PEG microwells

Seeding MCF-7 cells into microwells

The Ibidi-dishes with PEG microwell arrays were prepared on the day before cell seeding. First, the PBS in the Ibidi dish was carefully exchanged by cell culture media. In the cell seeding procedure we made sure never to let the hydrogel dehydrate. MCF-7 from a 70 % confluent flask, were seeded into the microwells at a seeding density of 1.5×10^5 cells per Ibidi dish well. After 3-4 hrs, cells that had not entered the wells were removed from the plateau surface by two rinsing steps. To create monolayers of cells with varying cell densities on the Col-I-coating, cells were seeded with 2×10^4 cells per Ibidi-dish well. The formation of 2D monolayers at these seeding densities was confirmed by confocal microscopy. Alternatively, cells were centrifuged into the wells for 3 min at 1100 rpm. When this procedure was used, 7×10^4 cells per array was sufficient for cluster formation. This method was applied for the experiment with the mAb13 antibody and in the E-cadherin knockdown experiments.

Drug assay

Cells were seeded into microwells as described above. After 24h or 48h preculture the cell culture media was exchanged to contain 100 nM Taxol or 0.01 % DMSO (v/v) in the controls. After 24h incubation, cells were fixed with ice-cold methanol (70 % (v/v) in PBS for 20 min), rinsed with PBS twice and incubated in PI/RNAse staining buffer (undiluted for 30 min at RT; BD Biosciences, Switzerland).

BrdU assay

BrdU incorporation in the nuclei of proliferating cells was used to determine proliferative rates. This protocol is explained in detail in Materials and Methods, Chapter 3. Incubation times used were consistently 6 h at the end of the assay except for the E-cadherin knockdown experiment where 8 h incubation was used.

Immunohistochemisty

E-cadherin staining of MCF-7 cells treated with the E-cadherin si-RNA or control si-RNA was performed as explained in Chapter 3, Materials and methods, section 3.4.3.

7.2.3 Imaging of single cells in 3D

Confocal imaging was employed to allow imaging of the clustered cells with single cell resolution, see Chapter 6 for a detailed description of the imaging method. In short, our approach made it possible to observe the position of single cells. Hence, cells localized in the centre or at the periphery of the cluster could be distinguished, as well as cells in contact with ECM proteins or not.

To assure a high quality in the acquisition of images and, at the same time, restrain experimental variables, a decision was early made to use MCF7 cultures and to acquire three individual z-sections per cluster in all experiments; z1, z2 and z3, where z3 represented the cells in direct contact with the matrix (i.e., bottom topographic location). The z-image planes were separated by ~15 μm to avoid overlapping assessments.

7.3 Results

7.3.1 Matrix adhesion plays a key role in the regulation of drug response in 3D

The importance of cell-matrix interactions, specifically matrix composition and 3D organization, in regulating altered drug responses have been highlighted in the literature (Aoudjit and Vuori, 2001; Serebriiskii *et al.*, 2008). Here we present a novel way to study matrix-dependent drug responses in 3D using Taxol and arrays of MCF-7 clusters. One advantage of culturing cells within these types of 3D environments is that the engineered microwell dimension determines the resultant cluster size. Therefore, this system allows the study of matrix-specific effects independently of matrix induced morphology changes.

Lam and Col-I are two highly relevant ECM proteins in breast cancer that represent epithelial and stromal (or mesenchymal) matrices, respectively. Details on matrix signaling in cancer progression are described in Chapter 1, section 1.2.1. The study of the effect of adhesion on these proteins is difficult in 2D, as MCF-7 cells do not form strong attachments to Lam (Yao *et al.*, 1996) and thus form clusters on top of a Lam gel or coating (Benton *et al.*, 2009) (Hirtenlehner *et al.*, 2002). When MCF-7 cells were cultured as 3D clusters in the protein-coated microwells (Ø = 90 μm) no

morphology differences could be observed regardless of the type of ECM protein (Fig. 7.1a and b). Therefore we considered this a suitable model to study the role of matrix interaction.

Initially, the effect of Lam and Col-I on MCF-7 proliferation was investigated. Fig. 7.1c shows that the proliferation rate after 48 h of culturing cells in Lam-coated microwells (32 ± 2 % proliferation) was not significantly different to proliferation after culture on Col-I (27 ± 3 % proliferation). In addition it was observed that the z-position within the cell cluster did not greatly affect proliferation (Fig. 7.1d). However, in Col-I microwells there was a small but significant difference in the proliferation rates of cells localized at the top of the clusters (i.e., z1) compared to the those located adjacent to the Col-I pre-coated surfaces (i.e., z3). The proliferation rate at the z1 location was 24 ± 3 % compared to 29 ± 4 % in z3 ($p<0.05$).

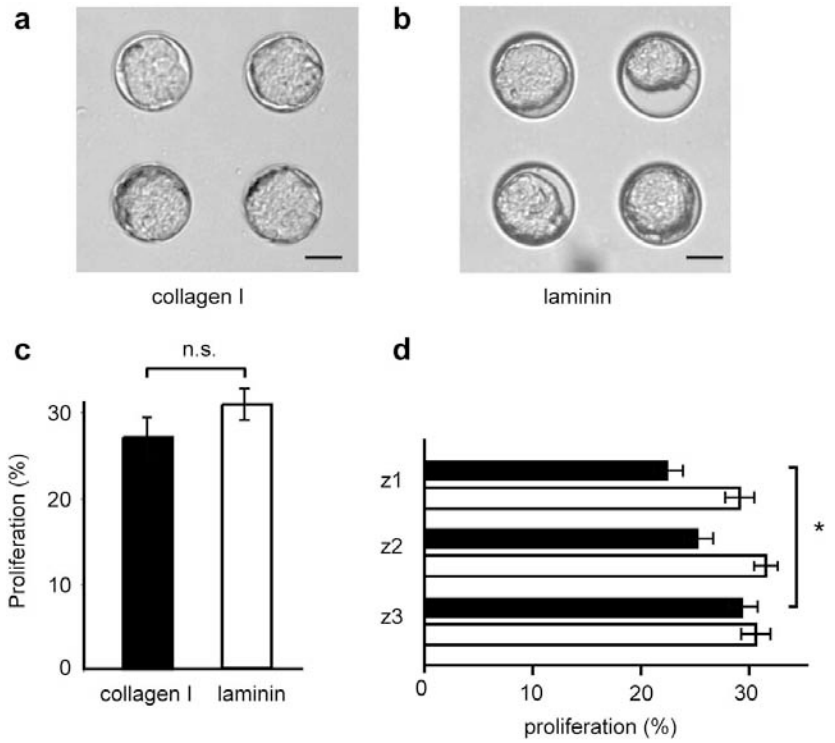

Figure 7.1: *Proliferation and cluster formation in the 100 µm wide microwells.* MCF-7 cells seeded in 100 µm wide microwells, coated with either Lam or Col-I, to form clusters similar in size did not show markedly different proliferation behaviour after 48h in culture (a). This behaviour was due to a homogenous behaviour throughout the cell cluster (b), however there was a small but significant decrease in proliferation with increasing distance from the Col-I interface. This could be due to a proliferation-inducing signal from Col-I in MCF-7 cells. The lower image shows clusters after 48h growth in Col-I and Lam wells respectively (c). Key: * = $p<0.05$: n.s. = not significant. Scale bars are 50 µm.

Collagen I interaction induces resistance to Taxol in 3D cultured cells

To study the effect of matrix on drug response we first investigated the response to Taxol in cell clusters that were precultured in Lam or Col-I-coated wells for a period of 24 h. In this experiment intriguing matrix effects were observed. After 24 h exposure to 100 nM Taxol, cell death was significantly lower in the microwells coated with the mesenchymal type of ECM i.e., Col-I, as opposed to in microwells coated with Lam, which represents the epithelial ECM (Fig. 7.2a). In Col-I-coated microwells the cell death was 19 ± 2 % lower ($p<0.001$) compared to cell death in cells cultured on Lam. These results suggest that the specific cell – Col-I interaction may impart a Taxol protective or Taxol resistance effect.

To study the effect of culture time in combination with signaling from the matrix, experiments were performed in which the clusters were cultured for 48 h before treatment. At this point, the observed ECM-specific effects were lost when Taxol-dependent cell death was evaluated (Fig. 7.2b). In this situation cell death was only 46 ± 3 % using Lam-coated wells, which is indistinguishable from the level of cell death observed in Col-I-coated microwells, 45 ± 4 %. We therefore hypothesized that other parameters than matrix interaction could play important roles in drug response in the 3D clusters.

Clarifying matrix-induced drug response in 3D by cell death distribution studies

To further understand the role of the specific matrix proteins on Taxol response, we quantified the level of cell death as a function of the position within the clusters (e.g. determining the amount of cell death at the individual image planes z1, z2 or z3).

The results showed that the largest difference between Col-I and Lam, as observed after 24 h pre-culture occurred at the bottom layers of the cluster, where direct cell-matrix interactions could be expected to be predominant (Fig. 7.2c). On Lam the drug response increased as the matrix interactions became prevalent (18 ± 4 % increase in cell death from z1 to z3, $p<0.001$) while Col-I showed the reverse trend (19 ± % decrease in cell death from z1 to z3, $p<0.001$). The drug response at plane z3 (bottom) was 73 ± 3 % cell death on Lam compared to 34 ± 3 % on Col-I ($p < 0.001$). A smaller difference following the same trend was observed in image plane z2, were cell death was 45 ± 2 % on Col-I, but 16 ± 3 % higher on Lam ($p<0.001$).

Interestingly, at a distance 35 μm away from the matrix interface, in the z1 slice, there was no significant difference in the response to Taxol on Lam vs. Col-I, respectively. In contrast, Taxol response in clusters that were pre-cultured for longer times, i.e. 48 h, were not significantly different regardless of ECM type and position within the cluster (Fig 7.2d).

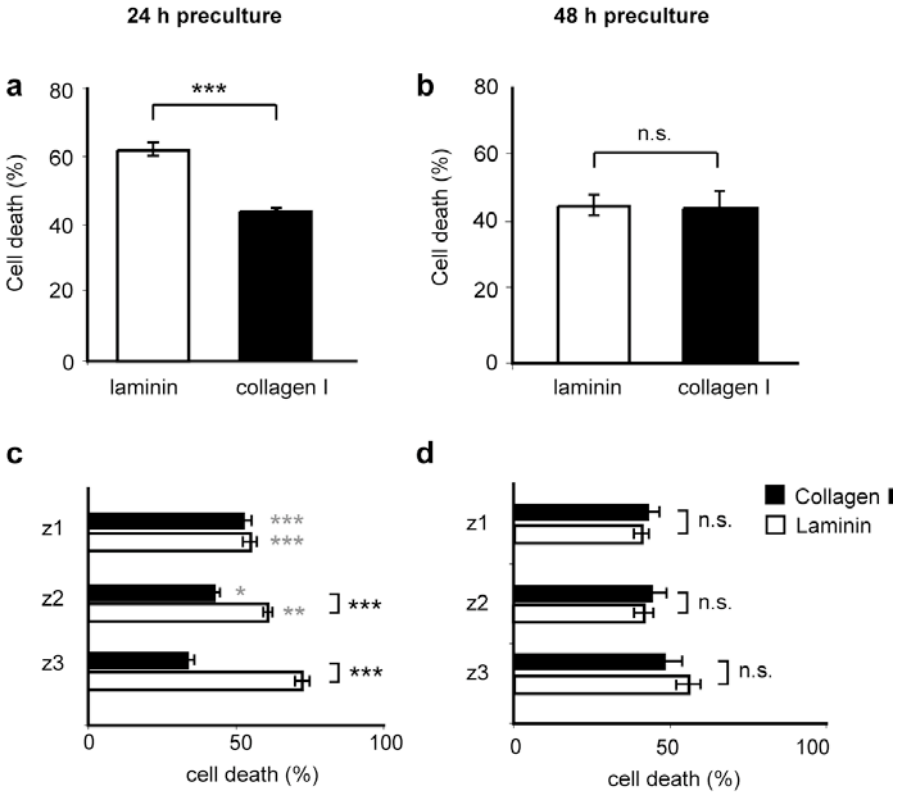

Figure 7.2: *Matrix and culture time dependence of drug response in 3D cultured cells.* The response to 24 h treatment with 100 nM Taxol in MCF-7 clusters after 24 h cluster formation is significantly higher in cells cultured in Lam-coated wells compared to microwells coated with Col-I (a). Conversely, when the clusters are pre-cultured for 48 h before treatment, there was no coating-dependence in the drug response (b). To further understand the effect of matrix on drug response, we assessed drug response at different locations in the clusters. The difference between Lam and Col-I at 24 h was predominant at the two z-positions z2 and z3 (c). Further away from the matrix coating the cell death was not coating-dependent. Interestingly, when cluster preculture was increased to 48 h, there was no significant difference in cell death between Col-I and Lam, for all measure positions in z (d). (*, ** and *** = $p<0.05$, $p<0.01$ and $p<0.001$ respectively. ns = not significant. The grey stars represent significant differences between z3 and the other images planes for Lam and Col-I respectively. Black stars represent comparisons between Lam and Col-I.)

In addition we determined the cell death distribution in the x-y plane. We found no significant differences in drug response between cells located within or at the edge of the clusters (Fig. 7.3). This finding confirmed our assumption that the behaviour of the cells within these clusters, with diffusion distances of < 50 μm, were not dependent on drug diffusion effects.

Inhibition of β1-integrin increases Taxol response in the 3D cultured cells

Previous work has highlighted the importance of integrin β1 for proliferation and survival signaling in breast cancer cells (Park *et al.*, 2006) (Zutter, 2007). To this end, we decided to question the role that major Col-I cell-adhesion receptors, specifically the β1-integrin, play in the observed 3D cluster Taxol responses and further relate the matrix-induced effects to proliferation. We used the well-characterized monoclonal antibody 13 (mAb13) that binds to integrin-β1 and favours its inactive conformation (Akiyama *et al.*, 1989). The mAb13 antibody was added 24 hours after cluster formation at a concentration of 50 μg/ml. This concentration was maintained for the rest of the experiment during subsequent media exchanges and in combination treatment with Taxol. The experimental scheme for the integrin-blocking experiment is outlined in Fig. 7.4a.

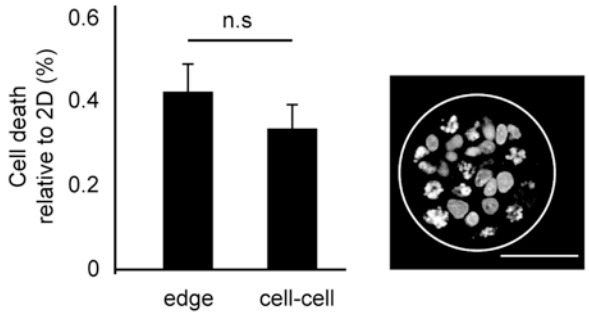

Figure 7.3 *MCF-7 cell death in the x-y plane.* The distribution of cell death in the x-y plane after 24h treatment with 10 nM Taxol showed no significant differences between the cells at the edge and the cells with only cell-cell contacts.

Initially, we intended to compare the effect of mAb13 treatment in 2D and 3D cluster grown cells. However, we observed an immediate (within 2 hrs) effect on cell morphology in the presence of mAb13. The morphology change was especially problematic in cell monolayers. Cells cultured on 200 μm wide Col-I patterns rounded up upon treatment and could therefore not serve as 2D controls (Fig. 7.4b).

As a consequence, we decided to only study the effect of mAb13 treatment in 3D. Minor morphology effects were observed also in 3D clusters, as demonstrated by the change in the area occupied by cells at the bottom of the clusters (z3) before and after mAb13 treatment (Fig. 7.4c). After treatment with mAb13, the area occupied by the cell cluster was significantly reduced at this position from 7850 ± 750 μm^2 in controls to 4850 ± 350 μm^2 after treatment, $p<0.05$.

When integrin-β1 binding was inhibited by mAb13 in combination with Taxol treatment, the average cell death was increased by 21 ± 5 % ($p<0.01$), in comparison to controls treated with only Taxol (Fig. 7.5a). This effect was only significant in the two image planes closest to the Col-I coating. In z2 and z3 the cell death was increased with mAb13 treatment by 20 ± 6 % ($p<0.01$) and 42 ± 4 % ($p<0.001$) respectively (Fig. 7.5b).

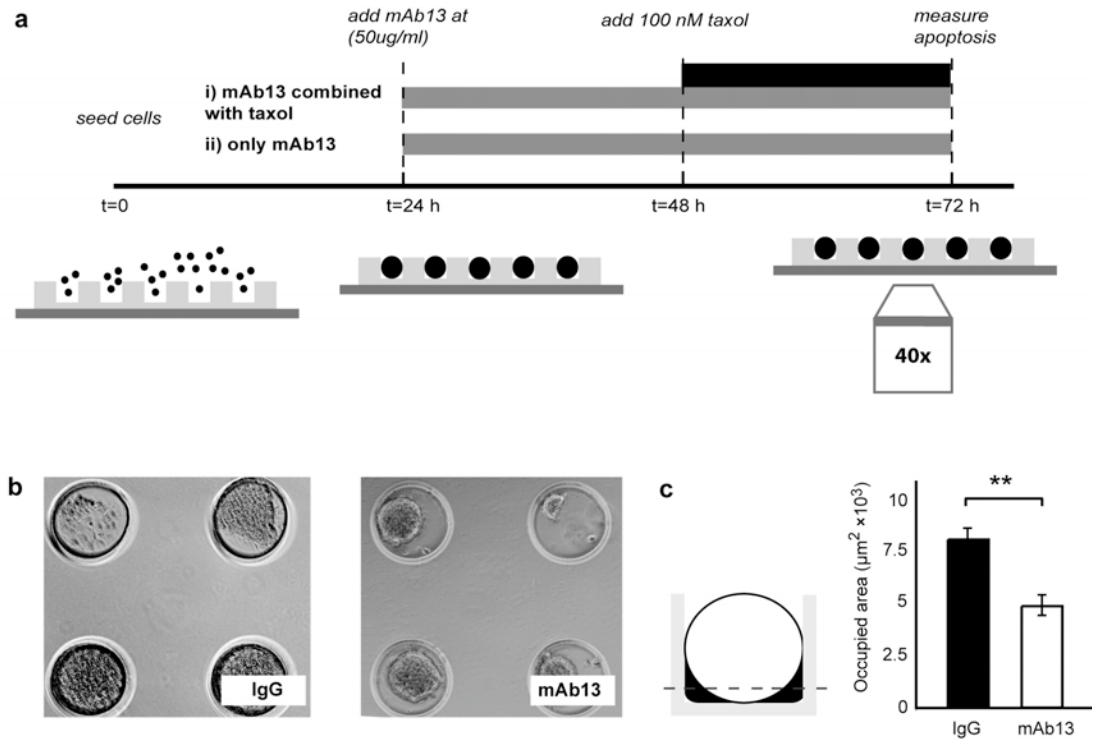

Figure 7.4: *Setup and morphology results for the combined treatment of mAb13 antibody and Taxol.* a) MCF-7 cells were seeded on Col-I-coated microwell arrays. After 24 h cluster formation the integrin β1-blocking antibody mAb13 was added to the culture for 24 h followed by a 24 h combined treatment with antibody and 100 nM Taxol. In control samples, only the mAb13 was added. 72 h after seeding, the rate of nuclear fragmentation was determined as a measure of apoptosis. b) Treatment with mAb13 caused cell colonies on Col-I to reduce the adhesion area with the matrix and round up. This was most clearly visible in monolayer cells, as shown in the transmission images in (b). Without treatment, cells spread to fill the 200 µm wide Col-I pattern, whereas after mAb13 treatment the cell colonies rounded up into 3D cell cluster. In cells that were grown in microwells, as clusters, the morphology change with mAb13 was less dramatic. However, it was observed that the area occupied by cells in the bottom z-image, z3, was significantly reduced from 7850 ± 750 μm^2 in controls to 4850 ± 350 μm^2 upon treatment (c).

Hence, this data suggests that the interaction with Col-I induced a protective effect on MCF-7 cells in their response to Taxol even after 48h cluster pre-culture, and furthermore, that integrin β1 may play a major role in this adhesion-mediated effect. Treatment with mAb13 alone did not lead to a significant increase in apoptosis; cell death was consistently below 3 % during mAb13 treatment (not shown). This shows that the combinatorial effect of Taxol treatment and β1-integrin-blocking was not cumulative but rather synergistic.

Interestingly, the increase in drug response upon β1-integrin-blocking did not relate to an increase in proliferation. Instead the mAb13 treatment significantly reduced

proliferation in the cells (fig. 7.5c). The average proliferation in the clusters was reduced by 10 ± 3 % in the presence of mAb13 ($p<0.01$). Our model system could additionally reveal that the proliferation was significantly affected by the antibody treatment only in the two images planes closest to the Col-I coating (Fig. 7.5d). The difference was 14 ± 3 % ($p<0.001$) and 10 ± 4 % ($p<0.05$) for z2 and z3, respectively. Hence, this further confirms that the antibody treatment predominantly affected the cells in contact with the Col-I matrix.

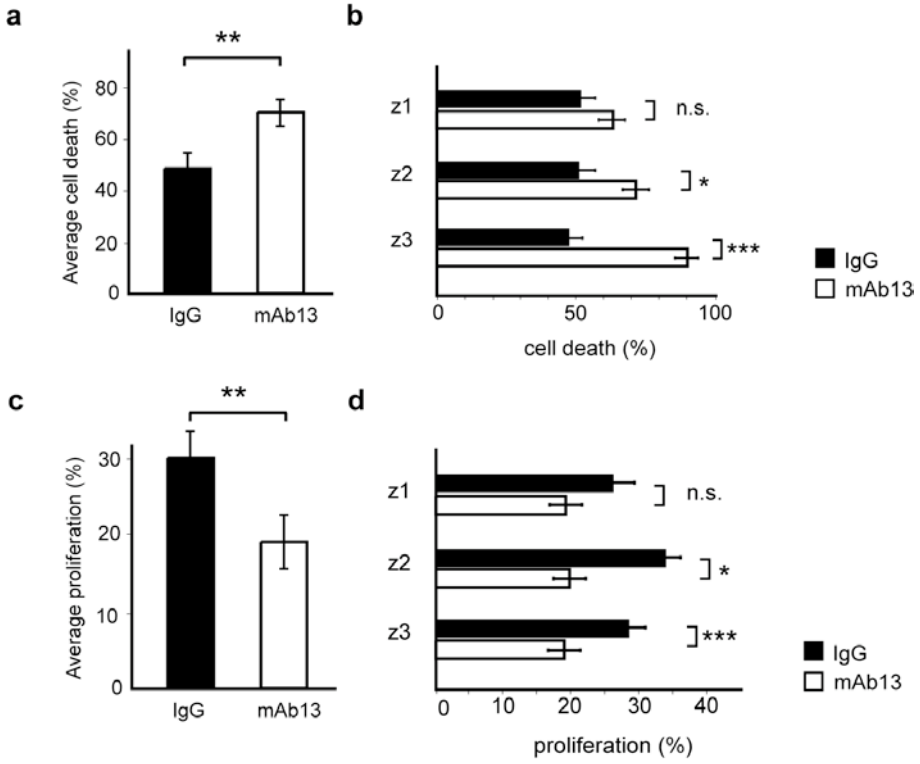

Figure 7.5: *Drug response and proliferation in Collagen I wells after blocking integrin β1.* When MCF-7 cell clusters cultured in Col-I microwells were treated with the integrin-blocking antibody mAb13, the response to Taxol was significantly increased (a). The effect was significant both in the response averaged over the clusters and at the individual z-image planes, with the exception of z1 (b). Integrin-blocking also affected the proliferation. The average proliferation after mAb13 treatment was significantly lower compared to IgG control (c). The z-plot revealed that this effect was predominantly a contribution from image plane z2 and z3, while there was not a significant difference in proliferation at z1 (d). (*, ** and *** represent 0.05, 0.01 and 0.001 respectively, n.s. = not significant)

7.3.2 Increased cell density reduces proliferation and drug response in 3D and 2D

In the above experiments we studied the influence of matrix coating under different experimental conditions. We found it interesting that matrix effects were dramatically less evident when cluster pre-culture times were increased in this model system. This could be due to altered signaling in the clusters with increased culture times, such as increased E-cadherin adhesions. Another explanation would be that it is due to a morphology change when cells are limited in space.

In order to get closer to the explanation of the observed behaviour we decided to determine the role of cell density in the 3D behaviour of cells. Cell density is a factor that includes morphology changes and increased cell-cell adhesion and is easily determined. Therefore it seemed like a good starting point. We determined cell density as the number of nuclei per area and measured for all positions throughout the cluster.

Cell density increased in clusters with culture time but do not correlate with a matrix-dependent behaviour

First, cell density was evaluated as a factor of matrix coating and culture time. It was found that the cell density after 24 h of preculture was not significantly different in Lam- versus Col-I-coated microwells (Fig. 7.6a). When cells in the clusters were allowed to proliferate for an additional 24 h (48 h) there was a significant increase in cell density in a matrix independent manner (Fig. 7.6a and b). The cell densities after 24 h preculture were 16 ± 1 and 17 ± 1 cells per slice in Lam and Col-I-coated wells respectively. After 48 h preculture the cell density significantly increased by 6 ± 2 cells per slice to 22 ± 2 cells in Col-I-coated microwells, $p<0.001$. In Lam-coated microwells the observed increase was from 9 ± 1 cells per slice, to 24 ± 1 cells, $p<0.001$.

These observations indicate that the effect of matrix-adhesion on drug response in 3D clusters may be masked by cell density-dependent factors with increased culture times. Furthermore, the results show that the increase in cell density in 3D clusters is independent of the type of matrix interface.

Large differences in drug response were found at the 24 h time point, which were revealed to be matrix and z-position-dependent. Therefore, the density distribution throughout the cluster at this time point was determined. Interestingly, no density effects with z direction were determined for Col-I (Fig. 7.6c). This indicates that the observed effects were purely matrix-dependent. In addition, no change in cell density was observed after blocking β1-integrin signaling (Fig. 7.6d), which further confirms that the matrix-dependent responses were density-independent.

In the Lam-coated microwells, there was a small difference in cell density between the bottom image plane (z3) and the rest at 24 h. The cell density was 13 ± 1 cells / area at z3, which is 4.5 ± 1 and 3 ± 1 lower than at position z1 and z2 respectively ($p<0.001$) (Fig. 7.6d).

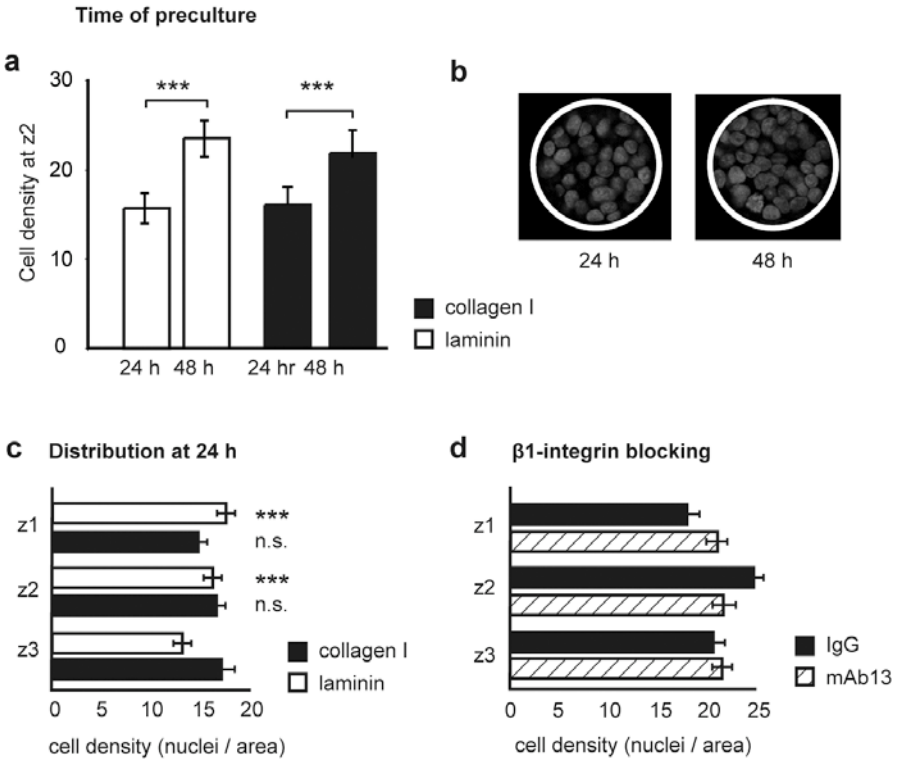

Figure 7.6: *Cell density distribution in z within cell clusters.* A factor that changed with time of preculture was cell density in the clusters, measured by the number of cells per z-image slice. Cell density was not significantly different between Lam and Col-I wells after 24 h preculture (a). When clusters were cultured for an additional 24 h, there was a strong increase in cell density that was again independent of matrix coating. (b) Shows example confocal images of MCF-7 cell nuclei in Col-I microwells after 24 h and 48 h preculture respectively. The culture of cells in Col-I-coated microwells did not induce density variations with position in z after 24h. In Lam-coated microwells there was a small change in density with position in z (c). Similarly, the inhibition of β1-integrin interactions with the matrix did not affect cell density (d). (* and *** represent $p<0.05$ and $p<0.001$, n.s. = not significant. All comparisons in c and d are within the same protein coating and refer to z3.)

Matching high 3D cell density in 2D reduces the dimensionality related differences in drug response

The observed effect of increased density with preculture time in 3D is interesting. It has been shown that the formation of cell-cell contacts, which presumably should increase with 3D cell culture and cell density, has an effect on drug response (St Croix, 1998). Here we decided to design an experiment to investigate to what extent increased cell density in 3D can explain differences in drug response and proliferation

between 3D and 2D. Before proceeding with this work, the difference in drug response between 3D culture of cells in 100 μm microwells and cells grown on flat hydrogels was examined to confirm that dimensionality affected drug response in the model platform used in this work. This experiment was performed entirely on Col-I.

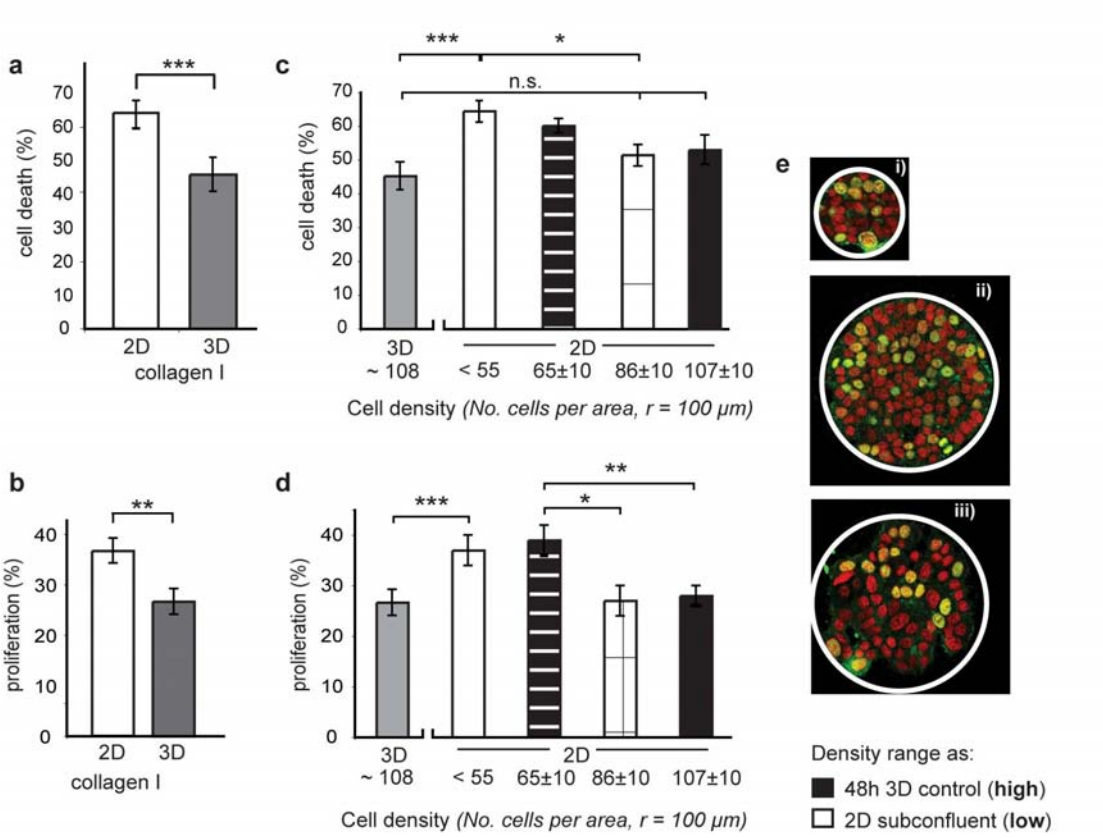

Figure 7.7: *The role of density in drug response in 3D determined by cell density studies on 2D collagen I patterns.* It was observed in previous experiments that cell density increased with time of culture of 3D clusters, hence we explored the role of density in the 3D-specific drug response. First, it was confirmed that the response to 100 nM Taxol treatment was significantly lower in 3D clusters grown in 100 μm wide microwells, compared to when cells were grown on flat hydrogel substrates (a). In the next step, we tested the role of cell density on drug response in 2D by the culture of cells on 200 μm wide Col-I patterns. It was found that drug response was significantly reduced with increasing cell density (b). When the cell density was matched in 2D and 3D, there is only a small difference in drug response, which is no longer significant. Proliferation, as measured by BrdU incorporation, was higher for cells grown in 2D compared to in 3D (c), hence, correlating nicely with the drug response observed. Furthermore, when cell density in 2D was increased, proliferation decreased (d). A significant decrease in proliferation compared to a sub-confluent situation was observed at a cell density of 86 cells per area. At matching densities in 2D and 3D there was no significant difference in proliferation. e) Cells with incorporated BrdU were stained by immunhistochemistry using a primary antibody for BrdU and a secondary antibody conjugated to Alexa Fluor 488. Here, i) cells in 100 μm wide 3D clusters at high density, ii) cells at high density on 200 μm wide 2D patterns and iii) cells at low density on 200 μm wide 2D patterns. All experiments were performed on Col-I-coated substrates.

Indeed, it was found that cells cultured in 3D clusters showed significantly lower drug response compared to cells cultured on a flat (2D) hydrogels (45 ± 4 % and 63 ± 2 % cell death respectively, $p<0.001$) (Fig. 7.7a). Next, we determined the effect of dimensionality on proliferation in these cells. We found that the reduced drug response in 3D correlated with a reduction in cell proliferation (Fig. 7.7b). Cells in 3D proliferated at a 10 ± 4 % lower rate than in 2D, where proliferation rate was 37 ± 3 %, $p<0.05$. Although the absolute difference in drug response and proliferation were not the same, the relative values are similar. Drug response was increased 1.4 fold in 2D, which correlated with a 1.3 fold increase in proliferation. This hints at a direct relationship between proliferation and drug response.

To elucidate the effect of cell density we designed an experiment, which involved the culture of cells at different cell densities. We used 200 μm wide circular Col-I patterns in the microstructured PEG hydrogel (Fig. 2.1) to control the number of cells per area. Cells seeded in the larger microwells did not form cell clusters, regardless of the seeding density tested, and were thus in a 2D environment. The cell seeding density was optimized so that a wide range of cell densities could be obtained, from low, sub-confluent density with <55 cells per pattern to high cell density with about 100 cells per pattern, which was comparable to the cell density in a 48 h pre-cultured 3D cluster.

The effect of cell density on drug response in 2D is shown in Fig. 7.7c. Drug response was significantly reduced with increasing cell density. At the lowest cell density (<55 cells per pattern) the cell death was 63 ± 3 %, which is 11 ± 4 higher than at a cell density of 76-96 cells per pattern ($p<0.05$). The highest 2D cell density, with 97-107 cells per pattern, matched the cell density in 3D. At this high cell density, cell death was slightly, but not significantly, greater in 2D.

Dimensionality related differences in proliferation are completely abolished at matched cell densities

To elucidate the role of proliferation in the observed cell density mediated drug responses we proceeded to measure the rates of proliferation at the various cell densities. The effect of cell density on proliferation was first observed at a density of about 86 cells per pattern (Fig. 7.7d and e). At this density proliferation was 25 ± 3 %, which is 12 ± 4 % lower than at the lowest cell density ($p<0.05$), which represents a sub-confluent cell layer. . At the highest cell density of 100 cells per pattern, which matches the cell density in 3D, the proliferation was 28 ± 2 %. This proliferation rate was not significantly different to the one measured in 3D cultured cells, which was 27 ± 2 %.

7.3.3 The role of E-cadherin for drug response in 3D cultured cells

While cell density is an interesting parameter to explore in drug response, it is actually composed of several different factors. These include increased cell-cell contacts, morphology changes and changes in cellular and nuclear size. Previous studies revealed a correlation between increased E-cadherin and growth suppression in 3D cultured cancer cells (St Croix *et al.*, 1998), which furthermore correlated to a reduced drug response (St Croix *et al.*, 1996). Hence, we decided to knockdown E-cadherin in the MCF-7 cells to investigate to what extent it could explain the observed effects of cell density on proliferation and thereby also on drug response.

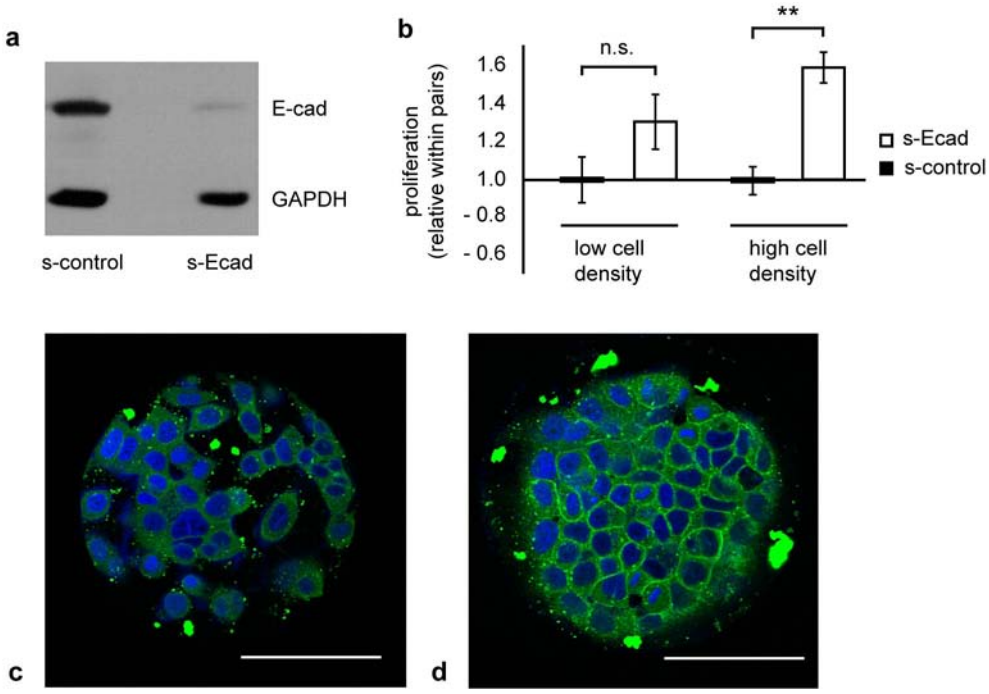

Figure 7.8: *E-cadherin affected cell proliferation but not morphology in MCF-7 cells.* E-cadherin knockdown was confirmed by western blot. GAPDH levels were used to account for differences in total cell numbers (a). When E-cadherin was depleted from the MCF-7 cells, they showed increased proliferation on the 2D Col-I patterns (b). The extent of the effect of the knockdown was shown to be dependent on the cell density. At low densities the relative proliferation increase of 0.3 fold was not significant. On the other hand, at high cell densities, the proliferation increased 0.6 fold compared to si-RNA control and 0.3 fold compared to the proliferation levels at low density. Hence, these data indicates that E-cadherin is responsible for the reduced proliferation previously observed at high cell densities. E-cadherin stain after knockdown with si-RNA was clearly different when compared to the 2D control without knockdown. The E-cadherin stain is of higher intensity at the cell-cell contacts in control (d), while homogenous staining of the cells was observed after E-cadherin knockdown (c).

Evaluation of knockdown levels

The efficiency of the E-cadherin knockdown was evaluated by Western blot analyses of the cell lysates. Of the two E-cadherin si-RNA tested; s-2769 and s-2770 the s-s2769 showed best blocking of expression results, with knockdown levels above 80 % at both 48h and 72 hrs after transfection (Fig. 7.8a).

E-cadherin regulates proliferation but not morphology of MCF-7 cells

E-cadherin knockdown caused only a modest effect on cell morphology in the MCF-7 cells cultured on the 2D Col-I patterns. After knockdown, cells still grew as colonies with cell-cell contacts. However, the staining of intracellular E-cadherin showed a distinct difference after knockdown. In control cells E-cadherin was clearly present at high concentrations at cell-cell contacts (Fig. 7.8d), conversely after knockdown, homogenous intracellular staining was observed (Fig. 7.8c).

Subsequently, the effect of knockdown on cell proliferation was determined. Interestingly, the knockdown of E-cadherin at high cell densities showed a significant increase in proliferation compared to control (Fig. 7.8b). The proliferation increased 0.6 fold compared to si-RNA control and 0.3 fold compared to the proliferation levels at low density. This difference corresponds directly to the relative difference between low and high density in untransfected cells expressing E-cadherin (Fig 7.7d). At low cell density, there was also a relative increase in proliferation after knockdown, which was not unexpected, as cell-cell contacts were also present in these samples. Therefore, E-cadherin can be expected to play a role in proliferation also at low densities. However, the fact that the increase was much smaller than at high density and insignificant to control underlies the increased importance of E-cadherin at high cell densities.

7.4 Discussion

7.4.1 The role of matrix adhesion in 3D drug response

An advantage of the microwell array is that it offers an in *vivo* like 3D environment, with a high control of extrinsic parameters. Thereby different parameters, like matrix composition, can be studied independently of other parameters. Here, matrix-induced drug response was studied in an early cancer model using MCF-7 cell clusters. In this experiment the role of two especially relevant matrix proteins was compared; Lam, a protein predominantly present in the early cancer niche and Col-I, which first comes into contact with cancer cells at a later stage in cancer progression.

A conventional way to study the role of matrix adhesion on a certain cell behaviour is to culture cells on different protein coatings on a flat substrate. However, with this method it can be difficult to compare the role of matrix due to protein-specific effects on cell morphology (Benton *et al.*, 2009). In contrast, with the microwell array no morphological differences in the 3D clusters were observed, irrespective of the matrix used. Therefore, we conclude that any differences in cell behaviour on this platform could be regarded as being imparted predominantly by the assorted ECMs. Initially, the effect of matrix coating on proliferation was determined. After 48 h cell culture, proliferation was found to be independent of matrix coating and position in the cluster. An exception was the position nearest to the Col-I coating, where there was a small but significant increase in proliferation. This modest, yet consistent, observation may reflect a proliferation-promoting signal imparted by the underlying Col-I, described previously in the literature (Hirtenlehner *et al.*, 2002).

The use of the high-resolution imaging readout showed that the cell response to Taxol was clearly dependent on the z-position in the 3D cell cluster. Cells in contact with the Col-I matrix, at the bottom part of the cluster, were significantly less responsive to treatment, compared to cells found in areas where cell-cell contacts were dominant. This behaviour was the direct opposite on Lam, where a higher drug response was observed in the cell layer with Lam-contact. Therefore it was concluded that the Col-I-interaction either directly or indirectly made the cells less responsive to or protected from Taxol treatment. The reduction in drug response with the z-position in the Lam clusters could be due to other factors, such as enhanced cell-cell interactions. In a following experiment it was shown that after 48 h preculture, the drug response was not significantly different on Col-I and Lam, independently of z-position. Thereby, it was clear that effects other than the matrix adhesion must be important for the 3D drug response in this model. In another model system, the time-dependent exchange or removal of the Col-I coating could be an explanation for these effects. However, because MCF-7 cells are tumorigenic and therefore not very migrative, such changes are less likely to influence our results. In addition, the collagen is crosslinked within the PEG hydrogel, and therefore would not be so easily removed as a physisorbed coating.

Subsequently, the contribution of the integrin β1 towards the Col-I-dependent effects was explored. In addition, the role of proliferation in the matrix-dependent drug response was investigated. When the activity of integrin β1 was blocked using the mAb13 antibody, drug response was increased, especially in the part of the cluster interacting with the matrix. This shows that β1 integrin is one of the major mediators of the matrix-dependent drug response on Col-I. This was also demonstrated by Aoudjit *et al.*, who further showed that the Col-I-dependent drug response could be related to the Col-I-specific integrin heterodimer α2β1 (Aoudjit and Vuori, 2001).

Interestingly, blocking β1 antibody induced reduced cell proliferation. This data is in agreement with previous observations suggesting that β1-integrin-blocking in MCF-7 cells in Matrigel reduced their proliferation and increased the efficiency of radiation therapy (Park *et al.*, 2006) (Park *et al.*, 2008). The increased susceptibility to radiotherapy could further be related to downregulation of Akt signaling, which promotes cell-survival downstream of β1-integrin signaling. The elucidation of the β1 integrin downstream signaling that leads to a decrease in drug response lies beyond the scope of this study. However, as drug response showed a negative correlation to proliferation, we propose that anti-apoptosis signaling is more important in this specific case (Meads *et al.*, 2009).

7.4.2 The role of cell density in 3D drug response

It was interesting to see that the differences in drug response between Lam and Col-I were not observed in cells that had been cultured for 48 h before treatment. One parameter that differed between clusters pre-cultured for 24 and 48 h was cell density. We hypothesized, that if increased cell density drives reduced drug response, then changes in cell density could also explain the effects of matrix adhesion. However, this theory could be ruled out, as there was no correlation between matrix effects on drug response and cell density. Instead, the Col-I-dependent drug response was concluded to be solely matrix-dependent.

Cell density as a factor in drug response was further investigated by comparing drug response in 3D cell clusters with cells cultured on 2D patterns at different cell densities. We initially showed that cells were less susceptible to Taxol and showed a reduced proliferation in 3D in comparison to 2D. Using the 2D patterns with controlled density, we could show that this dimensionality effect could be almost directly explained by increased cell density in 3D culture. In the results, we found similar drug response in 3D grown cells as in cells at high cell density on the 2D patterns. There was a tendency for higher drug response in 2D even in the samples with a high cell density, but it was insignificant from the drug response in 3D. Altering the cell density also altered the proliferation, so that at high cell densities, the proliferation matched that observed in 3D cultured cells. This result indicates that there was a direct link between proliferation and drug response in these experiments.

3D cell culture has repeatedly been shown to give a lower response to chemotherapeutics in comparison to cells cultured on flat substrates (Dhiman *et al.*, 2005) (St Croix *et al.*, 1996) (Fischbach *et al.*, 2007). This has been presumed to be due to increased levels of the cyclin-dependent kinase inhibitor p27, leading to reduced cell growth (St Croix *et al.*, 1996). Further parameters that are considered important in the diverse drug response between 2D and 3D are morphology and

phenotype changes, such as increased malignant potential (Fischbach *et al.*, 2007) and the limited diffusion of drugs and nutrients (Horning *et al.*, 2008). However, because of the complexity of the model systems used in these studies it was often difficult to determine the role of different parameters on drug response independently of each other to elucidate if there were interrelationships.

In contrast, in the 3D environment of the microwells several extrinsic parameters can be controlled and therefore their role in cell behaviour can be investigated independently of each other. In the cell clusters prepared in the 90 μm microwells, diffusion distances are less than 50 μm and therefore effects of diffusion are expected to be minor. In addition, culturing cells in the microwells controls morphology. Thereby, we can expect the measured alternations in drug response to be only governed by matrix and cell-cell interactions.

We concluded that the main reason for a dimensionality effect in this system, was increase in cell-cell adhesion and reduced proliferation at high cell densities. The knockdown of E-cadherin using si-RNA supported this conclusion, as the reduction of E-cadherin expression in cells at high densities caused a reversion of the proliferation inhibition. The resulting proliferation matched the proliferation observed in untransfected cells cultured at a low density. Hence, this data indicates that E-cadherin-mediated cell-cell adhesion was a major factor in inducing the down-stream signaling that resulted in a lower susceptibility to Taxol.

The direct relationship between proliferation and drug response in the density-dependent effects would seem to contradict the traditional view of cancer cells. Normal cells have a density-dependent proliferation, but the loss of contact inhibition is a typical hallmark of cancer. A recent study showed that the growth suppression mechanism relies on a tunable interplay between E-cadherin and growth factor concentrations (Kim *et al.*, 2009). Normal cells that form extensive E-cadherin adhesions become less responsive to EGF and therefore growth arrested.

One reason for the uncontrolled growth of cancer cells is that this growth regulation by E-cadherin is severely altered (Osborne *et al.*, 1982) (Kim *et al.*, 2009) or the cells no longer express E-cadherin. However, MCF-7 cells, being an early tumorigenic cancer cell line, expresses high levels of E-cadherin and still show some growth inhibition (Perrais *et al.*, 2007). St Croix *et al.* showed that induced E-cadherin-signaling in another cancer cell would indeed affect their behaviour and for example made the cells grow denser in 3D clusters (St Croix *et al.*, 1998). Hence, cancer cells can still be responsive to the E-cadherin signaling, which has shown to alter proliferation leading to resistance to drug treatment (St Croix *et al.*, 1996). Thus previous research supports our data that E-cadherin can be an important mediator of reduced drug response cancer. Hence, while not expected for all cancers, E-cadherin signaling and increased cell density seem to play an important role in early cancer.

7.4.3 Relationship between proliferation and drug response at different culture conditions

In this chapter we have presented a study of the combinatorial effect of Taxol treatment and microenvironmental parameters on drug response. The microenvironmental parameters; dimensionality of the culture environment as well as cell density showed a direct relationship between the effect on proliferation and drug response. Increasing the cell density in 2D, as well culturing cells in 3D, resulted in a reduced drug response, which was accompanied by a reduction in proliferation (Fig. 7.9b and c). This indicates that these microenvironmental parameters affect drug response largely by the regulation of the cell cycle. In contrast, interfering with the matrix adhesion, by blocking of integrin β1, was shown to increase drug response, while it induced a reduction in proliferation (Fig. 7.9a). Clearly, this drug response effect is not proliferation-dependent, but may instead be attributed to anti-apoptosis signaling downstream of integrin ligation.

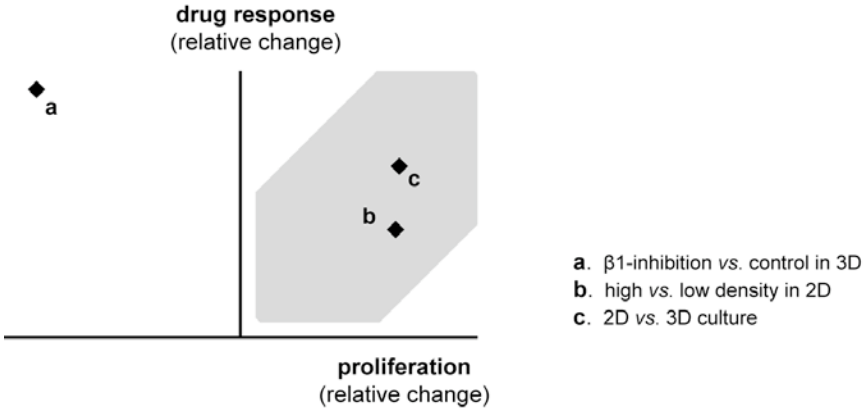

Figure 7.9: *The relationship between proliferation and drug response.* In the experiments comparing different extrinsic factors, we investigated the relationship between proliferation and microenvironment induced drug response. The graph shows the relative change in proliferation and drug response for each of the microenvironmental parameters tested. Initially, we found a direct relationship between proliferation changes and drug response for parameters related to dimensionality and cell density (b and c in the graph). However, in the experiments investigating the role of matrix adhesion, the relationship was somewhat different. For example, β1 integrin inhibition gave a decrease in proliferation while the drug response was increased, indicating that this response was governed by anti-apoptotic signalling (a).

The signaling from adhesion receptors induces a multivariate effect on signaling pathways, controlling both cell growth and survival (Meads, 2009). Anti-apoptosis signaling has frequently been reported as a down-stream effect of matrix adhesion, which could explain a reduced drug response (Aoudjit and Vuori, 2001) (Park *et al.*, 2008). However, matrix-dependent drug response has also shown to be related to decreased proliferation and p27 upregulation (Hazlehurst *et al.*, 1999). Hence, a

complex array of signaling pathways is activated by matrix interactions. Consequently, a direct relationship between its effect on proliferation and the response to chemotherapeutic drugs is typically not observed.

Most likely the crosstalk between different signals in a given microenvironmental setting will determine and tune the role of a certain extrinsic parameter. The relationship between proliferation as well as anti-apoptosis signaling and drug response is likely to be involved in the response to most cancer drugs. Independently of the mode of action, whether it is a general effect or a specific activity against a certain biochemical mechanism, most cancer drugs lead to inhibition of normal cell function and apoptosis.

The study of the relationship between proliferation and drug response proves intriguing insights into the signaling pathways occurring in different microenvironmental settings. These results could be of interest in the search for methods to predict treatment in patients. With more reliable markers for treatment prediction it would be possible to perform patient specific therapy, hence increasing overall efficiency. Proliferation is one phenotype-related parameters that has been highlighted as a possible predictor of therapy. For example it is known that dormant cancer cells survive treatment with cytotoxics (Naumov *et al.*, 2003) and form micrometastases many years after treatment. However, it has been shown that proliferation values can not always predict the response to chemotherapeutics (Aas *et al.*, 2003) (De Azambuja *et al.*, 2007). One explanation for this could be the effect of microenvironmental parameters with multivariate influence on signaling pathways in cell growth and survival, as highlighted in our results. Therefore, although proliferation is a useful predictive tool, it is important to have a clear picture of the factors that can modulate the relationship between proliferation and drug response.

7.5 Conclusions

In summary, this work showed that a microwell array based on the PEG hydrogel could be used to create an *in vivo* relevant model of early cancer. In this model, several parameters of the *in vivo* microenvironment, including matrix interface and cell-cell contacts, could be controlled. By the use of confocal imaging and sub-cellular resolution, drug response could be determined by apoptosis markers. This also enabled the analysis of the distribution of cell death in different areas of the 3D cell cluster. Therefore it was possible to differentiate between signals from cells in contact with matrix and the signals from cells with only cell-cell interactions.

With this model we could observe that matrix-induced drug response plays an important role also in 3D cultured cells. In addition, it was confirmed that this effect was independent of other parameters, such as morphology effects and cell density. On

the other hand, cell density was shown to be another important determinate of drug response. Crosstalk between these two effects was determined in 3D at high densities, where the effects of matrix were no longer observed. The comparison of different cell densities in 2D revealed that cell density could completely explain the effect of 3D culture on both drug response and proliferation. Finally a direct relationship between drug response and proliferation with cell density changes was observed, which could be correlated to increased E-cadherin levels at higher cell density. On the contrary, this was not observed for matrix dependent changes of drug response. This result indicates that both cell cycle regulation and anti-apoptosis signaling was involved in determining the drug response in this 3D model of early cancer.

Most importantly, this work shows that relatively simple models, like this microwell array for multicellular cancer cell culture, can be used in the first step towards more *in vivo* relevant models in drug development. Such models should be important to obtain more *in vivo* predictive results in general, but especially to test the efficiency of microenvironment targeted drugs *in vitro*.

CHAPTER 8

Conclusions and Outlook

8.1 Conclusions

The overall goal of this thesis was to develop 3D cancer models based on cell culture platforms with controlled extrinsic parameters. In extension, we aimed at establishing these models for the study of the tumour microenvironment as a determinant of drug response and thereby also cell adhesion-mediated drug resistance. Cell culture models that mimic aspects of the *in vivo* tumour environment can increase the predictivity of cancer drug development. The microwell platforms are advantageous compared to standard culture substrates as they allow for 3D culture, that has a higher relevance for *in vivo*, but with the same control of extrinsic parameters as can be obtained in 2D culture.

Therefore these platforms offer a unique opportunity to investigate the role of different extrinsic parameters independently of other parameters. Here we present two models, of different complexity, for 3D culture of cancer cells. Firstly, a PDMS microwell array previously developed in our lab by M. Dusseiller and M. Ochsner and secondly a PEG hydrogel based microwell array, developed in the lab of M. Lütolf. These platforms represent open microfabricated systems, that are advantageous as they offer control of the culture environment at the same time as they are simple to use and mostly easy compatible with standard cell culture formats (well-plates) and imaging methods.

The further development of these platforms towards the indicated use included the development of protein patterning procedures, assay development, in particular the choice of relevant cells and apoptosis read-out, and the establishment of imaging protocols. A large part of this thesis constitutes the evaluation of these platforms as breast cancer models and the application of the models to study the role of extrinsic parameters on drug response. The parameters investigated include dimensionality, matrix adhesion, cell-cell adhesion and cell density.

8.1.1 Development of new *in vitro* cancer models

A single cell culture platform for long-term studies based on the PDMS microwell array

Some cell assays, such as differentiation, protein expression and drug response require longer culture times, up to a week. Therefore, a platform for long-term cell culture was developed. This was done by optimization of the coating procedure of the PDMS microwell array developed by Dusseillller *et al.* (Dusseiller *et al.*, 2005). This microwell array was originally produced by microfabrication into PDMS and surface modified to coat protein only inside the microwells and PLL-g-PEG on the plateau areas. However, with this platform culture times were limited, as shown by lost pattern fidelity after only 2 days in experiments with mesenchymal stem cells (MSCs).

The stability of patterned substrates for cell culture is always an issue and is dependent on the substrate, the non-adhesive coating, as well as on the cells that are cultured on the patterns. In the new coating procedure we took advantage of the stable interaction between the well-characterized block-co-polymer Pluronics and the hydrophobic surface of native PDMS. In addition to the development of a printing-based protocol for functionalization of the array with proteins in the microwells and non-adhesive coating on the plateau, microfluidic patterning was used to create multiple patterns per array.

The quality of the new platform was subsequently evaluated by the culture of MSCs. Single MSCs were shown to be constrained to the microwells after 7 days in culture, which was a great improvement compared to the original approach (Rottmar *et al.*, 2009). In addition it was found that constraining the mesenchymal stem cells into microwells of 30×30×10 μm did not hinder them from differentiating into osteoclasts when cultured in differentiation media.

Finally, a first feasibility experiment towards a modified version of the new coating procedure was presented. Optimal patterning in terms of reproducibility and stability would theoretically be obtained if stamping could be eliminated from the fabrication process. Therefore we presented a strategy to produce microwells with microfluidic patterning, which would be possible in a design where microwells are connected by thin channels. Preliminary experiments were promising as they showed that the coating of thin channels by the proposed method would in principle be feasible and support cell adhesion only in the channels. This topic was not further developed in this thesis as the main direction was the application of controlled cell culture platforms for drug testing and this was achievable with the already developed methods.

Development of a the PEG-hydrogel-based platform towards a breast cancer model

A PEG-hydrogel microwell array was previously developed in the lab of M. Lütolf. It has been used for the study of the differentiation of isolated, single stem cells. Especially it has been applied for the investigation of the role of matrix composition in the stem cell niche (Lutolf *et al.*, 2009). The material characteristics of the PEG hydrogel platform makes it interesting for cancer cell culture with high *in vivo* relevance. The PEG polymer network has a low rigidity, approaching that of the tumour tissue. In addition, this microwell array allows for stable culture of 3D clusters with low variation in cluster size.

In this work, we first evaluated the coating of the microwells with three different matrix proteins that all are important at different stages of breast cancer. In all cases; for Lam, Col-I and Fn, protein transfer onto the hydrogel was obtained, as determined by fluorescence microscopy. Furthermore, we developed an imaging strategy based on confocal microscopy and the use of fluorescent molecules to stain specific markers within the cells. This strategy enabled the analysis of cell behaviour throughout the 3D cluster. Thereby the signal from cells in contact with the matrix and cells in areas of only cell-cell adhesion could be separated. High-resolution imaging enabled sub-cellular resolution and the use of high-content screening protocols for more precise determination of response. In the drug experiments we determined drug response by apoptosis levels through quantification of the ratio of fragmented nuclei.

Two different cancer models were evaluated with the platform representing early and later stages of breast cancer, using the cell lines MCF-7 and MDA-MB-231 respectively. Cells were shown to reduce their proliferation in the cluster in comparison to culture on TCPS. This effect was the most dramatic for MDA-MB-231 cells, indicating that they were strongly affected by this culture environment. Possibly these effects on proliferation could be due to the reduced matrix interaction when the cells were cultured in the constrained environment of the microwell.

It is possible that the environmental conditions in a cell culture model induce phenotypic changes of the cells. Recently, it was shown in a model mimicking the metastatic niche, that the extrinsic parameters induced the initiation of the mesenchymal epithelial reverting transition (MErT) (Benton *et al.*, 2009). There are many open questions to MErT and it would therefore be potentially be very interesting to study. However, the culture in the microwells did not induce E-cadherin re-expression. This behaviour was independent of the matrix interface, as no difference was seen for Lam and Col-I. Therefore, the proliferation effects were probably not related to a phenotype change, such as the MErT. In the light of these results, an early cancer model using MCF-7 cells was chosen as the most relevant system to study using this platform.

8.1.2 Application of engineered *in vitro* models to study the role of the microenvironment in cancer drug response

The role of extrinsic parameters on drug response using the reductionist 3D models of the PDMS microwell array

The PDMS platform was used as the most reductionist model of a 3D cell environment. With this model we were interested to see if extrinsic parameters that have previously shown to affect drug response, would also prove to be important when the complexity of the culture environment was reduced. To maintain the simplicity of this platform, but still allow the exploration of the importance of cell-cell contacts, this study concentrated on single cells and small cell cluster with less than six cells. Our first results show that the 3D environment of the microwell gave a reduced response to Taxol and further that the same trend was observed for two different matrix proteins; Col-I and Fn. These results could be explained by cell-shape changes in 3D, which may have an indirect effect on the extent of cell-cell adhesion.

One advantage of this platform is that within the microwell the number of cells in contact is controlled. The cluster size within the wells can be tuned by well size and seeding density. We used this property to study the role of cell-cell interaction in the response to Taxol. By comparison of single cells to cells forming cell-cell contacts it was found that the formation of cell-cell contacts made cells less susceptible to Taxol treatment. The presence and amount of cell-cell contacts have previously proved important for drug response in larger 3D cell-clusters (Green *et al.*, 2004). However, it was interesting to see that these effects could be observed already in these small clusters. One explanation could be that the culture in microwells forced the cells to take on a morphology, which was similar to that in a larger 3D cluster.

A striking result was that one contact was enough to give an effect and no significant increase was observed at multiple contacts. On the other hand, Perrais *et al.*, showed that the most dramatic effect of E-cadherin ligation is at the first cell contact (Perrais *et al.*, 2007). Hence, it may be that in small cell-cluster the difference between no contact and contact give the greatest effect on the downstream signaling. In this light, the presence of one or four cell contacts does not make a difference. This result is also in correlation with previous results from measuring the effect of cell contacts and spreading on the proliferation of endothelial cells (Nelson and Chen, 2002). Similarly to our results, it was found that the largest effect occurred going from single to pairs of cells. Additionally, in these cells the spreading area was shown to be a stronger signal for proliferation than cell-cell contacts.

The study was completed by a comparison to a more *in vivo* like cell-derived matrix. The PDMS microwell array is a very reductionist 3D model and it could be questioned whether the observed effects are representative for *in vivo*. Interestingly, we found a trend of reduced drug response both upon culture in the cell-derived 3D matrix and in the Fn-coated microwells. The effect was significantly stronger in the cell-derived matrix. Nevertheless, this indicates that we were able to mimic some aspects of the more complex environment of the matrices within the 3D environments of this *in vitro* model.

Microenvironment as a determinant of drug response in a model of early breast cancer using the PEG hydrogel microwell array

The PEG hydrogel microwell array was used as an *in vivo*-like model of cancer to study cell-adhesion mediated drug resistance. In a first study, we modelled the primary and a more progressed cancer environment by the use of Lam and Col-I-coating respectively. With this model we could observe that matrix-induced drug resistance, which has been observed in 2D *in vitro* experiments (Aoudjit and Vuori, 2001), played an important role for cells cultured in 100 μm wide clusters. In addition, it was confirmed that this effect was independent of other parameters, such as morphology effects and cell density. On the other hand, cell density was revealed to be another important determinate of drug response.

Crosstalk between these two effects was observed in 3D at high cell densities, where the effects of matrix were no longer observed. Comparing different cell densities in 2D, it could be shown that cell density was a major factor in this model, completely explaining the effect of 3D culture on drug response and proliferation. Furthermore, knocking down E-cadherin expression we could show that increased E-cadherin at elevated cell density was the determinant of these effects.

In the experiments in the PEG hydrogel, drug response and proliferation were determined in parallel. The results indicated that both cell-cycle regulation and anti-apoptosis signaling was involved in determining the drug response of the 3D cell clusters in this early cancer cell model.

On the one hand, there was a direct relationship between drug response and proliferation with density variation. Therefore the determining effect of cell density on drug response seemed to be alteration of the cell cycle e.g. by increase of the cyclin dependent kinase inhibitor p27 (St Croix *et al.*, 1996) (Fig. 8.1a). On the other hand, drug response alterations with matrix adhesion showed not to follow the trend in proliferation and therefore anti-apoptosis signaling can be expected to be the major cause (Fig.8.1b). Anti-apoptosis signaling is one of the pathways that have shown to be altered in matrix-mediated drug resistance e.g. by increase in Akt (serine/threonine

Kinase) phosphorylation (Aoudjit and Vuori, 2001) (Folgiero *et al.*, 2008). In contrast to cell-cell adhesion, integrin-mediated adhesion to matrix is known to increase the rates of cell cycle progression (Zutter, 2007). However, it has been found for some cancer cells, such as hematopoietic cell lines, that matrix adhesion also induce CAM-DR by increased p27 levels and cell cycle arrest (Hazlehurst *et al.*, 2003). Therefore, even though the matrix dependent resistance observed in our model seemed to be proliferation independent, this may not be true for all systems.

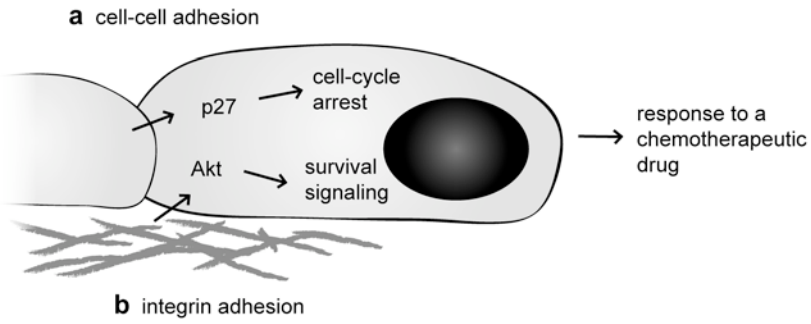

Figure 8.1: *Adhesion dependent drug response.* Dynamic signaling interactions between the cancer cells and the tumour microenvironment induce a transient drug resistance in the cells. Both signaling from the adhesion to other cells and from matrix adhesions via integrins are factors that result in this effect. In our experiments it was found that cell-cell adhesion-dependent drug resistance correlated to changes in proliferation (a). In the literature there is indeed evidence that link cell-cell adhesion and resistance, often via increased levels of the cyclin-dependent kinase inhibitor p27 (St Croix *et al.*, 1998). On the other hand matrix-dependent resistance was found to not follow the same pattern as proliferation. Therefore we hypothesize that these effect were mainly governed by anti-apoptosis signaling (b). It has been reported that matrix-adhesion can induce resistance in cancer cells by increased phosphorylation of the serine/threonine Kinase; Akt. Interestingly, it has also been shown that the expression pattern of integrins and extracellular matrix protein change with tumour progression to increased resistance (Sherman-Baust *et al.*, 2003).

The observations from our controlled 3D models can be set in relationship to what has been observed in other model systems. In some model systems, such as the multi-cellular tumour spheroids (Ivascu and Kubbies, 2007) and scaffold growth of cells (Dhiman *et al.*, 2005), cells predominantly form cell-cell adhesion. Therefore, cell cycle regulation can be predicted to be the major cause of resistance. However, an additional effect in these 3D models, especially in multi-cellular tumour spheroids, comes from diffusion limitations. On the other hand, cells cultured in models such as the cell-derived matrices were cells are mainly interacting with the matrix (Serebriiskii *et al.*, 2008) are more likely to show matrix-dependent resistance governed by anti-apoptosis signaling.

An intermediate situation with cells growing in cluster, but in contact with the ECM matrix, can be modelled by encapsulation in an ECM gel (Park *et al.*, 2008) or by culture on the PEG hydrogel microwell platform. These systems represent the *in vivo* environment of early cancer or in the metastatic niche. For these models it can be predicted that both anti-apoptosis signaling and cell cycle regulation are important signaling pathways involved in the regulation of drug response. Which of the effects that are likely to be dominant is also dependent on which cell type that is under study because of differences in integrin and E-cadherin expression.

Comparison of the findings from the two platforms

The PDMS microwell array and the PEG-hydrogel microwell array as presented here, represent two different *in vitro* platforms, at different positions along the scale from very reductionist models to more *in vivo*-like, complex models. However, because the cell type (MCF-7) and drug (Taxol) was chosen to be the same in the two systems, we can attempt to compare the findings from the two platforms.

In both systems, matrix composition was shown to play a role in determining the responsiveness to Taxol. While the drug response was higher on Col-I than on Fn in the PDMS platform, drug response increased additionally on Lam in comparison to Col-I on the PEG platform. The drug responsiveness of cells cultured on each of the three proteins on the two different platforms was not conducted in parallel, however it would seem possible that the matrix-induced drug response is lower for Col-I than for Lam, but lowest for Fn.

This would correlate to the importance of these proteins during different stages of cancer progression. Lam is predominantly present at early stages of epithelial cancers and Col-I is first an important protein when the cancer cells come in contact with the surrounding stroma (Cukierman and Bassi, 2010). Finally, Fn has shown to correlate to more aggressive, later stage cancer (Yao *et al.*, 2007). This result draws a parallel with the results obtained by Sherman-Baust *et al.*. They found a relationship between upregulation of certain proteins during cancer progression and the development of stronger matrix-induced resistance (Sherman-Baust *et al.*, 2003). This supports a hypothesis of progressive increase of the effect of adhesion-dependent resistance. In short; the further in cancer progression, the more time the cancer has had to adapt to its environment and develop adhesion-dependent survival mechanisms.

Cell-cell adhesion is another parameter that was investigated in both model systems. In the PDMS system it was found that one cell-cell contact was enough to induce a reduced response to Taxol. This is off course a rather artificial situation, which is difficult to correlate with the *in vivo* environment. However, it still indicates the strength of the signaling from cell-cell contacts on drug response. A similar result was

observed in the more *in vivo* relevant hydrogel model, as Taxol response decreased with increased cell density.

A characteristic of increased cell density is enhanced cell-cell contacts and thereby increased E-cadherin signaling (St Croix *et al.*, 1998). Therefore the role of cell-cell adhesion on drug response in the two systems agreed. However, on the PDMS platform it was revealed that the effect of cell-cell contacts was matrix dependent. The cell adhesion-dependent reduction in drug response was significant on Fn but not on Col-I. This result is in disagreement with what was observed on the PEG platform, where increased cell density and thereby cell-cell contacts showed to play an important role also on Col-I. However, it may be that on Col-I the sensitivity to the signaling from cell-cell contacts is reduced and hence that more cell-contacts are needed for the effect to become significant.

8.2 Outlook

The next step in the development of these models would be to establish a protocol for evaluation of high content read-out with a minimum of three markers for apoptosis per experiment. Multiple parameters for the assessment of drug response could help to provide more insight into the apoptosis pathways used by the cells, especially when correlated with their position within a cluster. In addition, determining downstream signaling in parallel to apoptosis would allow for the correlation of apoptosis levels with the increase in signaling molecules involved in resistance, such as Akt and cyclin-dependent kinases.

A next step would also be to perform a screen for CAM-DR with different cell lines. This work nicely shows the importance of the interaction with certain extrinsic parameters and the advantage of performing this study in the microwell array. However, most of the observed effects were not dramatic. Probably, the extent of CAM-DR is cell-line dependent. Integrin expression changes with cancer progression and these effects may be much more dramatic for a cell line further down the cancer progression e.g. the MDA-MB-231 cells. This also emphasizes that it is crucial that the right cell lines are used in the development of more specific treatments, such as integrin-targeting drugs.

In this work we performed a first feasibility test for the use of this system to study the metastatic niche. There are many open questions as to how metastatic cells switch phenotype at the metastatic site. Additionally, microenvironment-induced drug response in the metastatic niche is a highly relevant topic. Therefore it would be worth investing some time into understanding how this platform could be used to mimic the metastatic niche and possibly force MErT.

A natural application of the hydrogel platform would have been to test rigidity-dependent responses. However, while the hydrogel rigidity could easily be varied by polymer concentration, the protein coating was shown to be rigidity dependent. Hence, in order to investigate the role of these two parameters independently, further engineering would be needed. For such experiments we should also bear in mind that until now, very little is known about the effect of rigidity on drug response in cancer. Therefore, in an initial investigation of this relationship it would be sensible to screen for rigidity-dependent drug responses, testing a large range or rigidities, cell types and drugs. A first step in this direction was recently presented by Tilghman *et al.*. They investigated rigidity-dependent growth patterns of 17 different cancer cells and found both rigidity responsive and non-responsive cells (Tilghman *et al.*, 2010).

Another possible application of the PEG microwell array would be to use it for more high-throughput investigation of cell-interaction with cell-derived ECM matrices. As an outlook for the microwell work we present an engineering approach to produce cell-derived matrices in microwells.

8.2.1 Development of a new method for more high-throughput experimentation with cell-derived matrices

Cell-derived matrices, produced by fibroblasts, represent the ECM of the cancerous stroma and can be used to study the effect of the ECM on cancer cell migration (Castelló-Cros and Cukierman, 2009) and on matrix-dependent drug response (Serebriiskii *et al.*, 2008). The stroma changes in parallel with the cancer cells during cancer progression and therefore plays a crucial role in cancer. Recently it was shown that the gene expression of cancer cells can predict clinical outcome of cancer (Finak *et al.*, 2008). Therefore, methods that can provide further insight into cancer-stroma interactions could play an important role in the development of better therapies.

One advantage of cell-derived matrices is that by using a specific cell type, the origin and stage of the cancer environment can be reproduced *in vitro*. However, today the preparation, decellularization and handling of these matrices constitute tedious work. The resulting ECM matrices are very fragile, which leads to a certain un-reproducibility in the work. Here we propose the synthesis of matrices is microwells to obtain a system that is less fragile and more reproducible. In addition, by synthesis of the cell-derived matrix in small microwells the variability in matrix height can be expected to be less compared to when 96-well culture dishes are used, which would be advantageous for a more high-throughput imaging.

Preparation of cell-derived matrices in a microwell array

For the synthesis of cell-derived matrices within the PEG hydrogel based microwell array, the microwells were coated with Fn and matrix was prepared as described in

Materials and Methods, Chapter 3. NIH-3T3 cells were seeded for 2 days in Fn-coated microwells in medium containing 50 µg/ml Fn. To visualize the matrix prepared by the cells, the Fn in the media was mixed with (33% v/v) fluorescently labelled Fn. After matrix synthesis was complete, the cells were lyzed as described in chapter 3, section 3.5. After repeated rinsing in PBS and incubation in PBS overnight, the matrix could be used as a culture substrate for other cells. The matrices were imaged with confocal microscopy and their thickness determined to be about 5 µm. Fig 8.2a shows that the matrices filled the whole area of the microwell.

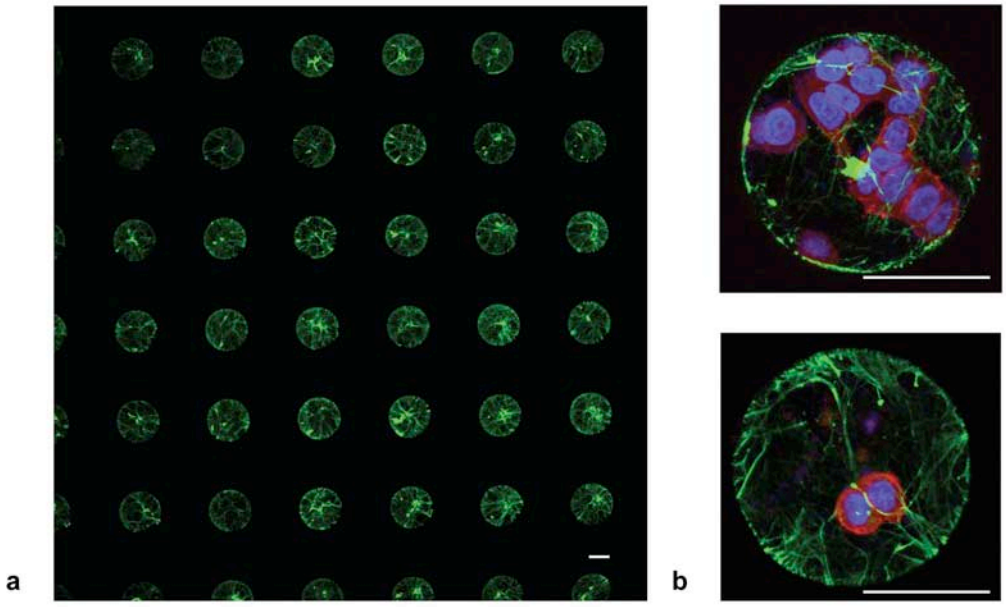

Figure 8.2: *Cell-derived matrix formation in PEG microwells.* Cell-derived Fn matrices were produced at the bottom of 100 and 200 µm wide microwells by culture of overconfluent NIH-3T3 fibroblasts for 2 days in cell-culture media enriched with 50 µg/ml Fn. For imaging purposes 1/3 of the Fn was replaced by Fn labelled with Alexa Fluor 488. After decellularization, the Fn component of the matrix could be visualized on a confocal microscope (a). The matrices were shown to form in all the microwells in the array and complete cover the bottom of the well. The matrices can be used for several types of investigations for example to study matrix-induced drug resistance and its dependence on cancer progression. Here we show reseeded MCF-7 cells that adhere in the matrices (b). The images are obtained on a confocal microscope, but with a pinhole adjusted to produce an image slice of ca 5 µm. Green is Fn, red is F-actin and blue is nuclei. Scale bar is 50 µm.

Reseeding of cancer cells into cell-derived matrices

To test the feasibility of reseeding cells in the matrix-coated microwell array, we seeded breast carcinoma cells (MCF-7) at low density. After 24 h, the cells were fixed and stained with phalloidin for actin and Hoechst for cell nuclei. Figure 8.2b shows the cells growing in the matrix. The cells are adhering to the matrix fibers, are partially integrating into the matrix but still form strong cell-cell contacts. A

mesenchymal cell can be expected to show stronger integration with the matrix, leading to 3D invasion.

8.2.2 Potential and limitations of microwell based models in drug development

In this work it was shown that microwells could be used to study 3D cell clusters in a controlled environment, where different extrinsic parameters can be independently controlled. Additionally, the cell clusters prepared in the arrays were very homogenous in size and could be viewed as individual experimental units. We expect that this increased reproducibility of experiments, in comparison to when less controlled cell culture is used.

However, there are some limitations with this setup that should be mentioned here. One is that microwell arrays are not completely controlled systems, as in this open setup solute concentrations and flow can not be controlled on the microscale. This could be solved by integration of the microwell array into a microfluidic system. Potentially, this could be very interesting, as drug concentration could be controlled over time to mimic the drug concentration decay in the body. However, this would position this platform into a different category of *in vitro* models. One advantage of the current setup is certainly the simplicity in seeding and analyzing cells, and the possibility to integrate it into standard formats, such as the 8-well Ibidi dishes and 96-well plates.

In order to use this experimental platform in drug development, some further development of the platform would be needed. In drug development, when comparing different cell lines and drugs, it is important to achieve a certain throughput. The throughput could be increased by producing the PEG-hydrogels in a larger format, such as a in a 96-well plate, and applying automated imaging. Another way to increase throughput would be to increase the multiplexing of the platform. With the current design, microwells cannot be individually addressed and therefore, only one experimental condition can be tested per array. However, it would not be simple to solve the problem with addressability, as the microwells are too small for spotting techniques, which typically renders spots in the dimensions of 200 – 300 μm, depending on the substrate. As mentioned previously, this problem could be solved by integration into a microfluidic system.

Nevertheless, some of the mentioned limitations can be overcome. Therefore, the microwell arrays discussed in this thesis still have a great potential as platforms that can be used to provide more insight into CAM-DR. Initially they may find application in basic research, but with some adaptations such methods may also be used in drug development. The Fn-matrix-filled microwell arrays offer a unique opportunity for more high-throughput investigations with this very relevant *in vitro* model.

References

Aas, T., Geisler, S., Eide, G.E., Haugen, D.F., Varhaug, J.E., Bassøe, A.M., Thorsen, T., Berntsen, H., Børresen-Dale, A.L., Akslen, L.A*., et al.* (2003). *Predictive value of tumour cell proliferation in locally advanced breast cancer treated with neoadjuvant chemotherapy*. Eur J Cancer **39**, 438-446.

Akiyama, S.K., Yamada, S.S., Chen, W.-T., and Yamada, K.M. (1989). *Analysis of fibronectin receptor function with monoclonal antibodies: Roles in Cell Adhesion, Migration, Matrix Assembly, and Cytoskeletal Organization*. J Cell Biol **109**, 863-875.

Alberts, B., Johnson, A., Lewis, J., Raff, M., Roberts, K., and Walter, P. (2002). Molecular Biology of the Cell (Garland Science).

Aoudjit, F., and Vuori, K. (2001). *Integrin signaling inhibits paclitaxel-induced apoptosis in breast cancer cells*. Oncogene **20**, 4995-5004.

Azioune, A., Storch, M., Bornens, M., Théry, M., and Piel, M. (2009). *Simple and rapid process for single cell micro-patterning*. Lab Chip **9**, 1640-1642.

Balis, F. (2002). *Evolution of Anticancer Drug Discovery and the Role of Cell-Based Screening box, p. 85*. J Natl Cancer Inst.

Benton, G., Crooke, E., and George, J. (2009). *Laminin-1 induces E-cadherin expression in 3-dimensional cultured breast cancer cells by inhibiting DNA methyltransferase 1 and reversing promoter methylation status*. FASEB J **23**, 3884-3895.

Berthier, E., Surfus, J., Verbsky, J., Huttenlocher, A., and Beebe, D.J. (2010). *A high-content chemotaxis assay for patient diagnosis*. Integr Biol **2**, 630-638.

Bewick, M.A., and Lafreine, R.M. (2006). *Adhesion dependent signalling in the tumour microenvironment: The future of drug targetting*. Curr Pharm Des **12**, 2833-2848.

Bhadriraju, K., and Chen, C.S. (2002). *Engineering cellular microenvironments to improve cell-based drug testing*. Drug Discovery Today **7**, 612-620.

Bissell, M., and LaBarge, M. (2005). *Context, tissue plasticity, and cancer Are tumor stem cells also regulated by the microenvironment?* Cancer Cell **7**, 17-23.

Bissell, M.J., Radisky, D.C., Rizki, A., Weaver, V.M., and Petersen, O.W. (2002). *The organizing principle: microenvironmental influences in the normal and malignant breast*. Differentiation **70**, 537-546.

Bleicher, Bohm, H., Muller, K., and Alanine, A. (2003). *Hit and lead generation: Beyond high-throughput screening*. Nat Rev Drug Discov **2**, 369-378.

Boxshall, K., Wu, M.-H., Cui, Z., Cui, Z., Watts, J.F., and Baker, M.A. (2006). *Simple surface treatments to modify protein adsorption and cell attachment properties within a poly(dimethylsiloxane) micro-bioreactor*. Surf Interface Anal **38**, 198-201.

Boyle, P., and Levin, B. (2008). World Cancer Report (World Health Organization).

Butcher, D.T., Alliston, T., and Weaver, V.M. (2009). *A tense situation: forcing tumour progression*. Nat Rev Cancer **9**, 108-122.

Castelló-Cros, R., and Cukierman, E. (2009). *Stromagenesis during tumorigenesis: characterization of tumor-associated fibroblasts and stroma-derived 3D Matrices*. Methods mol biol/extracellular matrix protocols **522**, 275-305.

Castelló-Cros, R., Khan, D.R., Simons, J., Valianou, M., and Cukierman, E. (2009). *Staged stromal extracellular 3D matrices differentially regulate breast cancer cell responses through PI3K and beta1-integrins*. BMC Cancer **9**, 94.

Chang, A., and Garrow, G. (1995). *Pilot-study of vinorelbine (navelbine) and paclitaxel (taxol) in patients with refractory breast-cancer and lung-cancer*. Seminars in Oncology **22**, 66-71.

Chao, Y.L., Shepard, C.R., and Wells, A. (2010). *Breast carcinoma cells re-express E-cadherin during mesenchymal to epithelial reverting transition*. Mol Cancer **9**, 179.

Chen, C., Mrksich, M., Huang, S., Whitesides, G., and Ingber, D.E. (1997). *Geometric Control of Cell Life and Death*. Science **276**, 1425-1428.

Chen, S., Jiang, X., and Whitesides, G. (2005). *Microengineering the environment of mammalian cells in culture*. MRS Bulletin **30**, 194-201.

Choi, N.W., Cabodi, M., Held, B., Gleghorn, J.P., Bonassar, L.J., and Stroock, A.D. (2007). *Microfluidic scaffolds for tissue engineering*. Nat Mater **6**, 908-915.

Christel, M.D. (2009). *From Pipeline to market. Pipelines bulk up as industry shakes up R&D, a surge in clinical projects spurs hope.* R&D Directions **15**, 12-89.

Cree, I., Glaysher, S., and Harvey, A. (2010). *Efficacy of anti-cancer agents in cell lines versus human primary tumour tissue*. Curr Opin Pharmacol **4**, 375-379.

Cukierman, E., and Bassi, D.E. (2010). *Physico-mechanical aspects of extracellular matrix influences on tumorigenic behaviors*. Semin Cancer Biol **20**, 139-145.

Cukierman, E., and Khan, D.R. (2010). *The benefits and challenges associated with the use of drug delivery systems in cancer therapy*. Biochemical pharmacology **80**, 762-770.

Damiano, J.S., and Dalton, W.S. (2000). *Integrin-mediated drug resistance in multiple myeloma*. Leukemia & Lymphoma **38**, 71-81.

Dancey, J.E., and Chen, H.X. (2006). *Strategies for optimizing combinations of molecularly targeted anticancer agents*. Nature Rev Drug Discov **5**, 649-659.

De Azambuja, E., Cardoso, F., De Castro, G., Colozza, M., Mano, M.S., Durbecq, V., Sotiriou, C., Larsimont, D., Piccart-Gebhart, M.J., and Paesmans, M. (2007). *Ki-67 as prognostic marker in early breast cancer: a meta-analysis of published studies involving 12 155 patients*. British journal of cancer **96**, 1504-1513.

De Silva, M., Desai, R., and Odde, D. (2004). *Micro-patterning of animal cells on PDMS substrates in the presence of serum without use of adhesion inhibitors*. Biomed Microdevices **6**, 219-222.

Debnath, J., and Brugge, J. (2005). *Modelling glandular epithelial cancers in three-dimensional cultures*. Nat Rev Cancer.

Debnath, J., Muthuswamy, S., and Brugge, J. (2003). *Morphogenesis and oncogenesis of MCF-10A mammary epithelial acini grown in three-dimensional basement membrane cultures*. Methods **30**, 256-268.

Denys, H., Braems, G., Lambein, K., Pauwels, P., Hendrix, A., De Boeck, A., Mathieu, V., Bracke, M., and De Wever, O. (2009). *The extracellular matrix regulates cancer progression and therapy response: implications for prognosis and treatment*. Curr Pharm Des **15**, 1373-1384.

Desgrosellier, J.S., and Cheresh, D.A. (2010). *Integrins in cancer: biological implications and therapeutic opportunities*. Nat Rev Cancer **10**, 9-22.

Dhiman, H., Ray, A.R., and Panda, A.K. (2005). *Three-dimensional chitosan scaffold-based MCF-7 cell culture for the determination of the cytotoxicity of tamoxifen*. Biomaterials **26**, 979-986.

Discher, D., Janmey, P., and Wang, Y. (2005). *Tissue cells feel and respond to the stiffness of their substrate: Materials and biology*. Science **310**, 1139-1143.

Dunn, J.C., Yarmush, M.L., Koebe, H.G., and Tompkins, R.G. (1989). *Hepatocyte function and extracellular matrix geometry: long-term culture in a sandwich configuration [published erratum appears in FASEB J 1989 May;3(7):1873]*. FASEB J **3**, 174-177.

Durand, R., and Olive, P. (2001). *Resistance of tumor cells to chemo-and radiotherapy modulated by the three-dimensional architecture of solid tumors and spheroids.* Methods in cell biology **64**, 211.

Dusseiller, M., Schlaepfer, D., Koch, M., Kroschewski, R., and Textor, M. (2005). *An inverted microcontact printing method on topographically structured polystyrene chips for arrayed micro-3-D culturing of single cells*. Biomaterials **26**, 5917-5925.

Dusseiller, M., Smith, M.L., Vogel, V., and Textor, M. (2006). *Microfabricated three-dimensional environments for single cell studies*. Biointerphases **1**, 1-4.

Engler, A., Rehfeldt, F., Sen, S., and Discher, D. (2007). *Microtissue elasticity: measurements by atomic force microscopy and its influence on cell differentiation*. Methods in cell biology **83**, 521-545.

Engler, A., Sen, S., Sweeney, H., and Discher, D. (2006). *Matrix elasticity directs stem cell lineage specification*. Cell **126**, 677-689.

Even-Ram, S., and Yamada, K.M. (2005). *Cell migration in 3D matrix*. Curr Opin Cell Biol **17**, 524-532.

Faia-Torres, A., Goren, T., Textor, M., and Pla-Roca, M. (2011). Patterned Biointerfaces. In Comprehensive Biomaterials (Elsevier).

Falconnet, D., Csucs, G., Grandin, H.M., and Textor, M. (2006). *Surface engineering approaches to micropattern surfaces for cell-based assays*. Biomaterials **27**, 3044-3063.

Fang, C., Wang, Y., Vu, N.T., Lin, W.-Y., Hsieh, Y.-T., Rubbi, L., Phelps, M.E., Mueschen, M., Kim, Y.-M., Chatziioannou, A.F.*, et al.* (2010). *Integrated Microfluidic and Imaging Platform for a Kinase Activity Radioassay to Analyze Minute Patient Cancer Samples*. Cancer Res **70**, 8299-8308.

Fehm, T., Becker, S., Duerr-Stoerzer, S., Sotlar, K., Mueller, V., Wallwiener, D., Lane, N., Solomayer, E., and Uhr, J. (2007). *Determination of HER2 status using both serum HER2 levels and circulating tumor cells in patients with recurrent breast cancer whose primary tumor was HER2 negative or of unknown HER2 status*. Breast Cancer Res **9**.

Finak, G., Bertos, N., Pepin, F., Sadekova, S., Souleimanova, M., Zhao, H., Chen, H., Omeroglu, G., Meterissian, S., Omeroglu, A.*, et al.* (2008). *Stromal gene expression predicts clinical outcome in breast cancer*. Nature Medicine **14**, 515-527.

Fink, J., Théry, M., Azioune, A., Dupont, R., Chatelain, F.O., Bornens, M., and Piel, M. (2007). *Comparative study and improvement of current cell micro-patterning techniques*. Lab Chip **7**, 672.

Fischbach, C., Chen, R., Matsumoto, T., Schmelzle, T., Brugge, J.S., Polverini, P.J., and Mooney, D.J. (2007). *Engineering tumors with 3D scaffolds*. Nat Meth **4**, 855-860.

Flaim, C.J., Chien, S., and Bhatia, S.N. (2005). *An extracellular matrix microarray for probing cellular differentiation*. Nat Meth **2**, 119-125.

Folgiero, V., Avetrani, P., Bon, G., Di Carlo, S.E., Fabi, A., Nisticò, C., Vici, P., Melucci, E., Buglioni, S., Perracchio, L.*, et al.* (2008). *Induction of ErbB-3 Expression by α6β4 Integrin Contributes to Tamoxifen Resistance in ERβ1-Negative Breast Carcinomas*. PLoS ONE **3**.

Friedl, P., Zanker, K.S., and Brocker, E.B. (1998). *Cell migration strategies in 3-D extracellular matrix: differences in morphology, cell matrix interactions and integrin function.* Microsc Res Tech **43**, 369-378.

Friedrich, J., Ebner, R., and Kunz-Schughart, L. (2007). *Experimental anti-tumor therapy in 3-D: Spheroids - old hat or new challenge?* Int J of Radiation Biol **83**, 849-871.

Friedrich, J., Seidel, C., Ebner, R., and Kunz-Schughart, L. (2009). *Spheroid-based drug screen: considerations and practical approach*. Nature Protocols **4**, 309-324.

Ganser, A., Roth, G., van Galen, J.C., Hilderink, J., Wammes, J.J.G., Müller, I., van Leeuwen, F.N., Wiesmüller, K.-H., and Brock, R. (2009). *Diffusion-driven device for a high-resolution dose-response profiling of combination chemotherapy*. Anal Chem **81**, 5233-5240.

Gardner, S.N., and Fernandes, M. (2003). *New tools for cancer chemotherapy: computational assistance for tailoring*. Mol Cancer Ther **2**, 1079-1084.

Gasparri, F. (2009). *An ovierview of cell phenotypes in HCS: limitations and advantages*. Expert Opin Drug Discov **4**, 643-657.

Gawlitta, D., Oomens, C.W.J., Baaijens, F.P.T., and Bouten, C.V.C. (2004). *Evaluation of a continuous quantification method of apoptosis and necrosis in tissue cultures*. Cytotehnology **46**, 139-150.

Gidrol, X., Fouqué, B., Ghenim, L., Haguet, V., Picollet-D'hahan, N., and Schaack, B. (2009). *2D and 3D cell microarrays in pharmacology*. Curr Opin Pharmacol **9**, 664-668.

Goffin, J.M., Pittet, P., Csucs, G., Lussi, J.W., Meister, J.-J., and Hinz, B. (2006). *Focal adhesion size controls tension-dependent recruitment of α-smooth muscle actin to stress fibers*. The Journal of Cell Biology **172**, 259-268.

Gómez-Sjöberg, R., Leyrat, A.A., Pirone, D.M., Chen, C.S., and Quake, S.R. (2007). *Versatile, fully automated, microfluidic cell culture system*. Anal Chem **79**, 8557-8563.

Grantab, R., Sivananthan, S., and Tannock, I. (2006). *The penetration of anticancer drugs through tumor tissue as a function of cellular adhesion and packing density of tumor cells*. Cancer Res **66**, 1033-1039.

Green, S.K., Francia, G., Isidoro, C., and Kerbel, R.S. (2004). *Antiadhesive antibodies targeting E-cadherin sensitize multicellular tumor spheroids to chemotherapy in vitro*. Molecular Cancer Therapeutics **3**, 149-159.

Griffith, L.G., and Schwartz, M.A. (2006). *Capturing complex 3D tissue physiology in vitro*. Nat Rev Mol Cell Biol **7**, 211-224.

Gudjonsson, T., Rønnov-Jessen, L., and Villadsen, R. (2003). *To create the correct microenvironment: three-dimensional heterotypic collagen assays for human breast epithelial morphogenesis and neoplasia*. Methods **30**, 247-255.

Håkanson, M., Textor, M., and Charnley, M. (2011). *Engineered 3D environments to elucidate the effect of environmental parameters on drug response in cancer*. Integr Biol, 1-8.

Hazlehurst, L.A., Argilagos, R.F., and Dalton, W.S. (2007). *β1 integrin mediated adhesion inreases Bim protein degradation and contributes to drug resistance in leukaemia cells*. British journal of haematology **136**, 269-275.

Hazlehurst, L.A., Landowski, T.H., and Dalton, W.S. (2003). *Role of the tumor microenvironment in mediating de novo resistance to drugs and physiological mediators of cell death*. Oncogene **22**, 7396-7402.

Hazlehurst, L.A., Wisner, L., and Dalton, W.S. (1999). *Activation of β1 integrin induces intrinsic drug resistance in the myeloma 8226 cell line: correlation with decreased proliferative index and increased p27 levels*. Proc AACR **40**, 324-.

Hehlgans, S., Haase, M., and Cordes, N. (2007). *Signalling via integrins: implications for cell survival and anticancer strategies*. BBA-Reviews on Cancer **1775**, 163-180.

Heino, J. (2000). *The collagen receptor integrins have distinct ligand recognition and signaling functions*. Matrix Biology **19**, 319-323.

Henley, D., Isbill, M., Fernando, R., Foster, J.S., and Wimalasena, J. (2006). *Paclitaxel induced apoptosis in breast cancer cells requires cell cycle transit but not Cdc2 activity*. Cancer Chemother Pharmacol **59**, 235-249.

Herrmann, R., Fayad, W., Schwarz, S., Berndtsson, M., and Linder, S. (2008). *Screening for Compounds That Induce Apoptosis of Cancer Cells Grown as Multicellular Spheroids*. J Biomol Screening **13**, 1.

Hirschhaeuser, F., Menne, H., Dittfeld, C., West, J., Mueller-Klieser, W., and Kunz-Schughart, L.A. (2010). *Multicellular tumor spheroids: An underestimated tool is catching up again*. J Biotechnol **148**, 3-15.

Hirtenlehner, K., Pec, M., Kubista, E., and Singer, C.F. (2002). *Extracellular matrix proteins influence phenotype and cytokine expression in human breast cancer cell lines*. Eur Cytokine Network **13**, 234-240.

Holmes, F.A., Walters, R.S., Theriault, R.L., Forman, A.D., Newton, L.K., Raber, M.N., Buzdar, A.U., Frye, A.U., and Hortobagyi, G.N. (1991). *Phase-II trial of taxol, an active-drug in the treatment of metastatic breast-cancer*. Journal of the National Cancer Institute **83**, 1797 -1805.

Hood, J., Bednarski, M., Frausto, R., Guccione, S., Reisfeld, R., Xiang, R., and Cheresh, D.A. (2002). *Tumor regression by targeted gene delivery to neovasculature*. Science **296**, 2404-2407.

Horning, J.L., Sahoo, S.K., Vijayaraghavalu, S., Dimitrijevic, S., Vasir, J.K., Jain, T.K., Panda, A.K., and Labhasetwar, V. (2008). *3-D Tumor Model for In Vitro Evaluation of Anticancer Drugs*. Mol Pharmaceutics **5**, 849-862.

Ioachim, E., Charchanti, A., and Briasoulis, E. (2002). *Immunohistochemical expression of extracellular matrix components tenascin, fibronectin, collagen type IV and laminin in breast cancer: their prognostic value and role in tumor invasion and progression*. Eur J Cancer **38**, 2362-2370.

Ivascu, A., and Kubbies, M. (2007). *Diversity of cell-mediated adhesions in breast cancer spheroids.* International journal of oncology **31**, 1403.

Jodele, S., Blavier, L., Yoon, J.M., and DeClerck, Y.A. (2006). *Modifying the soil to affect the seed: role of stromal-derived matrix metalloproteinases in cancer progression*. Cancer Metastasis Rev **25**, 35-43.

Jones, T., Carpenter, A., Lamprecht, M., Moffat, J., Silver, S., Grenier, J., Root, D., Golland, P., and Sabatini, D. (2009). *Scoring diverse cellular morphologies in image-based screens with iterative feedback and machine learning*. PNAS **106**, 1826-1831.

Jordan, M.A., and Wilson, L. (1998). *Microtubules and actin filaments: dynamic targets for cancer chemotherapy*. Curr Biol **10**.

Joyce, J., and Pollard, J. (2009). *Microenvironmental regulation of metastasis*. Nat Rev Cancer **9**, 239-252.

Kamb, A., Wee, S., and Lengauer, C. (2007). *Why is cancer drug discovery so difficult?* Nat Rev Drug Discov **6**, 115-120.

Kasili, P.M., Song, J.M., and Vo-Dinh, T. (2004). *Optical sensor for the detection of caspase-9 activity in a single cell*. J Am Chem Soc **126**, 2799-2806.

Kenny, P., Lee, G., Myers, C., Neve, R., Semeiks, J., Spellman, P., Lorenz, K., Lee, E., Barcellos-Hof, M.H., Petersen, O.*, et al.* (2007). *The morphologies of breast cancer cell lines in three-dimensional assays correlate with their profiles of gene expression*. Mol Oncol **1**, 84-96.

Kim, J.-H., Kushiro, K., Graham, N.A., and Asthagiri, A.R. (2009). *Tunable interplay between epidermal growth factor and cell-cell contact governs the spatial dynamics of epithelial growth*. Proc Natl Acad Sci USA **106**, 11149-11153.

Kim, K.K., Kugler, M.C., Wolters, P.J., Robillard, L., Galvez, M.G., Brumwell, A.N., Sheppard, D., and Chapman, H.A. (2006). *Alveolar epithelial cell mesenchymal transition develops in vivo during pulmonary fibrosis and is regulated by the extracellular matrix*. Proc Natl Acad Sci USA **103**, 13180-13185.

Kim, M.S., Yeon, J.H., and Park, J.-K. (2007). *A microfluidic platform for 3-dimensional cell culture and cell-based assays*. Biomed Microdevices **9**, 25-34.

Knudson, A.G. (1971). *Mutations and Cancer: Statistical study of retinoblastoma*. PNAS **68**, 820-823.

Koenig, A., Mueller, C., Hasel, C., Adler, G., and Menke, A. (2006). *Collagen type I induces disruption of E-cadherin-mediated cell-cell contacts and promotes proliferation of pancreatic carcinoma cells*. Cancer Research **66**, 4662-4671.

Kola, I., and Landis, J. (2004). *Can the pharmaceutical industry reduce attrition rates?* Nat Rev Drug Discov **3**, 711-715.

Kostic, A., Lynch, C.D., and Sheetz, M.P. (2009). *Differential matrix rigidity response in breast cancer cell lines correlates with the tissue tropism*. PLoS ONE **4**, e6361.

Kubow, K.E., Klotzsch, E., Smith, M.L., Gourdon, D., Little, W.C., and Vogel, V. (2009). *Crosslinking of cell-derived 3D scaffolds up-regulates the stretching and unfolding of new extracellular matrix assembled by reseeded cells*. Integr Biol **1**, 635-648.

Kumar, S., and Weaver, V.M. (2009). *Mechanics, malignancy, and metastasis: The force journey of a tumor cell*. Cancer and metastasis reviews **28**, 113-127.

Kunz-Schughart, L.A., and Knuechel, R. (2002). *Tumor associated fibroblasts (Part II): functional impact on tumor tissue*. Histol Histopathol **2**, 623-637.

Kuschel, C., Steuer, H., Maurer, A.N., Kanzok, B., Stoop, R., and Angres, B. (2006). *Cell adhesion profiling using extracellular matrix protein microarrays*. BioTechniques **40**, 523-531.

Labarge, M.A., Nelson, C.M., Villadsen, R., Fridriksdottir, A., Ruth, J.R., Stampfer, M.R., Petersen, O.W., and Bissell, M.J. (2009). *Human mammary progenitor cell fate decisions are products of interactions with combinatorial microenvironments*. Integr Biol **1**, 70.

Landro, J.A. (2000). *HTS in the new millennium: the role of pharmacology and flexibility*. J Pharmacol Toxicol Methods **44**, 273-289.

Lang, P., Yeow, K., Nichols, A., and Scheer, A. (2006). *Cellular imaging in drug discovery*. Nat Rev Drug Discov **5**, 343-356.

Lee, G.Y., Kenny, P.A., Lee, E.H., and Bissell, M.J. (2007). *Three-dimensional culture models of normal and malignant breast epithelial cells*. Nat Meth **4**, 359-365.

Lee, M., Kumar, R., Sukumaran, S., Hogg, M., Clark, D., and Dordick, J. (2008). *Three-dimensional cellular microarray for high-throughput toxicology assays*. Proceedings of the National Academy of Sciences **105**, 59.

Lee, S., Rico, I., Müller, M., and Spencer, N. (2004). *Influence of molecular architecture on the adsorption of Poly(ethylene oxide)-Poly(propylene oxide)-Poly(ethylene oxide) on PDMS surfaces and implications for aqueous lubrication*. Macromolecules **37**, 8349-8356.

Levental, I., Georges, P., and Janmey, P. (2007). *Soft biological materials and their impact on cell function*. Soft Matter **3**, 299-306.

Levental, K.R., Yu, H., Kass, L., Lakins, J.N., Egeblad, M., Erler, J.T., Fong, S.F.T., Csiszar, K., Giaccia, A., Weninger, W*., et al.* (2009). *Matrix Crosslinking Forces Tumor Progression by Enhancing Integrin Signaling*. Cell **139**, 891-906.

Li, G., Liu, T., Tarokh, A., Nie, J., Guo, L., Mara, A., Holley, S., and Wong, S. (2007). *3D nuclei segmentation based on gradient flow tracking*. BMC Cell Biology **8**.

Li, J.-T., and Caldwell, K.D. (1996). *Plasma protein interactions with pluronic-treated colloids*. Coll Surf B: Biointerfaces **7**, 9-22.

Lii, J., Hsu, W.-J., Parsa, H., Das, A., Rouse, R., and Sia, S.K. (2008). *Real-time microfluidic system for studying mammalian cells in 3D microenvironments*. Anal Chem **80**, 3640-3647.

Lindstrom, S., and Andersson-Svahn, H. (2010). *Overview of single-cell analyses: microdevices and applications*. Lab Chip **10**, 3363-3372.

Liu, M.C., and Tai, Y.-C. (2011). *A 3-D microfluidic combinatorial cell array*. Biomed Microdevices **13**, 191-201.

Liu, W., and Chen, C. (2007). *Cellular and multicellular form and function☆*. Advanced Drug Delivery Reviews **59**, 1319-1328.

Liu, W., Li, L., Wang, X., Ren, L., Wang, X., Wang, J., Tu, Q., Huang, X., and Wang, J. (2010). *An integrated microfluidic system for studying cell-microenvironmental interactions versatilely and dynamically*. Lab Chip **10**, 1717-1724.

Lövborg, H., Nygren, P., and Larsson, R. (2004). *Multiparametric evaluation of apoptosis: effects of standard cytotoxic agents and the cyanoguanidine CHS 828*. Mol Cancer Ther **3**, 521-526.

Lovchik, R., Arx, C., Viviani, A., and Delamarche, E. (2008). *Cellular microarrays for use with capillary-driven microfluidics*. Anal Bioanal Chem **390**, 801-808.

Lussi, J., Falconnet, D., Hubbell, J., Textor, M., and Csucs, G. (2006). *Pattern stability under cell culture conditions—A comparative study of patterning methods based on PLL-g-PEG background passivation*. Biomaterials **27**, 2534-2541.

Lutolf, M., Doyonnas, R., Havenstrite, K., Koleckar, K., and Blau, H.M. (2009). *Perturbation of single hematopoietic stem cell fates in artificial niches*. Integr Biol **1**, 59-69.

Lutolf, M.P., and Hubbell, J.A. (2005). *Synthetic biomaterials as instructive extracellular microenvironments for morphogenesis in tissue engineering*. Nat Biotech **23**, 47-55.

Lwin, T., Hazlehurst, L., Dessureault, S., Lai, R., Bai, W., Sotomayor, E., Moscinski, L.C., Dalton, W.S., and Tao, J.G. (2007). *Cell adhesion induces p27Kip1-associated cell-cycle arrest through down-regulation of the SCFSkp2 ubiquitin ligase pathway in mantle-cell and other non-Hodgkin B-cell lymphomas*. Blood **110**, 1631-1638.

Maffini, M.V., Soto, A.M., Calabro, J.M., Ucci, A.A., and Sonnenshein, C. (2004). *The stroma as a crucial target in rat mammary gland carcinogenesis*. J Cell Sci **117**, 1495-1502.

Mamounas, E.P., Bryant, J., Leinbersky, B., Fehrenbacher, L., Sedlacek, S.M., Fisher, B., Wickerham, D.L., Yothers, G., Soran, A., and Wolmark, N. (2005). *Paclitaxel after doxorubicin plus cyclophosphamide as adjuvant chemotherapy for node-positive breast cancer: Results from NSABP B-28*. Journal of clinical oncology **23**, 3686-3696.

Marlind, J., Pisoni, I., and Neri, D. (2006). *Tumor vascular targeting*. Drugs of the future **31**, 901-913.

Martinez, M.M., Reif, R.D., and Pappas, D. (2010). *Detection of apoptosis: A review of conventional and novel techniques*. Anal Methods **2**, 996.

Maziasz, T., Kadambi, V.J., Silverman, L., Fedyk, E., and Alden, C.L. (2010). *Predictive Toxicology Approaches for Small Molecule Oncology Drugs*. Toxicology Pathology **38**, 148-164.

McBeath, R., Pirone, D.M., Nelson, C.M., Bhadriraju, K., and Chen, C. (2004). *Cell shape, cytoskeletal Tension, and RhoA regulate stem cell lineage commitment*. Developmental Cell **6**, 483-495.

Meads, M., Gatenby, R., and Dalton, W. (2009). *Environment-mediated drug resistance: a major contributor to minimal residual disease*. Nat Rev Cancer **9**, 665-674.

Menendez, J., Ropero, S., del Mar Barbacid, M., Montero, S., Solanas, M., Escrich, E., Cortes-Funes, H., and Colomer, R. (2002). *Synergistic interaction between vinorelbine and gamma-linolenic acid in breast cancer cells*. Breast Caner Research and Treatment **72**, 203-219.

Mercey, E., Obeid, P., Glaise, D., Calvo-Munoz, M.-L., Guguen-Guillouzo, C., and Fouque, B. (2010). *The application of 3D micropatterning of agarose substrate for cell culture and in situ comet assays*. Biomaterials **31**, 3156-3165.

Meyvantsson, I., Warrick, J., Hayes, S., Skoien, A., and Beebe, D. (2008). *Automated cell culture in high density tubeless microfluidic device arrays*. Lab Chip **8**, 717-724.

Michalet, X., Pinaud, F.F., Bentolila, L.A., Tsay, J.M., Doose, S., Li, J.J., Sundaresan, G., Wu, A.M., Gambhir, S.S., and Weiss, S. (2005). *Quantum dots for live cells, in vivo imaging and diagnostics*. Science **307**, 538-544.

Michel, R., Lussi, J., Csucs, G., Reviakine, I., Danuser, G., Ketterer, B., Hubbell, J., Textor, M., and Spencer, N. (2002). *Selective Molecular Assembly Patterning: A New Approach to Micro- and Nanochemical Paterning of Surfaces for Biological Applications*. Langmuir **18**, 3281-3287.

Minchinton, A., and Tannock, I.F. (2006). *Drug penetration in solid tumors* Nature reviews cancer **6**, 583-592.

Miroshnikova, Y.A., Jorgens, D.M., Spitio, L., Auer, M., Sarang-Sieminski, A.L., and Weaver, A. (2011). *Epithelial morphogenesis within synthetic 3D matrix with tunable mechanical properties*. Phys Biol **8**.

Morgan, D.O. (2007). The cell cycle: principles of control (New Science Press).

Mori, Y., Shimizu, N., Dallas, M., Niewolna, M., Story, B., Williams, P., Mundy, G., and Yoneda, T. (2004). *Anti-alpha 4 integrin antibody suppresses the development of multiple myeloma and associated osteoclastic osteolysis*. Blood **104**, 2149-2154.

Morley, N., Rapp, A., Dittmar, H., Salter, L., Gould, D., Greulich, K.O., and Curnow, A. (2006). *UVA-induced apoptosis studied by the new apo/necro-Comet-assay which distinguishes viable, apoptotic and necrotic cells*. Mutagenesis **21**, 105-114.

Mulvey, C.S., and Sherwood, C.A. (2009). *Wavelength-dependent backscattering measurements for quantitative real-time monitoring of apoptosis in living cells*. J Biomed Optics **14**.

Muñoz-Pinedo, C., Green, D.R., and van den Berg, A. (2005). *Confocal restricted-height imaging of suspension cells (CRISC) in a PDMS microdevice during apoptosis*. Lab Chip **5**, 628-633.

Murphy, E., Majeti, B., Barnes, L., Makale, M., Weis, S., Lutu-Fuga, K., Wrasidlo, W., and Cheresh, D.A. (2008). *Nanoparticle-mediated drug delivery to tumor vasculature suppresses metastasis*. PNAS **105**, 9343-9348.

Nagrath, S., Sequist, L., Maheswaran, S., Bell, D., Irimia, D., Ulkus, L., Smith, M., Kwak, E., Digumarthy, S., and Muzikansky, A. (2007). *Isolation of rare circulating tumour cells in cancer patients by microchip technology*. Nature **450**, 1235-1239.

Naumov, G., Townson, J., MacDonald, I., Wilson, S., Bramwell, V., Groom, A., and Chambers, A. (2003). *Ineffectiveness of doxorubicin treatment on solitary dormant mammary carcinoma cells or late-developing metastases*. Breast cancer research and treatment **82**, 199-206.

Nelson, C., and Bissell, M. (2005). *Modeling dynamic reciprocity: engineering three-dimensional culture models of breast architecture, function, and neoplastic transformation*. Seminars in Cancer Biology **15**, 342-352.

Nelson, C., and Chen, C. (2002). *Cell-cell signaling by direct contact increases cell proliferation via a PI3K-dependent signal*. FEBS Letters **514**, 238-242.

Nelson, C., Inman, J., and Bissell, M. (2008a). *Three-dimensional lithographically defined organotypic tissue arrays for for quantitative analysis of morphogenesis and neoplastic progression*. Nature Protocols **3**, 674-678.

Nelson, C., Raghavan, S., Tan, J., and Chen, C. (2003). *Degradation of Micropatterned Surfaces by Cell-Dependent and-Independent Processes*. Langmuir **19**, 1493-1499.

Nelson, C.M., Khauv, D., Bissell, M.J., and Radisky, D.C. (2008b). *Change in cell shape is required for matrix metalloproteinase-induced epithelial-mesenchymal transition of mammary epithelial cells*. J Cell Biochem **105**, 25-33.

Nelson, C.M., Vanduijn, M.M., Inman, J.L., Fletcher, D.A., and Bissell, M.J. (2006). *Tissue Geometry Determines Sites of Mammary Branching Morphogenesis in Organotypic Cultures*. Science **314**, 298-300.

Ng, C.P., and Pun, S.H. (2008). *A perfusable 3D cell-matrix tissue culture chamber for in situ evaluation of nanoparticle vehicle penetration and transport*. Biotechnology and Bioengineering **99**, 1490-1501.

Niles, A., Moravec, R.A., and Riss, T.L. (2008). *Update on in vitro cytotoxicity assays for drug development*. Expert Opin Drug Discov **3**, 655-669.

Ochsner, M., Dusseiller, M.R., Grandin, H.M., Luna-Morris, S., Textor, M., Vogel, V., and Smith, M.L. (2007). *Micro-well arrays for 3D shape control and high resolution analysis of single cells*. Lab Chip **7**, 1074-1077.

Ochsner, M., Textor, M., Vogel, V., and Smith, M.L. (2010). *Dimensionality controls cytoskeleton assembly and metabolism of fibroblast cells in response to rigidity and shape*. PLoS ONE **5**, 9445-.

Ong, S.-M., Zhang, C., Toh, Y.-C., Kim, S.H., Foo, H.L., Tan, C.H., van Noort, D., Park, S., and Yu, H. (2008). *A gel-free 3D microfluidic cell culture system*. Biomaterials **29**, 3237-3244.

Onishi, T., Hayashi, N., Theriault, R.L., Hortobagyi, G.N., and Ueno, N.T. (2010). *Future directions of bone-targeted therapy for metastatic breast cancer*. Nat Rev Clin Oncol **7**, 641-651.

Oreffo, R., Bord, S., and JT, T. (1998). *Skeletal progenitor cells and ageing human populations*. Clin Sci **5**, 594-555.

Osborne, C., Hamilton, B., and Nover, M. (1982). J Clin Endocrinol Metab **55**, 86-93.

Pantel, K., Alix-Panabières, C., and Riethdorf, S. (2009). *Cancer micrometastases*. Nature Reviews Clinical Oncology **6**, 339-351.

Paris, S., and Sesboue, R. (2004). *Metastasis models: the green fluorescent revolution?* Carcinogenesis **25**, 2285-2292.

Park, C.C., Zhang, H., Pallavicini, M., Gray, J.W., Baehner, F., Park, C.J., and Bisell, M.J. (2006). *β1 Integrin Inhibitory Antibody Induces Apoptosis of Breast Cancer Cells, Inhibits Growth, and Distinguishes Malignant from Normal Phenotype in Three Dimensional Cultures and In vivo*. Cancer Res **66**, 1526-1535.

Park, C.C., Zhang, H.J., Yao, E.S., Park, C.J., and Bissell, M.J. (2008). *β1 Integrin Inhibition Dramatically Enhances Radiotherapy Efficacy in Human Breast Cancer Xenografts*. Cancer Res **68**, 4398-4405.

Park, E.S., Brown, A.C., Difeo, M.A., Barker, T.H., and Lu, H. (2010). *Continuously perfused, non-cross-contaminating microfluidic chamber array for studying cellular responses to orthogonal combinations of matrix and soluble signals*. Lab Chip **10**, 571.

Paszek, M., Zahir, N., Johnson, K., Lakins, J., Rozenberg, G., Gefen, A., Reinhart-King, C., Margulies, S., Dembo, M., Boettiger, D.*, et al.* (2005). *Tensional homeostasis and the malignant phenotype*. Cancer Cell **8**, 241-254.

Patel, S., Jenkins, J., Papadopolous, N., Burgess, M., Plager, C., Gutterman, J., and Benjamin, R. (2001). *Pilot study of Vitaxin - An angiogenesis inhibitor - In patients with advanced leiomyosarcomas*. Cancer **92**, 1347-1348.

Pavlovich, A.L., Manivannan, S., and Nelson, C.M. (2010). *Adipose Stroma Induces Branching Morphogenesis of Engineered Epithelial Tubules*. Tissue Eng Part A **16**, 3719-3726.

Perrais, M., Chen, X., Perez-Moreno, M., and Gumbiner, B.M. (2007). *E-cadherin homophilic ligation inhibits cell growth and epidermal growth factor receptor signaling independently of other cell interactions*. Molecular Biology of the Cell **18**, 2013-2025.

Pla-Roca, M., Leulmi, R.F., Djambazian, H., Sundararajan, S., and Juncker, D. (2010). *Addressable nanowell arrays formed using reversibly sealable hybrid elastomer-metal stencils*. Anal Chem **82**, 3848-3855.

Prestwich, G.D. (2008). *Evaluating drug efficacy and toxicology in three dimensions: Using synthetic extracellular matrices in drug discovery*. Acc Chem Res **41**, 139-148.

Prozialeck, W.C., Edwards, J.R., Lamar, P.C., Liu, J., Vaidya, V.S., and Bonventre, J.V. (2009). *Expression of kidney injury molecule-1 (Kim-1) in relation to necrosis and apoptosis during the early stages of Cd-induced proximal tubule injury*. Toxicology and Applied Pharmacology **238**, 306-314.

Ramm, P. (2005). *Image-based screening: a technology in transition*. Curr Opin Biotech **16**, 41-48.

Rehfeldt, F., Engler, A., Eckhardt, A., Ahmed, F., and Discher, D. (2007). *Cell responses to the mechanochemical microenvironment—Implications for regenerative medicine and drug delivery☆*. Adv Drug Delivery Rev **59**, 1329-1339.

Reif, R.D., Martinez, M.M., Wang, K., and Pappas, D. (2009). *Simultaneous cell capture and induction of apoptosis using and anti-CD95 affinity microdevice*. Anal Bioanal Chem **395**, 787-795.

Ringel, I., and Horwitz, S. (1987). *Taxol is converted to 7-Epitaxol, a biologically active isomer, in cell culture medium*. J Pharmacol Exp Ther **242**, 692-698.

Roberge, M. (2000). *Cell-based screen for antimitotic agents and indentification of analogues of rhizoxin, eleutherobin and paclitaxel in natural extracts*. Cancer Res **60**, 5052-5058.

Rønnov-Jessen, L., and Bissell, M. (2008). *Breast cancer by proxy: can the microenvironment be both the cause and consequence?* Trends in Molecular Medicine **15**, 5-13.

Ronnov-Jessen, L., Petersen, O., and Bissell, M.J. (1996). *Cellular changes involved in conversion of normal to malignant breast: Importance of the stromal reaction*. Physiological Reviews **76**, 69-125.

Rottmar, M., Håkanson, M., Smith, M.L., and Maniura-Weber, K. (2009). *Stem cell plasticity, osteogenic differentiation and the third dimension*. J Mater Sci: Mater Med **21**, 999-1004.

Schauer, K., Duong, T., Bleakley, K., Bardin, S., Bornens, M., and Goud, B. (2010). *Probabilistic density maps to study global endomembrane organization*. Nat Meth **7**, 560-566.

Serebriiskii, I., Castelló-Cros, R., Lamb, A., Golemis, E., and Cukierman, E. (2008). *Fibroblast-derived 3D matrix differentially regulates the growth and drug-responsiveness of human cancer cells*. Matrix Biol **27**, 573-585.

Shain, K.H., and Dalton, W.S. (2001). *Cell adhesion is a key determinant in de novo multidrug resistance (MDR): new targets for the prevention of acquired MDR*. Mol Cancer Ther **1**, 69-78.

Sherman-Baust, C., Weeraratna, A., Rangel, L., Pizer, E., Cho, K., Schwartz, D., Schock, T., and Morin, P. (2003). *Remodeling of the extracellular matrix through overexpression of collagen VI contributes to cisplatin resistance in ovarian cancer cells*. Cancer Cell **3**, 377-386.

Shi, J., Orth, J.D., and Mitchison, T. (2008). *Cell type variation in responses to antimitotic drugs that target microtubules and kinesin-5*. Cancer Res **68**, 3269-3276.

Siebers, M.C., Walboomers, X.F., van den Dolder, J., Leeuwenburgh, S.C.G., Wolke, J.G.C., and Jansen, J.A. (2008). *The behavior of osteoblast-like cells on various substrates with functional blocking of integrin-beta1 and integrin-beta3*. J Mater Sci Mater Med **19**, 861-868.

Sleeman, J., and Cremers, N. (2007). *New concepts in breast cancer metastasis: tumor initiating cells and the microenvironment*. Clinical and Experimental Metastasis **24**, 707-715.

Sminia, P., Acker, H., Eikesdal, H., Kaaijk, P., Enger, P., Slotman, B., and Bjerkvig, R. (2003). *Oxygenation and response to irradiation of organotypic multicellular spheroids of human glioma*. Anticancer Res **23**, 1461-1466.

Sodunke, T.R., Turner, K.K., Caldwell, S.A., McBride, K.W., Reginato, M.J., and Noh, H.M. (2007). *Micropatterns of Matrigel for three-dimensional epithelial cultures*. Biomaterials **28**, 4006-4016.

Song, L., and Tsuan, R. (2004). *Transdifferentiation potential of human mesenchymal stem cells derived from bone marrow*. FASEB J **18**.

Spink, B., Cole, R., Katz, B., Gierthy, J., Bradley, L., and Spink, D. (2006). *Inhibition of MCF-7 breast cancer cell proliferation by MCF-10A breast epithelial cells in coculture*. Cell Biology International **30**, 227-238.

St Croix, B., Florenes, V., Rak, J., Flanagan, M., Bhattacharya, N., Slingerland, J., and Kerbel, R. (1996). *Impact of the cyclin-dependent kinase inhibitor p27(Kip1) on resistance of tumor cells to anticancer agents*. Nature Medicine **2**, 1204-1210.

St Croix, B., Sheehan, C., Rak, J.W., Flørenes, V.A., Slingerland, J.M., and Kerbel, R.S. (1998). *E-Cadherin-dependent growth suppression is mediated by the cyclin-dependent kinase inhibitor p27(KIP1)*. The Journal of Cell Biology **142**, 557-571.

Starkuviene, V., and Pepperkok, R. (2007). *The potential of high-content high-throughput microscopy in drug discovery*. Brit J Pharmacol **152**, 62-71.

Steeg, P.S. (2006). *Tumor metastasis: mechanistic insights and clinical challenges*. Nature medicine **12**, 895-904.

Strobl, J.S., Nikkhah, M., and Agah, M. (2010). *Actions of the anti-cancer drug suberoylanilide hydroxamic acid (SAHA) on human breast cancer cytoarchitecture in silicon microstructures*. Biomaterials **31**, 7043-7050.

Sung, J.H., and Shuler, M.L. (2009). *A micro cell culture analog (mu CCA) with 3-D hydrogel culture of multiple cell lines to assess metabolism-dependent cytotoxicity of anti-cancer drugs*. Lab Chip **9**, 1385-1394.

Sutherland, R.M. (1988). *Cell and environment interactions in tumor microregions: the multicell spheroid model*. Science **240**, 177-184.

Takayama, S., Ostuni, E., LeDuc, P., Naruse, K., Ingber, D.E., and Whitesides, G.M. (2001). *Subcellular positioning of small molecules*. Nature **411**, 1016.

Tan, J.L., Liu, W., Nelson, C.M., Raghavan, S., and Chen, C.S. (2004). *Simple approach to micropattern cells on common culture substrates by tuning substrate wettability*. Tissue Engineering **10**, 865-872.

Tanaka, M., Bateman, R., Rauh, D., Vaisberg, E., Ramachandani, S., Zhang, C., Hansen, K.C., Burlingame, A.L., Trautman, J.K., Shokat, K.M.*, et al.* (2005). *An Unbiased Cell Morphology–Based Screen for New, Biologically Active Small Molecules*. PLoS Biol **3**.

Teicher, B.A. (2009). *Acute and chronic in vivo therapeutic resistance*. Biochemical pharmacology **77**, 1665-1673.

Tenstad, E., Tourovskaia, A., Folch, A., Myklebost, O., and Rian, E. (2010). *Extensive adipogenic and osteogenic differentiation of patterned human mesenchymal stem cells in a microfluidic device*. Lab Chip **10**, 1401-1409.

Théry, M., Jiménez-Dalmaroni, A., Racine, V., Bornens, M., and Jülicher, F. (2007). *Experimental and theorectical study of mitotic spindle orientation*. Nature **447**, 493-496.

Théry, M., Pépin, A., Dressaire, E., Chen, Y., and Bornens, M. (2006). *Cell distribution of stress fibres in response to the geometry of the adhesive environment*. Cell Motil Cytoskeleton **63**, 341-355.

Théry, M., Racine, V., Pepin, A., Piel, M., Chen, Y., Sibarta, J.-B., and Bornens, M. (2005). *The extracellular matrix guides the orientation of the cell division axis*. Nat Cell Biol **7**, 947-953.

Tilghman, R.W., Cowan, C.R., Mih, J.D., Koryakina, Y., Gioeli, D., Slack-Davis, J.K., Blackman, B.R., Tschumperlin, D.J., and Parsons, J.T. (2010). *Matrix Rigidity Regulates Cancer Cell Growth and Cellular Phenotype*. PLoS ONE **5**, e12905.

Trusheim, M.R., Berndt, E.R., and Douglas, F.L. (2007). *Stratified medicine: strategic and economic implications of combining drugs and clinical biomarkers*. Nature Reviews drug discovery **6**, 287-293.

Tsai, J., and Kam, L. (2009). *Rigidity-Dependent Cross Talk between Integrin and Cadherin Signaling*. Biophys J **96**, L39-L41.

van der Kuip, H., Mürdter, T., Sonnenberg, M., McClellan, M., Gutzeit, S., Gerteis, A., Simon, W., Fritz, P., and Aulitzky, W. (2006). *Short term culture of breast cancer tissues to study the activity of the anticancer drug taxol in an intact tumor environment*. BMC Cancer **6**, 86.

Wang, H., Dembo, M., and Wang, Y. (2000). *Substrate flexibility regulates growth and apoptosis of normal but not transformed cells*. Am J Physiol Cell Physiol **279**, C1345-C1350.

Wang, H., Fu, W.L., Im, J.H., Zhou, Z.Y., Santoro, S.A., Iyer, V., DiPersio, C.M., Yu, Q.C., Quaranta, V., Al-Medhi, A.*, et al.* (2004). *Tumor cell α3β1 integrin and vascular laminin-5 mediate pulmonary arrest and metastasis*. J Cell Biol **164**, 935-941.

Wang, Z., Kim, M.-C., Marquez, M., and Thorsen, T. (2007). *High-density microfluidic arrays for cell cytotoxicity analysis*. Lab Chip **7**, 740.

Weaver, V., and Bissell, M. (1999). *Functional culture models to study mechanisms governing apoptosis in normal and malignant mammary epithelial cells*. Journal of mammary gland biology and neoplasia **4**, 193-201.

Weaver, V.M., Lelièvre, S., Lakins, J.N., Chrenek, M.A., Jones, J.C.R., Giancotti, F., Werb, Z., and Bisell, M.J. (2002). *B4 integrin-dependent formation of polarized three-dimensional architecture confers resistance to apoptosis in normal and malignant mammary epithelium*. Cancer Cell **2**, 205-216.

Wheelock, M.J., Shintani, Y., Maeda, M., Fukumoto, Y., and Johnson, K.R. (2008). *Cadherin switching*. Journal of Cell Science **121**, 727-735.

Wittekind, C., and Neid, M. (2005). *Cancer invasion and metastasis*. Oncology **69**, 14-16.

Wlodkovic, D., and Cooper, J.M. (2010). *Tumors on chips: oncology meets microfluidics*. Curr Opin Chem Biol **14**, 556-557.

Wlodkovic, D., Faley, S., Zagnoni, M., Wikswo, J.P., and Cooper, J.M. (2009). *Mirofluidic singel-cell array cytometry for the analysis of tumor apoptosis*. Anal Chem **81**, 5517-5523.

Wong, A., and Gumbiner, B. (2003). *Adhesion-independent mechanism for suppression of tumor cell invasion by E-cadherin*. J Cell Biol **161**, 1191-1203.

Wu, G., Irvine, J., Luft, C., Pressley, D., Hodge, C.N., and Janzen, B. (2003). *Assay development and high-throughput sreening of caspases in mirofluidic format*. Combinatorial chemistry & High throughput screening **6**, 303-312.

Wu, L.Y., Di Carlo, D., and Lee, L.P. (2008). *Microfluidic self-assembly of tumor spheroids for anticancer drug discovery*. Biomed Microdevices **10**, 197-202.

Yao, C., Ziober, B., Squillace, R., and Kramer, R. (1996). *alpha 7 integrin mediates cell adhesion and migration on specific laminin isoforms*. Journal of Biological Chemistry **271**, 25598-25603.

Yao, E., Zhang, H., Chen, Y., Lee, B., and Chew, K. (2007). *Increased ß1 Integrin Is Associated with Decreased Survival in Invasive Breast Cancer*. Cancer Res.

Ye, N., Qin, J., Shi, W., Liu, X., and Lin, B. (2007). *Cell-based high content screening using an integrated microfluidic device*. Lab Chip **7**, 1696-1704.

Yeung, T., Georges, P.C., Flanagan, L.A., Marg, B., Ortiz, M., Funaki, M., Zahir, N., Ming, W., Weaver, V., and Janmey, P.A. (2004). *Effects of substrate stiffness on cell morphology, cytoskeletal structure, and adhesion*. Cell Motil Cytoskeleton **60**, 24-34.

Younan, X., and Whitesides, G. (1998). *Soft lithography*. Annu Rev Marer Sci, 33.

Young, E.W.K., and Beebe, D.J. (2010). *Fundamentals of microfluidic cell culture in controlled microenvironments*. Chem Soc Rev **39**, 1036.

Zahir, N., and Weaver, V. (2004). *Death in the third dimension: apoptosis regulation and tissue architecture*. Current opinion in genetics & development **14**, 71-80.

Zutter, M.M. (2007). *Integrin-mediated adhesion: Tipping the balance between chemosensitivity and chemoresistance*. Adv Exp Med Biol **608**, 87-100.